

https://dspace.org/

Nano-Embedded Bioplatform for Ocular Delivery of Genetic Material

Sikhosana, Nombeko

2025
University of the Witwatersrand, Johannesburg
https://hdl.handle.net/10539/50012
Sikhosana, Nombeko. (2025). Nano-Embedded Bioplatform for Ocular Delivery of Genetic Material [PhD thesis, University of the Witwatersrand, Johannesburg]. WIReDSpace. https://hdl.handle.net/10539/50012

Downloaded from a DSpace repository. https://dspace.org/

Nano-Embedded Bioplatform for Ocular Delivery of Genetic Material

Nombeko Sikhosana

A thesis submitted to the Faculty of Health Sciences, University of the Witwatersrand, in fulfilment of the requirements for the degree of Doctor of Philosophy



Supervisors:

Professor Yahya Essop Choonara

Professor Lisa Du Toit

Dr Pavan Walvekar

Department of Pharmacy and Pharmacology, School of Therapeutic Sciences, Faculty of Health Sciences, University of the Witwatersrand, Johannesburg

Dr Naseer Ally

Division of Ophthalmology, Department of Neurosciences, School of Clinical Medicine, Faculty of Health Sciences, University of the Witwatersrand, 7 York Road, Parktown, Johannesburg 2193, South Africa

Johannesburg, South Africa, 2025

DECLARATION

I, **Nombeko Sikhosana**, declare that this thesis is my work except where expressly indicated in the text for outsourced analysis. It has been submitted for the Doctor of Philosophy degree in the Faculty of Health Sciences at the University of the Witwatersrand, Johannesburg, South Africa. It has not been submitted before any degree or examination at this or any other University.



18th June 2025

ANIMAL ETHICS DECLARATION

I, Nombeko Sikhosana, hereby confirm that the study entitled “Nano-embedded 3D bioplatform for Ocular Tissue Regeneration” was approved by the University of the Witwatersrand's Animal Ethics Screening Committee (AESC), with Ethics Clearance Number AESC21-04-016.

APPENDIX B

RESEARCH OUTPUTS

Research output

Nombeko Sikhosana, Pavan Walvekar, Lisa C. du Toit and Yahya E. Choonara. Evaluation of the Efficacy of a Polymer-Lipid Conjugated Cationic Ocular Nanosystem for Enhanced Gene Delivery *In Vitro:* Manuscript submitted to the Journal - *Drug Delivery and Translational Research.* Awaiting reviewer response.

Nombeko Sikhosana, Pavan Walvekar, Lisa C. du Toit, Naseer Ally, and Yahya E. Choonara. Advances in Nucleic Acid Delivery Platforms Targeting Posterior Segment Eye Diseases: Review submitted to the Journal: *Expert Opinion on Drug Delivery* - Awaiting reviewer response.

Research presentation

Nombeko Sikhosana, Pavan Walvekar, Lisa C. du Toit and Yahya E. Choonara. Nano-embedded 3D bioplatform for ocular tissue regeneration. 16th Early Career Scientist Convention, SAMRC, Cape Town Headquarters (Online), 25 - 26 October 2022.

APPENDIX C1

Nombeko Sikhosana, Pavan Walvekar, Lisa C. du Toit and Yahya E. Choonara. Nano-embedded 3D bioplatform for ocular tissue regeneration: Development of a novel gene delivery system. University of Venda, 2023 Young Scientists' conference, 12 - 13 June 2023.

APPENDIX C2

Nombeko Sikhosana, Pavan Walvekar, Lisa C. du Toit and Yahya E. Choonara. Nano-embedded 3D bioplatform for ocular tissue regeneration: Development of a novel gene delivery system. University of KwaZulu Natal, The Capital Resort, Zimbali, APSSA 2023 Conference, 31 Aug - 02 September 2023.

APPENDIX C3

ABSTRACT

This thesis explores gene therapy as a promising strategy for treating retinal degenerative diseases, with a particular focus on the development and future of gene delivery vectors. Effective gene delivery systems must be biocompatible and versatile, capable of encapsulating and delivering various nucleic acid payloads. However, current vectors often face limitations such as immunogenicity, low payload capacity, non-specific tropism, and suboptimal transfection efficiency. Numerous studies over the past decade highlight that the limited success of gene therapy is largely due to the inefficiencies of these delivery systems. To address this, the thesis proposes a biocompatible, cationic gene delivery nanosystem targeting CD44 receptors on retinal pigment epithelium (RPE) cells. This targeted approach enhances tissue specificity and supports nucleic acid encapsulation and delivery. A dual delivery system was developed comprising a thermoresponsive hydrogel designed to encapsulate the nanosystem and support ocular cell proliferation for tissue regeneration. The gene delivery vehicle referred to as the nano-polyplex was constructed using hyaluronic acid (HA) conjugated to 2-aminobenzimidazole and oleylamine, forming an amphiphilic, cationic structure. Upon loading with the plasmid pcDNA6.2-EmGFP (pEmGFP), the nano-polyplex exhibited spherical morphology, with particle sizes ranging from 75 nm (unloaded) to 150 nm–3.6 μm (loaded), and zeta potentials ranging from 2.5 mV to 27 mV, depending on the nitrogen-to-phosphate (N:P) ratio. Encapsulation efficiencies exceeded 90% for most N:P ratios, except for N:P 5, which achieved 19.5%. The formulations effectively protected pEmGFP from nuclease degradation and enabled sustained release over 96 hours. Cell viability remained above 90% across all tested formulations. Transfection efficiency, evaluated via GFP expression and fluorescence microscopy, was highest for the N:P 15 formulation. In Phase II, the nano-polyplex was embedded in a pluronic-chitosan hydrogel to form the Gen-I system, a "Trojan horse" platform enabling sustained gene delivery and promoting cell viability. The Gen-I system supported cell survival and proliferation over 36 hours in vitro. A seven-day pilot in vivo study demonstrated the system’s safety and the sustained presence of pEmGFP following intravitreal administration, with only moderate inflammation observed. Collectively, this work presents a novel, biocompatible gene delivery platform with targeted tropism and regenerative potential for retinal gene therapy applications.

ACKNOWLEDGEMENTS

I would like to thank Prof. Yahya Choonara, Dr Pavan Wilvekar, Prof. Lisa Du Toit, Dr Kuben Naidoo and Dr Naseer Ally for allowing me the opportunity to work with them, mentoring me and playing a significant role in my growth during my Postgraduate studies. May their teachings be manifested in all I do.

I sincerely thank my financial sponsors: Bongani Mayosi National Health Scholar Programme, the Medical Research Council (MRC), the National Research Foundation (NRF) and the University of the Witwatersrand.

Lastly, I also thank and appreciate Ms Busi Nompumelelo, Mr Kleinbooi Mohlabi, Mr Bafana Temba and Ms Tshidi Mosete for their technical and administrative assistance during my research. I also thank all members of the Wits Advanced Drug Delivery Platform (WADDP), particularly Mashudu, Leon, Dr Ngema, Atang, Ahmed, Brian, Jonathan, Theresa and Clarence, for making my time socially engaging.

DEDICATION

I dedicate this, previous and future works to my late grandmother (love of my life) who saw in me immense potential from a very young age. I also dedicate this to my late father who always pushed me to achieve the best and my mother who always listens to my complaints with no judgement and enjoys taking part in insane conversations with me, thanks mom 🙂. Major thanks to my siblings (Nyaniso, Themba and Kuntsu), my nieces (Amahle, Akhona and Anathi), my cousin Themba and my nephews (Anele, Luthando, Mangaliso and Luyanda). Love you guys…

TABLE OF CONTENTS

ANIMAL ETHICS DECLARATION ii

RESEARCH OUTPUTS AND iii

ABSTRACT iv

ACKNOWLEDGEMENTS v

DEDICATION vi

TABLE OF CONTENTS viii

LIST OF FIGURES xvi

LIST OF TABLES xxi

LIST OF EQUATIONS xxii

LIST OF ABBREVIATIONS xxiii

CHAPTER ONE

Background and Motivation for the Formulation of a Nano-embedded 3D-bioplatform for Ocular Tissue Regeneration

1. Introduction 1

1.1. Rationale and motivation for this study 4

1.2. Novelty of the study 5

1.3. Nano-embedded bioplatform (Gen-I): concept and outline 6

1.4. Aim and objectives of this study 6

1.5. Overview of this Thesis 7

1.6. References 9

CHAPTER TWO

Advances in Nucleic Acid Delivery Platforms Targeting Posterior Segment Eye Diseases

2. Introduction 12

2.1. Background on Posterior Segment Eye Diseases 12

2.2. Challenges and Limitations of Current Therapies 17

2.3. Gene therapy: A Brief Synopsis 18

2.3.1. Overview of Gene delivery essentials 19

2.4. Overview on viral vector-based gene delivery 20

2.4.1. Viral vector-based gene therapies targeting PSEDs 21

2.4.2. Novel approaches to ocular gene therapy: Optogenetic therapy and RPE regeneration 22

2.4.3. Limitations 24

2.5. Non-viral vector nucleic acid-based therapy background 28

2.5.1. A brief description of the gene delivery process 30

2.5.2. The advent of non-viral based gene delivery systems: Polymer-based nanosystems 30

2.5.3. Lipid-based nucleic acid delivery systems 34

2.5.4. Bioconjugates, Bioresponsive, Hybrid and cell-aided gene delivery nanosystems 37

2.5.4.1. siRNA modification as a form of protection/delivery 37

2.5.4.2. Bioresponsive gene delivery nanosystems 37

2.5.4.3. Lipid-polymer (‘Hybrid’) delivery nanosystems 39

2.5.4.4. The “Trojan horse” gene delivery Strategy 41

2.5.5. Inorganic based gene delivery systems 43

2.6. Conclusion and way forward 45

2.7. Expert opinion 46

2.8. References 48

CHAPTER THREE

Evaluation of the Efficacy of a Polymer-Lipid Conjugated Cationic Nanosystem for Enhanced Gene Delivery *In Vitro*

3. Introduction 64

3.1. Experimental section 66

3.1.1. Synthesis of the amphiphilic cationic copolymer 67

3.1.1.1. Sodium hyaluronate conversion 67

3.1.1.2. Synthesis of HA-2AB conjugates 67

3.1.1.3. Quaternisation of HA-2AB (synthesis of a cationic copolymer) 67

3.1.1.4. Synthesis of cationic self-assembling nanosystem (HA-2AB+-OLA) 67

3.1.2. Physicochemical characterisation of the HA-2AB+-OLA copolymer 68

3.1.3. Isolation and Purification of pcDNA6.2-EmGFP from Transformed Escherichia coli 69

3.1.4. Preparation and characterisation of nano-polyplex Formulation: pcDNA6.2-EmGFP loaded nanosystem 69

3.1.5. Entrapment/Gel retardation analysis and Encapsulation efficiency 70

3.1.6. Nuclease Protection assay and pDNA stability 71

3.1.7. In vitro release studies of the nano-polyplex system 71

3.1.8. Stability studies 71

3.1.9. Cell culture 71

3.1.10. Cell cytotoxicity 72

3.1.11. In vitro cell transfection and Fluorescent cell imaging 72

3.1.12. Flow cytometry 73

3.1.13. Real-time quantitative pCR for emGFP expression in vitro 73

3.1.14. Statistical analysis 73

3.2. Results and Discussion 74

3.2.1. Confirmation of HA-OLA-2AB+ conjugate by 1H NMR spectroscopy 75

3.2.2. Interpretation of the vibrational transitions for structural analysis of HA-2AB+-OLA copolymer 76

3.2.3. Evaluating Phase transitions of HA-2AB+-OLA conjugate using X-ray Diffraction 77

3.2.4. Thermal stability of composites 78

3.2.5. Differential scanning calorimetry 80

3.2.6. Formation of the nano-polyplex system 80

3.2.7. Evaluating the Encapsulation Efficiency of the Nano-polyplex system 83

3.2.8. Evaluation of pcDNA6.2-EmGFP degradation by endonucleases 84
3.2.9. Evaluation of in vitro pcDNA6.2-EmGFP release from the cationic- amphiphilic nano-polyplex system 85
3.2.10. Assessment of the nano-polyplex system biocompatibility and safety profile in HEK 293 and hRPE cell line 87
3.2.11. In vitro transfection efficiency and gene expression as analysed by GFP detection 88
3.2.11.1. GFP detection in nano-polyplex transfected HEK 293 cells 88
3.2.11.2. hRPE cells fail to express GFP following transfection 90
3.3. Concluding remarks 90
3.4. References 92

CHAPTER FOUR

Preliminary investigation of smart hydrogel systems for cell encapsulation and delivery to promote tissue regeneration

4. Introduction 97

4.1. Materials and Methods 99

4.1.1. Construction and characterisation of the Gen-I system: Box-Behnken Design 99

4.1.2. Gelation Characterisation and Injectability Assessment 100

4.1.3. Physicochemical and structural characterisation of hydrogels 101

4.1.4. Rheological analysis of the Gen-I system 101

4.1.5. Gen-I Degradation profile and stability 102

4.1.6. Maintenance of Cell culture 102

4.1.7. Cell Viability and Proliferation assay 103

4.1.8. Statistical analysis 104

4.2. Results and Discussion 104

4.2.1. Design of Experiments - The Box-Behnken Design matrix 104

4.2.2. Structural and Thermal Characterisation of the Gen-I system 109

4.2.2.1. Assessment of Gen-I chemical composition and molecular structure 109

4.2.2.2. Assessment of Gen-I system composition and thermal stability 110

4.2.2.3. Electron microscopy for the evaluation of the surface topography and composition of the Gen-I system 111

4.2.3. Mechanical and rheological properties of the Gen-I system 112

4.2.5. Gen-I system safety profile and cell viability monitoring following cell seeding 116

4.3. Concluding remarks 118

4.4. References 120

CHAPTER FIVE

Pilot study: *In vivo* evaluation of Novel Gen-I system safety profile and GFP expression in the retina of New Zealand White Rabbits

5. Introduction 125

5.1. Materials and Methods 126

5.1.1. Materials 126

5.1.2. Animal housing and welfare 127

5.1.3. Preparation of formulations and intravitreal administration of the intervention 127

5.1.4. Euthanisia, enucleation and sampling 129

5.1.5. Histomorphological and GFP expression analysis 129

5.1.6. pcDNA6.2-EmGFP in vivo Quantification 130

5.2. Results and Discussion 130

5.2.1. Animal postoperative assessment, recovery, and behaviour 130

5.2.2. Histological analysis of ocular tissue 131

5.2.3. Quantitative analysis of pcDNA6.2-EmGFP and GFP expression 133

5.3. Concluding Remarks 136

5.4. References 138

CHAPTER SIX

Conclusion and Recommendations

6. Conclusion 141

6.1. Concluding Insights 141

6.2. Recommendations 143

6.3. References 144

APPENDICES

Appendix A: Supplementary Material 145

Appendix B: Animal Ethics Clearance Certificate 150

Appendix C: Research Outputs 151

Appendix D: Originality report 154

LIST OF FIGURES

Figure 1.1	A schematic representation of the study design for the development of the proposed novel amphiphilic cationic pEmGFP loaded nano-polyplex system for the in vitro analysis and the Gen-I system for in vitro and in vivo delivery and analysis.	7
Figure 2.1	Schematic representation of healthy retina, choroid, and retinal pigment epithelium (RPE) cells	13
Figure 2.2	Schematic representation of PSEDs, namely Retinitis pigmentosa, Glaucoma, Early Age-related Macular degeneration and Diabetic retinopathy, Diabetic macular oedema and advanced age-related AMD and associated pathologies	14
Figure 2.3	Summary of gene therapy delivery modalities. In vivo, gene therapy involves the administration of genetic material encapsulated within a delivery vector directly into the patient. Ex vivo gene therapy involves the extraction of cells from a patient or an allogenic source; the extracted cells are genetically modified using a vector containing a therapeutic transgene. This is followed by the selection and expansion of the modified cells in culture and infusion to reintroduce them into the patient.	19
Figure 2.4	Representation of non-viral gene therapy mediated by cellular internalisation via endocytosis. The cytosol is the destination for RNA payload, whilst the cell nucleus is the target for DNA delivery mediated by the nuclear pore	20
Figure 2.5	a) HEK293-GIRK cells transiently transfected with different Opsin-mKate fusion proteins show robust membrane expression (exemplified for OPN1MW(CT mGluR6)-mKate and Mela(CTmGluR6)-mKate). b–h) To assess the relative efficacies at which opsin constructs activate G-proteins in the Gαi/o class, we screened all opsin constructs in HEK293-GIRK cells. h–j) In vivo screening of treated blind (>24 weeks) rd1 mice in a naïve optomoter reflex task.	25
Figure 2.6	Delivery of the protein RDS/normal mouse peripherin (NMP) as facilitated by CK30PEG nanoparticles to photoreceptors leads to functional rescue of the rds heterozygous phenotype in mice.	32

Figure 2.7 In vivo gene silencing efficacy. Eyes of nude mice were inoculated with WERI-Rb-1-luci cells, and the mice were divided into four groups, administered with normal saline, naked siRNA, siRNA/PA/89WP, and siRNA/Lipo, respectively. Each siRNA formulation contained 1.5 μg siRNA and was applied three times daily via topical installation. 35

Figure 2.8 A) A Schematic representation of the structural organisation of different LNP variants encapsulating mRNA cargo. B) Lipid composition of LNP variants in the study. C Schematic illustration exhibiting delivery of LNPx via subretinal route, retinal imaging and processing, as well as CRISPR-Cas9 editing mechanism. D) Representative fundus imaging showing editing events mediated by Cas9-sgAi9-LNPx. E) Quantification of tdTomato signal in fundus images. F) Representative flat mount images showing gene editing events in the RPE. G) Quantification of gene editing events in the RPE. H) Quantification of editing events by next-generation sequencing showed increased edits in the Cas9-sgAi9 37

Figure 2.9 Anti-neovascularization of PACD/siRNA in an OIR mouse model 40

Figure 2.10 LPD-mediated Rpe65 gene delivery in Rpe65 knockout mice rescues cone cell death 41

Figure 2.11 Targeted delivery of MSC-hybrid-siRNA NPs and therapeutic efficacy in a laser-induced CNV mouse model 43

Figure 3.1 Schematic of synthesis of HA-OLA-2AB^{+} derivative using EDC/NHS conjugation chemistry. Hyaluronic acid (HA, 85 kDa); HA-conjugated to 2AB (133 Da) and OLA (267 Da). 72

Figure 3.2 ^{13}C nuclear magnetic resonance (NMR) spectra of native polymers and the synthesised conjugate. 73

Figure 3.3 Physicochemical characterisation of HA_2AB_OLA copolymer. a) Comparative FTIR spectra of the individual components, HA, 2AB, OLA and HA_2AB_OLA participating in the formation of HA-OLA-2AB. The individual constituents/reactants (HA, 2AB, OLA and HA-OLA-2AB) used in the formulation of the cationic copolymer were observed and analysed to detect the occurrence of actual conjugation. The FTIR spectra were recorded in the range of 850 to 4000 cm-1. 75

b) X-ray Diffraction (XRD) Analysis of Pure Hyaluronic Acid (HA) and the synthesized conjugate polymer HA-2AB-OLA. The XRD pattern reveals the characteristic peaks associated with an amorphous structure and thus absence of a well defined crystal lattice

Figure 3.4 **Thermal stability of the polymer composite, HA_2AB_OLA.** a) The TGA spectra represent the thermal stability, decomposition, and degradation profiles of key components in the synthesis of the hyaluronic acid (HA) conjugate, HA-OLA-2AB. A significant decomposition for HA is indicated by a sharp mass reduction between 229.8 - 509.3 °C in comparison to the synthesised polymer. The modifications on HA slightly impacted its thermostability, as evidenced by the observed variations in mass loss during degradation. b) Differential scanning calorimetry curves illustrating the thermal behavior and properties of: pure hyaluronic acid (HA) with characteristic degradation peak at 233.69 °C, 2-aminobenzimidazole (2AB) with its sharp peak at 230.44 °C synonymous with its melting point, hyaluronic acid conjugated to Oleylamine (HA-OLA) and the final synthesized conjugate polymer, HA-OLA-2AB^{+} both showing presence of two concurrent endothermic peak which may be indicative of multiple processes occurring during the heating process. 76

Figure 3.5 DLS results of the various NP formulations. Mean size (d.nm) and zeta potential (mV) of different formulations of HA-OLA-2AB^{+}/pDNA nanocomplexes prepared by complexation of pDNA with the amphiphilic and cationic conjugate HA-OLA-2AB^{+}. Data from experiments are presented as the mean ± SD, n =3 (**** denote $p < 0.0001$). 78

Figure 3.6 DLS results (Zeta potential and mean NP diameter) of the nano-polyplex system stability test following 28 days storage at 4 - 8°C. 79

Figure 3.7 Encapsulation efficiency of the nanocomplex, Gel retardation and Nuclease protection assay. (A) The pDNA encapsulation efficiency (EE%) of different NP ratio formulations. With the amount of HA-OLA-2AB+ increasing, EE % significantly differed across formulations. (B) Gel retardation assay of HA-OLA-2AB+ DNA (1 µg) at N/P ratios of 10 - 40. (C) Nuclease protection assay analysis. In vitro cumulative pcDNA release profile from different NP formulation ratios of HA-OLA-2AB+ /pcDNA. Data from experiments are presented as the mean ± SD, n =3 (**** denote $p < 0.0001$). 81

Figure 3.8 Cell viability of HA-OLA-2AB+ /pcDNA NPs formulations on the Hek 293 T and hRPE cell lines. Measurements were carried out by MTT assay with comparison to untreated cells as the positive control. Values of MTT assay are given in percentages and normalized to blank control as 100%. Data from experiments are presented as the mean ± SD, n = 6 (**** denote p < 0.0001). 83

Figure 3.9 Transfection efficiency of HA_2AB+_OLA/pEmGFP formulation. (A) Fluorescence microscopy images showing EmGFP transfected HEK 293 cells. (B) Corrected fluorescence intensity as determined by Image J. (C) EmGFP mRNA quantification using qPCR. Data from experiments are presented as the mean ± SD, n =3 (**** denote p < 0.0001). 84

Figure 3.10: Transfection efficiency of nano-polyplex system in HEK 293 and hRPE cells. Images were taken 72 h post-transfection with: HEK 293 cells only (A), free pcDNA6.2-EmGFP (B),Lipofectamine 3000/pcDNA6.2-EmGFP (C), Nano-polyplex (D), hRPE cells only (E), pcDNA6.2-EmGFP (F), Lipofectamine 3000/pcDNA6.2-EmGFP (G) and Nano-polyplex (H). (I) EmGFP mRNA quantification results using qPCR. Data from experiments are presented as the mean ± SD, n =3 (* denote p < 0.05). Scale bar 50 µm 86

Figure 4.1: Three-dimensional (3D) and contour response surface plots of (A) Gelation temperature, (B) Gelation temperature, (C) Injectability (21 Gauge needle), (D) Injectability (25 Gauge needle). 103

Figure 4.2: Structural analysis for Gen-I system, Pluronic®F127, Chitosan and the nano-poplex using FTIR. 105

Figure 4.3: Thermograms of individual polymers and the composite Gen-I system as a function of temperature. 106

Figure 4.4: Scanning electron micrographs of the surface morphology of composite gel matrix (left) and Gen-I system (right). 107

Figure 4.5: Rheological characterisation of the optimised Gen-I system. (a) Inversion test for the assessment of gelation behaviour. (b) Temperature ramp at constant shear rate. (c) Frequency sweep at 37 °C. (d) Shear thinning behaviour of the Gen-I system at 37 °C. (d) Steady shear stress ramps on the Gen-I system at 37 °C. Stress ramps from 0 to 350 Pa in 1000 s 109

Figure 4.6: Degradation profiles of Gen-I system, Pluronic F127 and Pluronic F127_chitosan hydrogels in culture media (pH 7.2 to 7.4) at 37 °C (mean ± S.D., n = 3, $p < 0.05$) 111

Figure 4.7: Safety profile of the Gen-I system on HEK293 and hRPE cells. a,b) Cell viability of HEK293 and hRPE cells using the MTT assay at 48h and 72 h. Live cell staining (Calcein AM) and nucleic acid staining (DAPI) of c) non-encapsulated hRPE cells and d) Gen-I encapsulated hRPE cells at timepoint 48h. Scale bar: 50 µm. (Data from experiments are presented as the mean ± SD, n = 3). 112

Figure 5.1: Pilot study design (allocation of animals to groups) 121

Figure 5.2: Depiction of surgical setup, intravitreal administration of intervention and postoperative application of chloramphenicol ointment. 122

Figure 5.3: Histological slides of enucleated eyes on day 7. Tissue from negative control eyes showing (A) retina, (B) choroid, (C) sclera and (D) optic nerve at 10x and 20x magnification (Scale bar = 1000 µm) . (E - H) ocular tissue from Lipofectamine 3000_ pcDNA6.2-EmGFP (positive control) administered eyes (scale bar = 1000 µm). (I - L) histological images of ocular tissue from Gen-I system administered eyes (scale bar = 1000 µm). Symbols in the histopathological images indicate the following: circle = plasma cells; square =gliosis; triangle = lymphocytes; star = lymphocytic cuffing, dotted = vacuolization, black arrow = neutrophils, red arrow = congested vasculature. 125

Figure 5.4: pcDNA6.2-EmGFP concentrations quantified in aspirated vitreous humour using the PicoGreen dsDNA assay. Data are presented as mean ± standard deviation (SD) from [n] biological replicates. Statistical significance was determined using ONE-WAY ANOVA, with $p < 0.0001$ (****) considered significant. 127

LIST OF TABLES

Table 2.1:	Drug classes and therapies for posterior segment diseases currently approved by the FDA or used off-label	15
Table 2.2:	Viral vector-based gene therapies for posterior segment diseases	27
Table 4.1:	Independent and dependent variables for factorial design.	75
Table 4.2:	Summary of the DOE (Box-Behnken statistical design) generated formulations for the optimisation of the Gen-I system and responses obtained from *in vitro* testing.	100
Table 4.3:	Regression analysis summary for responses Y1, Y2, Y3 and Y4	101
Table 5.1	RT-PCR Cq Data	129

EQUATIONS

Equation 3.1	Crystallinity Index	65
Equation 3.2	Braggs law	68
Equation 3.3	Crystallite size	69
Equation 3.4	% Encapsulation efficiency	97
Equation 3.5	% Cell viability	98
Equation 4.1	% Degradation	98
Equation 4.3	Regression Model 1	101
Equation 4.4	Regression Model 2	102
Equation 4.5	Regression Model 3	102
Equation 4.6	Regression Model 4	102
Equation 4.7	Bingham liquid mode	110

ABBREVIATIONS

AMD	Age-related Macular Degeneration
AREC	Animal Research Ethics Committee
CD44	Cluster Differentiation Factor 44
DAPI	4′,6-diamidino-2-phenylindole
DMEM	Dulbecco’s Modified Eagle Medium
DNA	Deoxyribonucleic acid
DR	Diabetic Retinopathy (DR)
ECM	Extracellular Matrix
E.E	Encapsulation Efficiency
FBS	Foetal Bovine Serum
FTIR	Fourier Transform Infrared
HA	Hyaluronic acid
hRPE	Human Retinal Pigment cells
mRNA	Messenger Ribonucleic acid
PSEDs	Posterior Segment Eye Diseases
siRNA	Short interference Ribonucleic acid
SEM	Scanning Electron Microscope
TEM	Transmission Electron Microscopy
VEGF	Vascular Endothelial Growth Factor

CHAPTER ONE

Background and Motivation for the Formulation of a Nano-embedded 3D-bioplatform for Ocular Tissue Regeneration

1. Introduction

The estimated global life expectancy was 71.1 years in 2022, a rise from the 1950s 46.5 years; projections indicate that by 2050, the global life expectancy will be 77.3 years (World Economic Forum, 2023). This, along with changing socio-economic conditions has led to changes in lifestyle, therefore generating a shift in disease prevalence towards non-communicable and age-related illnesses (Steinmetz et al., 2021). Inadvertently, this has culminated in increased incidence of retinal degenerative diseases such as age-related macular degeneration (AMD), diabetic retinopathy (DR) and glaucoma. A clear link between these eye conditions is ageing and diabetes mellitus (DM), whose rise is estimated to reach 700 million cases globally by 2045 (Teo et al, 2021). A study aimed at assessing the global prevalence of DR among people with diabetes reported 103.12 million cases of DR (22.27%), 28.54 million for vision-threatening diabetic retinopathy (VTDR - 6.17%) and 18.83 million (4.07%) cases for clinically significant macular oedema (CSME) in 2020 (Teo et al., 2021). Furthermore, global projections as estimated by the International Diabetes Federation (IDF), are expected to reach 160.50 million for diabetic retinopathy, 44.82 million (VTDR), and 28.61 million (CSME), by 2045 respectively. Based on a pooled analysis of various hospital-based studies, the prevalence of diabetic retinopathy is reported to be 31.6% in Africa (Tilahun et al., 2020).

Unlike diabetic retinopathy, other major posterior segment eye diseases (PSED) are not only dependent on the predisposition to diabetes mellitus but also result from multiple factors such as age, genetics and high blood pressure, amongst others; one such multifactorial PSED is age-related macular degeneration (AMD). There are over 200 million cases of AMD globally, constituting 9% of all cases of blindness (Chaudhuri et al., 2023). By 2040, the prevalence of AMD is estimated to reach 300 million cases (Jiang et al., 2023; Vyawahare and Shinde, 2022), with most patients afflicted by AMD aged 50 years and above. The age selectiveness of AMD is attributed to the disruptions that commonly occur during the normal ageing process. This is frequently accompanied by the dysfunction of essential homeostatic processes, particularly those responsible for the renewal of cellular constituents, proteostasis, genomic stability, maintenance of correct epigenetic regulation and clearance of waste molecules (López-Otín et al., 2013). Inefficiencies in these mechanisms result in the gradual accumulation of crosslinked protein aggregates and lipofuscin granules in neurons (Moreno-García et al., 2018). The cross-linked nature of these complexes makes them

resistant to degradation, thus preventing lysosomal clearance (macroautophagy inhibition) and promoting the accumulation of lipofuscin in the cytoplasm of post-mitotic cells such as nerve cells (Moreno-García et al., 2018). This mechanism not only affects the transport of oxygen and essential nutrients (e.g., vitamin A) to the retinal pigment epithelial cell layer (RPE) and thus the photoreceptors but also contributes to the formation of reactive oxygen species and the activation of the pro-apoptotic cascade, resulting in RPE and photoreceptor atrophy (‘macular degeneration’). Another PSED commonly associated with ageing is glaucoma. Glaucoma is characterised by factors such as chronic inflammation, deficiency in anti-inflammatory bioactive lipids/cytokines, the aberrant expression of vascular endothelial growth factor (VEGF), and the presence of angiotensin II and prostaglandins (Casson, 2022). Glaucoma is a leading cause of severe and irreversible vision loss, affecting over 70 million people globally and resulting in more than 10% of bilateral blindness (Parihar, 2016). Its association with diabetes has been reported in multiple studies and meta-analyses which have demonstrated the role of diabetes in changing intraocular pressure (Kanamori et al., 2004). Convincingly, pathophysiological modifications such as microvascular endothelial dysfunction, blood flow dysregulation, and retinal nerve fibre layer defects seen in diabetics, correlate with those seen in glaucoma patients (Li et al., 2021).

Apart from environmental factors having a significant impact on the development of PSEDs, inherited genetic mutations are also capable of initiating the degeneration of the retina (Kolb et al., 1995). Pathologies related to retinal degeneration include a group of hereditary eye disorders called Retinitis Pigmentosa (RP) (Kolb et al., 1995). RP is the most common type of retinal dystrophy and affects individuals <60 years. Although characterised by varying phenotypes and genotypes, common symptoms include, nyctalopia and loss of peripheral vision eventually leading to blindness (Wu et al., 2023). Similarly to other PSEDs, available treatment modalities for RP are limited and require intraocular administration which has multiple drawbacks as frequent dosing is necessary to ensure therapeutic efficiency (Iyer et al., 2019). The invasiveness of the procedure may result in intraocular pressure, endophthalmitis, retinal detachment, and vitreous haemorrhage (Jager et al., 2004). Therefore, current advancements in retinal degeneration therapy are focusing on developing replacement therapies which can achieve sustained intraocular delivery, thus, reducing the number of required doses, reducing ophthalmological risk and offering economic benefit to patients. Additionally, the multifactorial and early-stage asymptomatic nature of PSEDs contributes to failure in early detection, difficulties in elucidating their exact mechanism of pathogenesis and developing efficient therapies requiring the investigation of broadly effective and innovative therapies. An exemplary innovative approach involves the development of vector based gene therapies capable of achieving targeted-controlled therapeutic delivery, similar to Luxturna (voretigene neparvovec-rzyl) which is a groundbreaking therapy for the treatment of Leber’s congenital amaurosis resulting from a

mutation in the rpe65 gene through the delivery of a functional copy of rpe65 to retinal cells (Padhy et al., 2020). Luxturna results in vision improvement, however, in the long term, fails to halt progressive degeneration of photoreceptors (Wang et al., 2020). Additionally, it makes use of an adeno-associated viral vector to deliver the *rpe65* gene, this vector has potential immunogenic effects and could cause adverse effects and reduce the efficacy of the treatment with multiple doses.

The use of viral vectors in gene therapy delivery has become the cornerstone of modern medicine, availing a much more efficient approach to precision medicine. However, viral vectors are constrained by several limitations such as limited genetic cargo, possibility of insertional mutagenesis and off-target effects, pre-existing immunity in some patients can cause immunogenic effects and depending on the viral vector, they can have narrow (adeno-associated viruses and retroviruses) or broad (adenoviruses and lentiviruses) tropism which can have unfavourable downstream effects depending on the application (Ghosh et al., 2020). Therefore, this study is aimed at fabricating a biocompatible smart hydrogel incorporating a polymeric non-viral gene delivery system. The composite gene delivery nanosystem embedded in a thermoresponsive hydrogel was delivered into the posterior segment of the New Zealand White rabbit eye model, genetic material analysed for stability and entrapment within the optimised nanosystem and the thermogel assessed for for its cell encapsulation, viability maintenance, and potential delivery properties. The incorporation of the nanosystem in the thermogel controls the release of the genetic material to be distributed throughout the target tissue. Biocompatible materials such as hyaluronic acid, pluronic F-127, oleylamine, 2-aminobenzimidazole and chitosan were the polymers of choice for the construction of the composite gene delivery nanosystem. The hybrid gene delivery system was designed to encapsulate genetic material and form an ocular matrix (hydrogel) to support cell delivery. Once in the ocular space, the matrix is expected to degrade through phase transition and solubilisation and release genetic material in a controlled manner.

The selection of the model genetic material for this study was guided by considerations of accessibility and practicality, with pcDNA™6.2/c-EmGFP-DEST being chosen for the study. This vector was selected as it can function as a non-toxic marker and allows for easy integration of a gene of interest to the fluorescent protein Emerald Green Fluorescent Protein (EmGFP) sequence (in future studies) which allows for non-invasive detection and monitoring of gene expression of recombinant protein. This fluorescent marker allows for precise tracking and validation of gene transfection and delivery. Moreover, its compatibility with standard transfection protocols and established use in mammalian transfection studies make it an optimal choice as a model for initial studies, providing a robust platform for evaluating gene delivery efficiency and efficacy in the ocular space.

1.1. Rationale and motivation for this study

Despite the continued advances made in the field of gene therapy and its growing importance in the future of precision medicine, numerous challenges remain. Significantly, these include the potential genotoxic effects associated with integrating viral vectors (Kohn et al., 2023), the electrostatic repulsion between the phospholipid bilayer and genetic material, along with the extremely short half-life of nucleic acid *in vivo* as they are prone to degradation by nucleases (Wang et al., 2023). Essential to note, most FDA-approved gene therapies utilise viral-based vectors for gene delivery, which have immense benefits in ensuring optimal gene delivery but have significant downsides. Most gene therapies use adeno-associated viral vectors to achieve optimum delivery. Although these vectors are associated with minimal pathogenicity, broad tropism, and relatively long-term gene expression, AAVs safety profile, particularly in high doses, remains a concern along with its immunogenic potential and adverse effects (neurotoxicity and hepatotoxicity) (Wang et al., 2024). Therefore, this study aims to overcome such drawbacks by designing a biocompatible hybrid nanosystem engineered to:

- Target cells expressing CD44 receptors through binding of hyaluronic acid incorporated in the nanosystem, this increases the precision of gene delivery and eliminates off-target effects.
- Achieve efficient cell transfection through endocytosis and with the ability to cross target cellular barriers by controlling the size of the nanosystem.
- Carry and deliver large genetic materials (>4.5 kilobases) without eliciting an immune response.
- Promote endosomal escape through the manipulation of its pH.
- Protect genetic material from degradation by nucleases and other environmental factors, ensuring the integrity of the genetic material during delivery.
- Achieve sustained gene delivery.
- Encapsulate and deliver cells in future retinal cell regenerative studies.

The use of polymeric material in the fabrication of the gene delivery nanosystem offers a more versatile alternative that allows for a tailored approach to disease treatment. Additionally, designing novel gene delivery nanosystems that aims to address existing challenges by enhancing efficiency, specificity and safety contributes to the body of scientific knowledge regarding gene delivery vector construction. By expanding our insight of the role of polymeric materials in optimising gene delivery vehicles, this research has the potential to positively contribute to the field, potentially leading to effective gene therapy based treatments for a variety of diseases and genetic disorders. The outcomes of this work could pave the way for the discovery of personalised gene therapies and ultimately, improve patient outcomes.

In the context of retinal degeneration therapies, existing therapies are only capable of treating symptoms and slowing down the degenerative process but fail to treat the underlying cause of degeneration, halting it or restoring vision loss. The only FDA approved ocular gene therapy, Luxturna, requires subretinal injections which have shown significant improvement in patient visual acuity (Fu et al., 2018), however, subsequent analyses have raised some concerns regarding the durability of the therapy and its effectiveness amongst patients with varying genetic backgrounds. A key limiting factor of the therapy is the requirement of viable retinal cells for viral vector transduction and expression of functional Retinal pigment epithelium-specific 65 kDa protein (RPE65) (Stingl et al., 2023). Therefore, a dual approach for retinal degenerative diseases is necessary to achieve gene delivery, retinal cell support and proliferation for ultimate tissue regeneration. In corroboration with this, this study focused on the fabrication of a cell supporting matrix, capable of promoting cell encapsulation, proliferation, and differentiation. Polymers capable of supporting cell growth such as hyaluronic acid, pluronic and chitosan were used in the construction of a biocompatible thermo-matrix. The use of the thermogel matrix would not only confer cell scaffold properties but would also ensure prolonged diffusion of the genetic material at the target site, therefore enhancing duration of gene expression and therapeutic effect, reducing the need for multiple administrations.

1.2. Novelty of the study

The novelty of this study involves the delivery of genetic material using a combinatorial approach which would enable the delivery of genetic material along with sustenance of underlying retinal cells in the case of ocular degenerative diseases. The potential scientific or societal advantages that inspired this study include:

- Addressing the Treatment Gap for Retinal Degeneration: The need for alternative treatment approaches for retinal degeneration, particularly in genetic retinopathies which have significant treatment barriers
- Advancing Scientific Knowledge in Gene Delivery Nanosystems: This study presents an opportunity to significantly expand current scientific understanding and contribute to breakthroughs in the construction and development of more efficient and targeted gene delivery nanosystems.
- Enhancing Cost-Effectiveness and Patient Compliance: The opportunity to reduce the cost of current therapies and improve patient compliance, as current retinal degenerative therapies require multiple administrations whose activity is often short-lived.

1.3. Nano-embedded bioplatform (Gen-I): concept and outline

The *in situ* forming Nano-embedded bioplatform was designed such that it is capable of sustained release of genetic material, promotion of gene delivery, supporting cell encapsulation and growth through the transportation of nutrients, waste and gas exchange. The bioplatform was formulated as an injectable thermoreversible hydrogel preferably composed of polymers that promote tissue health and that mimic the extracellular matrix (ECM) of the posterior segment of the eye such as: Hyaluronic acid, Collagen, and Alginate amongst others (Lee and Mooney, 2001). The Gen-I system is expected to have a combinatorial effect to drive targeted gene delivery and expression using the designed nanosystem and subsequently, support cell viability via the smart hydrogel portion of the Gen-I system for the ultimate goal of tissue regeneration and timely deposition of healthy ECM.

1.4. Aim and objectives of this study

The aim of this research was to develop a stable nano-embedded bioplatform (Gen-I) capable of reliably driving controlled gene delivery in the eye for potential expression and as a scaffold for cell growth and proliferation. In order to achieve this aim, the following objectives are delineated:

1. Identification and/or preparation of model genetic material.
2. Synthesis of non-viral gene delivery nano-complex systems capable of genetic material protection and delivery.
3. Characterisation of DNA-nanoparticle: size, surface and thermal stability, morphology, *in vitro* plasmid DNA release, cell uptake and targeting efficacy.
4. Design and construction of a smart hydrogel encapsulating nanoparticles to generate a hybrid bioplatform system, Gen-I, with inherent nucleic acid and cell encapsulation and regenerative properties.
5. Physicochemical and physicomechanical characterisation of the bioplatform (nano-free and nano-enabled), using techniques such as Nuclear magnetic resonance (NMR), Thermogravimetrist analysis (TGA), Scanning electron microscopy (SEM), X-ray diffraction (XRD) and rheology; with determination of the genetic material delivery- and regenerative potential of the Gen-I.
6. Assessment of the stability, preclinical safety and efficacy of the Gen-I *in vitro* and *in vivo* in the New Zealand Albino rabbit eye model.

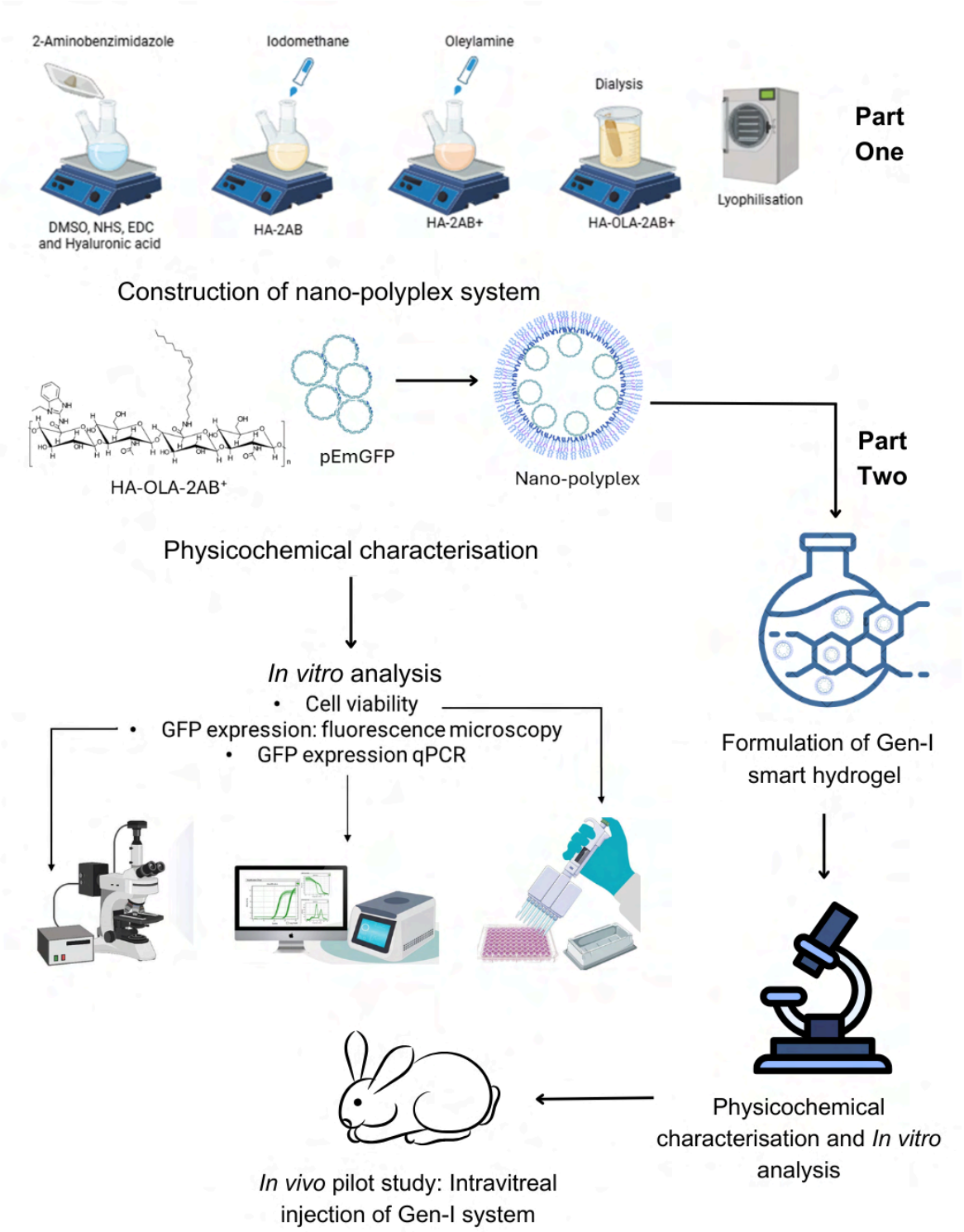

Figure 1.1. A schematic representation of the study design for the development of the proposed novel amphiphilic cationic pEmGFP loaded nano-polyplex system for the *in vitro* analysis and the Gen-I system for *in vitro* and *in vivo* delivery and analysis.

1.5. Overview of this Thesis

The thesis outline is composed of multiple chapters that provide comprehensive insights into the background of retinal degeneration, the current gene therapeutic approach, and the

design and construction of novel non-viral gene delivery systems and possibly cell delivery depots for future studies focused on retinal degenerative diseases.

Chapter One

This chapter highlights the global epidemiological status of retinal diseases, along with the current and projected future burden. Furthermore, key standard pathological features amongst the different types of posterior segment eye diseases are discussed along with an in depth discussion of their contribution to retinal degeneration. The central insufficiency of current therapies is their inability to achieve sustained therapeutic outcome or halt the underlying degenerative process and the lack of varying treatments for existing retinopathies. This chapter also emphasises the importance to investigate alternative approaches to treat retinal degenerative diseases and therefore the rationale of the study which is outlined in the conceptualisation and outline of the project is highlighted.

Chapter two

This review underscores the expansive breadth of the application of gene therapy in the treatment of ophthalmological diseases, with a particular emphasis on conditions affecting the posterior segment of the eye. By focusing on this specific area, the review illuminates the critical need for innovative therapeutic approaches to address the complexities of ocular disorders. It highlights ongoing advancements in the design of gene therapies and delivery systems, aimed at overcoming the inherent limitations of conventional treatments. Notably, the review delves into the synergistic integration of gene transfer, viral vs non-viral gene delivery system and a myriad of gene therapy approaches.

Chapter three

This chapter details the synthesis and characterisation of a novel cationic-amphiphilic gene delivery nanosystem (Nano-polyplex) composed of biocompatible polymers, hyaluronic acid, oleylamine, and amino benzimidazole. It also outlines the analysis of the physicochemical and mechanical properties of the synthesised composite (Nano-polyplex), including pertinent information such as morphology, its capacity to encapsulate, drive sustained release, and protect genetic cargo from nucleases and degradation. Moreover, this chapter details the *in vitro* safety profile of the constructed nanosystem and its ability to promote gene expression.

Chapter four

Delineates the fabrication of a nanosystem delivery platform, which would promote cell survival and proliferation and ultimate tissue regeneration. An in depth analysis of the design approach is conducted using the design of experiment (Box-Behnken design) approach. The final formulation referred to as the Gen-I system is characterised and assessed for its capacity to act as a cell encasing platform for cell delivery.

Chapter five

This chapter presents the *in vivo* analysis of the Gen-I system's safety profile and its ability to facilitate GFP expression. Histopathological assessments of ocular tissues and RNA expression analysis were conducted to evaluate GFP expression levels in the intervention group compared to the positive control group. The findings emphasize the importance of carefully selecting the site of gene therapy administration, duration of the study and optimising gene concentrations for improved efficacy.

Chapter six

This section provides an overview of the study, summarises the findings and limitations, and provides recommendations for future work.

1.6. References

Casson, R.J., 2022. Medical therapy for glaucoma: A review. Clin. Experiment. Ophthalmol. 50, 198–212. https://doi.org/10.1111/ceo.13989

Chaudhuri, M., Hassan, Y., Bakka Vemana, P.P.S., Bellary Pattanashetty, M.S., Abdin, Z.U., Siddiqui, H.F., 2023. Age-Related Macular Degeneration: An Exponentially Emerging Imminent Threat of Visual Impairment and Irreversible Blindness. Cureus 15, e39624. https://doi.org/10.7759/cureus.39624

Fu, X., Huu, V.A.N., Duan, Y., Kermany, D.S., Valentim, C.C.S., Zhang, R., Zhu, J., Zhang, C.L., Sun, X., Zhang, K., 2018. Clinical applications of retinal gene therapies. Precis. Clin. Med. 1, 5–20. https://doi.org/10.1093/pcmedi/pby004

Ghosh, S., Brown, A.M., Jenkins, C., Campbell, K., 2020. Viral Vector Systems for Gene Therapy: A Comprehensive Literature Review of Progress and Biosafety Challenges. Appl. Biosaf. 25, 7–18. https://doi.org/10.1177/1535676019899502

Iyer, S., Radwan, A.E., Hafezi-Moghadam, A., Malyala, P., Amiji, M., 2019. Long-acting intraocular Delivery strategies for biological therapy of age-related macular degeneration. J. Controlled Release 296, 140–149. https://doi.org/10.1016/j.jconrel.2019.01.007

Jager, R.D., Aiello, L.P., Patel, S.C., Cunningham, E.T., 2004. RISKS OF INTRAVITREOUS INJECTION: A COMPREHENSIVE REVIEW: Retina 24, 676–698. https://doi.org/10.1097/00006982-200410000-00002

Jiang, B., Jiang, C., Li, J., Lu, P., 2023. Trends and disparities in disease burden of age-related macular degeneration from 1990 to 2019: Results from the global burden of disease study 2019. Front. Public Health 11. https://doi.org/10.3389/fpubh.2023.1138428

Kanamori, A., Nakamura, M., Mukuno, H., Maeda, H., Negi, A., 2004. Diabetes has an additive effect on neural apoptosis in rat retina with chronically elevated intraocular pressure. Curr. Eye Res. 28, 47–54. https://doi.org/10.1076/ceyr.28.1.47.23487

Kohn, D.B., Chen, Y.Y., Spencer, M.J., 2023. Successes and challenges in clinical gene therapy. Gene Ther. 30, 738–746. https://doi.org/10.1038/s41434-023-00390-5

Kolb, H., Fernandez, E., Nelson, R. (Eds.), 1995. Webvision: The Organization of the Retina and Visual System. University of Utah Health Sciences Center, Salt Lake City (UT).

Lee, K.Y., Mooney, D.J., 2001. Hydrogels for Tissue Engineering 12.

Li, Y., Mitchell, W., Elze, T., Zebardast, N., 2021. Association Between Diabetes, Diabetic Retinopathy, and Glaucoma. Curr. Diab. Rep. 21, 38. https://doi.org/10.1007/s11892-021-01404-5

López-Otín, C., Blasco, M.A., Partridge, L., Serrano, M., Kroemer, G., 2013. The Hallmarks of Aging. Cell 153, 1194–1217. https://doi.org/10.1016/j.cell.2013.05.039

Moreno-García, A., Kun, A., Calero, O., Medina, M., Calero, M., 2018. An Overview of the Role of Lipofuscin in Age-Related Neurodegeneration. Front. Neurosci. 12. https://doi.org/10.3389/fnins.2018.00464

Padhy, S.K., Takkar, B., Narayanan, R., Venkatesh, P., Jalali, S., 2020. Voretigene Neparvovec and Gene Therapy for Leber's Congenital Amaurosis: Review of Evidence to Date. Appl. Clin. Genet. 13, 179–208. https://doi.org/10.2147/TACG.S230720

Parihar, J.K.S., 2016. Glaucoma: The 'Black hole' of irreversible blindness. Med. J. Armed Forces India 72, 3–4. https://doi.org/10.1016/j.mjafi.2015.12.001

Stingl, Krunoslav, Kempf, M., Jung, R., Kortüm, F., Righetti, G., Reith, M., Dimopoulos, S., Ott, S., Kohl, S., Stingl, Katarina, 2023. Therapy with voretigene neparvovec. How do we measure success? Prog. Retin. Eye Res. 92, 101115. https://doi.org/10.1016/j.preteyeres.2022.101115

Teo, Z.L., Tham, Y.-C., Yu, M., Chee, M.L., Rim, T.H., Cheung, N., Bikbov, M.M., Wang, Y.X., Tang, Y., Lu, Y., Wong, I.Y., Ting, D.S.W., Tan, G.S.W., Jonas, J.B., Sabanayagam, C., Wong, T.Y., Cheng, C.-Y., 2021. Global Prevalence of Diabetic Retinopathy and Projection of Burden through 2045: Systematic Review and Meta-analysis. Ophthalmology 128, 1580–1591. https://doi.org/10.1016/j.ophtha.2021.04.027

Tilahun, M., Gobena, T., Dereje, D., Welde, M., Yideg, G., 2020. Prevalence of Diabetic Retinopathy and Its Associated Factors among Diabetic Patients at Debre Markos Referral Hospital, Northwest Ethiopia, 2019: Hospital-Based Cross-Sectional Study. Diabetes Metab. Syndr. Obes. 13, 2179–2187. https://doi.org/10.2147/DMSO.S260694

Vyawahare, H., Shinde, P., 2022. Age-Related Macular Degeneration: Epidemiology, Pathophysiology, Diagnosis, and Treatment. Cureus 14, e29583. https://doi.org/10.7759/cureus.29583

Wang, C., Pan, C., Yong, H., Wang, F., Bo, T., Zhao, Y., Ma, B., He, W., Li, M., 2023. Emerging non-viral vectors for gene delivery. J. Nanobiotechnology 21, 272. https://doi.org/10.1186/s12951-023-02044-5

Wang, J.-H., Gessler, D.J., Zhan, W., Gallagher, T.L., Gao, G., 2024. Adeno-associated virus as a delivery vector for gene therapy of human diseases. Signal Transduct. Target. Ther. 9, 78. https://doi.org/10.1038/s41392-024-01780-w

Wang, X., Yu, C., Tzekov, R.T., Zhu, Y., Li, W., 2020. The effect of human gene therapy for RPE65-associated Leber's congenital amaurosis on visual function: a systematic review and meta-analysis. Orphanet J. Rare Dis. 15, 49. https://doi.org/10.1186/s13023-020-1304-1

World Economic Forum, 2023. Global life expectancy is changing around the world [WWW Document]. World Econ. Forum. URL

https://www.weforum.org/stories/2023/02/charted-how-life-expectancy-is-changing-around-the-world/ (accessed 2.3.25).

Wu, K.Y., Kulbay, M., Toameh, D., Xu, A.Q., Kalevar, A., Tran, S.D., 2023. Retinitis Pigmentosa: Novel Therapeutic Targets and Drug Development. Pharmaceutics 15, 685. https://doi.org/10.3390/pharmaceutics15020685

CHAPTER TWO

Advances in Nucleic Acid Delivery Platforms Targeting Posterior Segment Eye Diseases

2. Introduction

2.1. Background on Posterior Segment Eye Diseases

The retina is considered an extension of the brain and central nervous system, responsible for transducing light to neurochemical signals and relating specific information to the brain (Joselevitch, 2008). Multiple layers of neurons, with unique morphologies and functions, interconnected by synapses make up the retina **(Figure 2.1)** (Mahabadi and Al Khalili, 2022). Within each layer, an incredible diversity of cells function in the visual pathway. Degeneration of these neuronal cells due to genetic disposition, viral/bacterial infection, old age, and variable lifestyle choices is implicated in posterior segment eye diseases (PSEDs) which result in visual impairment and blindness. PSEDs are diseases affecting the retina, choroid and optic nerve, these primarily include glaucoma, retinitis pigmentosa, age-related macular degeneration (AMD) and diabetic retinopathy (DR), amongst others (**Figure 2.2**) (Bastawrous et al., 2014; World Health Organization, 2019).

The multifactorial and early-stage asymptomatic nature of PSEDs contributes to failure in early detection, challenges in developing effective therapies, and difficulties in elucidating their exact mechanism of pathogenesis. Common features of PSEDs include an increased production of angiotensin II, generation of reactive oxygen species (ROS) and pro-inflammatory factors such as vascular endothelial growth factor (VEGF) and prostaglandins. These factors often elicit the destruction of the blood-retina barrier, cause retinal ischemia, neovascularisation, haemorrhage, microaneurysms and retinal pigment epithelium-photoreceptor atrophy (Anderson et al., 2002; Beltramo and Porta, 2013; Das, 2016; Lin et al., 2020) (Figure 2.2). The multifactorial retinal diseases mentioned before result in similar clinical manifestations; therefore, treatments focusing on overlapping affected biological pathways such as reducing inflammation, controlling VEGF expression and restoring the blood-retinal barrier) has led to significant advances in treating PSEDs (Howell et al., 2011). The advent of anti-vascular endothelial growth factor agents; Ranibizumab 0.3 mg (Lucentis®; Genentech, Inc., South San Francisco, CA), Aflibercept 2.0 mg (Eylea®; Regeneron Pharmaceuticals, Inc., Tarrytown, NY, and the off label and the relatively inexpensive, Bevacizumab 1.25 mg (Avastin®; Genentech, Inc., South San Francisco, CA) (Al-Hussainy et al., 2008; Flockerzi et al., 2017; Ghanchi et al., 2022) (Table 1) has revolutionised the treatment of AMD, DMO and DR. Although the outlined anti-VEGF agents differ in structure, molecular weight, pharmacodynamics and pharmacokinetics, they have all

demonstrated significant ability to arrest disease progression and reduce the risk of vision loss (Boyer et al., 2013; van Asten et al., 2018). Additionally, the FDA's approval of the bispecific antibody Vabysmo™ (Roche, Basel, Switzerland), targeting angiogenesis and vascular permeability, has increased the arsenal for treating PSEDs (Ghanchi et al., 2022). Prior to the FDA's approval of the aforementioned therapies, the gold standard of care for wet AMD and DMO was laser photocoagulation, which requires the use of a laser to cauterise aberrant 'leaky blood vessels' (Al-Hussainy et al., 2008). However, this process can cause fibrosis and possible retinal detachment, and if not performed properly, it might also result in irreversible vision loss.

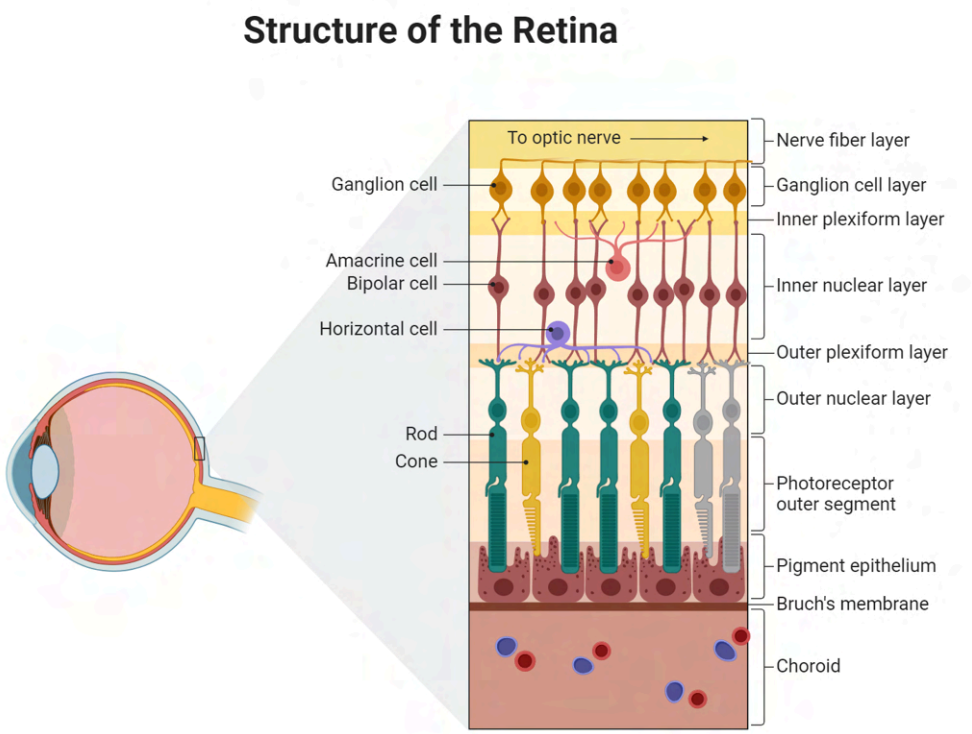

Figure 2.1: Schematic representation of healthy retina, choroid, and retinal pigment epithelium (RPE) cells (Adapted from: (Ren and Léveillard, 2022).

Whilst the PSEDs noted above are multifactorial in nature, inherited retinitis pigmentosa (RP) has a purely genetic basis. However, both contribute to the progressive degeneration of retinal tissue with a divergent aetiology and onset. RP is a group of mainly hereditary retinal degenerative diseases with varied inheritance patterns (e.g., autosomal recessive, autosomal dominant and X-linked forms) and mutations in at least 50 separate complementary genes reported to encode rod-related molecules (Murakami et al., 2015; Wang et al., 2019). RP is characterised by progressive vision loss due to abnormalities in photoreceptors (mainly rods) and RPE because of rod degeneration, which is subsequently accompanied by microenvironmental changes, such as nutrient deprivation, inflammation, oxidation, and loss

of trophic factors (Murakami et al., 2015). This drives cone cell death ('necrosis'), and thus loss of cone-mediated vision which is the most debilitating aspect of RP. Currently, there are only two FDA-approved therapies for RP, (i) the epiretinal implant, Argus II device, which provides artificial vision (Ghodasra et al., 2016) and (ii) the Adeno Associated serotype 2 viral vector (AAV-2) based gene therapy, Luxturna® (voretigene neparvovec-rzyl), which is only viable for patients with a genetic mutation in the *rpe65* gene coding for RPE65 protein (found in RPE cells) essential in the visual cycle (Ciulla et al., 2020; Dhurandhar et al., 2021).

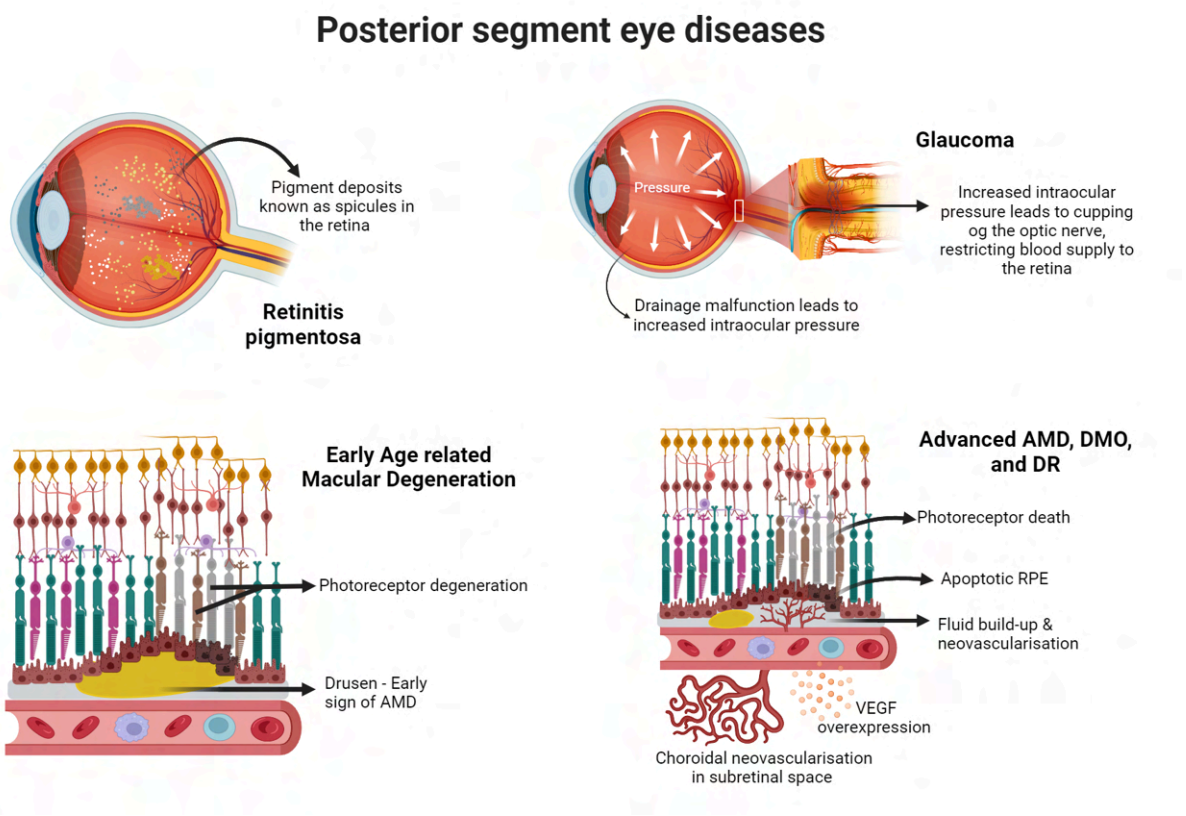

Figure 2.2: Schematic representation of PSEDs, namely Retinitis pigmentosa, Glaucoma, Early Age-related Macular degeneration and Diabetic retinopathy, Diabetic macular oedema and advanced age-related AMD and associated pathologies.

Table 2.1: Drug classes and therapies for posterior segment diseases currently approved by the FDA or used off-label

Drugs and Classes	Disease Target	Site of administration	Mechanism of Action	Reference
Class: Anti-angiogenic (tyrosine kinase inhibitors) **Drugs:** Ranibizumab, Bevacizumab and Brolucizumab (All FDA Approved)	AMD, DMO, Branch Retinal Venous Occlusion (BRVO), Central Retinal Venous Occlusion (CRVO), myopic CNV	Administered via intravitreal injection into the vitreous cavity once per month for the first three months, then once every 2 to 3 months	Humanised monoclonal antibodies that bind and inhibit vascular endothelial growth factor A (VEGF-A). Through binding to VEGF-A, the therapies interrupt the interaction of VEGF with its receptors, preventing the subsequent growth of new blood vessels.	(Ghanchi et al., 2022)
Class: Anti-angiogenic (tyrosine kinase inhibitors) **Drug:** Aflibercept (FDA Approved)	AMD, DMO, BRVO, CRVO, myopic CNV	Administered by intravitreal injection every month for the first 3 months, followed by intravitreal injection once every 2 months.	Aflibercept is a decoy receptor that binds VEGF-A, VEGF-B and placental growth factor (PIGF). This results in reduced VEGF and PIGF activity, reducing the growth of subsequent growth of new blood vessels	(Ghanchi et al., 2022)
Class: Complement factor inhibitors **Drugs:** ● POT-4/AL78898A – Peptide (Clinical Trials) ● Lampalizuma (Clinical Trial) – Fab fragment of humanised IgG murine anti-factor D antibody	Neovascular AMD Geographic Atrophy	Intravitreal administration Intravenous administration	POT-4/AL78898A targets C3 Lampalizuma targets Factor D	(Park et al., 2019)

● Eculizumab (Clinical Trials) – Humanized monoclonal antibody	Geographic Atrophy		Eculizumab – Humanized monoclonal antibody from murine anti-human C5 antibody m5G1	
Class: Corticosteroids **Drugs:** ● Dexamethasone implant (IDI) (Ozurdex; Allergan Inc, Irvine, CA) ● Fluocinolone acetonide implant (ILUVIEN®) ● Triamcinolone acetonide	DMO, DR and AMD	Dex: Intravitreal implant with up to 6 months of sustained drug release Fluo: Implanted into the vitreous cavity with a sustained release of 36 months Tria: Intravitreal injection	Dex: Bind to steroid receptors, altering gene expression by promoting anti-inflammatory genes Fluo: Binding of fluocinolone to glucocorticoid receptor alters the expression of genes mediating the synthesis of inflammatory mediators Tria: Has anti-inflammatory, anti-permeability, and anti-angiogenic properties, which help maintain the BRB & facilitate the reabsorption of exudates.	(Karti and Saatci, 2018) (Sarao et al., 2014) (Flockerzi et al., 2017)

2.2. Challenges and Limitations of Current Therapies

The alleviation of the pathophysiological symptoms associated with PSEDs has been of great focus, as such, there is a library of reviews that have thoroughly outlined and discussed FDA approved therapeutics and those still under clinical investigation (Ammar et al., 2020; Ghanchi et al., 2022; Singh et al., 2019; Wang et al., 2019). Although existing therapies show some efficacy, they are fraught with challenges and are linked to a comparatively high treatment burden (Sivaprasad and Oyetunde, 2016). For instance, FDA approved anti-VEGF therapies (Ranibizumab and Aflibercept) require multiple intravitreal injections, this can lead to ocular complications such as raised intraocular pressure, cataracts, transient blurry vision, retinal detachment, endophthalmitis and intravitreal hemorrhages (Giannaccini et al., 2014). An alternative, safer approach to intraocular injections for ocular diseases involves the use of eye drops and ointments. Generally, topical administration of drugs is often preferred over surgeries as it is the most convenient, safer, and patient compliant route of delivery. However, the associated drugs fail to reach the posterior segment of the eye in adequate concentration, as only ~5% of medicines applied topically diffuse through the anterior chamber, limiting their therapeutic efficacy (Jumelle et al., 2020). Moreover, the corneal epithelium, sclera, choroid, Bruch's membrane and retinal pigmented epithelium amongst others (see Figure 1), act as barriers to drug transport therefore resulting in low drug bioavailability in the posterior segment of the eye (Rodrigues et al., 2018). Additionally, the complex anatomy and physiology of the eye and the presence of the blood retinal barrier (BRB) are the main limiting factors for efficient drug delivery as they result in poor tissue specificity, short drug retention time and poor absorption of some drugs due to the presence of tight junctions and efflux transporters. Alternatively, the BRB is responsible for conferring the eye's immune privilege making it an ideal environment for direct therapy delivery. Therefore, achieving ideal drug bioavailability requires posterior administration (i.e. subretinal, suprachoroidal, subconjunctival and intravitreal injection), however this can have significant drawbacks as current therapies tend to require multiple intraocular injections.

Notably, standard-of-care therapies fail to treat retinal degeneration resulting from genetic mutations and, importantly, reverse the degeneration of retinal cells. Therefore, broadly effective treatments, like gene therapies, are crucial for treating vision loss regardless of specific genetic mutations or underlying pathologies. To improve ophthalmic drug bioavailability and overcome the drawbacks of conventional therapies, novel drug delivery systems (NDDS) coupled with gene therapy have been developed. NDDSs are capable of improving 'drug' bioavailability, avoiding off-target effects, achieving sustained and controlled therapeutic release, and reducing the frequency of injections required. Preferred NDDSs have prolific features such as non-immunogenicity, good histocompatibility, biocompatibility and increased patient compliance (Yadav et al., 2019). The coupling of NDDSs with gene

therapy has the capacity to treat genetic diseases, overcome drug tolerance or resistance inherent in traditional small drug molecules and eliminate the need for continuous therapeutic administration thus overcoming efficacy challenges (Gurevich and Gurevich, 2015; Heyde et al., 2010). The adaptation of gene therapy has the potential to offer longer-lasting transformational clinical benefit as it can circumvent limitations associated with conventional therapies. To this end, the use of gene therapy in combination with NDDSs has garnered much attention as a novel approach to overcoming limitations associated with current PSED therapies. Gene therapy has the unique ability to achieve durable and potentially curative clinical benefit through a single dose, as it affords sustained production of therapeutic proteins endogenously and obviates the need for lifelong therapeutic administration (Dunbar et al., 2018). Therefore, this review aims to highlight key developments in gene therapy involving the engineering and application of novel drug delivery systems for the treatment of PSEDs. It discusses viral and non-viral gene delivery systems in detail, focusing on non-viral systems. The review also thoroughly analyses current progress in the research of gene-based therapies and their application in treating and managing key posterior segment eye diseases.

2.3. Gene therapy: A Brief Synopsis

Gene therapy has become a growing subject of interest as it provides an opportunity to develop a ‘one-time treatment option’ adept in permanently correcting genetic errors and treating incurable diseases. Additionally, the opportunity to manipulate the human genome through localised genetic modifications affords researchers an opportunity to focus on gene therapy as an exciting avenue for the treatment of a variety of diseases (Massadeh and Al Aamery, 2016). Therefore, multiple gene therapy approaches are currently being investigated as possible alternatives to traditional therapies. There are four major modalities to gene therapy: (i) Gene replacement (delivery of a functional gene copy to a specific target cell or tissue to restore the function of a specific set of genes and change the expression make-up of the cells), (ii) gene silencing (regulation of gene expression by preventing a specific gene from being expressed), (iii) gene addition (gene overexpression, addition of an additional - copy of a gene to promote expression of a specific protein) and (iv) gene editing (involves the addition, deletion or change of a gene using a tool such as CRISPR/Cas9) (Bulcha et al., 2021a). These gene-based therapeutic techniques can be applied *in vivo* or *ex vivo*. *Ex vivo* gene therapy involves removing affected target cells and genetically engineering them to correct the disease phenotype, followed by subsequent re-introduction to patients. *In vivo* application involves the simple administration of a gene therapy through specific delivery routes (e.g., intravenous) **(Figure 2.3)**.

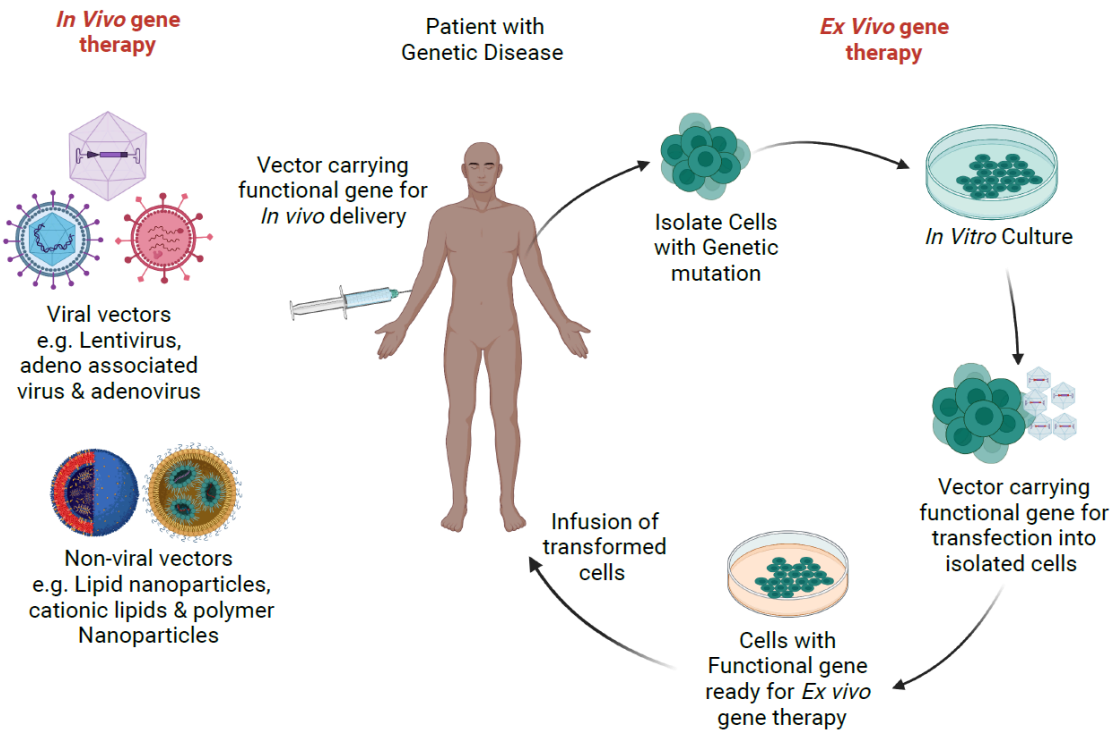

Figure 2.3: Summary of gene therapy delivery modalities. In vivo gene therapy involves the administration of genetic material encapsulated within a delivery vector directly into the patient. Ex vivo gene therapy consists of traction of cells from a patient or an allogenic source, the extracted cells are genetically modified using a vector containing a therapeutic transgene. This is followed by the selection and expansion of the modified cells in culture, and infusion to reintroduce them into the patient. (Image adapted from (Bulcha et al., 2021a).

2.3.1. Overview of Gene delivery essentials

Noteworthy, simply delivering genetic material (gene therapy) using either the *in vivo* or the *ex vivo* technique is insufficient, thus requiring a more nuanced approach. As such, gene therapy remains an elusive area of research, as it requires the design of vectors capable of protecting genetic cargo from nucleases, carrying large genetic material, achieving efficient and targeted gene release, being non-immunogenic, achieving endosomal escape and ease of mass purification and production (Gonçalves and Paiva, 2017). Notably, gene therapy design must also promote nuclear translocation where gene expression is required (Figure 2.4). For this purpose, the development of vectors possessing the aforementioned characteristics is essential. Thus, two classes of gene delivery methods exist, namely, viral and non-viral gene delivery vectors. Both methods are used to deliver genetic material, however each one has limitations. This review aims to highlight the key developments in gene delivery vectors (viral and non-viral). A thorough analysis of the design and construction

of non-viral gene delivery systems is conducted, along with their application in the treatment and management of key PSEDs.

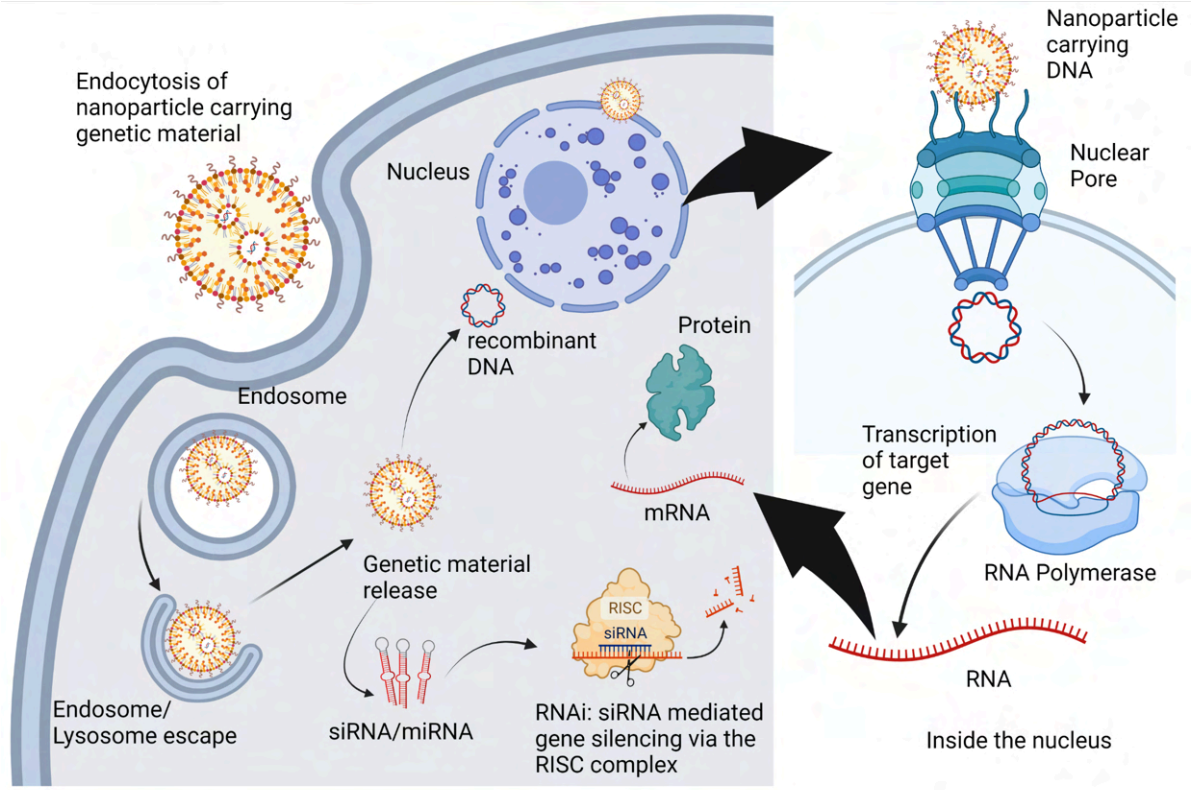

Figure 2.4: Representation of non-viral gene therapy mediated by cellular internalization via endocytosis. The cytosol is the destination for RNA payload whilst the cell nucleus is the target for DNA delivery mediated by the nuclear pore.

2.4. Overview on viral vector-based gene delivery

Viruses have been shown to provide extensive mutual benefit to humans, whether through their role in immunity against bacterial pathogens, destruction of tumour cells or their role in modulating our gut microbiome, they have a significant role in our survival (Goswami et al., 2019). The inherent nature of viruses as genetic engineers allows us to manipulate their key properties for gene delivery. Essential viral properties often considered by researchers for gene delivery include their ability to carry genetic cargo, transduction efficiency of target cells accompanied by stable gene expression, epichromosomal or genome integration (only certain viruses have this ability), viral propagation, targeted delivery, and modification of viral genome (Wang et al., 2024).

Through exploiting these features, viruses can be used as gene therapy vectors capable of efficiently modifying gene expression in a programmable manner, providing an opportunity to treat a variety of diseases and effectively immunise against severe disease.

Exploitation of viruses for use in gene therapy is possible through their modification, i.e., replacement of the viral genome with a therapeutic gene cassette, therefore inhibiting their inherent replication and pathogenic nature (Shirley et al., 2020). Characteristics such as vector tropism, mode of vector transfer, cargo space, the need for genome integration and immunotoxicity determine the nature of the viral vector chosen for a particular application (Shirley et al., 2020). A significant amount of gene therapies under development, clinical trials and approved by the FDA make use of one of the following viral vectors; retroviruses (lentiviruses), Adenoviruses (Ads) or Adeno Associated Viruses (AAVs) (Bulcha et al., 2021b). Adenovirus-based vectors are mainly being applied for vaccines (COVID-19 and Ebola vaccines) and cancer therapy development as they effectively activate CD8+ T cells (Bulcha et al., 2021b; Xie et al., 2023), whilst the most commonly used viruses for gene delivery are AAVs (typically used for in vivo gene therapy, as are adenoviruses) and lentiviruses (popular in ex vivo gene therapies) (Bulcha et al., 2021b). AAV vectors have emerged as the vector of choice in most *in vivo* applications as extensive advancements have been made in developing their recombinant counterparts which are replication incompetent, have incorporate an external cassette housing transgene of interest along with accompanying regulatory elements and inverted terminal repeats essential for vector production and stable episomal DNA (Byrne et al., 2025). Additionally, recombinant AAVs have wide tropism, broad tissue transduction capability and considerable safety profile in comparison to other viral vectors (Pupo et al., 2022). Likewise, lentiviruses, particularly third generation self-inactivating lentiviral vectors have also garnered interest for application in neovascualr AMD targeting gene therapy (Iqball et al., 2023). They are commonly used for correcting genetic mutations by introducing therapeutic genes to diseased cells. Their unique ability to translocate across the nuclear pore, integrate into the genome of cells and transduce non dividing cells offers them a key advantage in gene therapy (Milone and O'Doherty, 2018).

2.4.1. Viral vector-based gene therapies targeting PSEDs

Lentiviral vectors have been utilised in multiple studies and clinical trials, one that stands out involves the use of a non integrating equine infectious anemia virus-derived lentiviral vector to deliver angiostatin and endostatin expressing genes via subretinal administration (RetinoStat®) (Lauer et al., 2016). RetinoStat® is designed to treat neovascular AMD through the sustained expression of the anti-angiogenic factors, angiostatin and endostatin, thereby controlling the formation of aberrant blood vessels in patients with AMD. Preclinical studies using New Zealand White rabbits and rhesus macaques demonstrated transient inflammation which resolved one month after intervention and sustained expression of the therapeutic proteins for six months (Table 2) (Binley et al., 2012; Widdowson et al., 2010). Recently, a Phase I clinical trial study has shown significant safety and tolerability in patients, along with long term expression of the anti-angiogenesis factors (Lauer et al., 2016). Other lentiviral-based ocular gene therapies include BD311, an integrase-deficient lentiviral vector for the delivery of the VEGF-A gene (Early Phase I Clinical Trials) (Shanghai BDgene Co., Ltd., 2022) and OXB-203, developed for the delivery of an aflibercept encoding gene using lentiviral vectors derived from HIV and EIAV (Iqball et al., 2023).

The first and only ocular FDA approved gene replacement therapy is Voretigene neparvovec-rzyl (Luxturna™; Spark Therapeutics, Inc.), used for the treatment of a severe form of Leber congenital amaurosis type 2 (LCA2) (Russell et al., 2017) (Table 2). LCA is a severe inherited retinal dystrophy that causes blindness in childhood. Biallelic mutations in the gene rpe65, coding for RPE65 protein (found in RPE cells) essential in the visual cycle and normal vision, occur and thus impact an individual's visual acuity (Dhurandhar et al., 2021). Luxturna uses an AAV serotype 2 (AAV2) vector to deliver a functional copy of the rpe65 gene to quiescent RPE cells and utilises the host's gene expression machinery to make functional RPE protein, therefore rescuing the mutated phenotype. Although Luxturna improves vision and retinal sensitivity, subsequent studies have shown that this is not sustained, as photoreceptors steadily degenerate, matching those of untreated patients (Fu et al., 2018; Wang et al., 2020). Wang et al., (2020) suggest that the short-term visual function rescue can be attributed to the fact that the gene therapy only addresses the biochemical chromophore deficiency in LCA2 patients without dealing with the progressive degeneration of photoreceptors. Additionally, Luxturna requires the presence of viable photoreceptors, therefore, the development of therapies capable of treating advanced retinal degeneration (absence of photoreceptors) and which are not limited to specific genetic mutations is important.

2.4.2. Novel approaches to ocular gene therapy: Optogenetic therapy and RPE regeneration

There are scenarios where genetic defects are secondary to photoreceptor damage, therefore, better results can be achieved through focusing on unconventional forms of gene therapy such as optogenetic strategies to restore vision, particularly in instances where conventional gene therapy fails. Optogenetics is mainly utilised in advanced disease, whereby the lack of photoreceptors limits therapeutic efficacy (Dhurandhar et al., 2021). Interestingly, the versatility of this approach, unlike most therapeutic interventions, allows for universal effectiveness in treating retinal insults, regardless of the genetic origin of a disease (McClements et al., 2020). Viral vectors can be used to deliver light sensitive opsins (melanopsin and rhodopsin) to functioning inner retinal cells (bipolar/ ganglion cells) thus converting them to light sensitive cells. An example is the landmark study conducted by Bi et al. (2006), in which a gene encoding the Chlamydomona reinhardtii light-sensitive protein, channelrhodopsin (ChR2), was delivered to the surviving inner retinal neurons of mice using an AAV vector. ChR2 is a light-activated cation channel that induces neuronal action potentials and depolarisation (Britt et al., 2012). The ectopic expression of the ChR2 under the CMV/beta-actin promoter converted these cells to photosensitive cells, therefore, imparting light sensitivity to degenerate retinas (Bi et al., 2006). Key challenges highlighted by the study include the possible immunogenicity of using non-human opsonin genetic material, the need to optimize transgene expression, signal amplification by the photopigment, detection of non-toxic light levels for the stimulation of ChR2 sensor or even increased risk of producing phototoxic effects particularly in larger animal models (McClements et al., 2020).

Subsequent studies became cognizant of these limitations, with multiple optogenetic proteins and light-activated photoswitches developed resulting in the advent of multiple clinical trial studies (NCT02556736, NCT03326336, NCT04945772, and NCT04278131) (AbbVie, 2024; Bionic Sight LLC, 2023; GenSight Biologics, 2022; Nanoscope Therapeutics Inc., 2024). A fascinating optogenetic approach for vision restoration is outlined in the NCT04278131 (BS01) clinical trial. The assessment of BS01 therapy, which utilises AAV2 to deliver the optogenetic gene, Chronos, to retinal ganglion cells. Multiple animal models (mice, rats and non human primates) were used to assess the safety profile and preclinical efficacy of the therapy (Bionic Sight LLC, 2023; Yan et al., 2023). Phase 1/2 Clinical trial data showed tolerance of a broad range of treatment doses, restored light perception and detection of motion (Bionic Sight LLC, 2023). Similarly, Multi characteristic opsin (MCO) AAV2 based therapy (Dibas et al., 2024) and AAV2_G-protein coupled receptor (GPCR) opsins chimeras (Kralik et al., 2022) studies have shown significant improvements in visual acuity when targeting ON bipolar cells. Significantly, the use of chimera based gene therapies, namely,

the bipolar cell targeting GPCR opsin AAV2.7m8 vector based therapy have the potential to preserve the natural retinal circuitry thus restoring vision and visual behavior. Kralik et al., (2022) investigated multiple GPCR opsin chimeras and showed their ability to achieve stable expression in HEK293_GIRK cells using the fluorescent protein mKate2, which aids in membrane localisation as GPCR opsins are expected to localise in the membrane (Figure 5a). Additionally, cells expressing melanopsin and OPN1MW based chimeras showed significant currents (Figure 5b,c). Importantly bleach stability (important role in vision restoration) was observed for Mela(CTmGluR6) expressing cells, particularly when orange backlight (595 nm; 5×1015 photons/cm2/s) was used (Figure 5f,g). This is because melanopsin is known to be robustly light-sensitive and capable of responding to sustained or repetitive light without rapid desensitisation. Additionally, The orange light allows sustained activation without overwhelming the system, maintaining consistent response amplitudes. Substantially, the intravitreal administration of the AAV2.7m8 vector_GPCR_opsin constructs under the control of the hGRM6 promoter in blind rd1 mice resulted in vision restoration across all interventions, notably, Mela(CTmGluR6) (0.37 ± 07 cyc/deg, $n = 16$) significantly outperformed all variants (Figure 5i). Visual acuity and contrast sensitivity thresholds were not significantly different to that seen in wild type C57BL/6 mice (Figure 5j). Therefore, these findings suggest that a bipolar targeting GPCR opsins chimera gene therapy approach holds promise for treating individuals with advanced retinal degenerative diseases.

These therapies show immense promise in treating AMD by addressing resulting abnormalities. However, transient gene expression and their inability to reverse the damage to the RPE layer which is essential in maintaining photoreceptor health remain key limiting factors. Strategies for replacing diseased RPE have been undertaken, regrettably, none have proven effective and safe enough to apply as a standard of treatment (Zhou et al., 2024). Therefore, adopting in situ RPE regeneration by harnessing its inherent proliferative capacity can significantly enhance therapeutic outcomes and provide complementary mechanisms to restore tissue damage. Normally, RPE cells are arrested in the G1 phase of the cell cycle (quiescent, non proliferating), delivery of the E2F2 transcription factor can induce cells to bypass G1 arrest, thereby inducing regeneration by mitosis (Kampik et al., 2017). Kampik and colleagues used VSV-G lentiviral vector to subretinally deliver E2F2 in an RPE-deficient mouse model (RPECreER/DTA) (Longbottom et al., 2009). E2F2 expression resulted in a 34% increase in central RPE cell density without disruption of the RPE monolayer. This study served as a proof of concept for in situ RPE regeneration which can serve as a strategy aimed at preserving and restoring RPE integrity and in turn protection of photoreceptors.

2.4.3. Limitations

While viral vector based gene therapy has had some noteworthy success and holds hope for the future, it still has drawbacks. Despite the success of Luxturna, independent studies have reported local and systemic immune responses and ocular inflammation (gene therapy-associated uveitis) following therapeutic delivery, negating the immune privilege of the eye (Bucher et al., 2021). Moreover, progressive reduction in AAV mediated gene therapy efficacy has been reported, this is due to possible targeting of the transgene product by the cellular and humoral immune responses or deactivation of the gene by episomal silencing and or most likely, activation of the immune system against the transduced cells in response to “viral infection of cells” which can damage the retina and other ocular tissues, thus compromising any required repeat injections of the therapy (Bucher et al., 2021; Shen et al., 2020). Importantly, the formation of neutralizing antibodies (NABs) against AVV vectors has been widely reported in other routes of *in vivo* administration. NABs have been associated with reduced gene transfer, prevention of therapeutic re-administration and alterations in vector biodistribution (Shirley et al., 2020). Ongoing research into these challenges is yielding technological breakthroughs that have the potential to surpass current medicines and realise the potential of viral vectors.

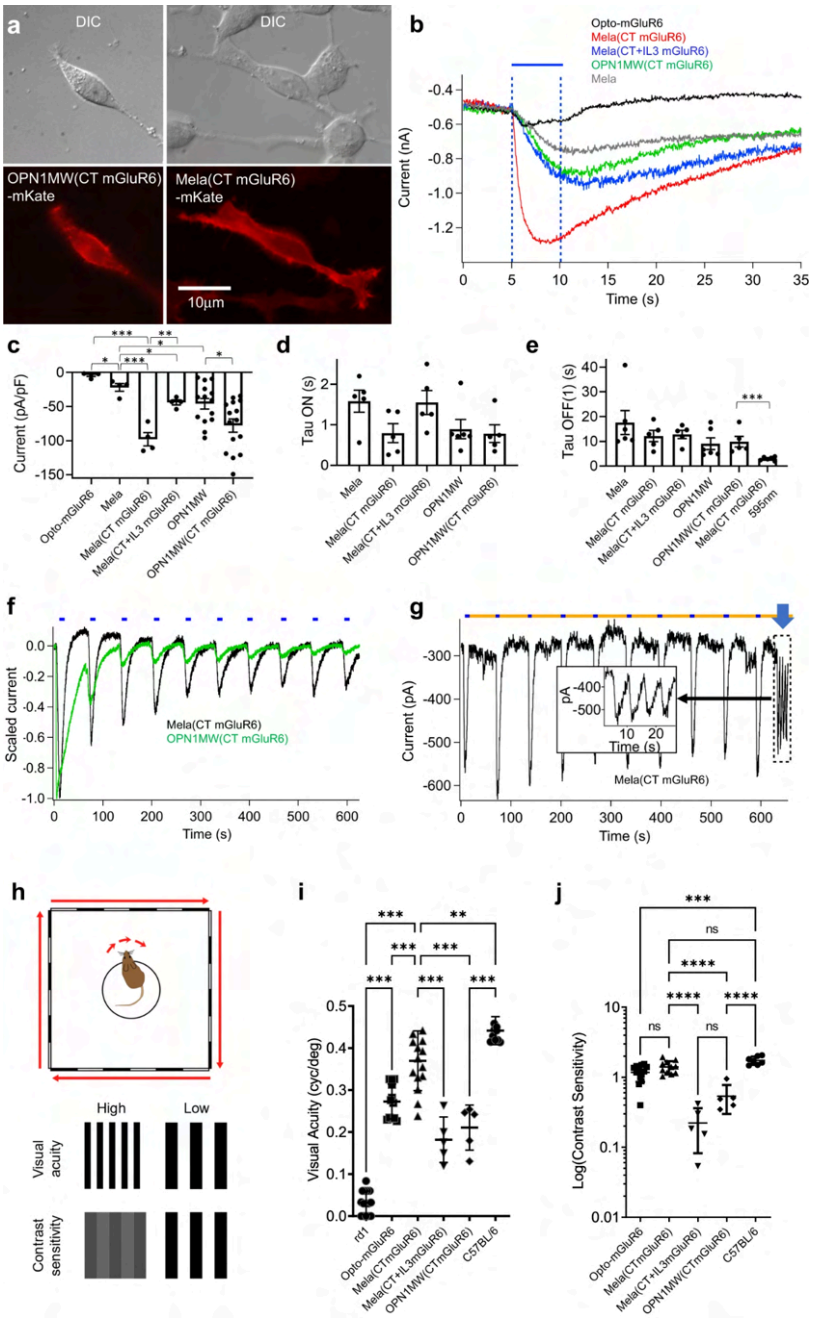

Figure 2.5: a) HEK293-GIRK cells transiently transfected with different Opsin-mKate fusion proteins show robust membrane expression (exemplified for OPN1MW(CT mGluR6)-mKate and Mela(CTmGluR6)-mKate). **b–h)** To assess the relative efficacies at which opsin constructs activate G-proteins in the Gαi/o class, we screened all opsin constructs in HEK293-GIRK cells. **h–j)** *In vivo* screening of treated blind (>24 weeks) rd1 mice in a naïve optomoter reflex task.

Table 2.2: viral vector-based gene therapies for posterior segment diseases

Gene therapy and delivery system (FDA approved and Under Clinical trial)	Disease Target	Site of administration	Mechanism of Action	Reference
RetinoStat® Phase I Clinical Trial	Age-related macular degeneration (AMD) and diabetic retinopathy (DR)	Subretinal administration	Uses a recombinant equine infectious anaemia virus to deliver genes encoding angiostatin and endostatin	(Lauer et al., 2016)
RGX-314: Anti-VEGF_AAV8 (RegenXbio® Inc.) Phase II Clinical Trial	Wet AMD, DR and other chronic retinal diseases	RGX-314 is designed to be a one time therapy administered subretinally. Recent clinical trials tested suprachoroidal administration as well.	AAV8 vector carrying a gene encoding the Anti-VEGF monoclonal antibody fragment is administered subretinally patients with ocular neovascularization. In vivo expression of the Anti-VEGF antibody blocks the expression of VEGF, controlling the angiogenesis.	(Bordet and Behar-Cohen, 2019; Regenxbio Inc., 2022)
HMR59: CD59_AAV2 (Janssen Pharmaceuticals Inc) Phase II Clinical Trial	Late-stage Severe AMD (Geographic atrophy; GA)	Administered as a one-time Intravitreal injection	HMR59 utilises the AAV2 vector to deliver a functional copy of the CD59 gene enabling the retina to express sufficient levels of the protein and thus regulate the complement pathway and preserve vision.	(Puliafito and Wykoff, 2019)

GT005: CF-I_AAV2 (Gyroscope Therapeutics Ltd, NCT03846193) - Phase I/II Clinical Trial	Late-stage Severe AMD (Geographic atrophy; GA)	Administered as a one-time investigational subretinal injection	CFI gene is delivered subretinally using AAV2 vector to patients with GA. Functional CFI gene promotes proper modulation of the complement pathway	(Gyroscope Therapeutics Limited, 2022)
ADVM-022: AAV.7m8-aflibercept (Eylea, Regeneron Pharmaceuticals) - Phase I/II Clinical Trial	Neovascular (Wet) Age-related Macular Degeneration and Diabetic Macular Oedema	Administered intravitreally as a one-time treatment	ADVM-022 is aimed at providing expression of aflibercept at levels affording protection from neovascularization for the lifetime of the patient following a single IVT dosing.	(Gelfman et al., 2021; Grishanin et al., 2019)
EDIT-101: Cas9a_gRNAs_AAV5 (Editas Medicine Inc.) Phase I/II Clinical Trial	Leber's congenital amaurosis type 10	Onetime subretinal delivery (Targeting photoreceptors)	EDIT-101 is designed to correct a point mutation in the CEP290 gene, the IVS26 mutation, that leads to incorrect splicing of the CPE290 transcript and a dysfunctional CEP290 protein.	(Editas Medicine Inc, 2022; Maeder et al., 2019)

2.5. Non-viral vector nucleic acid-based therapy background

The rapid progress made in the search for ideal gene delivery vectors seems promising; however, reports on adverse events in some patients who have received viral vector-based gene therapy have been reported. Thus pointing out the existing challenges restricting the wide adaptation and applicability of viral vectors. Continued advancements in the field of material science and polymer nanocomposite engineering have vastly contributed to our understanding of nanoscale materials. The insights gained from this have been translocated into the field of gene delivery, resulting in the development of nonviral vectors capable of overcoming limitations associated with viral delivery vehicles. To date, a variety of nanomaterials have been investigated for potential use as gene delivery vectors. These include organic nanomaterials i.e., lipid/polymer-based nanosystems and inorganic nanomaterials such as; graphene (carbon nanotubes), iron oxide and gold nanomaterials (Paul et al., 2014; Riley and Vermerris, 2017). The following have been noted as key benefits for the use of non-viral vector; potential to carry large genetic material, high chemical versatility allowing for surface modification which is beneficial for directed targeting, relative non-toxicity and negligible or non-immunogenicity (Chen et al., 2020). The low cost to commercialisation compared to viral vectors is also a key advantage in the use of non-viral vectors (Chen et al., 2020). Nevertheless, non-viral vectors are often characterised by transient gene expression and low transfection efficiency which may limit their overall effectiveness (Park et al., 2012). Currently, modifications to non-viral vectors exist, which can help in overcoming these limitations (Santana-Armas and Tros de Ilarduya, 2021).

Amongst various materials used in drug delivery, biodegradable polymers have been recognized as excellent candidates for the design and development of nanocarriers. The freedom to synthesize customisable polymers enables scientists to design nanocarriers with desired characteristics for varying applications. For efficient gene delivery, preference tends to be directed to the use of biocompatible ionizable cationic polymers and lipids (ideal pKa = 5 - 7) with facile chemistry (ease of synthesis and functionalization) and efficient entrapment of genetic material (Rai et al., 2019). The cationic nature of these polymers allows for efficient genetic material complexation via polymer-genetic material electrostatic interaction (Shmueli et al., 2010). The positive charge present on the nanosystem also facilitates endosomal escape and thus the release of the genetic material at the site of action via the proton sponge effect (Freeman et al., 2013). The proton sponge effect refers to the presence of weakly basic molecules buffering the pH of the endosome thus resulting in osmotic swelling, rupture of the endosomal membrane and release of encapsulated therapeutics (Madkhali et al., 2019). Multiple studies have reported on the benefits of using cationic polymers, particularly their role in improving encapsulation and delivery of genetic material to certain tissues, however, cationic polymers also adversely trigger acute cell necrosis and

mitochondrial leakage which results in inflammation (Liu et al., 2018; Wei et al., 2015). In relation to ocular delivery, the positive charge on these nanocarriers restricts their movement across the vitreous of the eye due to the presence of negatively charged glycosaminoglycans (mainly hyaluronic acid) that fill the spaces within the collagen fibres (Mains and Wilson, 2013). This superficial anionic charge of the vitreous humor retards the diffusion of cationic particles across the vitreous to the retina, thereby limiting therapeutic bioavailability (Varela-Fernández et al., 2020). Conversely, the vitreous humor, even in the liquified state, remains non-restrictive to anionic and neutral nanocarriers and molecules (del Amo et al., 2017). Therefore, coating of cationic nanoparticles with anionic or neutral groups may improve delivery and reduce toxicity (Fröhlich, 2012).

Other properties with significant effect on the design of effective nanocarriers involve the polymer's molecular weight, composition, and solubility. Since both natural and synthetic polymers encompass some of these properties, they have been used in the construction of gene delivery nanoparticles. Natural polymers such as polysaccharides and proteins are fast becoming key materials in nanocarrier development as they possess mucoadhesive properties, good biocompatibility, cytocompatibility and reactive sites that can be exploited for ligand conjugation, modification and or crosslinking (Dang and Leong, 2006). This allows researchers to tailor the polymers for a wide range of applications (Dang and Leong, 2006). Natural polymers commonly used in gene delivery studies include hyaluronic acid, dextran, β-cyclodextrin, chitosan, gelatin and albumin (Zhang et al., 2018). In contrast to natural polymers, synthetic polymers have a controlled-uniform chemical structure, as a result, they do not exhibit the variation seen in the production of natural polymers. Their biologically inert nature makes them ideal materials, as they often don't elicit an immune response, and their active sites can be utilised to enhance their properties and interaction with target cells (Chen et al., 2020; Song et al., 2018). Common synthetic polymers used in gene therapy include; polyethylenimine (PEI), Poly(2-N-(dimethylaminoethyl) methacrylate) (PDMAEMA), and poly(L-lysine) (PLL) (Chen et al., 2020).

The first type of non-viral vectors to be investigated were synthetic cationic lipid-based nanoparticles (Felgner et al., 1987). These particles electrostatically interact with the negatively charged phosphate groups of the genetic material backbone, thus forming lipoplexes (nanoparticles). According to Felgner et al. (1987) the lipoplexes can protect the DNA from nuclease degradation, deliver the genetic material to the mammalian cells and drive gene expression. This research broadened the possibilities for designing non-viral gene therapy vectors using lipids and other materials. Since then, a wide array of nonviral vectors have been constructed using different nanomaterials. For the purpose of this review, the use of such nanomaterials in gene therapy delivery for PSEDs has been reviewed below.

2.5.1. A brief description of the gene delivery process

Gene therapy remains a challenging area of research due to the complexity of designing an optimal vector. An ideal vector must protect the genetic cargo from nucleases, accommodate large genetic material, ensure efficient and targeted gene release, evade immune detection, facilitate effective endosomal escape, and allow for scalable purification and production (Gonçalves and Paiva, 2017). Significantly, gene delivery vectors should have mechanisms that support nuclear translocation of genetic material where necessary, to facilitate gene expression (Figure 2.4). As mentioned previously, vectors are used to package genetic material and introduce it to host cells, the mechanism of vector internalisation adopted following the interaction of the vector with the cell membrane is generally endocytosis (Figure 2.4) and is dependent on the presence of adapted proteins, membrane lipids, and interaction with surface receptors. The endocytosis of vectors/nanoparticles occurs either via phagocytosis which is performed by specialized cells or through pinocytosis which is the uptake of fluids and dissolved molecules (Acharya et al., 2018). Following cellular uptake, the vectors must escape the acidic environment of the vesicle (compartments lysosome and endosome) via the proton-sponge mechanism or swelling and local mechanical disruption. Subsequently, the vectors become degraded thus releasing/unpacking the genetic material. Depending on the genetic material encapsulated, different pathways are activated (Figure 2.4). In the case of DNA based gene therapy, following endosomal escape, DNA is translocated into the nucleus via the nuclear pore for transcription,and eventual protein expression, alternatively, mRNA does not require nuclear translocation and therefore directly undergoes translation in the cytoplasm, facilitating expedient protein expression (Figure 2.4). Gene therapy based on RNAi, requires its incorporation into RNA-induced silencing complex (RISC) in the cytosol, where it interacts with Argouate 2 component, resulting in duplex unwinding and degradation of the target mRNA which results in the suppression of target protein expression (Figure 2.4).

2.5.2. The advent of non-viral based gene delivery systems: Polymer-based nanosystems

Considered one of the first non-viral vector gene delivery systems showing promise, polyethylene glycol (PEG) substituted 30-mer lysine peptide (CK30PEG) nanocarrier used in multiple gene delivery studies, ocular, brain and in the Phase I/II cystic fibrosis clinical trials has shown versatility and effectiveness (Suk et al., 2011). The CK30PEG nanocarriers has shown excellent transfection in both mitotic and quiescent cells, this is attributed to their relatively small size, stability in the presence of nucleases, interaction with the cell surface nucleolin and non-degradative delivery to the nucleus (Cai et al., 2009). These properties, along with its large genetic cargo (20 kilobase pairs) supported its adoption in the

investigation of the role of gene therapy in the rescue of heterozygous retinitis pigmentosa (rds+/-) murine. Cai et al., (2009) used a mouse model that is heterozygous for the retinal degeneration slow (rds) gene. Attenuated expression of the RDS protein resulted in a phenotype resembling pathological abnormalities seen in RP such as abnormal rod and cone development and their eventual degeneration (Travis et al., 1991). Cai et al., (2009), therefore subretinally administered CK30PEG nanoparticles carrying a functional copy of the rds/ normal mouse peripherin (NMP) gene, one under the control of the ubiquitously expressed chicken beta-actin promoter (CBA) and the second under the control of photoreceptor-specific promoter for the human interphotoreceptor retinoid-binding protein (IRBP). CK30PEG nanoparticles carrying rds/NMP gene under the control of CBA promoter sustained gene expression in photoreceptors for up to four months with no evidence of toxicity. Importantly, the intervention resulted in the improvement of rod function and the restoration of cone function with biochemical rescue of RP in the mouse model (Figure 2.5).

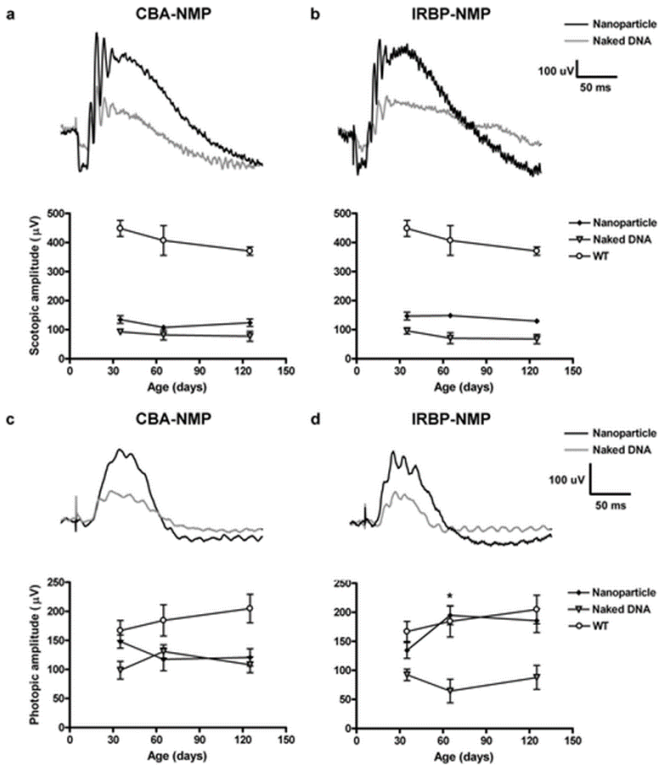

Figure 2.6: Delivery of the protein RDS/normal mouse peripherin (NMP) as facilitated by CK30PEG nanoparticles to photoreceptors leads to functional rescue of the rds heterozygous phenotype in mice. Cai et al (2009).

Promising results from previous studies using CK30PEG nanoparticles have prompted further investigation of their efficiency in packaging and delivery of larger genetic material. Unlike the currently approved RP gene therapy (Luxturna) which utilises an AAV vector with a limited genetic capacity of 5.7 kilobase pairs, CK30PEG nanoparticles can deliver genes of up to 15 kilobase pairs to the eye (Han et al., 2012). One distinctive study exploited the large capacity of CK30PEG nanoparticles in the delivery of the rhodopsin (rho) gene as well as its flanking non-coding sequences (promoter, introns, enhancers and scaffold/matrix attachment regions (S/MARs) etc.) to rho knockout mice with RP (Han et al., 2015). Delivery of the rho gene and flanking non-coding sequence using CK30PEG led to significant functional and structural improvements in rods and cones which were sustained for up to eight months post CK30PEG_rho genomic DNA delivery compared to CK30PEG_rho cDNA (rho gene only). This significant difference in therapeutic efficacy and gene expression level suggests the importance of including native expression elements (introns, promoters and other elements) to promote the efficiency of some gene therapies.

A notable mention in the advent of non-virus based gene delivery vectors is the cationic polymer, poly (β-amino esters) (PBAEs), which has proven beneficial for the delivery of therapeutics. PBAEs are synthesized via the copolymerisation of amine and diacrylate to form biodegradable positively charged co-polymers (Perni and Prokopovich, 2017). The positive charge on PBAE is conferred by secondary and tertiary amines which promote complexation with genetic material to form polyelectrolyte complexes or nanoplexes, and facilitate endosomal escape (Kim et al., 2016). To investigate the effectiveness of PBAEs for ocular gene delivery, a VEGF-cDNA complexed with PBAEs was suprachoroidally injected in wildtype rats. Two weeks post administration, expression levels of VEGF in the RPE and choroid were elevated (Shen et al., 2020). After 8 weeks of injection, overexpression of VEGF resulted in early-stage neovascularisation, which later progressed to subretinal fibrosis after 5 months causing AMD. VEGF expression was sustained for 8 months, this provided a new model for retinal neovascularisation studies. The therapeutic potential of PBAEs was explored by delivering a cDNA expressing anti-VEGF protein subretinally to rho/VEGF transgenic mice. Thirty five days post injection, retinal flat mounts demonstrated reduced subretinal neovascularisation, this was maintained for up to seventy days (Shen et al., 2020).

Careful selection of the route of administration for gene therapy delivery is essential. The delivery of therapeutics via the vitreous often results in vitreous retardation, aggregation and immobilisation of the therapy (particularly cationic constituents) and therefore insufficient titters reaching the retina, prompting the need for strategies to overcome these limitations (Peeters et al., 2005). This can be made possible through the design and development of coated nanoparticles, which have great mobility within the vitreous humor, efficiently interact with the target cell membrane and achieve successful cell uptake and transfection (Martens

et al., 2015). The presence of hyaluronic acid in the vitreous humor, retina and along with the dominant presence of CD44 receptors (to which hyaluronic acid is a ligand) on some retinal cells and RPE (Liu et al., 1997; Shinoe et al., 2010) has prompted researchers to consider hyaluronic acid as a possible polymer for efficient and targeted delivery of genetic material to the retina. Martens et al., (2015), developed cationic nanoparticles using the bioreducible polymer p(CBA-ABOL), which is a linear poly(amido amine) with repetitive disulfide linkages, prepared by Michael-type polyaddition, carrying a plasmid vector and coated them with hyaluronic acid. This conferred the nanocarriers with an anionic surface, did not affect encapsulation of GFP expressing plasmid DNA, and improved intravitreal mobility of the nanoparticles. Importantly, *in vitro* analysis of ARPE-19 cell transfection and GFP expression by the nanoparticles demonstrated promising results for CD44-HA mediated endocytosis (Martens et al., 2015).

Building on the advancements in gene delivery approaches discussed above, the focus now shifts to exploring gene delivery mechanisms specifically tailored for retinoblastoma treatment, offering a new frontier in ocular oncology. Retinoblastoma is the most common pediatric intraocular malignancy with an incidence of 1:15 000 to 20 000 live births and a 30% survival rate (Pandey, 2014). Retinoblastoma originates in the retina due to mutations in the RB transcriptional corepressor 1 (RB 1) gene which is a tumour suppressor gene. Polymer based nanoparticles such as the poly(ethylene glycol) grafted branched polyethyleneimine have been shown to efficiently transfect retinoblastoma Y79 cell lines and and promote gene expression of genetic cargo thereby prompting further investigation of polymer NPs for the treatment of retinoblastoma (Wang et al., 2022). A notable study employed a penetratin derivative, 89WP, functionalised nanosystem composed of polyamidoamine (PAMAM) dendrimer for the delivery of luciferase inhibiting siRNA labeled with 5-carboxyfluorescein (siRNA-FAM) (siRNA/PA/89WP) in orthotopic retinoblastoma mice. Briefly, delivery of siRNA/PA/89WP to WERI-Rb-1 luci cells (genetically modified to express luciferase) showed significantly higher fluorescence compared to the commercially available cationic liposomes, lipofectamine 2000 and sufficient safety profile and cellular internalisation using clathrin-mediated endocytosis (Gao et al., 2023). Importantly, significant *in vivo* retinal distribution of siRNA/PA/89WP was observed within two hours of installing the siRNA/PA/89WP system in the conjunctival sac of mice previously intravitreally inoculated with WERI-Rb-1 luci cells, showing the ocular permeability of the polyplex. However, fluorescence intensity decreased gradually to levels comparable with the naked siRNA group. siRNA/PA/89WP fluorescence intensity levels were 3x higher than those of naked siRNA and 1.5 times higher than those of lipofectamine_siRNA group. For gene silencing investigations, the interventions were delivered anteriorly using eye drops. Notably, rapid tumour growth was noted by significant increase in bioluminescence intensity in untreated and siRNA only treated groups, conversely siRNA/PA/89WP administration reduced

bioluminescence as a result of the inhibition of luciferase gene expression was noted (Figure 2.7). These results revealed that siRNA/PA/89WP could efficiently cross ocular barriers and deliver siRNA to tumour cells in the posterior segment of the eye.

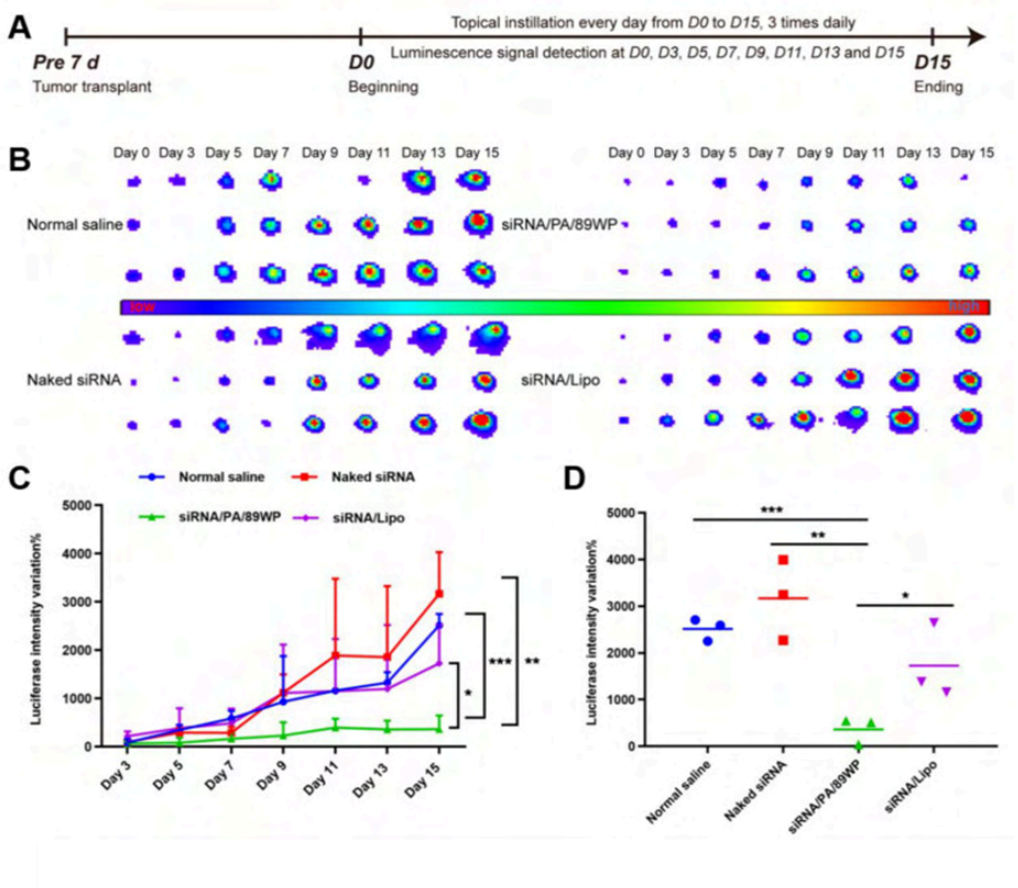

Figure 2.7: In vivo gene silencing efficacy. Eyes of nude mice were inoculated with WERI-Rb-1-luci cells, and the mice were divided into four groups, administered with normal saline, naked siRNA, siRNA/PA/89WP, and siRNA/Lipo, respectively. Each siRNA formulation contained 1.5 μg siRNA and was applied three times daily via topical installation. (A) Time schedule of tumour transplant, treatment, and evaluation of tumour-bearing mice. (B) Bioluminescence imaging of the eyes. (C) Semi-quantitative evaluation of changes in luciferase expression. (D) Comparison of changes in luciferase expression on day 15.

2.5.3. Lipid-based nucleic acid delivery systems

The versatility of Lipid-based nanosystems offers a plethora of benefits for nucleic acid delivery i.e.; amphiphilic nature, biocompatibility and the presence of cationic and helper lipid substitutes (Federica Ponti et al., 2021). To this end, lipid consideration in nanosystem synthesis has a significant effect on vector physicochemical properties. Saliently, surface charge has been shown to influence lipid nanoparticle (LNP) elimination, retinal distribution and siRNA delivery to different layers of the retina such as the ganglion cells and inner plexiform layer (Huang and Chau, 2019). Subsequent studies using amine lipidoid modified

LNPs with varying surface charges (5 to 34 mV) illustrated successful gene knockdown *in vitro* and *in vivo* following intravitreal administration in C57BL/6 mice (Huang and Chau, 2021). Comprehensively, neutral and mildly positive LNPs achieved less than 10% RNA-binding protein with multiple splicing (RBPMS) mRNA suppression, whilst LNPs with a surface charge of 31.2 mV achieved RBPMS mRNA suppression > 20% in retinal ganglion cells. This is indicative of the role of surface charge in promoting selective downregulation in target cells and promoting LNP diffusion across the vitreous and ILM to the RGC layer (Huang and Chau, 2019). Notably, Huang and Chau (2019) reported that majority of the LNPs intravitreally delivered in mice were cleared 24 hours after administration due to limited internalisation therefore showing importance of LNP modification for targeted delivery.

The ease of LNP surface modification/functionalisation and the inherent ability to accumulate in inflammatory microenvironments and choroidal neovascularisation lesions due to the enhanced permeability and retention (EPR) effect (Ideta et al., 2005) is a significant feature. Although this phenomenon is commonly found in tumour microenvironments, the neovascularisation in retinal degenerative diseases (AMD and DR) shares significant similarities with that of the tumours. Recently, Li et al (2023), leveraged the EPR effect in CNV mouse models through the co-delivery of quercetin and miR150 using Asp-Gly-Arg (NGR) peptide modified DDAB based solid lipid nanoparticles prepared by film ultrasonic method. The NGR modification of SLNs enhanced the uptake of the nanosystem *in vitro* using the HUVEC cell line, a model for angiogenesis and enhanced retinal co-retention. Significantly, quercetin and miR150 co-administration in CNV mice models downregulated CXCR4 and HIF-1α which play an essential role in the development of CNV in AMD patients (Cristante et al., 2023; Guerin et al., 2008) and resulted in visible inhibition of choroidal angiogenesis and partial restoration of retinal structure (Li et al., 2023).

As previously discussed, lipid based nanosystems are highly versatile, serving as effective delivery vehicles for siRNAs and miRNAs to regulate gene expression, and, as will be discussed, offering a promising modality for genome editing applications. Genome editing provides an exciting opportunity to tackle limitations often encountered by conventional gene replacement therapies, particularly autosomal dominant inherited retinal diseases. The adoption of gene editing techniques such as the CRISPR/Cas system allows for the correction of genetic mutations within the patient's own genome, permanent replacement or modification of defective target genes and correction of mutations in large genes (ABCA4 (6.8 kb) in Stargardt disease and USH2A (15.6 kb) in Usher syndrome type 2) which is commonly impossible in conventional gene replacement strategies due to vector limitations and possible need to fragment genes for efficient delivery (Dhurandhar et al., 2021; Fenner et al., 2022). To this end, Guatam et al. (2023) developed and investigated a translatable carboxy-ester - LNPx-based mRNA gene editing system for the the co-encapsulation and

subretinal delivery of caspase 9 (cas9) mRNA and single guide RNA (sgRNA) to Ai9 mice (Figure 2.8a,b).

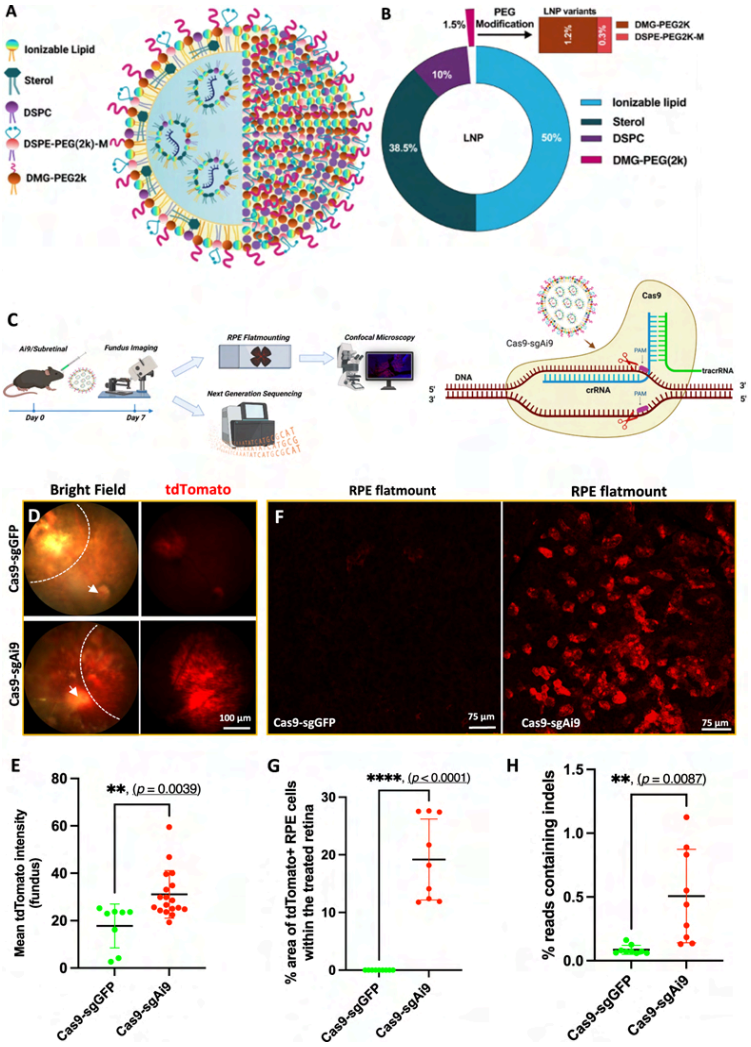

Figure 2.8: A) A Schematic representation of the structural organization of different LNP variants encapsulating mRNA cargo. B) Lipid composition of LNP variants in the study. C Schematic illustration exhibiting delivery of LNPx via subretinal route, retinal imaging and processing, as well as CRISPR-Cas9 editing mechanism. D) Representative fundus imaging showing editing events mediated by Cas9-sgAi9-LNPx. E) Quantification of tdTomato signal in fundus images. F) Representative flat mount images showing gene editing events in the RPE. G) Quantification of gene editing events in the RPE. H) Quantification of editing events by next-generation sequencing showed increased edits in the Cas9-sgAi9.

Seven days post-interventions imaging of test mice revealed a higher tdTomato fluorescence signal compared to the Cas9-sgGFP negative control group (Figure 2.7d,e). Additionally, retinal flat mounts showed 16.4% tdTomato positive RPE cells compared to the control group

(Figure 2.7g), with next-generation sequencing exhibiting a 5.94-fold higher level of indels/editing compared to negative control (Figure 7h). Beyond murine gene editing, lipid nanoparticle systems have also been evaluated for their capacity to deliver mRNA to diverse ocular tissues, including those of human origin (Chambers et al., 2024). To this end, LNPs loaded with mRNA encoding GFP and ciliary neutrophic factor were assessed for their potential to effectively transfect murine and human RPE cells. The efficient transfection of retinal cells in mouse RPE (*in vivo*) and human ocular tissue demonstrated the potential for LNPs to expand their clinical potential.

2.5.4. Bioconjugates, Bioresponsive, Hybrid and cell-aided gene delivery nanosystems

2.5.4.1. siRNA modification as a form of protection/delivery

As lipid and polymer based nanosystems differ from viruses in their broad tropism, surface modification is essential not only in improving efficacy but also in avoiding off-target effects of the genetic cargo. Notably, the halted Phase III clinical trial study for bevasiranib and AGN211745, siRNA based therapies for targeting VEGF-A and VEGFR1 overexpression in AMD respectively, showed significant off target effects involving the activation of Toll like receptor 3 and TRIF resulting in the secretion of Interleukin 12 and Interferon γ and localised inflammation affecting surrounding tissue and exacerbating disease progression (Kleinman et al., 2008). Additionally, results from the study showed subpar efficacy compared to existing therapies at the time. In some instances modifications beyond the nanosystem are deemed necessary, particularly to eliminate the unintended immune stimulation and off-target gene silencing by siRNAs. The modification of siRNAs has the potential to improve siRNA instability, cellular delivery, bioavailability and nucleic acid immunogenicity. Specifically, the conjugation of siRNA to 2′-O-hexadecyl (C16) has demonstrated sustained transthyretin RNA interference in the RPE of cynomolgus monkeys (Brown et al., 2022). Importantly, because multiple IRDs are related to dominant mutations in photoreceptor cells, silencing these genes by adopting modified siRNAs targeting photoreceptors specifically, even when intravitreally administered, is an exciting feat. Recently, a dozen configurations of siRNAs targeting the Huntingtin gene were synthesized and monitored for HTT protein reduction (Cheng et al., 2024). Significantly, the tetravalent siRNA, which had the highest valence, showed the best enrichment in photoreceptors following intravitreal administration in both C57BL/6J mice and porcine retinas. Silencing of HTT protein was observed for six and nine months in rodents and four months in the porcine retina (maximum duration of the experiment), indicating the potential for a single dose therapy annually.

2.5.4.2. Bioresponsive gene delivery nanosystems

An exciting avenue of functionalisation involves the introduction of bioresponsive moieties that are sensitive to various biochemical signals. The commonly exploited signals in this regard include the presence of reactive oxygen species, changes in pH and presence of certain enzymes in diseased tissues,these are often used for the development of stimuli-responsive delivery systems (Dou et al., 2020). Popular techniques for nanomaterial functionalisation include the (i) activation of esters to form amide bonds, (ii) click chemistry, which introduces compatible click functional groups and formation of stable conjugates, (iii) Thiol chemistry and (iv) ring open polymerisation reactions, which allow for the introduction of desired heteroatoms onto the polymer backbone, amongst others (Mauri et al., 2018). For example, an *in vivo* gene therapy approach utilising a self-assembled nanoparticle based on pH-sensitive amino lipids (prepared via a multicomponent reaction) to deliver therapeutic abca4 plasmid DNA to treat Stargardt macular degeneration has been investigated (Sun et al., 2020). Like RP, the rare autosomal recessive disease, caused by a monogenic mutation in abca4 gene can be associated with choroidal neovascularization complications (Querques et al., 2008). The attenuation of abca4 gene in Stargardt disease results in the accumulation of the photo-toxin N-retinylidene-N-retinyl ethanolamine bisretinoid (A2E) and lipofuscin in RPE phagosomes resulting in the eventual destruction of photoreceptors (Sun et al., 2020).

Presently, multiple therapeutics such as deuterated vitamin A, modulation of the complement system and cell therapy have been developed as a preventative measure for lipofuscin accumulation and rescue of macular degeneration. However, to the best of our knowledge, none have demonstrated significance in accomplishing clinical translation. A promising strategy involves the replacement of the mutated abca4 gene with a functional copy. The abca4 gene delivery system designed by Sun et al., (2020) uses oleic acid, ethylene-diamine and cysteine, it uses a pH dependent endosomal escape strategy and reductive cytosolic release of DNA to target tissue. Furthermore, for enhanced and photoreceptor directed gene expression, the abca4 gene was under the control of a bovine rho promoter. Subretinal administration of the eco/prho-abca4 lipid nanoparticles resulted in sustained gene expression eight months post injection, a 35% reduction in N-retinylidene-N-retinyl ethanolamine bisretinoid (A2E) photo-toxin accumulation, delayed disease progression in Stargardt disorder mice (abca4-/-) for at least six months after treatment, and improved dark adaptation (Sun et al., 2020). The role of pH responsive systems has also been recently shown through the design of a triblock copolymer (PEG-b-PAMA-b-P(C7A-r-DBA) for siVEGFA intravitreal delivery in a mouse model of hypoxia-induced angiogenesis (Guo et al., 2024). Administration of the pH-responsive system not only resulted in a wide distribution of siRNA within the different layers of the retina, showing the nanosystem can penetrate the inner blood-retina barrier but a reduction in CNV rate was observed in mice treated with the

system (PACD/siVEGFA), indicative of VEGF-A silencing which was comparable to that of the clinical drug, ranibizumab (Figure 2.9) (Guo et al., 2024).

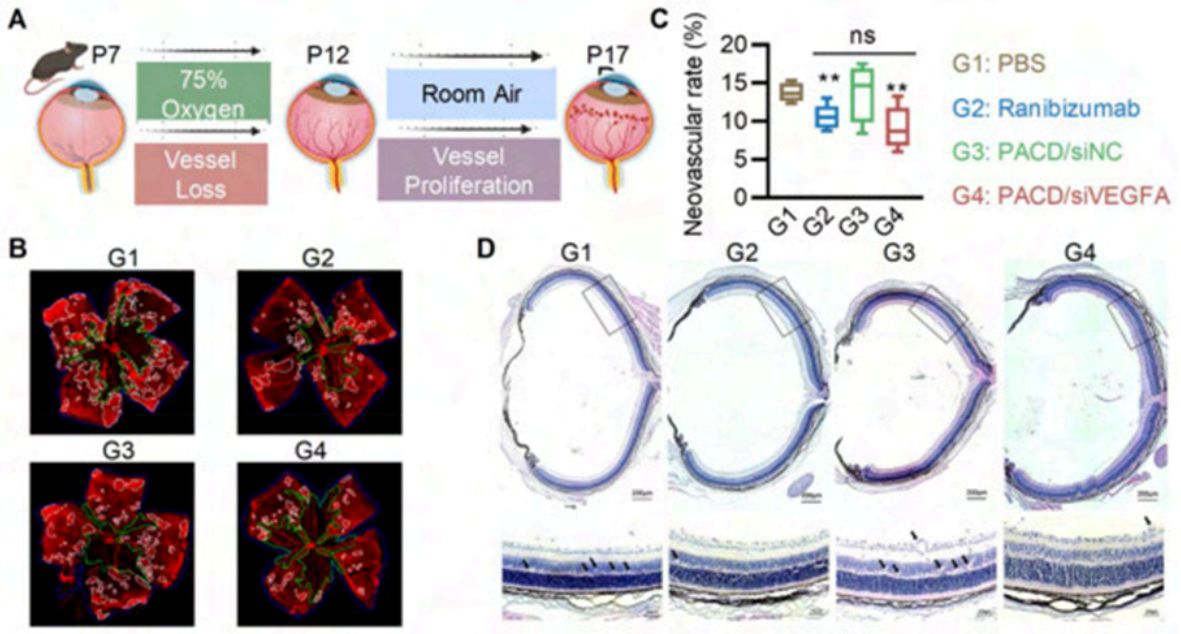

Figure 2.9: Anti-neovascularization of PACD/siRNA in an OIR mouse model (Guo et al., 2024).

The adoption of other stimuli response modalities for ocular delivery of nucleic acids has been investigated (X. Lin et al., 2021). Notably, a multifunctional-stimuli responsive silica nanosystem conferred with a disulfide bond for glutathione-responsive cargo release, conjugated to imidazole to aid in endosomal escape and functionalised with an all-trans-retinoic acid for enhanced RPE-specific internalisation, was synthesised and investigated for cas9/sgRNA ribonucleoprotein and mRNA (amongst other biomacromolecules) encapsulation and transfection (Wang et al., 2021). Consequently, SNP-based cas9/sgRNA ribonucleoprotein and mRNA delivery were achieved in the RPE of Ai14 transgenic mice along with high genome editing. (Wang et al., 2021). Therefore, adopting the multifunctional approach for gene delivery represents a powerful tool for advanced cargo delivery and optimum therapeutic outcomes.

2.5.4.3. Lipid-polymer ('Hybrid') delivery nanosystems

Hybrid systems (polymer-lipid nanosystems) offer the best of both worlds, the biomimetic nature of lipids and the structural functionality of polymers. Use of the hybrid system has shown improved drug bioavailability, flexibility in particle size design, increased drug loading, controlled system degradation, sustained release and steric stabilisation (Hadinoto et al., 2013). Earlier research on lipid-polymer systems (core shell type nanocarriers) demonstrated

the potential of these types of nanocarriers to serve as possible conduits for systemic administration in CNV treatment. This was particularly reported by Iriyama et al., (2011), who synthesised the polyion complex ([PEG-b-PAsp(DET)/ pDNA) encapsulating pDNA encoding sFlt-1 for systemic administration in CVN mice which showed a reduction in CNV lesions by 60% and low toxicity (Iriyama et al., 2011). Recently, a plethora of studies showing successful gene delivery by hybrid nanocarriers have been reported and have demonstrated vast potential for significant functionality of the nanocarriers. For example, to eliminate off-target therapeutic delivery and side effects, the development of functionalised hybrid nanoparticles capable of achieving tissue specific gene expression was conducted by Rajala et al., (2014).

Figure 2.10: LPD-mediated Rpe65 gene delivery in Rpe65 knockout mice, rescues cone cell

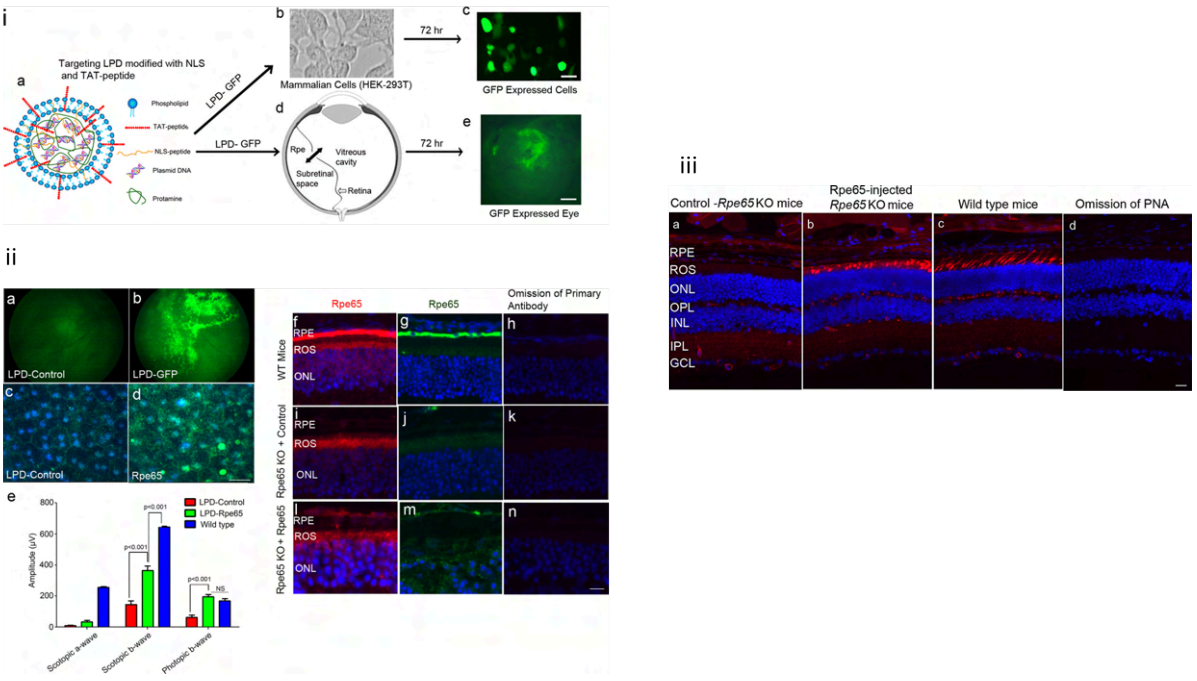

death (Rajala et al., 2014).

Importantly, functionalisation enhances the properties of nanocarriers, thus broadening their application. A good example of this is the creation of an artificial virus using biocompatible nanoparticles (Rajala et al., 2014). This involves the surface modification of nanoparticles via the attachment of receptor-specific ligands and peptides capable of maximizing gene delivery and expression *in vivo*. The formulated liposome-protamine-DNA complex (LPD) functionalised with a nuclear localisation signalling (NLS) peptide and a cell penetrating peptide through non-covalent bonding to facilitate effective gene administration to the eye is demonstrated in Figure 2.10. Using rpe65 knockout mice models, the authors confirmed cell-specific gene delivery and expression by the LPD system following subretinal administration, indubitably resulting in the preservation of cone receptors comparable to wild-type mice and rescue of the functional phenotype. In addition to promoting site specific

therapy delivery, functionalisation of nanomaterials can positively affect the surface chemistry, size, charge, hydrophobicity and hydrophilicity of the developed delivery system, therefore, changing its biocompatibility, biodistribution, solubility and clearance (Rajala et al., 2014; Thiruppathi et al., 2017). A more recent similar paper detailed a core-shell nanocarrier composed of dioleoylphosphatidylethanolamine (DOPE) linked to hyaluronic acid for CD44 targeting (outermost shell) with the inner core layer of the system composed of amino acid and NLS functionalised dendrimers and pH-sensitive lipids as part of the inner layer of the nanosystem (Tan et al., 2021). According to the study, *in vitro* analysis of the carrier proved an effective tool for the promotion of cellular uptake (ARPE-19 cells), endosomal escape and nuclear translocation. Significantly, nanocarriers encapsulating pFlt23K-EGFP construct (EGFP_pDNA carrying Flt23K), showed VEGF expression inhibition under hypoxia-like conditions along with relative safety levels and efficient transfection when administered *in vivo* (C57BL/6 female mice). Recently, a hybrid nanocarrier approach for the delivery of the Human Antigen R (HuR) siRNA aimed at targeting diabetic retinopathy was investigated (Supe et al., 2023). Thoroughly, HuR is an RNA binding protein that regulates multiple cellular pathways and angiogenic molecules, such as VEGF and the transforming growth factor beta 1 (TGFβ1) known to have a role in diabetic retinopathy as increased expression leads to vascular permeability and tissue fibrosis amongst other issues (Mohan et al., 2024). Liposomes prepared by thin film hydration were mixed with branched PEI_siRNA complex to yield ternary complexes (lipopolyplexes: LPPs) (Supe et al., 2023). *In vitro* studies using ARPE-19 cells demonstrated that the delivery of HuR siRNA showed efficient cellular uptake, downregulation of HuR mRNA and protein and VEGF. Additionally, the intravitreal delivery of these complexes in male streptozotocin induced DR Wistar rats reduced HuR and VEGF protein expression in the DR mice and thus serves as an interesting modality for further studies (Supe et al., 2023).

2.5.4.4. The “Trojan horse” gene delivery Strategy

The therapeutic potential of e*x vivo* gene therapy was reported by Abe et al. (2008) through the genetic modification of rat RPE cells using a cationic liposome to transfect a doxycycline responsive cDNA carrying the brain-derived neurotrophic factor gene (BDNF gene). Subretinal injection of the genetically modified RPE cells into littermates showed photoreceptor protection against phototoxicity (Abe et al., 2008). The groundwork established by researchers discussed above demonstrated the possibility of exogenous gene transfection of retinal cells and *ex vivo* gene delivery, paving the way for the use of stem cells as a conduit for gene delivery. Specifically, mesenchymal stem cells (MSCs) have been used as part of a trojan horse strategy to deliver nanoparticles encapsulating drug targets (Ouyang et al., 2020). Importantly, the intravenous transplantation of bone marrow derived MSCs have been shown to migrate to CNV lesions in CNV mice models with HIF-1α shown to inhibit -

CNV by downregulating multiple growth factors (namely, HIF-1α and VEGF) (Zhang et al., 2017). Interestingly, PLGA NPs loaded with HIF-1α silence the expression of HIF-1α in RPE cells, however, insufficient encapsulation efficiency and lack of animal studies made the nanosystem difficult to popularise (Figure 2.11) (Zhang et al., 2024). Given this, the "trojan horse" strategy seems promising, as cell mediated therapy has significantly better circulation time intravenously, has the ability to circumvent biological barriers and has abundant surface ligands that can aid with specific targets (Yu et al., 2020).

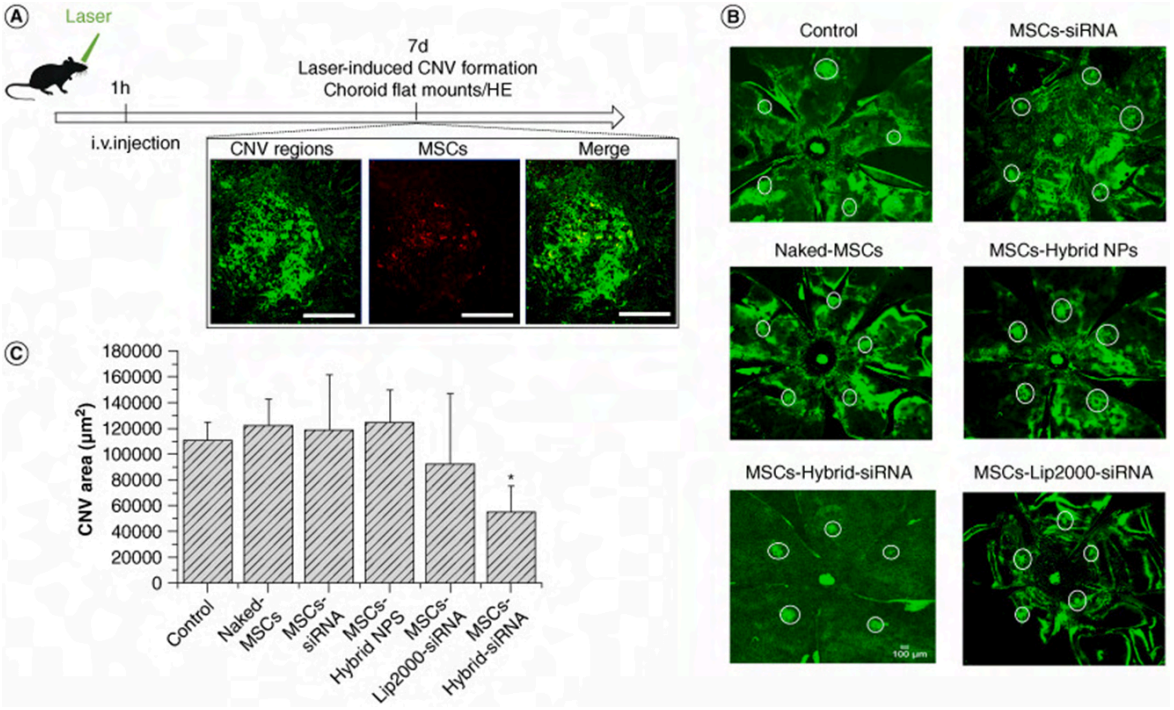

Figure 2.11: Targeted delivery of MSC-hybrid-siRNA NPs and therapeutic efficacy in a laser-induced CNV mouse model (Zhang et al., 2024).

MSCs transfected with PLGA_lipid hybrid nanoparticles loaded with HIF-1α siRNA were intravenously delivered to C57BL/6 CNV mouse model. Analysis showed modified MSCs migrated to CNV area without accrual in other organs, a significant reduction in CNV area following treatment was reported, however no significant difference in CNV thickness was observed. Despite promising data in this study, limitations such as scalability hinder wide clinical translation of the therapy (Zhang et al., 2024). An exciting and rapidly growing area of research involves the use of extracellular vesicles (EVs) as vehicles for gene and protein delivery, serving as a bridge facilitating cell-cell communication (Herrmann et al., 2021). Furthermore, investigations on the pathways involved in neural cell regeneration and the screening of genetic material that could possibly facilitate these processes has garnered significant interest (Barbato et al., 2017; Bringmann et al., 2009; Hamon et al., 2019). Naturally, mammalian cells, unlike zebrafish, are incapable of regenerating the retina following damage, leading to site restoration (Lindsey and Powers, 2007; Sherpa et al., 2008)

Notably, damage to zebrafish retina results in increased gene expression of Ascl1 in muller glia, unfortunately, Ascll1 is not expressed in mammalian muller glia following injury (Karl and Reh, 2010). However, forced expression through the coupled delivery of Ascl1 and a histone deacetylase inhibitor in mice has been shown to stimulate muller glia derived regeneration, advocating for the possible role of gene therapy in promoting endogenous retinal regeneration (Jorstad et al., 2017).

Of note is the investigation of EVs for their potential in inducing muller glia dedifferentiation and generation of proliferative progenitor cells in zebrafish eyes (Didiano et al., 2020). Briefly, EVs are known to carry protein, lipid and RNA cargo specific to certain cell types and functions. Therefore, Didiano et al., (2020) tested EVs from multiple cell lines capable of inducing muller glia derived proliferation. Isolated EVs intravitreally injected in zebrafish were screened for their ability to induce muller glia dedifferentiation and generation of proliferating progenitor cells. Significantly, small EVs from C6 glioma cells repeatedly induced muller glia reprogramming and generation of proliferative progenitor cells and resulted in increased expression of Ascl1a following their delivery. Screening of the EV cargos showed miR 124 enrichment which is known to induce Ascl1 expression therefore facilitating the repair of the retina (Didiano et al., 2020). Further investigations focused on the use of EVs is required to streamline the process of EV screening and understanding which components of the cargo are driving cell reprogramming and possible regeneration.

2.5.5. Inorganic based gene delivery systems

Inorganic nanosystems are typically composed of an inorganic core serving as a rigid support coated with polymers to confer biocompatibility and functionality. Importantly, the magnetic, loading and photoelectric properties of these nanomaterials enable their use as multifunctional systems, i.e. drug/gene delivery, radiotherapy, chemotherapy, diagnostics, and hyperthermal therapy delivery (Lin et al., 2021). Additionally, inorganic materials enable facile synthesis and tuning of nanosystem properties (size, loading efficiency, charge etc.) which facilitates the design of an ideal nanosystem. For example, amino funtionalisation of mesoporous silica-based nanoparticles (MSNs) has been shown to impact nanoparticle size, loading efficiency and improve nucleic acid entrapment (Valdés-Sánchez et al., 2022). Notably, Valdés-Sánchez et al., (2022), used amino functionalised MSNs to deliver the precursor mRNA (pre-mRNA) splicing factor 31 gene (PRPF31) which encodes for the splicing factor PRPF31, a component of the spliceosome involved in pre-mRNA splicing essential for the production of mature mRNA prior to translation (Aweidah et al., 2023). PRPF31 plays an important role in the survival and differentiation of retinal progenitor cells through its splicing role (Li et al., 2021). Therefore dysfunctional PRPF31 has been

implicated in autosomal dominant RP because mutations in PRPF31 affect spliceosome assembly which surprisingly only causes retina specific effects such as abnormal neural cell differentiation and apoptosis (Aweidah et al., 2023; Li et al., 2021). Safety profile of MSNs carrying prpf31_GFP DNA following subretinal delivery in C57BL/6 mice was analysed, fundus images and optical coherence tomography showed retinal morphology and thickness comparable to that observed in non treated eyes. Significantly, transgene expression of GFP and PRPF31 was reported in the retinal layers of the treated mice as depicted by the co-localisation of the stains, importantly, this did not affect RPE tight junctions (Aweidah et al., 2023). These data indicate the potential role of MSNs as gene delivery vehicles directing transfection directly to RPE cells *in vivo*.

An exciting avenue for inorganic NPs is their consideration in ophthalmic imaging or theranostic approaches. Gold NPs (AuNPs) in particular, have been investigated for use in ophthalmic imaging with focus on optical coherence tomography and photoacoustic imaging (Chen et al., 2021). Recently, Focus Ultrasound (FUS) mediated AuNPs were shown to efficiently traverse the BRB and colonise the RGC layer following intravenous delivery, therefore providing therapeutic and diagnostic benefit to retinal degenerative diseases (Park et al., 2024). Takeuchi et al (2020) designed an anti-angiogenic thiolated siRNA conjugated ultra-small AuNP system. The antiangiogenic behaviour of the siRNA-AuNPs was assessed on the HUVEC cell line using the Mtrigel-based tube formation assay. Treatment of HUVEC cells with the siRNA-AuNPsTube showed an overall significant safety profile and inhibition of tube formation ($67.6 \pm 5.4\%$) (Takeuchi et al., 2018). Unfortunately, no *in vivo* investigations were undertaken by the study, but preliminary data supports the need for further assessment of this system in an animal model.

Moreover, the ability of AuNPs to absorb and scatter light as a result of the oscillation of their free electrons following exposure/excitation by light is referred to as surface plasmon resonance (SPR) (Huang and El-Sayed, 2010). SPR band intensity and wavelengths can be tuned by controlling particle size, shape and local refractive index near the particle surface (Huang and El-Sayed, 2010). Therefore, the manipulation of SPR peaks in AuNPs to explore the ability of the nanosystems to target or bind different cell types (ganglion and bipolar cells specifically) and deliver genetic material by spatially targeted irradiation of near infrared light (NIR - 780 and 850 nm) has been investigated (Batabyal et al., 2021). To this end, Thy-1 (for ganglion cells) and PKCα antibody functionalisation of Au nanorods was conducted for optical delivery in retinal degenerated mice (B6. CXB1-Pde6brd10/J) (Batabyal et al., 2021). Gold nanorods (GNRs) were loaded with multi-characteristic opsin II (MCO-II) mCherry plasmid DNA and intravitreally delivered in B6. CXB1-Pde6brd10/J mice which were succeeded by irradiation using NIR (780 or 850nm) laser beam. Targeted *in vivo* delivery of Thy-1 and PKCα functionalised GNRs and MCO-II expression was reported in ganglion and

Bipolar cells respectively, following administration. The study demonstrated that field enhancement by GNRs transiently perforates the cell membrane, which aids in transduction of genetic cargo, and the use of GNRs and irradiation has the ability to enable multiple dosing without creating immunotoxicity.

Lastly, an interesting form of gene therapy showing significant promise in the treatment of PSEDs involves the use of antisense oligonucleotides and aptamers. Aptamers are single stranded nucleic acid molecules created (although some occur naturally) using a library of random sequences with the aim of selecting and amplifying for a sequence with specific target binding capabilities (Dunn et al., 2017). Considered affinity reagents, they tend to fold into 3D structures and target specific molecules (DNA, proteins, pathogenic cells, etc.) similarly to antibodies. However, unlike antibodies, they have low batch variability, low immunogenicity and are relatively inexpensive to generate. An innovative use of aptamers is their application in the inhibition of VEGF in Long-Evans pigmented rats using topically administered carbon dots carrying anti-VEGF aptamer (Shoval et al., 2019). According to Shoval et al., (2019), the use of carbon dots has the potential to successfully inhibit VEGF-stimulated angiogenesis in choroidal blood vessels. Briefly, synthesis of the Anti-VEGF aptamer conjugated carbon dots was conducted through surface modification with carboxylic acid to facilitate hybridisation to amino modified aptamer. The resulting hybrid system possessing luminescence properties can enable the use of the C-dots in gene delivery and use in bioimaging or as sensing conduits. Significantly, topical delivery of the aptamer:C-dots in Long-Evans pigmented rats, inhibited CNV comparable to bevacizumab and aflibercept. Additionally, the nanosystem enabled real-time monitoring of therapeutic concentrations *in vivo*, which can serve as the basis for further future studies as it has the potential to achieve non-invasive monitoring of drug concentration by fluorescence fundoscopy, which can aid in personalising the dosage to each patient.

2.6. Conclusion and way forward

The isolation and accessibility of the eye to non-invasive diagnostics/imaging approaches make the visualisation of neurons and blood vessels relatively less complicated and the detection of any subtle changes in the eye's physiology possible in comparison to other organs. Therefore, the possibility of direct therapeutic delivery to the retina with minimal systemic diffusion under visualization, the bilateral nature and symmetry of most inherited diseases and the availability of the contralateral eye to serve as a valuable 'untreated' control offer a huge advantage on the treatment and research of ocular diseases (Kumaran et al., 2018). Despite this and the technological advancement made thus far, the safe and efficient delivery of therapeutics to the posterior segment of the eye without the need for multiple ocular injections remains a challenge. Additionally, conventional pharmacological

interventions for PSEDs are limited in their capacity to reverse or regenerate lost photoreceptors and or RPE, they are only effective at slowing down progressive vision loss and preserving remnant vision. As previously discussed, the goal of PSED therapy is to reduce inflammation, restore blood–retinal barrier and importantly, achieve retinal-RPE restoration and regeneration (Xu and Chen, 2016). Although currently approved therapies manage to slow down the degenerative process, the need for multiple doses presents an immense challenge, necessitating the use of novel drug delivery systems and in particular, the adoption of gene therapy, to tackle some of the associated shortfalls. The promise shown by the only FDA-approved gene therapy, Luxturna, has expanded research for other gene based approaches. As reviewed above, the findings of clinical trials and research underway has aided in defining the window of opportunity for successful intervention of PSEDs. Although knowledge on the efficacy and safety of gene therapy is still limited, therefore necessitating in-depth long-term studies, current research and clinical trial results show significant promise. Essential to note is the focus needed on the activity and behaviour of the genetic material of interest once it reaches its target site (siRNAs and miRNAs in particular). Monitoring the efficacy of the therapy is not enough, examining the occurrence of unintended downstream effects of the therapy such as impacts on other unrelated pathways and possible offsite delivery of the genetic material is essential. To circumvent some of these limitations, the development and or use of biocompatible gene delivery vectors for targeted gene delivery and expression is essential. Greater efficiency and safety of gene transfer will be made possible by further advancements in vector design and delivery. By optimising the clinical trial design, outcomes can be evaluated more quickly and with more accuracy.

2.7. Expert opinion

The concept of delivering genetic material to target cells, resulting in corrected gene expression and therapeutic efficacy, was first proposed by Theodore Friedmann and later supported by George Stamatoyannopoulos (Papanikolaou and Bosio, 2021). For instance, the introduction of the hypoxanthine-guanine phosphoribosyltransferase (HPRT) gene into mutant mammalian cells provided the first demonstration of gene therapy changing the signature and character of mutant cells, this was a significant finding made by Dr Szybalska and Szybalski (Szybalska and Szybalski, 1962). Years later, the first human gene therapy trial to show significant clinical benefit was demonstrated in twins with an X-linked version of severe combined immune deficiency (SCID). SCID was due to a loss of function mutation in the gene encoding the interleukin-2 receptor gamma subunit or adenosine deaminase (ADA) (Kohn, 2000). Using a gamma-retroviral vector, the ADA gene was transfected into T cells of the SCID patients, resulting in effective treatment of the twins with SCID. Most notably, as recently as 2017, the approval of the first-ever gene therapy for retinal diseases, Luxturna, marked a significant milestone in the field. Unfortunately, it can only be implemented for the

treatment of the rare biallelic RPE65 mutation associated with retinal dystrophy, and as a result, remains extremely costly (US$850 000). Improvements in visual acuity remain non-ubiquitous amongst treated individuals, with only 50% of the treated patients meeting the FDAs requirements for meaningful vision improvement and some patients reported to experience permanent vision loss. Therefore a plethora of experimental therapies are being investigated and were reviewed above. One interesting therapy which shows promise is GenSight's optogenetic therapy (GS030) aimed at delivering genetic material encoding light sensitive proteins into the RGCs, bypassing the damaged photoreceptors (Sahel et al., 2021). This is particularly beneficial for end stage retinal degeneration, marked by loss of photoreceptors. As such, optogenetic therapy enables the treatment of a myriad of retinal diseases despite the original cause, its wide adaptability thus has a potential to reduce treatment cost for retinal degenerative diseases. Despite this, optogenetic therapies are currently unable to restore vision to natural levels and mostly require external devices (goggles) to facilitate vision restoration. Although currently investigated gene therapies show promising results, the fundamental problem with retinal degeneration, retinal cell loss, remains neglected. This is driven by the inability of mammalian neuronal cells to renew. Therefore, combining neuronal cell regeneration with gene therapy approaches is the key to tackling retinal degenerative diseases. An exciting avenue which has shown promise is the investigation of nucleic acids capable of facilitating neuronal cell dedifferentiation and in particular, the role of EVs in promoting retinal cell regeneration. Although this approach is still in its infancy, it has huge potential to revolutionise the field of retinal therapy. Notably, the adoption of CRISPR/Cas9 for this purpose shows significant potential in the replacement of mutated genes and the activation of key transcription factors and pathways (Ascl1, Sox2, Wnt, Notch etc.) for the reprogramming of certain retinal cells to photoreceptors. As CRISPR/Cas9 gene therapy is in its nascent stage, further investigations to ensure precise delivery and control whilst avoiding off-target effects and or tumorigenesis is essential. Importantly, the complex processes underlying retinal regeneration demand precise coordination in renewing various retinal cells and restoring the intricate neural networks involved. As a result, the goal of achieving effective tissue regeneration through gene therapy remains a challenging and distant objective.

Although currently investigated gene therapies show promising results, the fundamental problem with retinal degeneration, retinal cell loss, remains neglected. This is driven by the inability of mammalian neuronal cells to renew. Therefore, combining neuronal cell regeneration with gene therapy approaches is the key to tackling retinal degenerative diseases. An exciting avenue showing promise for targeted drug/gene delivery and retinal cell regeneration involves the use of extracellular vesicles as shown in the reviewed study (Jorstad et al., 2017; Durmaz et al., 2024). EVs offer a unique and biologically compatible avenue for gene delivery as they are capable of transporting nucleic acids, proteins and

signalling molecules to target cells with high specificity and minimal immunogenecity. Owing to their natural origin and modifiable surfaces, EVs can easily cross biological barriers whilst maintaining cargo integrity, ensuring precision gene delivery and cell-targeting. Additionally, in the context of retinal diseases, EVs extracted from stem cells are normally enriched with proteins, microRNAs, siRNAs, and mRNA (along with a plethora of other signaling molecules) known to modulate cell fate determination, tissue repair and cell de-differentiation pathways. Additionally, these molecules have shown potential in the reactivation of progenitor state of Müller glia and retinal epithelial cells in combination with the delivery of target genes for specific retinal insults offer an immense opportunity for future research on diseases demanding both the conrrection of genetic mutations and simultaneously tissue regeneration/repair. As such, the future of gene delivery vehicles in relation to retinal regenerative strategies lies in the refinement of genetic cargo loading, surface modification for cell-specific targeting and EV isolation strategies. Focusing on this could unlock, non-viral gene delivery system solutions capable of overcoming current limitations associated with synthetic nanoparticles and viral vectors. Such advancements could significantly accelerate the development of personalised, precision approaches to reprograming damaged tissue, paving the way for sustained, regenerative gene therapy strategies in vision restoration.

Despite promising preclinical outcomes in retinal gene therapy, translating these systems to the clinic is hindered by complex production processes, high costs, and the need for robust regulatory frameworks. Additionally, clinical trial research on the long-term efficacy of gene therapy and safety concerning continuous transgene expression has not presently been performed. Therefore, this must be considered along with techniques to regulate transgene expression *in vivo* should the levels of protein expression prove toxic. Unfortunately, gene therapy research has an unsavoury history of prioritising progress at the expense of safety. Even so, with careful consideration of the therapeutic efficacy and long-term safety in the design of gene therapies and the selection of accompanying vectors, gene therapy may bring significant progress in the development of widely effective next-generation therapeutics. Therefore, multidisciplinary collaboration is key to solving enduring challenges, making the integration of engineering, biology, and clinical science essential in bringing these therapies closer to patients who desperately need them.

2.8. References

AbbVie, 2024. Phase I/IIa, Open-Label, Dose-Escalation Study of Safety and Tolerability of Intravitreal RST-001 in Patients With Advanced Retinitis Pigmentosa (RP) (Clinical trial registration No. NCT02556736). clinicaltrials.gov.

Abe, T., Wakusawa, R., Seto, H., Asai, N., Saito, T., Nishida, K., 2008. Topical Doxycycline

Can Induce Expression of BDNF in Transduced Retinal Pigment Epithelial Cells Transplanted into the Subretinal Space. Invest. Ophthalmol. Vis. Sci. 49, 3631–3639. https://doi.org/10.1167/iovs.07-0947

Acharya, P.C., Fernandes, C., Mallik, S., Mishra, B., Tekade, R.K., 2018. Chapter 4 - Physiologic Factors Related to Drug Absorption, in: Tekade, R.K. (Ed.), Dosage Form Design Considerations, Advances in Pharmaceutical Product Development and Research. Academic Press, pp. 117–147. https://doi.org/10.1016/B978-0-12-814423-7.00004-6

Al-Hussainy, S., Dodson, P.M., Gibson, J.M., 2008. Pain response and follow-up of patients undergoing panretinal laser photocoagulation with reduced exposure times. Eye 22, 96–99. https://doi.org/10.1038/sj.eye.6703026

Ammar, M.J., Hsu, J., Chiang, A., Ho, A.C., Regillo, C.D., 2020. Age-related macular degeneration therapy: a review. Curr. Opin. Ophthalmol. 31, 215–221. https://doi.org/10.1097/ICU.0000000000000657

Anderson, D.H., Mullins, R.F., Hageman, G.S., Johnson, L.V., 2002. A role for local inflammation in the formation of drusen in the aging eye. Am. J. Ophthalmol. 134, 411–431. https://doi.org/10.1016/S0002-9394(02)01624-0

Aweidah, H., Xi, Z., Sahel, J.-A., Byrne, L.C., 2023. PRPF31-retinitis pigmentosa: Challenges and opportunities for clinical translation. Vision Res. 213, 108315. https://doi.org/10.1016/j.visres.2023.108315

Barbato, S., Marrocco, E., Intartaglia, D., Pizzo, M., Asteriti, S., Naso, F., Falanga, D., Bhat, R.S., Meola, N., Carissimo, A., Karali, M., Prosser, H.M., Cangiano, L., Surace, E.M., Banfi, S., Conte, I., 2017. MiR-211 is essential for adult cone photoreceptor maintenance and visual function. Sci. Rep. 7, 17004. https://doi.org/10.1038/s41598-017-17331-z

Bastawrous, A., Burgess, P.I., Mahdi, A.M., Kyari, F., Burton, M.J., Kuper, H., 2014. Posterior segment eye disease in sub-Saharan Africa: review of recent population-based studies. Trop. Med. Int. Health 19, 600–609. https://doi.org/10.1111/tmi.12276

Batabyal, S., Kim, S., Wright, W., Mohanty, S., 2021. Layer-specific nanophotonic delivery of therapeutic opsin-encoding genes into retina. Exp. Eye Res. 205, 108444. https://doi.org/10.1016/j.exer.2021.108444

Beltramo, E., Porta, M., 2013. Pericyte Loss in Diabetic Retinopathy: Mechanisms and Consequences. Curr. Med. Chem. 20, 3218–3225. https://doi.org/10.2174/09298673113209990022

Bi, A., Cui, J., Ma, Y.-P., Olshevskaya, E., Pu, M., Dizhoor, A.M., Pan, Z.-H., 2006. Ectopic Expression of a Microbial-Type Rhodopsin Restores Visual Responses in Mice with Photoreceptor Degeneration. Neuron 50, 23–33. https://doi.org/10.1016/j.neuron.2006.02.026

Binley, K., Widdowson, P.S., Kelleher, M., De Belin, J., Loader, J., Ferrige, G., Carlucci, M., Esapa, M., Chipchase, D., Angell-Manning, D., Ellis, S., Mitrophanous, K., Miskin, J., Bantseev, V., Nork, T.M., Miller, P., Naylor, S., 2012. Safety and Biodistribution of an Equine Infectious Anemia Virus-Based Gene Therapy, RetinoStat® , for Age-Related Macular Degeneration. Hum. Gene Ther. 23, 980–991. https://doi.org/10.1089/hum.2012.008

Bionic Sight LLC, 2023. Phase 1/2, Safety and Efficacy Trial of BS01, a Recombinant Adeno-Associated Virus Vector Expressing ChronosFP in Patients With Retinitis Pigmentosa (Clinical trial registration No. NCT04278131). clinicaltrials.gov.

Bordet, T., Behar-Cohen, F., 2019. Ocular gene therapies in clinical practice: viral vectors and nonviral alternatives. Drug Discov. Today 24, 1685–1693. https://doi.org/10.1016/j.drudis.2019.05.038

Boyer, D.S., Hopkins, J.J., Sorof, J., Ehrlich, J.S., 2013. Anti-vascular endothelial growth factor therapy for diabetic macular edema. Ther. Adv. Endocrinol. Metab. 4, 151–169. https://doi.org/10.1177/2042018813512360

Bringmann, A., Iandiev, I., Pannicke, T., Wurm, A., Hollborn, M., Wiedemann, P., Osborne, N.N., Reichenbach, A., 2009. Cellular signaling and factors involved in Müller cell gliosis: Neuroprotective and detrimental effects. Prog. Retin. Eye Res. 28, 423–451. https://doi.org/10.1016/j.preteyeres.2009.07.001

Britt, J.P., McDevitt, R.A., Bonci, A., 2012. Use of channelrhodopsin for activation of CNS neurons. Curr. Protoc. Neurosci. Editor. Board Jacqueline N Crawley Al CHAPTER, Unit2.16. https://doi.org/10.1002/0471142301.ns0216s58

Brown, K.M., Nair, J.K., Janas, M.M., Anglero-Rodriguez, Y.I., Dang, L.T.H., Peng, H., Theile, C.S., Castellanos-Rizaldos, E., Brown, C., Foster, D., Kurz, J., Allen, J., Maganti, R., Li, J., Matsuda, S., Stricos, M., Chickering, T., Jung, M., Wassarman, K., Rollins, J., Woods, L., Kelin, A., Guenther, D.C., Mobley, M.W., Petrulis, J., McDougall, R., Racie, T., Bombardier, J., Cha, D., Agarwal, S., Johnson, L., Jiang, Y., Lentini, S., Gilbert, J., Nguyen, T., Chigas, S., LeBlanc, S., Poreci, U., Kasper, A., Rogers, A.B., Chong, S., Davis, W., Sutherland, J.E., Castoreno, A., Milstein, S., Schlegel, M.K., Zlatev, I., Charisse, K., Keating, M., Manoharan, M., Fitzgerald, K., Wu, J.-T., Maier, M.A., Jadhav, V., 2022. Expanding RNAi therapeutics to extrahepatic tissues with lipophilic conjugates. Nat. Biotechnol. 40, 1500–1508. https://doi.org/10.1038/s41587-022-01334-x

Bucher, K., Rodríguez-Bocanegra, E., Dauletbekov, D., Fischer, M.D., 2021. Immune responses to retinal gene therapy using adeno-associated viral vectors – Implications for treatment success and safety. Prog. Retin. Eye Res. 83, 100915. https://doi.org/10.1016/j.preteyeres.2020.100915

Bulcha, J.T., Wang, Y., Ma, H., Tai, P.W.L., Gao, G., 2021a. Viral vector platforms within the

gene therapy landscape. Signal Transduct. Target. Ther. 6, 1–24. https://doi.org/10.1038/s41392-021-00487-6

Bulcha, J.T., Wang, Y., Ma, H., Tai, P.W.L., Gao, G., 2021b. Viral vector platforms within the gene therapy landscape. Signal Transduct. Target. Ther. 6, 53. https://doi.org/10.1038/s41392-021-00487-6

Byrne, B.J., Flanigan, K.M., Matesanz, S.E., Finkel, R.S., Waldrop, M.A., D'Ambrosio, E.S., Johnson, N.E., Smith, B.K., Bönnemann, C., Carrig, S. and Rossano, J.W., 2025. Current clinical applications of AAV-mediated gene therapy. Molecular Therapy, 33(6), pp.2479-2516.

Cai, X., Nash, Z., Conley, S.M., Fliesler, S.J., Cooper, M.J., Naash, M.I., 2009. A Partial Structural and Functional Rescue of a Retinitis Pigmentosa Model with Compacted DNA Nanoparticles. PLOS ONE 4, e5290. https://doi.org/10.1371/journal.pone.0005290

Chen, C.-K., Huang, P.-K., Law, W.-C., Chu, C.-H., Chen, N.-T., Lo, L.-W., 2020. Biodegradable Polymers for Gene-Delivery Applications. Int. J. Nanomedicine Volume 15, 2131–2150. https://doi.org/10.2147/IJN.S222419

Chen, F., Si, P., Zerda, A. de la, Jokerst, J.V., Myung, D., 2021. Gold nanoparticles to enhance ophthalmic imaging. Biomater. Sci. 9, 367–390. https://doi.org/10.1039/D0BM01063D

Cheng, S.-Y., Caiazzi, J., Biscans, A., Alterman, J.F., Echeverria, D., McHugh, N., Hassler, M., Jolly, S., Giguere, D., Cipi, J., Khvorova, A., Punzo, C., 2024. Single intravitreal administration of a tetravalent siRNA exhibits robust and efficient gene silencing in mouse and pig photoreceptors. Mol. Ther. - Nucleic Acids 35, 102088. https://doi.org/10.1016/j.omtn.2023.102088

Ciulla, T.A., Hussain, R.M., Berrocal, A.M., Nagiel, A., 2020. Voretigene neparvovec-rzyl for treatment of RPE65-mediated inherited retinal diseases: a model for ocular gene therapy development. Expert Opin. Biol. Ther. 20, 565–578. https://doi.org/10.1080/14712598.2020.1740676

Cristante, E., Liyanage, S.E., Smith, A.J., Ali, R.R., Bainbridge, J.W.B., 2023. Role of HIF1α and HIF2α in Cre Recombinase–Induced Retinal Pigment Epithelium Pathology and Its Secondary Effect on Choroidal Neovascularization. Am. J. Pathol. 193, 1694–1705. https://doi.org/10.1016/j.ajpath.2023.05.017

Dang, J.M., Leong, K.W., 2006. Natural polymers for gene delivery and tissue engineering. Adv. Drug Deliv. Rev., Gene Delivery for Tissue Engineering 58, 487–499. https://doi.org/10.1016/j.addr.2006.03.001

Das, U.N., 2016. Diabetic macular edema, retinopathy and age-related macular degeneration as inflammatory conditions. Arch. Med. Sci. AMS 12, 1142–1157. https://doi.org/10.5114/aoms.2016.61918

del Amo, E.M., Rimpelä, A.-K., Heikkinen, E., Kari, O.K., Ramsay, E., Lajunen, T., Schmitt, M., Pelkonen, L., Bhattacharya, M., Richardson, D., Subrizi, A., Turunen, T., Reinisalo, M., Itkonen, J., Toropainen, E., Casteleijn, M., Kidron, H., Antopolsky, M., Vellonen, K.-S., Ruponen, M., Urtti, A., 2017. Pharmacokinetic aspects of retinal drug delivery. Prog. Retin. Eye Res. 57, 134–185. https://doi.org/10.1016/j.preteyeres.2016.12.001

Dhurandhar, D., Sahoo, N.K., Mariappan, I., Narayanan, R., 2021. Gene therapy in retinal diseases: A review. Indian J. Ophthalmol. 69, 2257–2265. https://doi.org/10.4103/ijo.IJO_3117_20

Dibas, A., Batabyal, S., Kim, S., Carlson, M., Mohanty, S., Sharif, N.A., 2024. Efficacy of Intravitreal Multi-Characteristic Opsin (MCO-010) Optogenetic Gene Therapy in a Mouse Model of Leber Congenital Amaurosis. J. Ocul. Pharmacol. Ther. 40, 702–708. https://doi.org/10.1089/jop.2024.0084

Didiano, D., Abner, J.J., Hinger, S.A., Flickinger, Z., Kent, M., Clement, M.A., Balaiya, S., Liu, Q., Dai, X., Levine, E.M., Patton, J.G., 2020. Induction of a proliferative response in the zebrafish retina by injection of extracellular vesicles. Exp. Eye Res. 200, 108254. https://doi.org/10.1016/j.exer.2020.108254

Dou, Y., Li, C., Li, L., Guo, J., Zhang, J., 2020. Bioresponsive drug delivery systems for the treatment of inflammatory diseases. J. Controlled Release 327, 641–666. https://doi.org/10.1016/j.jconrel.2020.09.008

Dunbar, C.E., High, K.A., Joung, J.K., Kohn, D.B., Ozawa, K., Sadelain, M., 2018. Gene therapy comes of age. Science 359, eaan4672. https://doi.org/10.1126/science.aan4672

Dunn, M.R., Jimenez, R.M., Chaput, J.C., 2017. Analysis of aptamer discovery and technology. Nat. Rev. Chem. 1, 0076. https://doi.org/10.1038/s41570-017-0076

Durmaz, E., Dribika, L., Kutnyanszky, M. and Mead, B., 2024. Utilizing extracellular vesicles as a drug delivery system in glaucoma and RGC degeneration. Journal of Controlled Release, 372, pp.209-220.

Editas Medicine Inc, 2022. Editas Medicine Announces Dosing of First Pediatric Patient in the BRILLIANCE Clinical Trial of EDIT-101 for LCA10.

Federica Ponti, Matilde Campolungo, , Clara Melchiori, , Nina Bono, ,, Gabriele Candiani, 2021. Cationic lipids for gene delivery: many players, one goal. Chem. Phys. Lipids 235, 105032. https://doi.org/10.1016/j.chemphyslip.2020.105032

Felgner, P.L., Gadek, T.R., Holm, M., Roman, R., Chan, H.W., Wenz, M., Northrop, J.P., Ringold, G.M., Danielsen, M., 1987. Lipofection: a highly efficient, lipid-mediated DNA-transfection procedure. Proc. Natl. Acad. Sci. 84, 7413–7417. https://doi.org/10.1073/pnas.84.21.7413

Fenner, B.J., Tan, T.-E., Barathi, A.V., Tun, S.B.B., Yeo, S.W., Tsai, A.S.H., Lee, S.Y.,

Cheung, C.M.G., Chan, C.M., Mehta, J.S., Teo, K.Y.C., 2022. Gene-Based Therapeutics for Inherited Retinal Diseases. Front. Genet. 12. https://doi.org/10.3389/fgene.2021.794805

Flockerzi, V., Frohman, M.A., Brook, S., Geppetti, P., Hofmann, F.B., Michel, M.C., Page, C.P., Rosenthal, W., Wang, K., 2017. Pharmacologic Therapy of Ocular Disease. Handb. Exp. Pharmacol., Corticosteroids and Anti-Complement Therapy in Retinal Diseases 242, 389. https://doi.org/10.1007/164_2016_22

Freeman, E.C., Weiland, L.M., Meng, W.S., 2013. Modeling the Proton Sponge Hypothesis: Examining Proton Sponge Effectiveness for Enhancing Intracellular Gene Delivery through Multiscale Modeling. J. Biomater. Sci. Polym. Ed. 24, 398–416. https://doi.org/10.1080/09205063.2012.690282

Fröhlich, E., 2012. The role of surface charge in cellular uptake and cytotoxicity of medical nanoparticles. Int. J. Nanomedicine 7, 5577–5591. https://doi.org/10.2147/IJN.S36111

Fu, X., Huu, V.A.N., Duan, Y., Kermany, D.S., Valentim, C.C.S., Zhang, R., Zhu, J., Zhang, C.L., Sun, X., Zhang, K., 2018. Clinical applications of retinal gene therapies. Precis. Clin. Med. 1, 5–20. https://doi.org/10.1093/pcmedi/pby004

Gao, X., Fan, X., Jiang, K., Hu, Y., Liu, Y., Lu, W., Wei, G., 2023. Intraocular siRNA Delivery Mediated by Penetratin Derivative to Silence Orthotopic Retinoblastoma Gene. Pharmaceutics 15, 745. https://doi.org/10.3390/pharmaceutics15030745

Gelfman, C.M., Grishanin, R., Bender, K.O., Nguyen, A., Greengard, J., Sharma, P., Nieves, J., Kiss, S., Gasmi, M., 2021. Comprehensive Preclinical Assessment of ADVM-022, an Intravitreal Anti-VEGF Gene Therapy for the Treatment of Neovascular AMD and Diabetic Macular Edema. J. Ocul. Pharmacol. Ther. 37, 181–190. https://doi.org/10.1089/jop.2021.0001

GenSight Biologics, 2022. A Phase 1/2a, Open-Label, Non-Randomized, Dose-Escalation Study to Evaluate the Safety and Tolerability of GS030 in Subjects With Retinitis Pigmentosa (Clinical trial registration No. NCT03326336). clinicaltrials.gov.

Ghanchi, F., Bourne, R., Downes, S.M., Gale, R., Rennie, C., Tapply, I., Sivaprasad, S., 2022. An update on long-acting therapies in chronic sight-threatening eye diseases of the posterior segment: AMD, DMO, RVO, uveitis and glaucoma. Eye 36, 1154–1167. https://doi.org/10.1038/s41433-021-01766-w

Ghodasra, D.H., Chen, A., Arevalo, J.F., Birch, D.G., Branham, K., Coley, B., Dagnelie, G., de Juan, E., Devenyi, R.G., Dorn, J.D., Fisher, A., Geruschat, D.R., Gregori, N.Z., Greenberg, R.J., Hahn, P., Ho, A.C., Howson, A., Huang, S.S., Iezzi, R., Khan, N., Lam, B.L., Lim, J.I., Locke, K.G., Markowitz, M., Ripley, A.-M., Rankin, M., Schimitzek, H., Tripp, F., Weiland, J.D., Yan, J., Zacks, D.N., Jayasundera, K.T., 2016. Worldwide Argus II implantation: recommendations to optimize patient

outcomes. BMC Ophthalmol. 16, 52. https://doi.org/10.1186/s12886-016-0225-1

Giannaccini, M., Giannini, M., Calatayud, M.P., Goya, G.F., Cuschieri, A., Dente, L., Raffa, V., 2014. Magnetic Nanoparticles as Intraocular Drug Delivery System to Target Retinal Pigmented Epithelium (RPE). Int. J. Mol. Sci. 15, 1590–1605. https://doi.org/10.3390/ijms15011590

Gonçalves, G.A.R., Paiva, R. de M.A., 2017. Gene therapy: advances, challenges and perspectives. Einstein 15, 369–375. https://doi.org/10.1590/S1679-45082017RB4024

Goswami, R., Subramanian, G., Silayeva, L., Newkirk, I., Doctor, D., Chawla, K., Chattopadhyay, S., Chandra, D., Chilukuri, N., Betapudi, V., 2019. Gene Therapy Leaves a Vicious Cycle. Front. Oncol. 9, 297. https://doi.org/10.3389/fonc.2019.00297

Grishanin, R., Vuillemenot, B., Sharma, P., Keravala, A., Greengard, J., Gelfman, C., Blumenkrantz, M., Lawrence, M., Hu, W., Kiss, S., Gasmi, M., 2019. Preclinical Evaluation of ADVM-022, a Novel Gene Therapy Approach to Treating Wet Age-Related Macular Degeneration. Mol. Ther. 27, 118–129. https://doi.org/10.1016/j.ymthe.2018.11.003

Guerin, E., Sheridan, C., Assheton, D., Kent, D., Wong, D., Grant, M., Hiscott, P., 2008. SDF1-alpha is associated with VEGFR-2 in human choroidal neovascularisation. Microvasc. Res. 75, 302–307. https://doi.org/10.1016/j.mvr.2007.12.001

Guo, S., Li, C., Wang, C., Cao, X., Liu, X., Liang, X.-J., Huang, Y., Weng, Y., 2024. pH-Responsive polymer boosts cytosolic siRNA release for retinal neovascularization therapy. Acta Pharm. Sin. B 14, 781–794. https://doi.org/10.1016/j.apsb.2023.09.001

Gurevich, E.V., Gurevich, V.V., 2015. Beyond traditional pharmacology: new tools and approaches. Br. J. Pharmacol. 172, 3229–3241. https://doi.org/10.1111/bph.13066

Gyroscope Therapeutics Limited, 2022. HORIZON: A Phase II, Open-label, Outcomes-assessor Masked, Multicentre, Randomised, Controlled Study to Evaluate the Safety and Efficacy of Two Doses of GT005 Administered as a Single Subretinal Injection in Subjects With Geographic Atrophy Secondary to Age-related Macular Degeneration (Clinical trial registration No. NCT04566445). clinicaltrials.gov.

Hadinoto, K., Sundaresan, A., Cheow, W.S., 2013. Lipid–polymer hybrid nanoparticles as a new generation therapeutic delivery platform: A review. Eur. J. Pharm. Biopharm. 85, 427–443. https://doi.org/10.1016/j.ejpb.2013.07.002

Hamon, A., García-García, D., Ail, D., Bitard, J., Chesneau, A., Dalkara, D., Locker, M., Roger, J.E., Perron, M., 2019. Linking YAP to Müller Glia Quiescence Exit in the Degenerative Retina. Cell Rep. 27, 1712-1725.e6. https://doi.org/10.1016/j.celrep.2019.04.045

Han, Z., Banworth, M.J., Makkia, R., Conley, S.M., Al-Ubaidi, M.R., Cooper, M.J., Naash, M.I., 2015. Genomic DNA nanoparticles rescue rhodopsin-associated retinitis pigmentosa phenotype. FASEB J. 29, 2535–2544.

https://doi.org/10.1096/fj.15-270363

Han, Z., Conley, S.M., Makkia, R.S., Cooper, M.J., Naash, M.I., 2012. DNA nanoparticle-mediated ABCA4 delivery rescues Stargardt dystrophy in mice. J. Clin. Invest. 122, 3221–3226. https://doi.org/10.1172/JCI64833

Herrmann, I.K., Wood, M.J.A., Fuhrmann, G., 2021. Extracellular vesicles as a next-generation drug delivery platform. Nat. Nanotechnol. 16, 748–759. https://doi.org/10.1038/s41565-021-00931-2

Heyde, M., Partridge, K.A., Oreffo, R.O.C., Howdle, S.M., Shakesheff, K.M., Garnett, M.C., 2010. Gene therapy used for tissue engineering applications. J. Pharm. Pharmacol. 59, 329–350. https://doi.org/10.1211/jpp.59.3.0002

Howell, G.R., Macalinao, D.G., Sousa, G.L., Walden, M., Soto, I., Kneeland, S.C., Barbay, J.M., King, B.L., Marchant, J.K., Hibbs, M., Stevens, B., Barres, B.A., Clark, A.F., Libby, R.T., John, S.W.M., 2011. Molecular clustering identifies complement and endothelin induction as early events in a mouse model of glaucoma. J. Clin. Invest. 121, 1429–1444. https://doi.org/10.1172/JCI44646

Huang, X., Chau, Y., 2021. Enhanced Delivery of siRNA to Retinal Ganglion Cells by Intravitreal Lipid Nanoparticles of Positive Charge. Mol. Pharm. 18, 377–385. https://doi.org/10.1021/acs.molpharmaceut.0c00992

Huang, X., Chau, Y., 2019. Investigating impacts of surface charge on intraocular distribution of intravitreal lipid nanoparticles. Exp. Eye Res. 186, 107711. https://doi.org/10.1016/j.exer.2019.107711

Huang, X., El-Sayed, M.A., 2010. Gold nanoparticles: Optical properties and implementations in cancer diagnosis and photothermal therapy. J. Adv. Res. 1, 13–28. https://doi.org/10.1016/j.jare.2010.02.002

Ideta, R., Tasaka, F., Jang, W.-D., Nishiyama, N., Zhang, G.-D., Harada, A., Yanagi, Y., Tamaki, Y., Aida, T., Kataoka, K., 2005. Nanotechnology-Based Photodynamic Therapy for Neovascular Disease Using a Supramolecular Nanocarrier Loaded with a Dendritic Photosensitizer. Nano Lett. 5, 2426–2431. https://doi.org/10.1021/nl051679d

Iqball, S., Beck, D.K., Devarajan, G., Khoo, C.P., O'Connor, D.M., Ellis, S., Guzman, E., Mitrophanous, K.A., Lad, Y., 2023. Lentiviral delivered aflibercept OXB-203 for treatment of neovascular AMD. Mol. Ther. Methods Clin. Dev. 30, 350–366. https://doi.org/10.1016/j.omtm.2023.07.001

Iriyama, A., Oba, M., Ishii, T., Nishiyama, N., Kataoka, K., Tamaki, Y., Yanagi, Y., 2011. Gene Transfer Using Micellar Nanovectors Inhibits Choroidal Neovascularization In Vivo. PLOS ONE 6, e28560. https://doi.org/10.1371/journal.pone.0028560

Jorstad, N.L., Wilken, M.S., Grimes, W.N., Wohl, S.G., VandenBosch, L.S., Yoshimatsu, T., Wong, R.O., Rieke, F., Reh, T.A., 2017. Stimulation of functional neuronal

regeneration from Müller glia in adult mice. Nature 548, 103–107. https://doi.org/10.1038/nature23283

Joselevitch, C., 2008. Human retinal circuitry and physiology. Psychol. Neurosci. 1, 141–165. https://doi.org/10.3922/j.psns.2008.2.008

Jumelle, C., Gholizadeh, S., Annabi, N., Dana, R., 2020. Advances and limitations of drug delivery systems formulated as eye drops. J. Controlled Release 321, 1–22. https://doi.org/10.1016/j.jconrel.2020.01.057

Kampik, D., Basche, M., Luhmann, U.F.O., Nishiguchi, K.M., Williams, J. a. E., Greenwood, J., Moss, S.E., Han, H., Azam, S., Duran, Y., Robbie, S.J., Bainbridge, J.W.B., Larkin, D.F., Smith, A.J., Ali, R.R., 2017. In situ regeneration of retinal pigment epithelium by gene transfer of E2F2: a potential strategy for treatment of macular degenerations. Gene Ther. 24, 810–818. https://doi.org/10.1038/gt.2017.89

Karl, M.O., Reh, T.A., 2010. Regenerative medicine for retinal diseases: activating endogenous repair mechanisms. Trends Mol. Med. 16, 193–202. https://doi.org/10.1016/j.molmed.2010.02.003

Kim, J., Kang, Y., Tzeng, S.Y., Green, J.J., 2016. Synthesis and application of poly(ethylene glycol)-co-poly(β-amino ester) copolymers for small cell lung cancer gene therapy. Acta Biomater. 41, 293–301. https://doi.org/10.1016/j.actbio.2016.05.040

Kleinman, M.E., Yamada, K., Takeda, A., Chandrasekaran, V., Nozaki, M., Baffi, J.Z., Albuquerque, R.J.C., Yamasaki, S., Itaya, M., Pan, Y., Appukuttan, B., Gibbs, D., Yang, Z., Karikó, K., Ambati, B.K., Wilgus, T.A., DiPietro, L.A., Sakurai, E., Zhang, K., Smith, J.R., Taylor, E.W., Ambati, J., 2008. Sequence- and target-independent angiogenesis suppression by siRNA via TLR3. Nature 452, 591–597. https://doi.org/10.1038/nature06765

Kohn, D.B., 2000. Gene Therapy for XSCID: The First Success of Gene Therapy. Pediatr. Res. 48, 578–578. https://doi.org/10.1203/00006450-200011000-00002

Kralik, J., van Wyk, M., Stocker, N., Kleinlogel, S., 2022. Bipolar cell targeted optogenetic gene therapy restores parallel retinal signaling and high-level vision in the degenerated retina. Commun. Biol. 5, 1–15. https://doi.org/10.1038/s42003-022-04016-1

Kumaran, N., Michaelides, M., Smith, A.J., Ali, R.R., Bainbridge, J.W.B., 2018. Retinal gene therapy. Br. Med. Bull. 126, 13–25. https://doi.org/10.1093/bmb/ldy005

Lauer, A.K., Campochiaro, P.A., Sohn, E.H., Kelleher, M., Harrop, R., Loader, J., Ellis, S., Mitrophanous, K., 2016. Phase I Safety and Tolerability results for RetinoStat®, a Lentiviral Vector Expressing Endostatin and Angiostatin, in Patients with Advanced Neovascular Age-Related Macular Degeneration. Invest. Ophthalmol. Vis. Sci. 57.

Li, J., Liu, F., Lv, Y., Sun, K., Zhao, Y., Reilly, J., Zhang, Y., Tu, J., Yu, S., Liu, X., Qin, Y., Huang, Y., Gao, P., Jia, D., Chen, X., Han, Y., Shu, X., Luo, D., Tang, Z., Liu, M.,

2021. Prpf31 is essential for the survival and differentiation of retinal progenitor cells by modulating alternative splicing. Nucleic Acids Res. 49, 2027–2043. https://doi.org/10.1093/nar/gkab003

Li, W., Chen, L., Gu, Z., Chen, Z., Li, Hong, Cheng, Z., Li, Hanmei, Zou, L., 2023. Co-delivery of microRNA-150 and quercetin by lipid nanoparticles (LNPs) for the targeted treatment of age-related macular degeneration (AMD). J. Controlled Release 355, 358–370. https://doi.org/10.1016/j.jconrel.2023.01.080

Lin, G., Revia, R.A., Zhang, M., 2021. Inorganic Nanomaterial-Mediated Gene Therapy in Combination with Other Antitumor Treatment Modalities. Adv. Funct. Mater. 31, 2007096. https://doi.org/10.1002/adfm.202007096

Lin, X., Wu, X., Chen, X., Wang, B., Xu, W., 2021. Intellective and stimuli-responsive drug delivery systems in eyes. Int. J. Pharm. 602, 120591. https://doi.org/10.1016/j.ijpharm.2021.120591

Lin, Y., Xu, C.L., Breazzano, M.P., Tanaka, A.J., Ryu, J., Levi, S.R., Yao, K., Sparrow, J.R., Tsang, S.H., 2020. Progressive RPE atrophy and photoreceptor death in KIZ-associated autosomal recessive retinitis pigmentosa. Ophthalmic Genet. 41, 26–30. https://doi.org/10.1080/13816810.2020.1723116

Lindsey, A.E., Powers, M.K., 2007. Visual behavior of adult goldfish with regenerating retina. Vis. Neurosci. 24, 247–255. https://doi.org/10.1017/S0952523806230207

Liu, L., Liu, Y., Xu, B., Liu, C., Jia, Y., Liu, T., Fang, C., Wang, W., Ren, J., He, Z., Men, K., Liang, X., Luo, M., Shao, B., Mao, Y., Xiao, H., Qian, Z., Geng, J., Dong, B., Mi, P., Jiang, Y., Wei, Y., Wei, X., 2018. Negative regulation of cationic nanoparticle-induced inflammatory toxicity through the increased production of prostaglandin E2 via mitochondrial DNA-activated Ly6C+ monocytes. Theranostics 8, 3138–3152. https://doi.org/10.7150/thno.21693

Liu, N.-P., Roberts, W.L., Hale, L.P., Levesque, M.C., Patel, D.D., Lu, C.-L., Jaffe, G.J., 1997. Expression of CD44 and Variant Isoforms in Cultured Human Retinal Pigment Epithelial Cells 11.

Longbottom, R., Fruttiger, M., Douglas, R.H., Martinez-Barbera, J.P., Greenwood, J., Moss, S.E., 2009. Genetic ablation of retinal pigment epithelial cells reveals the adaptive response of the epithelium and impact on photoreceptors. Proc. Natl. Acad. Sci. 106, 18728–18733. https://doi.org/10.1073/pnas.0902593106

Madkhali, O., Mekhail, G., Wettig, S.D., 2019. Modified gelatin nanoparticles for gene delivery. Int. J. Pharm. 554, 224–234. https://doi.org/10.1016/j.ijpharm.2018.11.001

Maeder, M.L., Stefanidakis, M., Wilson, C.J., Baral, R., Barrera, L.A., Bounoutas, G.S., Bumcrot, D., Chao, H., Ciulla, D.M., DaSilva, J.A., Dass, A., Dhanapal, V., Fennell, T.J., Friedland, A.E., Giannoukos, G., Gloskowski, S.W., Glucksmann, A., Gotta, G.M., Jayaram, H., Haskett, S.J., Hopkins, B., Horng, J.E., Joshi, S., Marco, E.,

Mepani, R., Reyon, D., Ta, T., Tabbaa, D.G., Samuelsson, S.J., Shen, S., Skor, M.N., Stetkiewicz, P., Wang, T., Yudkoff, C., Myer, V.E., Albright, C.F., Jiang, H., 2019. Development of a gene-editing approach to restore vision loss in Leber congenital amaurosis type 10. Nat. Med. 25, 229–233. https://doi.org/10.1038/s41591-018-0327-9

Mahabadi, N., Al Khalili, Y., 2022. Neuroanatomy, Retina, in: StatPearls. StatPearls Publishing, Treasure Island (FL).

Mains, J., Wilson, C.G., 2013. The Vitreous Humor As a Barrier to Nanoparticle Distribution. J. Ocul. Pharmacol. Ther. 29, 143–150. https://doi.org/10.1089/jop.2012.0138

Martens, T.F., Remaut, K., Deschout, H., Engbersen, J.F.J., Hennink, W.E., van Steenbergen, M.J., Demeester, J., De Smedt, S.C., Braeckmans, K., 2015. Coating nanocarriers with hyaluronic acid facilitates intravitreal drug delivery for retinal gene therapy. J. Controlled Release 202, 83–92. https://doi.org/10.1016/j.jconrel.2015.01.030

Massadeh, S., Al Aamery, M., 2016. Nano-materials for Gene Therapy: An Efficient Way in Overcoming Challenges of Gene Delivery. J. Biosens. Bioelectron. 07. https://doi.org/10.4172/2155-6210.1000195

Mauri, E., Perale, G., Rossi, F., 2018. Nanogel Functionalization: A Versatile Approach To Meet the Challenges of Drug and Gene Delivery. ACS Appl. Nano Mater. 1, 6525–6541. https://doi.org/10.1021/acsanm.8b01686

McClements, M.E., Staurenghi, F., MacLaren, R.E., Cehajic-Kapetanovic, J., 2020., Optogenetic Gene Therapy for the Degenerate Retina: Recent Advances. Front. Neurosci. 14, 1187. https://doi.org/10.3389/fnins.2020.570909

Milone, M.C., O'Doherty, U., 2018. Clinical use of lentiviral vectors. Leukemia 32, 1529–1541. https://doi.org/10.1038/s41375-018-0106-0

Mohan, S.P., Nagarajan, H., Vetrivel, U., Ramasubramanyan, S., 2024. Human Antigen R -mediated modulation of Transforming Growth Factor Beta 1 expression in retinal pathological milieu. Biochem. Biophys. Rep. 39, 101807. https://doi.org/10.1016/j.bbrep.2024.101807

Murakami, Y., Ikeda, Y., Nakatake, S., Miller, J.W., Vavvas, D.G., Sonoda, K.H., Ishibashi, T., 2015. Necrotic cone photoreceptor cell death in retinitis pigmentosa. Cell Death Dis. 6, e2038–e2038. https://doi.org/10.1038/cddis.2015.385

Nanoscope Therapeutics Inc., 2024. A Phase 2b Randomized, Double-Masked, Sham-Controlled, Study to Evaluate the Efficacy and Safety of Intravitreal Injection of MCO-010 Optogenetic Therapy in Adults With Retinitis Pigmentosa [RESTORE] (Clinical trial registration No. NCT04945772). clinicaltrials.gov.

Ouyang, X., Wang, X., Kraatz, H.-B., Ahmadi, S., Gao, J., Lv, Y., Sun, X., Huang, Y., 2020. A Trojan horse biomimetic delivery strategy using mesenchymal stem cells for PDT/PTT therapy against lung melanoma metastasis. Biomater. Sci. 8, 1160–1170.

https://doi.org/10.1039/C9BM01401B

Pandey, A.N., 2014. Retinoblastoma: An overview. Saudi J. Ophthalmol. 28, 310–315. https://doi.org/10.1016/j.sjopt.2013.11.001

Papanikolaou, E., Bosio, A., 2021. The Promise and the Hope of Gene Therapy. Front. Genome Ed. 3, 4. https://doi.org/10.3389/fgeed.2021.618346

Park, H.-J., Yang, F., Cho, S.-W., 2012. Nonviral delivery of genetic medicine for therapeutic angiogenesis. Adv. Drug Deliv. Rev. 64, 40–52. https://doi.org/10.1016/j.addr.2011.09.005

Park, Y., Shin, J., Park, J., Kim, S., Park, J.H., Kim, J., Kim, C.S., Chang, J.W., Schuurmans, C., Aubert, I., Chang, W.S., Eom, K., 2024. Focused Ultrasound as a Novel Non-Invasive Method for the Delivery of Gold Nanoparticles to Retinal Ganglion Cells. Transl. Vis. Sci. Technol. 13, 5. https://doi.org/10.1167/tvst.13.5.5

Paul, A., Hasan, A., Kindi, H.A., Gaharwar, A.K., Rao, V.T.S., Nikkhah, M., Shin, S.R., Krafft, D., Dokmeci, M.R., Shum-Tim, D., Khademhosseini, A., 2014. Injectable Graphene Oxide/Hydrogel-Based Angiogenic Gene Delivery System for Vasculogenesis and Cardiac Repair. ACS Nano 8, 8050–8062. https://doi.org/10.1021/nn5020787

Peeters, L., Sanders, N.N., Braeckmans, K., Boussery, K., Van de Voorde, J., De Smedt, S.C., Demeester, J., 2005. Vitreous: A Barrier to Nonviral Ocular Gene Therapy. Invest. Ophthalmol. Vis. Sci. 46, 3553–3561. https://doi.org/10.1167/iovs.05-0165

Perni, S., Prokopovich, P., 2017. Poly-beta-amino-esters nano-vehicles based drug delivery system for cartilage. Nanomedicine Nanotechnol. Biol. Med. 13, 539–548. https://doi.org/10.1016/j.nano.2016.10.001

Puliafito, C.A., Wykoff, C.C., 2019. Looking ahead in retinal disease management: highlights of the 2019 angiogenesis, exudation and degeneration symposium. Int. J. Retina Vitr. 5, 22. https://doi.org/10.1186/s40942-019-0174-y

Pupo, A., Fernández, A., Low, S.H., François, A., Suárez-Amarán, L. and Samulski, R.J., 2022. AAV vectors: The Rubik's cube of human gene therapy. Molecular Therapy, 30(12), pp.3515-3541.

Querques, G., Bocco, M.C.A., Soubrane, G., Souied, E.H., 2008. Intravitreal ranibizumab (Lucentis) for choroidal neovascularization associated with Stargardt's disease. Graefes Arch. Clin. Exp. Ophthalmol. 246, 319–321. https://doi.org/10.1007/s00417-007-0689-z

Rai, R., Alwani, S., Badea, I., 2019. Polymeric Nanoparticles in Gene Therapy: New Avenues of Design and Optimization for Delivery Applications. Polymers 11. https://doi.org/10.3390/polym11040745

Rajala, A., Wang, Y., Zhu, Y., Ranjo-Bishop, M., Ma, J.-X., Mao, C., Rajala, R.V.S., 2014. Nanoparticle-Assisted Targeted Delivery of Eye-Specific Genes to Eyes Significantly Improves the Vision of Blind Mice In Vivo. Nano Lett. 14, 5257–5263.

https://doi.org/10.1021/nl502275s

Regenxbio Inc., 2022. A Randomized, Partially Masked, Controlled, Phase 2b/3 Clinical Study to Evaluate the Efficacy and Safety of RGX-314 Gene Therapy in Participants With nAMD (ATMOSPHERE) (Clinical trial registration No. NCT04704921). clinicaltrials.gov.

Ren, X., Léveillard, T., 2022. Modulating antioxidant systems as a therapeutic approach to retinal degeneration. Redox Biol. 57, 102510. https://doi.org/10.1016/j.redox.2022.102510

Riley, M., Vermerris, W., 2017. Recent Advances in Nanomaterials for Gene Delivery—A Review. Nanomaterials 7, 94. https://doi.org/10.3390/nano7050094

Rodrigues, G.A., Lutz, D., Shen, J., Yuan, X., Shen, H., Cunningham, J., Rivers, H.M., 2018. Topical Drug Delivery to the Posterior Segment of the Eye: Addressing the Challenge of Preclinical to Clinical Translation. Pharm. Res. 35, 245. https://doi.org/10.1007/s11095-018-2519-x

Russell, S., Bennett, J., Wellman, J.A., Chung, D.C., Yu, Z.-F., Tillman, A., Wittes, J., Pappas, J., Elci, O., McCague, S., Cross, D., Marshall, K.A., Walshire, J., Kehoe, T.L., Reichert, H., Davis, M., Raffini, L., George, L.A., Hudson, F.P., Dingfield, L., Zhu, X., Haller, J.A., Sohn, E.H., Mahajan, V.B., Pfeifer, W., Weckmann, M., Johnson, C., Gewaily, D., Drack, A., Stone, E., Wachtel, K., Simonelli, F., Leroy, B.P., Wright, J.F., High, K.A., Maguire, A.M., 2017. Efficacy and safety of voretigene neparvovec (AAV2-hRPE65v2) in patients with RPE65-mediated inherited retinal dystrophy: a randomised, controlled, open-label, phase 3 trial. Lancet Lond. Engl. 390, 849–860. https://doi.org/10.1016/S0140-6736(17)31868-8

Sahel, J.-A., Boulanger-Scemama, E., Pagot, C., Arleo, A., Galluppi, F., Martel, J.N., Esposti, S.D., Delaux, A., de Saint Aubert, J.-B., de Montleau, C., Gutman, E., Audo, I., Duebel, J., Picaud, S., Dalkara, D., Blouin, L., Taiel, M., Roska, B., 2021. Partial recovery of visual function in a blind patient after optogenetic therapy. Nat. Med. 27, 1223–1229. https://doi.org/10.1038/s41591-021-01351-4

Santana-Armas, M.L., Tros de Ilarduya, C., 2021. Strategies for cancer gene-delivery improvement by non-viral vectors. Int. J. Pharm. 596, 120291. https://doi.org/10.1016/j.ijpharm.2021.120291

Shanghai BDgene Co., Ltd., 2022. A Safety and Efficacy Study of VEGFA-targeting Gene Therapy to Treat Refractory Retinal and Choroidal Neovascularization Diseases (Clinical trial registration No. NCT05099094). clinicaltrials.gov.

Shen, J., Kim, J., Tzeng, S.Y., Ding, K., Hafiz, Z., Long, D., Wang, J., Green, J.J., Campochiaro, P.A., 2020. Suprachoroidal gene transfer with nonviral nanoparticles. Sci. Adv. https://doi.org/10.1126/sciadv.aba1606

Sherpa, T., Fimbel, S.M., Mallory, D.E., Maaswinkel, H., Spritzer, S.D., Sand, J.A., Li, L.,

Hyde, D.R., Stenkamp, D.L., 2008. Ganglion cell regeneration following whole-retina destruction in zebrafish. Dev. Neurobiol. 68, 166–181. https://doi.org/10.1002/dneu.20568

Shinoe, T., Kuribayashi, H., Saya, H., Seiki, M., Aburatani, H., Watanabe, S., 2010. Identification of CD44 as a cell surface marker for Müller glia precursor cells. J. Neurochem. 115, 1633–1642. https://doi.org/10.1111/j.1471-4159.2010.07072.x

Shirley, J.L., Jong, Y.P. de, Terhorst, C., Herzog, R.W., 2020. Immune Responses to Viral Gene Therapy Vectors. Mol. Ther. 28, 709–722. https://doi.org/10.1016/j.ymthe.2020.01.001

Shmueli, R.B., Anderson, D.G., Green, J.J., 2010. Electrostatic Surface Modifications to Improve Gene Delivery. Expert Opin. Drug Deliv. 7, 535–550. https://doi.org/10.1517/17425241003603653

Shoval, A., Markus, A., Zhou, Z., Liu, X., Cazelles, R., Willner, I., Mandel, Y., 2019. Anti-VEGF-Aptamer Modified C-Dots—A Hybrid Nanocomposite for Topical Treatment of Ocular Vascular Disorders. Small 15, 1902776. https://doi.org/10.1002/smll.201902776

Singh, R.P., Elman, M.J., Singh, S.K., Fung, A.E., Stoilov, I., 2019. Advances in the treatment of diabetic retinopathy. J. Diabetes Complications 33, 107417. https://doi.org/10.1016/j.jdiacomp.2019.107417

Sivaprasad, S., Oyetunde, S., 2016. Impact of injection therapy on retinal patients with diabetic macular edema or retinal vein occlusion. Clin. Ophthalmol. Auckl. NZ 10, 939–946. https://doi.org/10.2147/OPTH.S100168

Song, R., Murphy, M., Li, C., Ting, K., Soo, C., Zheng, Z., 2018. Current development of biodegradable polymeric materials for biomedical applications. Drug Des. Devel. Ther. 12, 3117–3145. https://doi.org/10.2147/DDDT.S165440

Suk, J.S., Boylan, N.J., Trehan, K., Tang, B.C., Schneider, C.S., Lin, J.-M.G., Boyle, M.P., Zeitlin, P.L., Lai, S.K., Cooper, M.J., Hanes, J., 2011. N-acetylcysteine Enhances Cystic Fibrosis Sputum Penetration and Airway Gene Transfer by Highly Compacted DNA Nanoparticles. Mol. Ther. 19, 1981–1989. https://doi.org/10.1038/mt.2011.160

Sun, D., Schur, R.M., Sears, A.E., Gao, S.-Q., Vaidya, A., Sun, W., Maeda, A., Kern, T., Palczewski, K., Lu, Z.-R., 2020. Non-viral Gene Therapy for Stargardt Disease with ECO/pRHO-ABCA4 Self-Assembled Nanoparticles. Mol. Ther. 28, 293–303. https://doi.org/10.1016/j.ymthe.2019.09.010

Supe, S., Upadhya, A., Tripathi, S., Dighe, V., Singh, K., 2023. Liposome-polyethylenimine complexes for the effective delivery of HuR siRNA in the treatment of diabetic retinopathy. Drug Deliv. Transl. Res. 13, 1675–1698. https://doi.org/10.1007/s13346-022-01281-9

Szybalska, E.H., Szybalski, W., 1962. GENETICS OF HUMAN CELL LINES, IV.

DNA-MEDIATED HERITABLE TRANSFORMATION OF A BIOCHEMICAL TRAIT. Proc. Natl. Acad. Sci. U. S. A. 48, 2026–2034.

Takeuchi, T., Tagami, T., Fukushige, K., Ozeki, T., 2018. Useful properties of siRNA-coated gold nanoparticles as a mini-nanocarrier platform for intraocular administration. J. Drug Deliv. Sci. Technol. 47, 411–416. https://doi.org/10.1016/j.jddst.2018.06.009

Tan, G., Liu, D., Zhu, R., Pan, H., Li, J., Pan, W., 2021. A core-shell nanoplatform as a nonviral vector for targeted delivery of genes to the retina. Acta Biomater. 134, 605–620. https://doi.org/10.1016/j.actbio.2021.07.053

Thiruppathi, R., Mishra, S., Ganapathy, M., Padmanabhan, P., Gulyás, B., 2017. Nanoparticle Functionalization and Its Potentials for Molecular Imaging. Adv. Sci. 4, 1600279. https://doi.org/10.1002/advs.201600279

Travis, G.H., Christerson, L., Danielson, P.E., Klisak, I., Sparkes, R.S., Hahn, L.B., Dryja, T.P., Sutcliffe, J.G., 1991. The human retinal degeneration slow (RDS) gene: Chromosome assignment and structure of the mRNA. Genomics 10, 733–739. https://doi.org/10.1016/0888-7543(91)90457-P

Valdés-Sánchez, L., Borrego-González, S., Montero-Sánchez, A., Massalini, S., de la Cerda, B., Díaz-Cuenca, A., Díaz-Corrales, F.J., 2022. Mesoporous Silica-Based Nanoparticles as Non-Viral Gene Delivery Platform for Treating Retinitis Pigmentosa. J. Clin. Med. 11, 2170. https://doi.org/10.3390/jcm11082170

van Asten, F., Michels, C.T.J., Hoyng, C.B., van der Wilt, G.J., Klevering, B.J., Rovers, M.M., Grutters, J.P.C., 2018. The cost-effectiveness of bevacizumab, ranibizumab and aflibercept for the treatment of age-related macular degeneration—A cost-effectiveness analysis from a societal perspective. PLoS ONE 13, e0197670. https://doi.org/10.1371/journal.pone.0197670

Varela-Fernández, R., Díaz-Tomé, V., Luaces-Rodríguez, A., Conde-Penedo, A., García-Otero, X., Luzardo-Álvarez, A., Fernández-Ferreiro, A., Otero-Espinar, F.J., 2020. Drug Delivery to the Posterior Segment of the Eye: Biopharmaceutic and Pharmacokinetic Considerations. Pharmaceutics 12, 269. https://doi.org/10.3390/pharmaceutics12030269

Wang, A.L., Knight, D.K., Vu, T.T., Mehta, M.C., 2019. Retinitis Pigmentosa: Review of Current Treatment. Int. Ophthalmol. Clin. 59, 263–280. https://doi.org/10.1097/IIO.0000000000000256

Wang, J., Wang, H., Zhao, P., Chen, Z., Lin, Q., 2022. Hyperbranched-star PEI-g-PEG as a nonviral vector with efficient uptake and hypotoxicity for retinoblastoma gene therapy application. Colloid Interface Sci. Commun. 50, 100647. https://doi.org/10.1016/j.colcom.2022.100647

Wang, J.-H., Gessler, D.J., Zhan, W., Gallagher, T.L., Gao, G., 2024. Adeno-associated virus as a delivery vector for gene therapy of human diseases. Signal Transduct. Target.

Ther. 9, 78. https://doi.org/10.1038/s41392-024-01780-w

Wang, X., Yu, C., Tzekov, R.T., Zhu, Y., Li, W., 2020. The effect of human gene therapy for RPE65-associated Leber's congenital amaurosis on visual function: a systematic review and meta-analysis. Orphanet J. Rare Dis. 15, 49. https://doi.org/10.1186/s13023-020-1304-1

Wang, Y., Shahi, P.K., Wang, X., Xie, R., Zhao, Y., Wu, M., Roge, S., Pattnaik, B.R., Gong, S., 2021. In vivo targeted delivery of nucleic acids and CRISPR genome editors enabled by GSH-responsive silica nanoparticles. J. Controlled Release 336, 296–309. https://doi.org/10.1016/j.jconrel.2021.06.030

Wei, X., Shao, B., He, Z., Ye, T., Luo, M., Sang, Y., Liang, X., Wang, W., Luo, S., Yang, S., Zhang, S., Gong, C., Gou, M., Deng, H., Zhao, Y., Yang, H., Deng, S., Zhao, C., Yang, L., Qian, Z., Li, J., Sun, X., Han, J., Jiang, C., Wu, M., Zhang, Z., 2015. Cationic nanocarriers induce cell necrosis through impairment of Na+/K+-ATPase and cause subsequent inflammatory response. Cell Res. 25, 237–253. https://doi.org/10.1038/cr.2015.9

Widdowson, P., Ellis, S., Binley, K., Nork, M., Miller, P., Bantseev, V., McCulloh, R., Kan, O., Naylor, S., 2010. Ocular Tolerance of an Eiav Based Lentiviral Vector Treatment for Neovascular Age-Related Macular Degeneration (Retinostat®) in Rabbits and Nonhuman Primate Models. Invest. Ophthalmol. Vis. Sci. 51, 3104.

World Health Organization, 2019. World report on vision. World Health Organization, Geneva.

Xie, L., Han, Y., Liu, Y., Zhou, Y., Yu, J., von Brunn, A., Lei, J., 2023. Viral vector-based cancer treatment and current clinical applications. MedComm – Oncol. 2, e55. https://doi.org/10.1002/mog2.55

Xu, H., Chen, M., 2016. Targeting the complement system for the management of retinal inflammatory and degenerative diseases. Eur. J. Pharmacol. 787, 94–104. https://doi.org/10.1016/j.ejphar.2016.03.001

Yadav, K.S., Rajpurohit, R., Sharma, S., 2019. Glaucoma: Current treatment and impact of advanced drug delivery systems. Life Sci. 221, 362–376. https://doi.org/10.1016/j.lfs.2019.02.029

Yan, B., Viswanathan, S., Brodie, S.E., Deng, W.-T., Coleman, K.E., Hauswirth, W.W., Nirenberg, S., 2023. A clinically viable approach to restoring visual function using optogenetic gene therapy. Mol. Ther. Methods Clin. Dev. 29, 406–417. https://doi.org/10.1016/j.omtm.2023.05.005

Yu, H., Yang, Z., Li, F., Xu, L., Sun, Y., 2020. Cell-mediated targeting drugs delivery systems. Drug Deliv. 27, 1425–1437. https://doi.org/10.1080/10717544.2020.1831103

Zhang, L., Qiang, W., Li, M.-Q., Wang, S.-J., Jia, W., Wang, R., Bai, S.-W., Wang, Q.-F., Wang, H.-Y., 2024. A drug delivery system of HIF-1α siRNA nanoparticles loaded by

mesenchymal stem cells on choroidal neovascularization. Nanomed. 19, 2171–2185. https://doi.org/10.1080/17435889.2024.2393075

Zhang, X., Wu, Q., Yang, S., 2017. Effects of siRNA-mediated HIF-1α gene silencing on angiogenesis in osteosarcoma. Pak. J. Med. Sci. 33, 341–346. https://doi.org/10.12669/pjms.332.12587

Zhang, Y., Sun, T., Jiang, C., 2018. Biomacromolecules as carriers in drug delivery and tissue engineering. Acta Pharm. Sin. B 8, 34–50. https://doi.org/10.1016/j.apsb.2017.11.005

Zhou, W., Chai, Y., Lu, S., Yang, Q., Tang, L., Zhou, D., 2024. Advances in the study of tissue-engineered retinal pigment epithelial cell sheets. Regen. Ther. 27, 419–433. https://doi.org/10.1016/j.reth.2024.04.008

CHAPTER THREE

In Vitro Evaluation of the Efficacy of a Polymer-Lipid Conjugated Cationic Nanosystem for Enhanced Gene Delivery

3. Introduction

DNA holds a considerable amount of information regularly decrypted to drive biological processes essential for life. Key environmental and genetic factors influence our phenotypic and genotypic makeup, ultimately shaping our predisposition to certain diseases. During cell division (meiosis, mitosis), gamete formation and development, harmful mutations may be introduced or inherited, manifesting as severe diseases. Considerable efforts have been made to develop treatments for inherited diseases such as posterior segment eye diseases (i.e. retinoblastoma, retinitis pigmentosa and age related macular degeneration) with limited therapeutic success. These include chemotherapeutics, protein therapies (e.g. Lucentis (ranibizumab) and Avastin (bevacizumab)) and surgery procedures, however, none of these are capable of tackling the underlying cause of the diseases (Goswami et al., 2019). Therefore, the investigation of alternative therapeutic approaches remains essential in addressing these conditions with a high degree of specificity.

The opportunity to manipulate the human genome through localised genetic modifications can serve as a replacement for conventional therapies, as it has unbridled promise in overcoming associated shortcomings (Massadeh and Al Aamery, 2016). To realise the full therapeutic potential of gene therapy, the development of advanced delivery vehicles is imperative. Exemplary gene delivery systems proficiently circumvent challenges such as immunogenicity, rapid clearance by the reticuloendothelial system (RES), low bioavailability (Li and Huang, 2009; Wang et al., 2023), instability and susceptibility to nucleases (Hill et al., 2016), which are intrinsic to the use of genetic materials. Notably, the effectiveness and safety of gene therapies heavily relies on the chosen vector or delivery system. While many FDA-approved gene therapies employ viral vectors due to their high tropism, transfection efficiency and wide investigation, they are often associated with immunogenicity, high production costs, and limited cargo capacity (Bulcha et al., 2021a; Zhao et al., 2021). Of significant concern is the propensity of some viral vectors, lentivirus and retrovirus in particular, to cause insertional mutagenesis resulting in the activation of proto-oncogenes and inactivation of tumor suppressors (Fan and Johnson, 2011). This underscores the importance of developing safe, cost-effective, and efficient non-viral delivery systems for gene therapy.

Lipid and polymer-based nanosystems have demonstrated substantial promise in overcoming some of the limitations associated with viral vectors (Raana et al., 2020; Wang et al., 2023). They have the potential to protect genetic material from degradation by nucleases,

facilitate cellular uptake, promote cytosolic release of encapsulated genetic material, and support nuclear translocation. Non-viral vectors commonly employ cationic lipids (e.g. DOTAP and DOTMA), polymers (Poly (β-amino esters) and PEI), and peptides (TAT and PLL) (Alfei, 2023; Ma et al., 2021). These spontaneously assemble with nucleic acid via electrostatic interactions, forming gene delivery complexes (Federica Ponti et al., 2021). Salient non-viral vector based gene therapies include the SARS COVID-19 vaccines Pfizer-BioNTech (Comirnaty) and Moderna (Spikevax). These are lipid based nanosystems for the delivery of mRNA encoding a membrane anchored, perfusion stabilised full length SARS-CoV-2 spike protein (BNT162b2 - Pfizer-BioNTech and mRNA-1273 - Moderna) (Wilson and Geetha, 2022). Although advances in these two vaccines exponentially expounded our advances in the development of mRNA-lipid based vaccines, further optimisation of the nanosystem was still required to reduce its immunogenicity, improve target specificity, enhance stability and translational efficiency, including storage conditions. Unlike lipid nanoparticles, polymeric based delivery vehicles have a significantly more improved stability and higher transfection efficiency *in vitro* and *in vivo* (Parveen et al., 2023). The HIV therapeutic vaccine candidate, DermaVir is one such gene therapy system utilising polymers for the delivery of a plasmid encoding 15 HIV-1 antigens for the priming of T lymphocytes and strengthening the body's immune response to infection (Casper et al., 2023; Lisziewicz et al., 2012). DermaVir is formulated using a 22kDa PEI polymer conjugated to mannobiose enabling its delivery via an occlusive skin patch. Interestingly, stability studies proved promising results for DermaVir, showing that it retained its properties for an extended amount of time (Casper et al., 2023).

The versatility offered by non-viral vectors enables researchers to modify and make them adaptable for specific therapeutic applications. Specifically, the customisable nature of polymers enables the integration of essential functionalities: pH, temperature and redox responsiveness, which can ensure site specific delivery, tunable degradation and controlled/sustained release of genetic cargo. Importantly, functional groups on polymers can further enable the conjugation of targeting ligand, antibodies or even aptamers endowing the delivery nanosystems with extensive functionality. The advantage of using polymers in gene delivery design can specifically be noted through the use of hyaluronic acid (HA), which does not only have multiple functional groups for functionalisation, but also has ligand capabilities (Almalik et al., 2013).

This study therefore presents the design of a high molecular weight HA-based cationic amphiphilic nanosystem for plasmid DNA (pcDNA6.2-EmGFP, described in section 3.1.3) delivery. HA has biocompatible and biodegradable properties which render it an ideal polymer for therapeutic delivery. Moreover, HA-based carrier systems hold the potential to target CD44 receptors, which are overexpressed in cancer stem cells and damaged retinal

pigment epithelial cells (Chandola et al., 2019; Yaghobi et al., 2021). The complexation of negatively charged genetic material with anionic HA can pose challenges, to overcome these, HA was modified using 2-aminobenzimidazole (2AB), resulting in a reduction of its negative charge density. The complexation of negatively charged genetic material with anionic hyaluronic acid (HA) can be challenging due to electrostatic repulsion. To address this, HA was chemically modified by conjugation with 2-aminobenzimidazole (2AB), effectively reducing its overall negative charge density. Notably, 2AB and its derivatives possess anti-inflammatory, antibacterial, and antioxidant properties (Javahershenas et al., 2024) thereby imparting multifunctional capabilities to the resulting nanosystem. Moreover, the presence of reactive functional groups (amides) in 2AB enables further modification and functionalization of the resulting copolymer, an important feature for achieving targeted and efficient gene delivery. Additionally, following endosomal uptake, the acidic environment within the endosome leads to protonation of the amide groups, triggering the proton sponge effect (Mehta et al., 2024). This effect promotes osmotic swelling and subsequent disruption of the endosomal membrane, thereby facilitating the efficient release of the genetic cargo into the cytoplasm (Mehta et al., 2024; Xu et al., 2021). Furthermore, 2AB introduces cationic sites that promote electrostatic interactions with nucleic acids, thereby enhancing nucleic acid entrapment and delivery efficiency. However, it should be noted that these are not anticipated to promote nuclear translocation, which typically requires the inclusion of a nuclear localization signal in the genetic material sequence utilised (Redrejo-Rodríguez et al., 2012). Subsequently, the HA-2AB complex underwent further modification with oleylamine (OLA), an unsaturated fatty amine whose primary amine functional group enables its use in the synthesis and functionalization of polymers, particularly for nanoparticle formation. Its selection was based on reported roles in controlling nanoparticle size and morphology, as well as preventing aggregation both during and after synthesis (Mourdikoudis et al., 2022). Thus conugation of OLA to the copolymer, HA-2AB, lead to the formation of an amphiphilic cationic delivery nanosystem capable of self-assembling with pcDNA6.2-EmGFP. This multifunctional nanosystem complex could hold the potential to enhance the residence time of the nanosystem and promote DNA bioavailability. This chapter primarily focused on the optimisation of pcDNA6.2-EmGFP entrapment efficiency and transfection via the nanosystem, particularly with reference to retinal pigment epithelial (RPE) cells and the Human Embryonic Kidney (HEK) 293 cell line. Various polymer-to-pcDNA6.2-EmGFP ratios were evaluated for biocompatibility, GFP expression and sustained release.

3.1. Experimental section

Materials: plasmid DNA (pcDNATM6.2/c-EmGFP/YFP-DEST/pcDNA6.2-EmGFP - 7442 bp) (Thermo Fisher Scientific, South Africa), DH5α competent cells (Promega, Madison), NucleoBond Xtra Midi plasmid extraction kit (Mecherey-Nagel, Separations, South Africa),

Ampicillin and Luria-Bertani broth (ThermoFischer, South Africa). Hyaluronic acid (HA) sodium salt from *Streptococcus equi* (85 kDa) (Sigma-Aldrich, South Africa), 2-Aminobenzimidazole (place), N-(3-dimethylaminopropyl)-N'-ethylcarbodiimide hydrochloride (EDC) and N-hydroxysuccinimide (NHS) (Sigma-Aldrich, South Africa). Tris-acetate-EDTA (TAE) Buffer (10 x) (place,), Sterile water (DNAse, RNAse-free) (Merck, South Africa), 1Kbp Top DNA Ladder, Agarose, ethidium bromide, DNaseI and BamHI (Thermo Fisher Scientific, South Africa). Human embryonic kidney cells (HEK 293) and retinal epithelial primary (hREP) cells, Dulbecco's Modified Eagle's Medium (DMEM)/Ham′s Nutrient Mixture F12 (1:1) medium (Sigma Aldrich, South Africa), penicillin/streptomycin, fetal bovine serum (FBS), Trypsin-EDTA and 3-[4,5-dimethylthiazol-2-yl]-2,5-diphenyltetrazolium bromide (MTT). Reagents and glassware were autoclaved where necessary before use.

3.1.1. Synthesis of the amphiphilic cationic copolymer

3.1.1.1. Sodium hyaluronate conversion

To aid in progressive chemical reactions, sodium hyaluronate was converted to its acidic form, HA, through dialysis in 0.3 M HCl solution. Briefly, sodium hyaluronate (1 g) was dissolved in 100 mL deionised water to form a clear viscous solution. This was dialysed (MWCO:12 kDa) for 24 hours against 3 L of a 0.3 M HCl solution and later washed in deionised water. Following conversion, HA solution was recovered by lyophilisation in a freeze-dryer (Labconco Freeze-Dry Systems, Labconco Corp., Kansas City, MO, USA).

3.1.1.2. Synthesis of HA-2AB conjugates

HA was chemically conjugated to 2-aminobenzimidazole (2AB) using EDC/NHS chemistry. To achieve 50% degree of substitution, 1 g of HA was dissolved in dimethylsulfoxide (DMSO) to form a clear solution. Subsequently, EDC and NHS were added and left to react at room temperature under stirring for 30 minutes, following this, 2-AB (198 mg) was added to the reaction and stirred for 16 hours. The final mixture was dialysed using cellulose dialysis membrane (MWCO ~ 12 -14 kDa) against deionised water for 24 hours. The purified product was then lyophilised and stored at room temperature (yield: white fibrous product).

3.1.1.3. Quaternisation of HA-2AB (synthesis of a cationic copolymer)

To facilitate nucleic acid entrapment via electrostatic interaction between the pDNA and the nanosystem, the HA-2AB conjugate was quarternised (cationised) using iodoethane. The copolymer HA-2AB (100 mg) was dissolved in DMSO and reacted with iodoethane (53 µL) for 14 hours at room temperature to form the cationic copolymer ($HA\text{-}2AB^{+}$) via the conversion of 2-AB amide groups into quaternary ammonium salts. The reaction was dialysed against deionised water for 24 hours using cellulose dialysis membrane (MWCO ~ 12 -14 kDa).

3.1.1.4. Synthesis of cationic self-assembling nanosystem (HA-2AB$^+$-OLA)

To synthesise the hybrid self-assembling nanosystem, an EDC/NHS two-step reaction was used to conjugate olelyamine to carboxylic acid groups of HA-2AB$^+$. In line with the aim of this study, OLA was chosen for its ability to contribute to the formation of biomimetic structures. Specifically, its hydrophobic alkyl tail and reactive amine group which allows for conjugation with the hydrophobically modified HA-2AB copolymer, facilitating the formation of self-assembling, vesicle-like nanoparticles that resemble cell membranes (Mourdikoudis et al., 2022). A grafting ratio of 33% was targeted. To achieve this, HA-2AB$^+$ (100 mg) was completely dissolved in DMSO, subsequently, EDC (133.5 mg) and NHS (160 mg) were added, and the reaction was left for 30 minutes, following which oleylamine (227.6 µL) was added and left under stirring for 36 hours. The reaction mixture was dialysed against deionised water for 24 hours using cellulose dialysis membrane (MWCO ~ 3.5 kDa) to purify the copolymer. Furthermore, the solution was freeze dried to obtain HA-2AB+-OLA conjugate (nanosystem).

3.1.2. Physicochemical characterisation of the HA-2AB$^+$-OLA copolymer

To explicate the chemical and physical properties of the synthesised polymer conjugate, multiple analytical techniques were utilised. ^{1}H and ^{13}C nuclear magnetic resonance (NMR) spectroscopy was carried out on a Bruker 400 MHz spectrometer (Bruker Corporation., USA) to determine the degree of modification of HA. The parent compounds and final product were prepared by dissolution in the appropriate solvent at room temperature. The samples were then transferred to 5 mm NMR tubes for acquisition of ^{1}H and ^{13}C spectra. Fourier transform infrared (FTIR) spectroscopy analysis was performed to confirm the formation of the HA-2AB+-OLA conjugate and to determine the chemical composition of the synthesised copolymer. Analysis was conducted using the Perkin Elmer Spectrum 2000 FTIR spectrometer with a MIRTGS detector (PerkinElmer Spectrum 100, Llantrisant, Wales, UK). To determine the crystallinity of the conjugate, X-ray diffraction spectroscopy was conducted (RIGAKU MiniFlex, RIGAKU Inc., Tokyo, Japan) at a scanning speed of 2°/min in the 2θ range of 10–90°. The degree of crystallinity/crystallinity index (%CI): I_c - intensity of crystalline peak and I_a - intensity of amorphous peak;

$$CI = \frac{Ic}{Ia} \times 100 \quad (3.1)$$

interplanar spacing within the conjugate (Braggs law): *d* - interplanar spacing, order of diffraction, diffraction peak at an angle (θ), X-ray wavelength (λ)

$$n\lambda = 2d\,sin\theta \quad (3.2)$$

and crystallite size (τ): D - Crystallite size (in nm), K - Scherrer constant, β = FWHM of the peak and θ = Bragg angle

$$D = \frac{K\lambda}{\beta cos\theta} \quad (3.3)$$

were determined using XRD data and Equation 3.1, 3.2 and 3.3

To ascertain the composition and thermal stability of the synthesised polymer, thermogravimetric analysis (TGA) was conducted, using Thermogravimetric Analyzer TGA 4000 (PerkinElmer Life And Analytical Sciences Inc., Waltham, MA, USA). Samples were weighed out and placed in crucibles. TGA analysis was performed under nitrogen, at a heating rate of 10 °C/min over a 30-900 °C range. Finally, differential scanning calorimetry (DSC) was also used to determine the thermal stability and compatibility of the compounds used in the synthesis of the polymer. A DSC-1 with STARe Thermal Analysis software (Mettler Toledo, Switzerland) was used. Samples were weighed out and placed in aluminium crucibles, sealed and heated at 30-300 °C, heating range 10 °C/min under constant nitrogen. The reference standard used was an empty aluminium crucible.

3.1.3. Isolation and Purification of pcDNA6.2-EmGFP from Transformed *Escherichia coli*

The GFP-expressing pcDNA6.2-EmGFP construct was obtained in a vial from ThermoFischer (Promega™). The pcDNA™6.2/c-EmGFP-DEST vector was selected as the model genetic material due to its accessibility, non-toxic fluorescent marker properties, and compatibility with standard transfection protocols, providing a reliable platform for evaluating gene delivery efficiency in ocular tissues. To amplify the plasmid for optimisation and downstream applications, XL10 gold competent cells were used for transformation and propagation of the plasmid according to the manufacturer's instructions. The transformed plasmid in bacterial suspension was streaked onto LB agar ampicillin (100 ug/mL) plates, and the plates were incubated at 37 °C for 18 h. A single colony from the plate was inoculated in 10 mL of LB media supplemented with ampicillin (50 µg/mL), and the starter culture was grown for 16 h with shaking at 37 °C (300 rpm). Next, 1 mL of the starter culture was added to 500 mL of LB-ampicillin (50 µg/mL) media and incubated at 37 °C for 18 h with shaking at 300 rpm. The pcDNA6.2-EmGFP construct was extracted and purified from the bacterial culture using Macherey-Nagel Nucleospin Plasmid Kit (Separations, South Africa) according to the manufacturer's protocol. The final pcDNA6.2-EmGFP concentration and purity were measured using the Nanodrop using the 260/280 ratio and ran on a 0.8 % agarose gel using 80 to 100 V.

3.1.4. Preparation and characterisation of nano-polyplex Formulation: pcDNA6.2-EmGFP loaded nanosystem

HA-2AB^{+}-OLA/pcDNA6.2-EmGFP nanoparticles (henceforth referred to as the nano-polyplex) were prepared by self assembly and electrostatic interaction of HA-2AB+-OLA with pcDNA6.2-EmGFP at different N/P ratios (N:P 1,5, 10 to 40). N:P ratios were defined as the molar ratio of the cationic groups (HA-2AB^{+}-OLA): anionic groups in the plasmid DNA backbone (phosphates). Stock solutions of HA-2AB^{+}-OLA (1 mg/mL) and pcDNA6.2-EmGFP(1 mg/mL) were diluted at predetermined concentrations based on the N:P ratios mentioned above using nuclease free water. The nano-polyplex system was vortexed for 30 seconds and incubated at room temperature to allow sufficient time for complexes to form completely. Complexation of HA-2AB^{+}-OLA nanosystem with pcDNA6.2-EmGFP into nano-polyplexes was verified by agarose gel electrophoresis, Transmission/Scanning electron microscopy (SEM & TEM) and Dynamic light scattering (DLS). For each of the following analyses, nanoparticles were prepared fresh each time.

The size, zeta potential, and stability of the prepared nanoparticles were determined using dynamic light scattering (DLS) employing a Zetasizer NanoZS (Malvern Instruments Ltd, Malvern, Worcestershire, UK). The HA-2AB^{+}-OLA nanosystem was filtered before pcDNA6.2-EmGFP complexation using a 0.22 µm filter.DLS measurements were conducted at a particle count of > 150 kcounts/s, followed by analysis of the size and zeta potential using the Zetasizer NanoZS. Nano-polyplex size distribution and zeta potential were measured, with consideration given to the intensity-weighted relative frequency. The structural, morphological and dimensional characterisation of the nano-polyplex was determined by transmission electron microscopy (TEM) (TEM, Hillsboro, OR, USA) and scanning electron microscopy (SEM) (ZEISS Electron Microscopy, Carl Zeiss Microscopy Ltd., Cambridge, UK) at a 50000 magnification. For TEM, 20 µL of the nano-polyplex suspension was placed on the TEM copper grid following ultrasonication. Negative staining of the grid was conducted using 2% uranyl acetate (pH 4.2 to 4.5) to enable visualisation of the nanoparticles under a transmission electron microscope. The copper grid was dried at room temperature and nanoparticle images were acquired. Samples for Scanning electron microscopy (SEM) were prepared by pipetting a suspension of the nanocomplex onto a SEM stub, the sample was dried and subsequently coated with 2x gold palladium before viewing at 60 KX using a scanning electron microscope.

3.1.5. Entrapment/Gel retardation analysis and Encapsulation efficiency

Following incubation at room temperature for 1 hour as previously stated, the different N/P ratio nano-polyplex systems along with controls, namely, free pcDNA6.2-EmGFP and

non-loaded nanosystem (HA-2AB$^+$-OLA) were loaded on 1% agarose gel to determine the entrapment or retardation efficiency of the nano-polyplex. Gels were prepared by heating 1% agarose in 1x Tris borate EDTA (TBE) buffer (Thermo Fisher Scientific, South Africa), adding 2 µL ethidium bromide following cooling and poured into casting trays to solidify. The samples were mixed with 6x DNA loading dye (New England Biolabs, South Africa). An electrical potential of 100V was applied to the gels for 40 minutes, and images captured using ChemiDoc XRS + gel imaging system (Bio-Rad Laboratories, USA). Subsequently, encapsulation efficiency was assessed by measuring the amount of unbound pcDNA6.2-EmGFP following entrapment by the nanosystem. Briefly, respective weight ratios of pcDNA6.2-EmGFP: nanosystem were prepared, the nano-polyplexes were vortexed and incubated at room temperature for 30 minutes. Samples were then centrifuged at 10 000 x g for 30 minutes and the supernatant analysed using the Quant-iT PicoGreen kit according to manufacturer's instructions. Fluorescence was measured using a microplate reader (Victor X3, PerkinElmer, Waltham, MA, USA), with excitation and emission wavelengths of 480 and 520 nm. The linear calibration curve of pcDNA (F = 79.8*x*+178: R^2 0.995) was used to determine the amount of pcDNA6.2-EmGFP and the equation below was used to indirectly determine the amount of unloaded vs loaded pcDNA

$$Encapsulation\ Efficiency\ = \frac{Amount\ of\ entrapped\ pcDNA}{Total\ amount\ of\ loaded\ pcDNA} \times 100 \qquad (3.4)$$

3.1.6. Nuclease Protection assay and pDNA stability

The degree of protection afforded by HA-OLA-2AB$^+$ nanosystem on the incorporated pcDNA6.2-EmGFP was assessed by incubating the nano-polyplex at different N/P ratios and pcDNA6.2-EmGFP (positive control) with 1 unit of DNase I per µg DNA in DNase buffer (100mM Tris/HCl, 20mM $CaCl_2$, 2mM $MgCl_2$) for 1 hour at 37 °C. Subsequently, 6X DNA loading dye was added to the samples, this includes samples whereby the entrapped DNA was de-complexed from the nanosystem (to assess the integrity of pcDNA6.2-EmGFP following enzyme digestion), the samples were electrophoresed at 100 V for 60 minutes on a 1% agarose gel to determine the degree of protection from nucleases (DNaseI).

3.1.7. *In vitro* release studies of the nano-polyplex system

To study the *in vitro* release profile of the nano-polyplex system, 1mg of the nanosystem was dispersed in phosphate buffer saline (pH 7.2) to mimic normal physiological conditions. The nanoparticles were loaded with 1 µg of pcDNA6.2-EmGFP in a final volume of 500 µL of nanosystem loaded in 1.5 ml Eppendorf tube and then shaken at 37 °C and 300 rpm. At predetermined time points, the tubes were removed from the incubator and centrifuged at 13 000 rpm for 10 minutes and the supernatants aspirated to quantify the amount of

pcDNA6.2-EmGFP released using Quant-iT PicoGreen assay (Thermofisher, South Africa) as per manufacturer's instructions. Background readings were corrected using the centrifuged supernatants from the control group consisting of free pcDNA6.2-EmGFP and non-loaded HA-OLA-2AB^{+} nanosystem.

3.1.8. Stability studies

Storage stability studies of the nano-polyplex systems were carried out at 4 °C and 25 °C for 28 days. After 28 days, an aliquot of the loaded nanoparticles was analysed for stability by looking at the particle size, zeta potential, encapsulation efficiency and pcDNA6.2-EmGFP integrity using gel electrophoresis. Data of the loaded nanoparticles overtime was compared across storage conditions and time points to evaluate ideal storage conditions for the nanoparticles.

3.1.9. Cell culture

Human Embryonic Kidney (HEK 293) cells and Human Retinal Pigment Epithelial (hRPE) cells were cultured in Dulbecco's Modified Eagle Medium (DMEM) and Dulbecco's Modified Eagle Medium/Nutrient Mixture F-12 (DMEM/F12) respectively, supplemented with 10% fetal bovine serum, 100 mg/mL streptomycin, and 100 U/mL penicillin (Thermofisher, South Africa). Cells were maintained in a humidified incubator at 37 °C and 5% CO_2.

3.1.10. Cell cytotoxicity

To evaluate the toxic effects of the different N:P ratio formulations of the nano-polyplex systems, HEK 293 cells were selected as the model cell line due to their reliable and reproducible behaviour as they ensure consistency in results. Briefly, HEK 293 and hRPE cells were grown in complete cell medium to 80% - 90% confluence and seeded into 96 well plates at a density of 1×10^4 cells per well in 0.1 mL of complete cell medium for 24 h to allow adequate cellular adherence. Subsequently, the different N:P ratio formulations were added into each well and the untreated groups served as positive controls and media only groups as blank control groups. The cells were incubated for 48 and 72 hours, subsequently, MTT assay was performed using the MTT Cell Proliferation Kit I (Roche, Basel, Switzerland). Briefly, 10 µL of MTT stock solution (5 mg/mL) was added to each well and incubated for 4 hours at 37 °C in 5% CO_2 (under humid conditions), followed by the addition of 100 µL of solubilising agent (acid-isopropanol; 0.04 N HCl in isopropanol) to dissolve the formed formazan crystals and incubated overnight at 37 °C in 5% CO_2. Absorbance was measured spectrophotometrically at 570 nm with reference at 620 nm using a multimodal microplate reader (Victor X3, PerkinElmer, Waltham, MA, USA). The absorbance measurements were

computed (mean ± standard deviation) and % cell viability was calculated and compared with untreated control (100%) using the following equation:

$$\%\ Cell\ viability\ =\ \frac{Abs\ (treated\ sample)}{Abs\ (Control)} \times 100 \quad (3.5)$$

where *Abs (treated sample)* is test absorbance, *Abs (control)* is positive absorbance in nm.

3.1.11. *In vitro* cell transfection and Fluorescent cell imaging

Transfection studies are essential in understanding gene delivery, release, expression and the transfection efficiency of a nanosystem. The transfection capacity of the different N:P ratios of the nano-polyplex systems was evaluated in HEK 293 and hRPE cells using the GFP expressing vector, pcDNA6.2-EmGFP. Following growth of cells in complete medium, the cells were seeded into 96 well plates at a density of 1–4 × 10^4 per well so as to ensure cells are 70 - 90% confluent before transfection and maintained in 100 µl of complete medium overnight. Subsequently, lipofectamine (following manufacturer's protocol), N:P 10 - 40 and 1 µg pcDNA6.2-EmGFP were prepared and added into each well with seeded cells and incubated for 4 hours in serum-free medium. Thereafter, minimal media was replaced with complete medium and cells were incubated for 48 hours post transfection. Detection of GFP expression following transfection was detected using the Celina S (Logos Biosystems, South Korea) fluorescence microscope with brightfield, fluorescent and merged images taken using 4x magnification and GFP- filter (Emission 475 nm and excitation 509 nm). All fluorescent images were taken under the same exposure and analysed using Image J software. Transfection efficiency and fluorescence intensity of the transfected cells versus control cells was measured using Image J software, additionally, transfected cells were further analysed using Flow cytometry for a more accurate assessment of transfection efficiency.

3.1.12. Flow cytometry

Following 48 hours of transfections, cells were harvested and prepared for flow cytometry analysis. Thoroughly, cells were detached using trypsin-EDTA and collected by centrifugation. The cell pellet was washed twice with PBS using centrifugation and later resuspended in 0.5 mL PBS (1 × 10^6 cells/mL). For GFP fluorescence detection, the BD LSR II flow cytometer (BD Biosciences, San Jose, CA) was used and set to alexa fluor 488 excitation laser and 510–530 nm emission filter. Instrument calibration was conducted using untransfected cells as the negative control (baseline autofluorescence) and lipofectamine 3000 transfected cells as the positive control. For each measurement, 30, 000 events were recorded and the data analysed using FACSDiva software (BD Biosciences, San Jose, CA).

3.1.13. Real-time quantitative pCR for emGFP expression *in vitro*

Following transfection of HEK 293 and hRPE cells by lipofectamine 3000 and Nanopolyplex system as detailed in section 3.1.9.2, cells were washed with PBS and detached using trypsin. Trypsin was deactivated using cell culture media and centrifuged. Pelleted cells were then stored in DNA/RNA Shield (Inqaba Biotech, South Africa) and sent to Inqaba Biotech for analysis. Reference gene β-ACTIN (Forward: 5'-CAGAAGGATTCCTATGTGGGC-3', Reverse: 5'-GAGGGCATACCCCTCGTAGAT-3') was quantified for normalising the expression levels of emGFP (Forward: 5'- GACGACGGCAACTACAAGAC -3', Reverse: 5 '-TGTCGGCGGTGATATAGACC- 3') in transfected cells.

3.1.14. Statistical analysis

The data is displayed as mean ± standard deviation. Statistical significance was assessed using the One way ANOVA test using Origin 2021b software, a p-value below 0.05 was regarded as statistically significant, * $p < 0.05$; ** $p < 0.01$; *** $p < 0.001$.

3.2. Results and Discussion

For this study, a novel self-assembling cationic nanosystem was designed as a non-viral vector for gene delivery using HA as the primary polymer. Although HA is biocompatible, biodegradable and is capable of promoting targeted delivery through interacting with CD44 receptors, its nucleic acid encapsulation capabilities are limited due to its anionic nature (Almalik et al., 2013). Therefore, the use of quaternised 2-aminobenzimidazole and oleylamine in the formation of the nanosystem has the potential to efficiently complex nucleic acids, aid in endosomal escape and facilitate *in vitro* transfection (Wang et al., 2021). Conjugation of HA to 2-AB allows for the formation of stable complexes with nucleic acids, which is essential in ensuring the protection of genetic material from degradation. Additionally, the cationic nature of 2-AB can facilitate nanosystem uptake, strong electrostatic interactions with nucleic acid and pH responsiveness i.e., facilitate nucleic acid release in response to changes in pH (specifically, endosomal pH environment). 2-AB, along with its derivatives, has been extensively utilised in drug development and shown to be biocompatible, exhibiting low cytotoxicity (Hsu et al., 2022). Following the formation of the HA-2AB$^+$ conjugate, the novel compound was further modified with the hydrophobic moiety, oleylamine (Figure 3.1). Previous research has shown that interaction of the cell membrane with an amphiphilic molecule promotes cell membrane adsorption and temporary loss of integrity, thus driving endosomal uptake and enhanced drug delivery (Bishop et al., 2015).

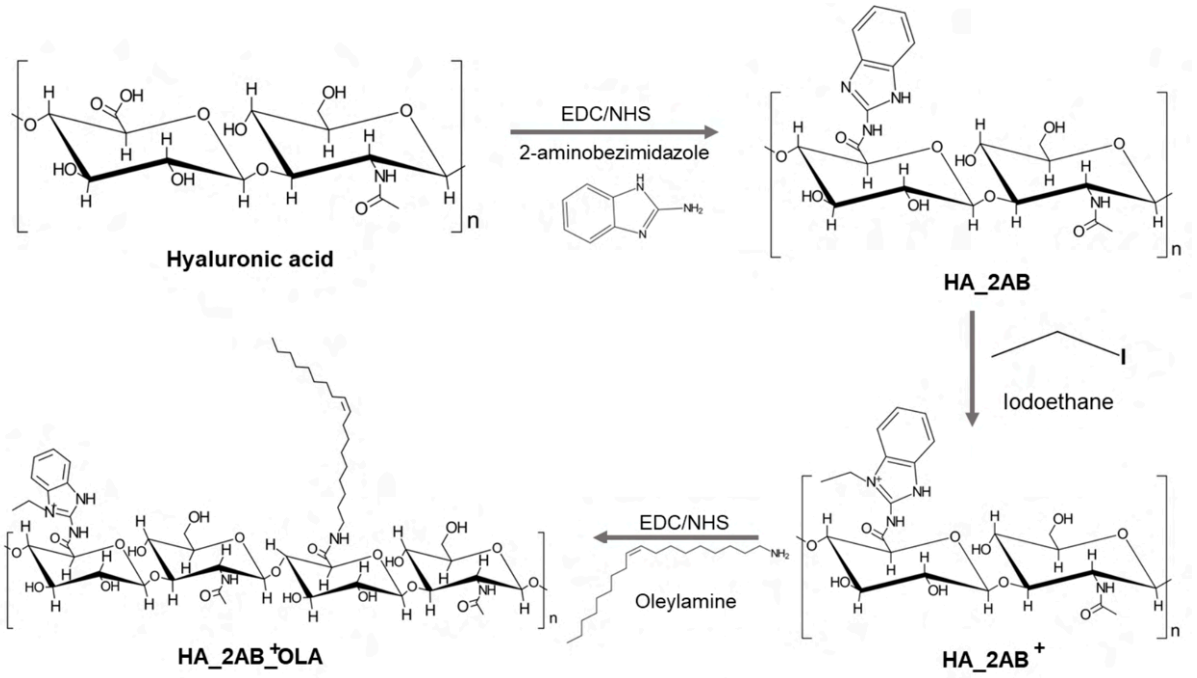

Figure 3.1: Schematic of synthesis of HA-OLA-2AB^{+} derivative using EDC/NHS conjugation chemistry. Hyaluronic acid (HA, 85 kDa); HA-conjugated to 2-AB (133 Da) and OLA (267 Da).

Therefore conjugating the hydrophilic compound, HA-2AB^{+}, to OLA was essential to ensure the formation of vesicle-like nanoparticles that resemble cell membranes. This structural mimicry supports both stability and cellular uptake, while offering potential for dual delivery of hydrophilic and hydrophobic therapeutics, including nucleic acids. As previously discussed, the design and construction of this self assembling cationic nanosystem was prepared through the synthesis of the derivative HA-2AB^{+}-OLA, using EDC/NHS chemistry (Figure 3.1). We hypothesize that the cationic-amphiphilic nanosystem and the anionic pcDNA6.2-EmGFP will form a stable nano-polyplex system via electrostatic interaction. The design and characterisation of the nano-polyplex systems are further discussed below.

3.2.1. Confirmation of HA-OLA-2AB^{+} conjugate by ^{1}H NMR spectroscopy

Confirmation of the conjugation was conducted using ^{1}H and ^{13}C NMR spectroscopy for the copolymer and the individual elements of the formulation (Figure 3.2). The ^{1}H and ^{13}C NMR signals obtained from the copolymer were compared to the individual components of the conjugate to verify the formation of new peaks. The ^{1}H NMR spectra of HA depicted a chemical shift at 4.5 ppm corresponding to the two protons bonded to the carbons adjacent to the oxygen atoms in the HA structure (Figure 3.2) (Youm et al., 2014). Additionally, a broad signal between 3.3 and 3.9 ppm is indicative of protons within the sugar rings and a chemical

shift of around 1.9 ppm corresponding to the methyl (-CH_3) protons of the N-acetyl group was present (Figure 3.2). The final conjugate, HA-2AB$^+$-OLA, revealed prominent chemical shifts of protons similar to those seen in the individual synthesis components (Figure 3.2). The peaks between 0.8 to 2.9 ppm align to those seen in the oleylamine hydrocarbon chain, a signal at 5.3 ppm suggests the presence of protons adjacent to oleylamine alkenes, and the peak at 7.9 ppm region of the spectra can be assigned to protons directly attached to the carbon bonded to nitrogen in the amides, and alternatively to the hydrogens in the imidazolium ring oF 2AB (Massahud et al., 2023; Tsai et al., 2016). To support the data, ^{13}C NMR was conducted on the compounds and validated the data obtained from ^1H NMR, with the formation of an amide bond between HA and 2AB confirmed by the presence of a peak at 173 ppm (Supplementary Figure 2).

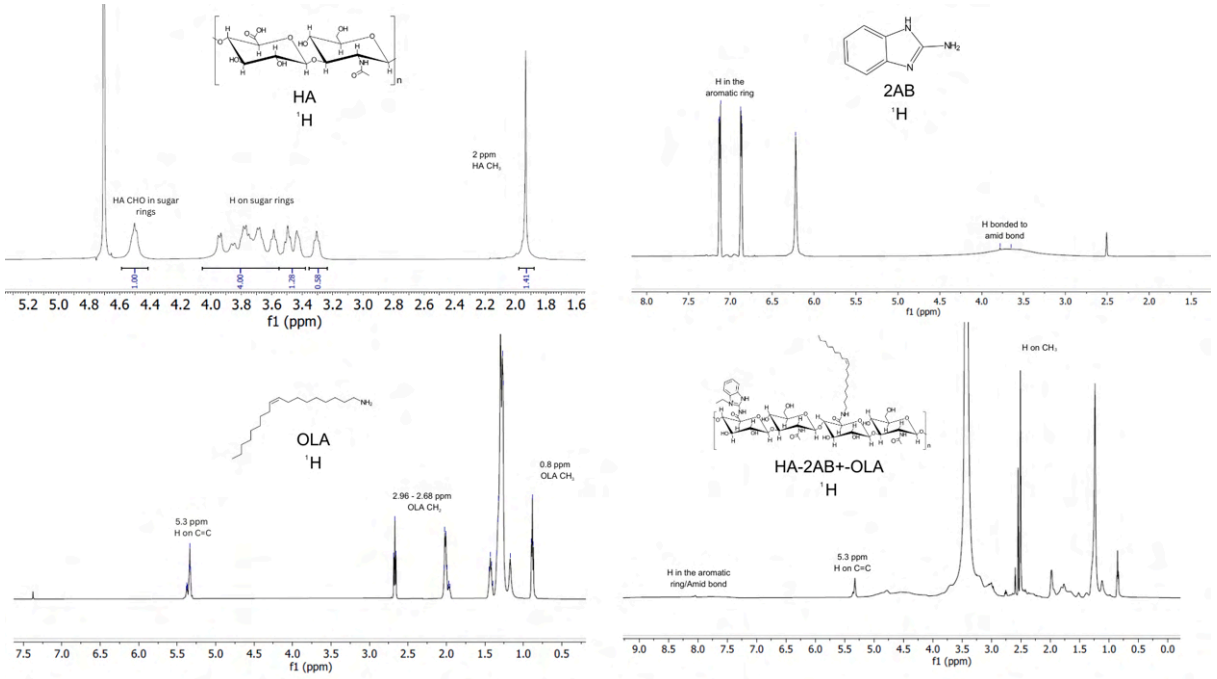

Figure 3.2: ^1H nuclear magnetic resonance (NMR) spectra of native polymers and the synthesised conjugate.

3.2.2. Interpretation of the vibrational transitions for structural analysis of HA-2AB$^+$-OLA copolymer

FTIR spectra were examined and analysed to compare the individual components (HA, 2-AB and OLA) with the produced copolymer (HA-2AB$^+$-OLA), in order to verify the formation of the copolymer. The FTIR spectra were captured within the range of 650 to 4000 cm^{-1}. Figure 3.3a depicts the FTIR spectra of the individual polymers involved in the synthesis process, as well as the final product. Each compound displayed its distinctive bands, indicating their characteristic properties as described henceforth. The spectra of HA showed a peak at 3276 cm^{-1} that corresponds to the stretching vibrations of amine (N-H) and hydroxyl (O-H) groups

and the 2918.36 cm^{-1} peak suggesting the presence of carbon-hydrogen bonds within the HA molecule, which are typically associated with the hydrocarbon backbone of the polysaccharide. Lastly, the bands at 1602 cm^{-1} and 1407 cm^{-1} correspond to the asymmetric (C=O) and symmetric (C-O) stretching modes of the carboxyl groups present in HA. These peaks indicate the presence of carboxylate functional groups (-COO-) within the HA molecule, which are derived from the uronic acid residues in its structure. The analysis of FTIR spectra revealed that the essential chemical structure of the native compounds is retained in the final conjugate HA-2AB^{+}-OLA. The FTIR analysis revealed characteristic peaks corresponding to the functional groups present in oleylamine, iodoethane, HA, and 2-AB. The strong broad band at 3278 cm^{-1} corresponds to the stretching vibrations of the amine (N-H) and hydroxyl (O-H) groups present in HA. The bands at 2921 cm^{-1} and 2852 cm^{-1} represent the stretching vibrations of the C-H bonds in the oleyl hydrocarbon chain (aliphatic hydrocarbons), the peak at 1636 cm^{-1} corresponds to the region of aromatic hydrocarbons in 2-AB, and the appearance of the peak at 1547 cm^{-1} indicates the site of conjugation, reflecting the formation of the amide covalent chemical bond (C-N stretch).

3.2.3. Evaluating Phase transitions of HA-2AB^{+}-OLA conjugate using X-ray Diffraction

Changes in HA structure, phase behaviour and degree of crystallinity as a result of 2-AB and OLA conjugation were assessed using X-ray diffraction. The data presented in Figure 3b confirms the amorphous nature of HA, showing a broad diffraction halo or signal at 2θ ≈ 43° (Lopez et al., 2020), additional diffraction peaks at 2θ ≈ 19.7°, 21.56° and 25.08° were also observed. Similarly, X-ray diffraction spectra for HA-2AB^{+}-OLA conjugate noted similar diffraction peaks 2θ ≈ 19.7°, 21.8°, 25° and 43° (Figure 3.3b) which depict a semi-crystalline/nanocrystalline structure. Conversely, a stronger diffraction signal was observed for HA-2AB^{+}-OLA which is indicative of high atomic density or molecular packing, prevalent in organised structures as demonstrated by the low interplanar distance between the crystal planes (Table 3.1). The slight broadening of the diffraction peaks is sometimes seen in nanoscale materials (nanocrystal structures) (Holder and Schaak, 2019) and is also indicative of the preservation of HA's disordered structure. Grafting of 2-AB and OLA to HA led to an increase in the crystallinity index from 63.8 % to 66.6% and crystallite size (Table 3.1) indicating the formation of a well ordered structure. Notably, the nanocrystalline nature of the conjugate will affect its thermal stability, surface area nucleic acid release properties and degradation rate (El Yousfi et al., 2023; Herdiana et al., 2022).

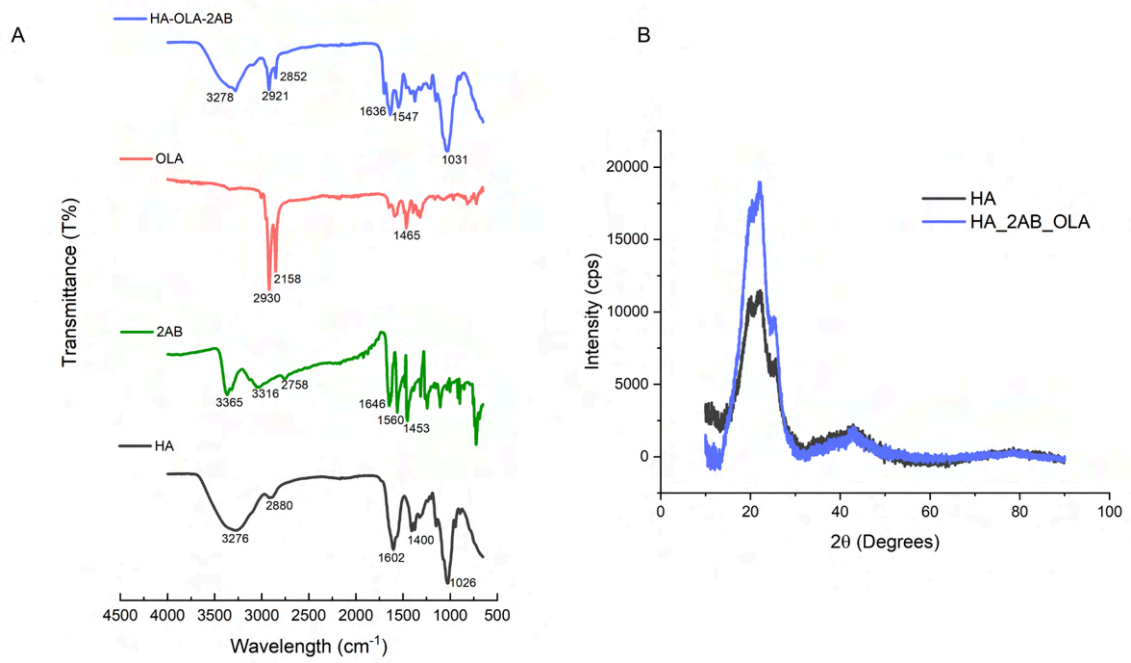

Figure 3.3: Physicochemical characterisation of HA_2AB_OLA copolymer. a) Comparative FTIR spectra of the individual components, HA, 2-AB, OLA and HA-2AB^{+}-OLA participating in the formation of HA-2AB^{+}-OLA. The FTIR spectra were recorded in the range of 850 to 4000 cm-1. b) X-ray Diffraction (XRD) Analysis of Pure Hyaluronic Acid (HA) and the synthesized conjugate polymer HA-2AB^{+}-OLA. The XRD pattern reveals the characteristic peaks associated with an amorphous structure and thus absence of a well defined crystal lattice.

Table 3.1: XRD based structural parameters of HA-2AB^{+}-OLA

Polymer	CI **(%)**	**D (nm)**	***d*** **(nm)**
Hyaluronic acid	63.8	8.35	2.07
HA-2AB^{+}-OLA	66.6	13.18	2.09

3.2.4. Thermal stability of composites

The thermal stability, decomposition and degradation of HA, copolymer (HA-OLA), 2-AB and the final synthesised derivative was investigated using thermogravimetric analysis. Figure 3.4a displays TGA spectra for the parent components and the final conjugate. HA demonstrated an initial weight loss (1.5%) below 100°C (onset temperature of degradation)

which is attributed to the loss of the bound and or adsorbed water as HA is very hygroscopic. Since HA is the main constituent in the conjugate, the hydration property of the polymer was retained in both the intermediate and final conjugate, as such, this resulted in similar weight loss patterns being observed between pure HA and the conjugates (initial mass loss 4.1% and 5.3% respectively at temperatures just below 100°C). A sharp reduction in mass was recorded between 229.8 - 509.3 °C, attributed to the decomposition of HA, this was followed by a gradual weight loss. A similar pattern of HA degradation has been reported in literature (Jiang et al., 2015). HA-OLA and HA-2AB^{+}-OLA curves show three distinct degradation regions similar to those observed in HA. The second and third regions starting at 199 and 454 °C for HA-OLA and 204 and 463 °C for HA-2AB^{+}-OLA are characteristic of a two stage polysaccharide degradation. The observed weight loss for the second region in the HA curve was 55.47 and 8.94% for the third region. Whilst the mass loss was 65.2% and 12.36% for HA-OLA and 67.3% and 6.96 % for HA-2AB^{+}-OLA respectively. This shows that modifications conducted on HA slightly altered its thermostability.

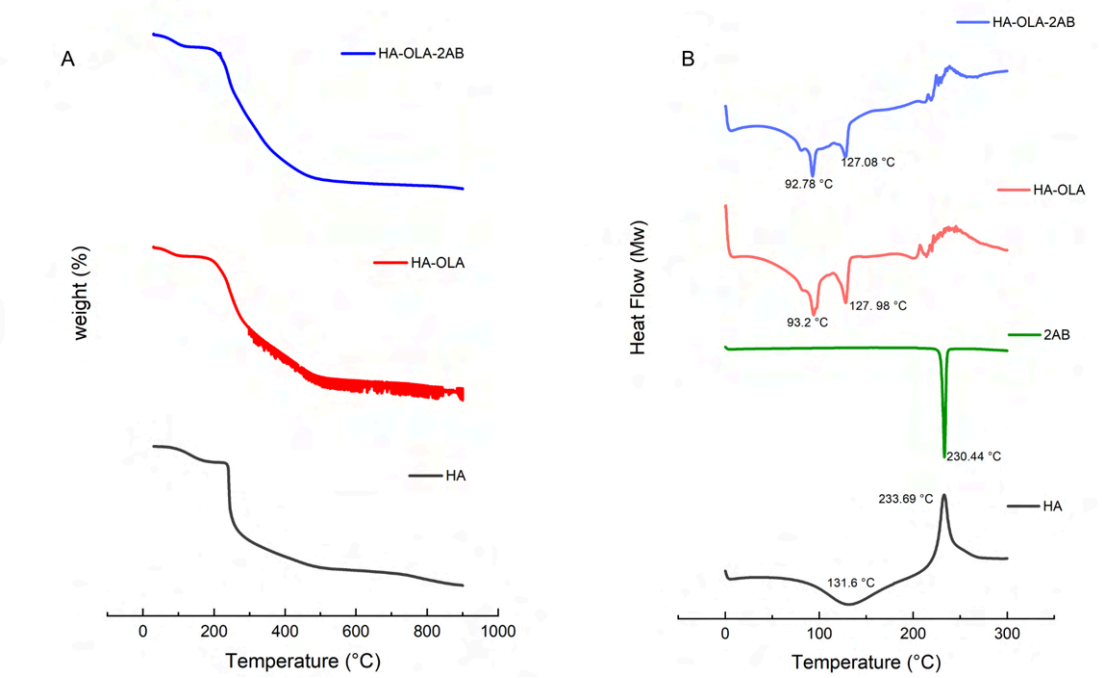

Figure 3.4: Thermal stability of the polymer composite, HA_2AB^{+}-OLA. a) The TGA spectra represent the thermal stability, decomposition, and degradation profiles of hyaluronic acid (HA), HA_OLA and HA-2AB^{+}-OLA. **b)** Differential scanning calorimetry curves illustrating the thermal behavior and properties of: pure HA, 2-aminobenzimidazole (2-AB), HA conjugated to Oleylamine (HA-OLA) and the final synthesized conjugate polymer, HA-2AB^{+}-OLA.

3.2.5. Differential scanning calorimetry

Differential scanning calorimetry was conducted to decipher the thermal behavior of the synthesised polymer, identifying its heat capacity and phase transitions. Figure 3.4b exhibits the DSC curves of the native compounds (HA, 2-AB) contrasted with the synthesised conjugates (HA-OLA and HA-2AB$^+$-OLA). HA displays a distinctive broad endothermic peak at 131.6 °C which may be indicative of the dehydration process as temperature rises and an exothermic transition (233.69 °C), correlating to its degradation (L. Han et al., 2012). A sharp endothermic peak at 230.4°C is observed for 2-AB; this phase transition is attributed to the compound's melting point. The DSC curve for HA-2AB$^+$-OLA largely resembles that of HA-OLA. The degradation peak of HA is slightly noticeable in the conjugates; the reduced clarity of the peak could be attributed to modification of the HA backbone. Two consecutive endothermic thermal events/phase transitions (± 92 and 127 °C) are observed in both the HA-OLA and HA-2AB$^+$-OLA conjugates which may be indicative of two separate but concurrent thermal events, such as dehydration and decomposition. Additionally, modification of HA via the 2-AB and OLA may have resulted in a different structural arrangement compared to pure HA, resulting in the conjugate existing in multiple phases. Both conjugates (HA-OLA and HA-2AB$^+$-OLA) exhibit a non-smooth curve which may be due to the chemical decomposition or degradation of the polymer, alternatively, this could be an indication of crystallization or polymer transition.

3.2.6. Formation of the nano-polyplex system

Prior to the formulation of the nano-polyplex system, pDNA extraction was carried out followed by assessment of its purity by measuring 260/280 and 260/230 purity ratios, which were 1.89 and 2.14 respectively. To optimise the delivery system, multiple formulations were synthesised using the **N** (moles of cationic charges in HA-2AB$^+$-OLA): **P** (moles of Phosphate groups in pDNA) ratio and further investigated. Nano-polyplex systems were prepared by mixing 1 µg pcDNA6.2-EmGFP with the synthesised conjugate (HA-2AB$^+$-OLA) at different ratios as explained in the experimental section. Subsequently, the hydrodynamic size and zeta potential of each formulation was determined using dynamic light scattering. An average hydrodynamic diameter of 73.85 nm and Zeta potential of 32 mV was observed for the non-loaded nanosystem with a relatively narrow size distribution (PDI ~0.270) (Figure 3.5c,d). Meanwhile, pcDNA6.2-EmGFP loading at different N:P ratios exhibited an N:P dependent size and zeta potential response. Notably, N:P ratio <15 demonstrated extensive nano-polyplex aggregation resulting in hydrodynamic diameter >270 nm and significantly lower zeta potential (2.9 mV; $p < 0.0001$) (Figure 3.5 c,d). Importantly, low N:P ratios nano-polyplexes are characterised by an increased nanoparticle size and low cationic

charge, consequent to inadequate nucleic acid charge neutralisation and condensation resulting in the formation of less compact-aggregated and unstable nano-polyplexes.

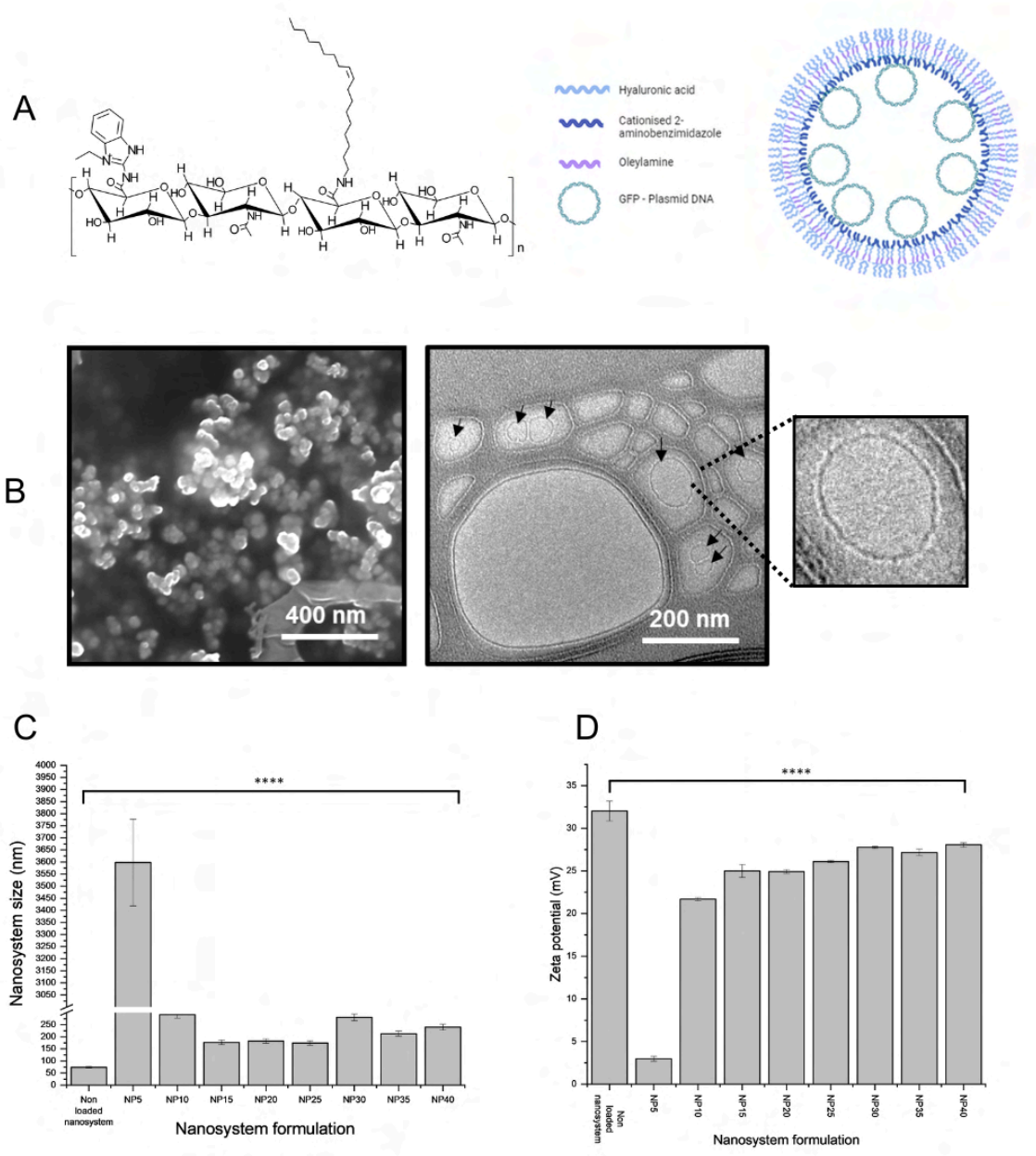

Figure 3.5: DLS results of the various NP formulations. (A) Structural representation of the nano-polyplex system. (B) TEM (right) and SEM micrographs (left) of nano-polyplex system. Insert on TEM micrograph is a zoom in one of the nano-polyplex systems to show the presence of a bilayer. (C) Mean size (d.nm) and (D) zeta potential (mV) of different formulations of the nano-polyplex system prepared by complexation of pcDNA6.2-EmGFP with the amphiphilic and cationic conjugate HA-2AB^{+}-OLA. Data from experiments are presented as the mean ± SD, n =3 (** $p < 0.01$, *** $p < 0.001$**** and $p < 0.0001$).

Conversely, N:P 15 to 25 nano-polyplex systems demonstrated an average particle size <200 nm (Figure 3.5 C,D) shown in previous studies to be ideal for receptor-mediated endocytosis which is typical in non-phagocytic cells like photoreceptors (Hillaireau and Couvreur, 2009). These formulations depict an 'optimal balance' in charge yielding efficient nucleic acid condensation and formation of stable complexes. Higher N:P ratio nano-polyplex systems (N:P 30 to 40) were marked by a hydrodynamic diameter >200 nm, which is the most preferable for uptake by phagocytic cells (e.g. hRPE cells) (Adijanto and Naash, 2015). As shown, N:P ratio modulates the degree of gene condensation and nanosystem stability leading to variations in charge and size. The overall morphology and size distribution of the nano-polyplex systems was confirmed by electron microscopy. SEM and TEM micrographs demonstrated spherical nanosystems with a mean diameter <200 nm and the presence of a bilayer structure (as seen in the insert - Figure 3.5b) similarly seen in polymersomes and liposomes (Jun et al., 2010). The presence of the bilayer confers versatility to the nano-polyplex system enabling its use as a dual drug encapsulation (hydrophobic and hydrophilic drugs) and delivery system (Fonseca et al., 2024).

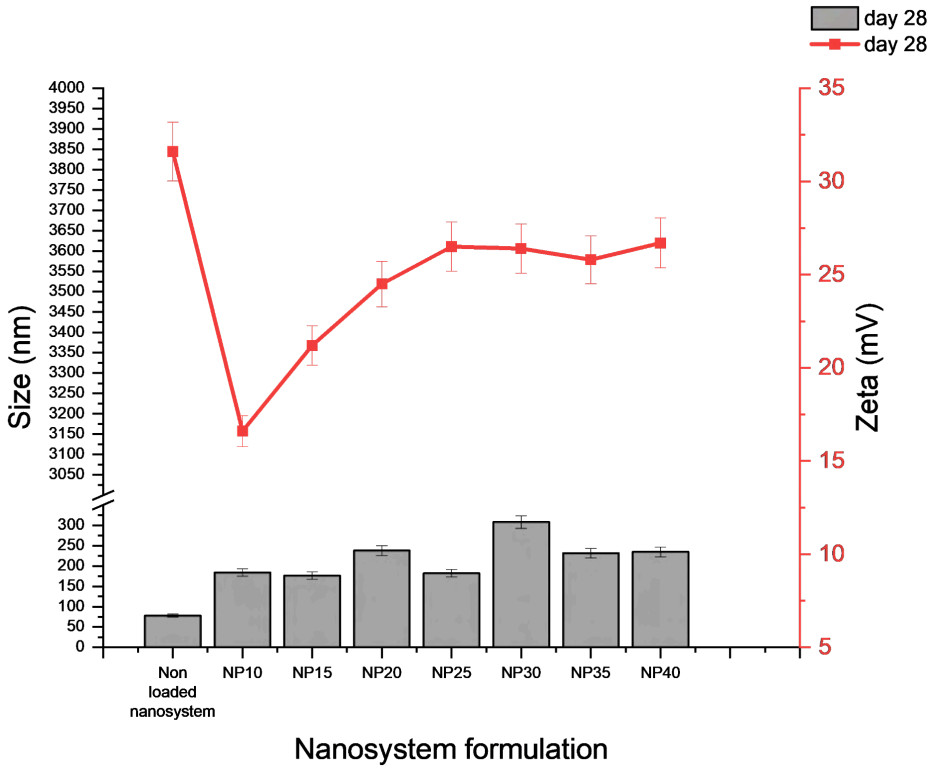

Figure 3.6: DLS results (Zeta potential and mean NP diameter) of the nano-polyplex system stability test following 28 days storage at 4 - 8°C.

The biomimetic nature of the system is comparable to that of the cell membrane, possibly resulting in improved nanosystem uptake by cells. Additionally, polymer-lipid based bilayers offer increased stability compared to liposomes, preventing premature degradation and sustained release (Fonseca et al., 2024). Importantly, stability of the unloaded and loaded nano-polyplex systems was assessed at cold storage temperature (4 to 8 °C) for 28 days. The size and zeta potential of the nano-polyplex systems remained relatively similar to day one after one month of storage, with pcDNA6.2-EmGFP integrity maintained (Figure 3.6).

3.2.7. Evaluating the Encapsulation Efficiency of the Nano-polyplex system

As part of the nanocarrier formulation process, key parameters such as encapsulation efficiency (drug loading), pharmacokinetic and pharmacodynamic characteristics, drug release kinetics and cell targeting features must be considered. Notably, encapsulation efficiency determines nucleic acid/drug release profile, bioavailability and biodistribution: a high entrapment efficiency ensures low levels of free DNA are in circulation thus minimising unintended off-target effects and cytotoxic (Mollé et al., 2022). Entrapment efficiency across different N:P ratio formulations was determined by measuring non-entrapped vs trapped pcDNA6.2-EmGFP using the ultrasensitive nucleic acid stain for double stranded DNA, PicoGreen, as outlined in Section 3.1.5. As shown in multiple studies, entrapment efficiency is dependent on nanocarrier charge (Brgles et al., 2008; Honary and Zahir, 2013), as such an increase in pcDNA6.2-EmGFP entrapment correlated (R^2 = 1) with increased Zeta potential (Figure 3.5d and 3.7a). Encapsulation efficiency was between 19.5 % to 99.7 % (Figure 6a), with N:P 20 to 40 demonstrating the highest entrapment efficiency attributable to strong electrostatic interactions between the anionic charge of pcDNA6.2-EmGFP and the cationic nanosystem. Furthermore, qualitative demonstration of pcDNA6.2-EmGFP entrapment was conducted using gel retardation assay and electrophoresis. This assay aids in confirming nano-polyplex system formation and analyses the binding affinity between genetic material and the nanosystem visually. Efficient entrapment of pcDNA6.2-EmGFP is indicated by the absence of visible nucleic acid band migration on the gel that is comparable to the negative control (free DNA) (Figure 3.6b). This supports the quantitative data showing complete nucleic acid complexation and formation of stable nano-polyplexes. Conversely, the presence of faint and or strong nucleic acid bands on the gel is indicative of unbound genetic material, lower entrapment efficiency and weakly formed nano-polyplex system as shown for N:P 5 nano-polyplex (Figure S3). Significantly, N:P 5 formulation was excluded in further studies due to low encapsulation efficiency.

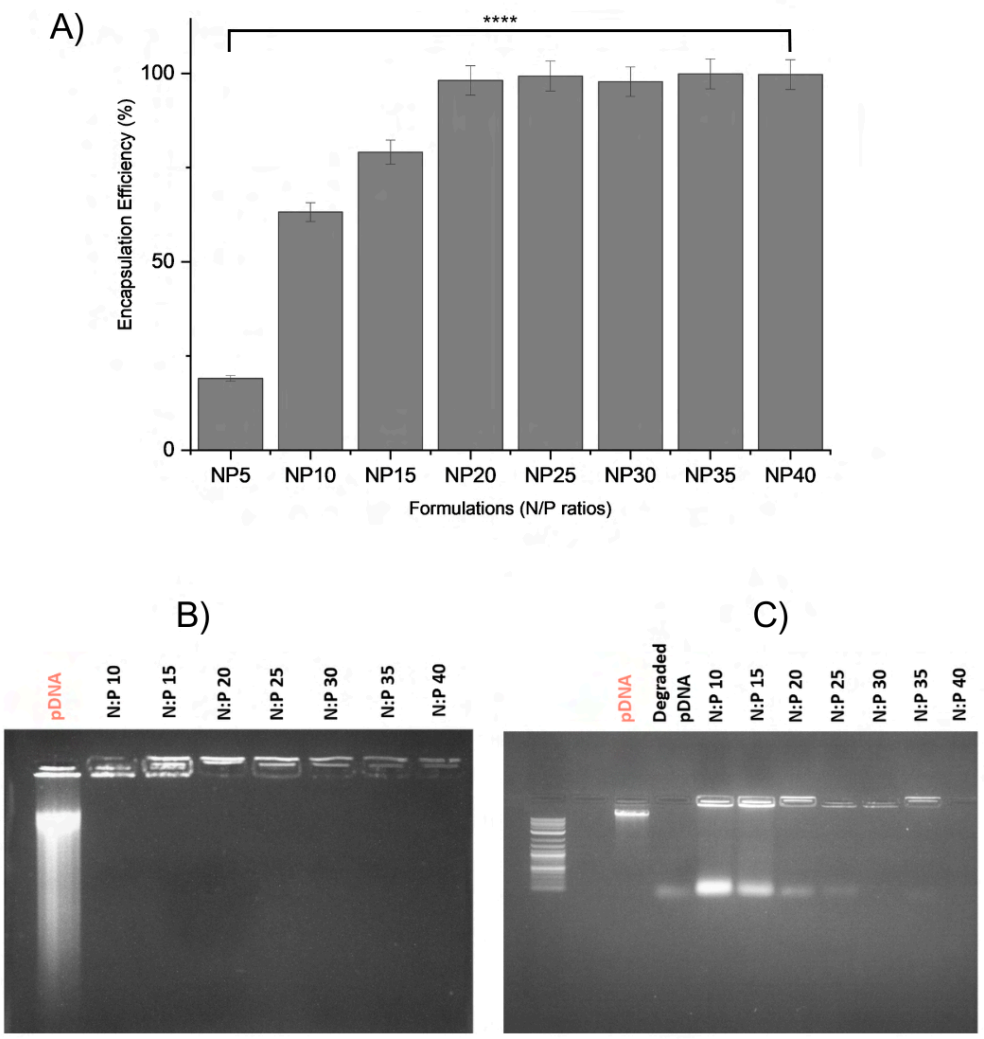

Figure 3.7: Quantitative and qualitative analysis of nano-polyplex system encapsulation efficiency. Gel retardation and Nuclease protection assay. (A) Nano-polyplex system encapsulation efficiency as determined using the Quant-iT PicoGreen kit. (B) Gel retardation assay qualitatively depicting varying degrees of nano-polyplex entrapment efficiency. (C) Nuclease (DNAseI) protection analysis by the varying N:P formulations of the nano-polyplex system. Data from experiments are presented as the mean ± SD, n =3 (**** denote $p < 0.0001$).

3.2.8. Evaluation of pcDNA6.2-EmGFP degradation by endonucleases

As previously stated, encapsulation efficiency contributes to nano-polyplex system stability and capacity to protect genetic material from degradation by nucleases (Kita and Dittrich, 2011). The detection of foreign genetic material by the innate immune system is often met by the action of nucleases which are responsible for the degradation of naked DNA *in vivo* (bloodstream and intracellular compartments) (Santa et al., 2021). Enhanced nucleic acid

stability is therefore essential to reduce the nucleic acid induced immunological effects and ensure a significant proportion reaches the target site. Therefore, the design of effective gene delivery systems capable of protecting nucleic acid from degradation is essential as uncomplexed nucleic acids are rapidly degraded by endonucleases, resulting in a half life of 10 minutes extracellularly and one hour intracellularly (Ha et al., 2011; Mullen et al., 2000; Vaughan et al., 2006), compared to complexed nucleic acid which can be three to six fold higher (Chiou et al., 1994). The stability of the constructed nano-polyplex system and the extent to which the nucleic acid is protected from degradation was therefore assessed by treating the free pcDNA6.2-EmGFP and the nano-polyplex systems (N:P 10 to 40) with the endonuclease, DNase I as elucidated in the methods section. Treatment of free pcDNA6.2-EmGFP resulted in its instant degradation, whereas the entrapped pcDNA6.2-EmGFP was protected from degradation at varying degrees across the different N:P ratios. Consistent with entrapment efficiency data, N:P 10 and 15 showed some degree of pcDNA6.2-EmGFP degradation as depicted by the smearing and fragmentation of nucleic acid (small fluorescent bands also present in free pcDNA6.2-EmGFP) (Figure 3.7c). Alternatively, higher N:P ratio formulations (N:P 20 to 40) showed lower rates of pcDNA6.2-EmGFP degradation indicative of the nano-polyplex potentially serving as an agent for protection against nucleases and thus ideal nanocarrier for genetic material (Figure 3.7c).

3.2.9. Evaluation of *in vitro* pcDNA6.2-EmGFP release from the cationic- amphiphilic nano-polyplex system

The main objective for gene delivery vehicles is to ensure protection, efficient encapsulation and sustained release of genetic cargo to the desired target sites. A significant advantage to using HA as one of the components in designing gene delivery nanosystems is its inherent biocompatible nature, CD44 receptor targeting capacity and presence of functional groups. To this end, carbodiimide crosslinking of HA with other polymers has been shown to slow down the degradation of the polymer *in vivo* (Tomihata and Ikada, 1997). Therefore, cross linking HA with the cationically modified 2-aminobenzimidazole enhances encapsulation efficiency as shown in Section 3.2.8, and has the potential to slow down the degradation of nanocarriers and provide sustained gene release. Accordingly, pcDNA6.2-EmGFP release from the nano-polyplex systems was quantified using the ultrasensitive nucleic acid stain for double stranded DNA, PicoGreen. The cumulative release profiles of the N:P ratio formulations N:P 10 to 40 are shown in Figure 3.8. All formulations released less than 30% of pcDNA6.2-EmGFP after 96 hours. The highest release was observed for N:P 20, releasing 26% over 96 hours. Nano-polyplex systems N:P 10, 15 and 20 showed higher release in the initial 24 hours, consistent with encapsulation efficiency results, particularly, N:P 10 and 15).

A gradual increase in pcDNA6.2-EmGFP release was observed for N:P 25 to 40 between 48 and 96 hours, reaching values between 12 and 17%. Importantly, compared to higher N:P ratio nano-polyplex systems, lower ratio systems were characterised by a relatively faster release within the first 10 hours; this could be attributed to nanosystem saturation with pcDNA6.2-EmGFP resulting in unbound nucleic acid being easily released into the medium. Additionally, lower N:P ratios of nano-polyplex systems are characterised by fewer charge interactions resulting in less compact but highly aggregated nanosystems increasing the available surface area for pcDNA6.2-EmGFP to easily diffuse across available pores.

The comparatively slower release observed in higher N:P ratio nano-polyplex systems could be attributed to the high electrostatic interactions between the genetic material and nanosystem, making diffusion incredibly difficult or steric hindrance (alternatively, formation of an ion shield) resulting in reduced pcDNA6.2-EmGFP diffusion. This charge dependence behaviour has been demonstrated and reported in previous studies (Xu and Szoka, 1996). Notably, N:P 20 deviates from this, showing a higher release profile than expected. This is possibly due to the formation of loosely packed pockets within the nano-polyplex allowing easy access for the release medium to facilitate diffusion, alternatively, N:P 20 may have a better dispersion which allows for efficient release of pcDNA6.2-EmGFP.

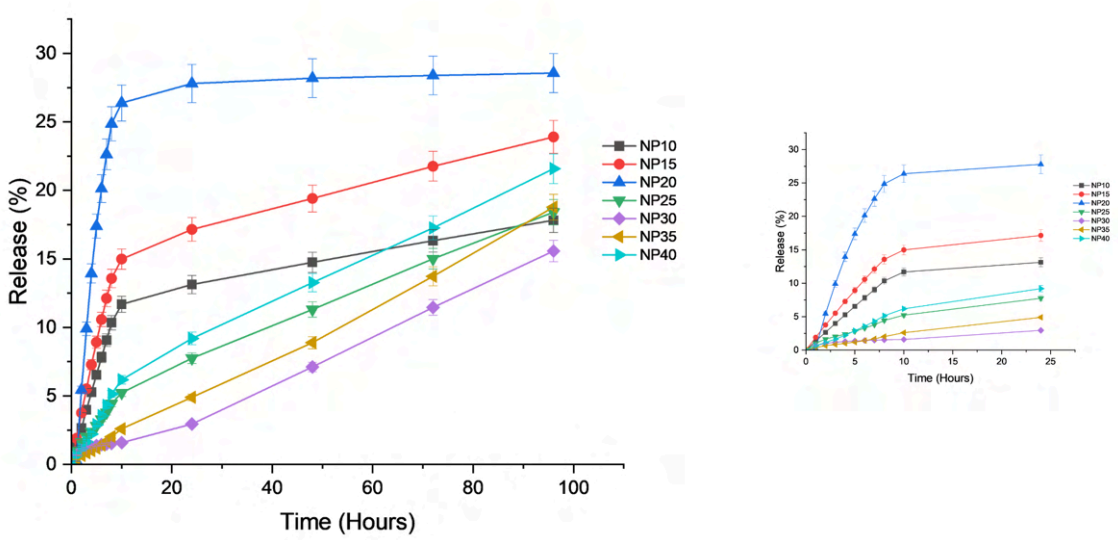

Figure 3.8: *In vitro* pcDNA6.2-EmGFP release profile from amphiphilic cationic nanosystem (HA-2AB^{+}-OLA) at pH 7.2 quantified using the Quant-iT PicoGreen assay. Insert on the right depicts the initial release phase (24h), showing early release rates of the nan-polyplex system. Data from experiments are presented as the mean ± SD, n = 3.

3.2.10. Assessment of the nano-polyplex system biocompatibility and safety profile in HEK 293 and hRPE cell line

The *in vitro* cytotoxicity of the different N:P ratio nano-polyplex formulations was evaluated using HEK 293 and hRPE cell lines. Following preparation of cell lines as outlined in Section 3.1.9, cells were treated with the nano-polyplex formulations, whilst untreated cells were observed as a positive control and cells treated with DMSO as the negative control. Following 72 hours of treatment, the nano-polyplex formulations showed a cell viability of 96% and above for both cell lines (Figure 3.9), indicating that the formulations were well-tolerated by the cells and thus did not induce significant toxicity. Notably, nanosystem only, N:P 15 and N:P 35 treated HEK 293 cells experienced slightly reduced viability. This could be attributed to prolonged exposure to the high cationic charge of the nanosystem which is known to disrupt the cell membrane by increasing its permeability resulting in the escape of cellular contents and inadvertently necrosis or apoptosis (Wei et al., 2015). Statistical analysis of the data using ONE WAY ANOVA indicated no statistically significant difference in cell viability amongst the groups, despite N:P 20 - 35, experiencing higher HEK 293 cell viability/growth. This can be attributed to moderate cationic charge density in these formulations which is ideal for promoting cell attachment and proliferation (Stamm et al., 2022), alternatively, this could be due to natural variations in cellular metabolism within the cells used, or slight errors during seeding. Similarly, biocompatibility of the nano-polyplex was observed in hRPE cells treated with various nano-polyplex N:P formulations.

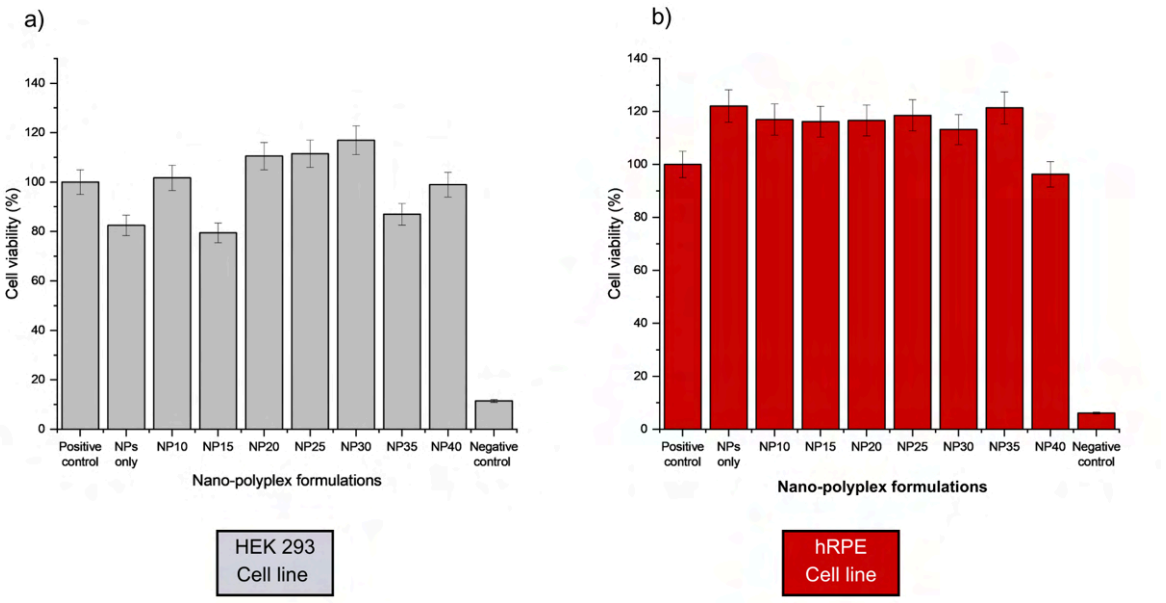

Figure 3.9: Cell viability of the a) HEK293 and b) hRPE cell lines treated with the varying nano-polyplex formulations. Measurements were carried out by MTT assay with comparison to untreated cells as the positive control. Values of MTT assay are given in percentages and

normalized to non-treated control as 100%. Data from experiments are presented as the mean ± SD, n = 6 (**** denote $p < 0.0001$).

3.2.11. *In vitro* transfection efficiency and gene expression as analysed by GFP detection

3.2.11.1. GFP detection in nano-polyplex transfected HEK 293 cells

To investigate general transfection efficiency of the nano-polyplex system, HEK 293 cells were selected as they are highly transfectable and ideal for optimising transfection protocols and testing the integrity of genetic material (Tan et al., 2021). hRPE cells were also chosen, as the primary aim of this research is to develop a non-viral gene delivery system targeting retinal cells. The *in vitro* transfection experiments were conducted as outlined in Section 3.1.9.2 using a green fluorescent protein expressing construct as a reporter gene. Non-transfected cells (negative control), free pcDNA6.2-EmGFP and lipofectamine 3000/pcDNA6.2-EmGFP treated cells (positive controls) were used as controls and N:P 10 to 40 nano-polyplexes as interventions, with GFP expression detected using fluorescence microscopy, quantitative PCR and flow cytometry. GFP signal in lipofectamine 3000 and nano-polyplex transfection HEK 293 cells was detected 72 hours post transfection (Figure 3.10 and Figure S4). Significant GFP expression was observed for lipofectamine 3000/pcDNA6.2-EmGFP treated HEK 293 cells as expected. Consistent with the release profile, N:P 15 and 20 showed relatively higher GFP signal compared to the other nano-polyplex ratio formulations (Figure S4), but lower GFP signal and expression compared to the positive control (Figure 3.10). Further quantitative data validation for GFP expression was conducted using flow cytometry to analyse transfection efficiency and detect GFP-positive cells. For this purpose, the fluorescence channel, Alexa Fluor 488 was selected as its emission spectra corresponds to that of GFP, with an excitation of 488 nm, and 50 000 total events were selected. A GFP positive gate was set to represent the GFP positive population. Percentage GFP detection in lipofectamine 3000/pcDNA6.2-EmGFP versus nano-polyplex system N:P 15 transfected HEK 293 cells was 2.4% and 1.0% respectively, thus showing positive transfection and GFP expression in both cell populations (Figure S4). Following the use of fluorescence based detection systems, qPCR was used to aid in the quantitative detection of Em(emerald) GFP mRNA levels and receive some insight into transcriptional activity of the cells following transfection. As shown in the bar graph - Figure 3.10I, RT-qPCR showed emGFP mRNA expression was higher for lipofectamine transfected cells compared to those of the nano-polyplex as expected due to the slow release by the system. Since levels of mRNA were 0.0319% of those detected in lipofectamine 3000 positive control, possible modifications to the nanosystem may need to be applied to improve efficiency in cell delivery. Nevertheless, these results demonstrate that the nano-polyplex

shows promise as a non-viral gene delivery system, driving controlled gene release and expression.

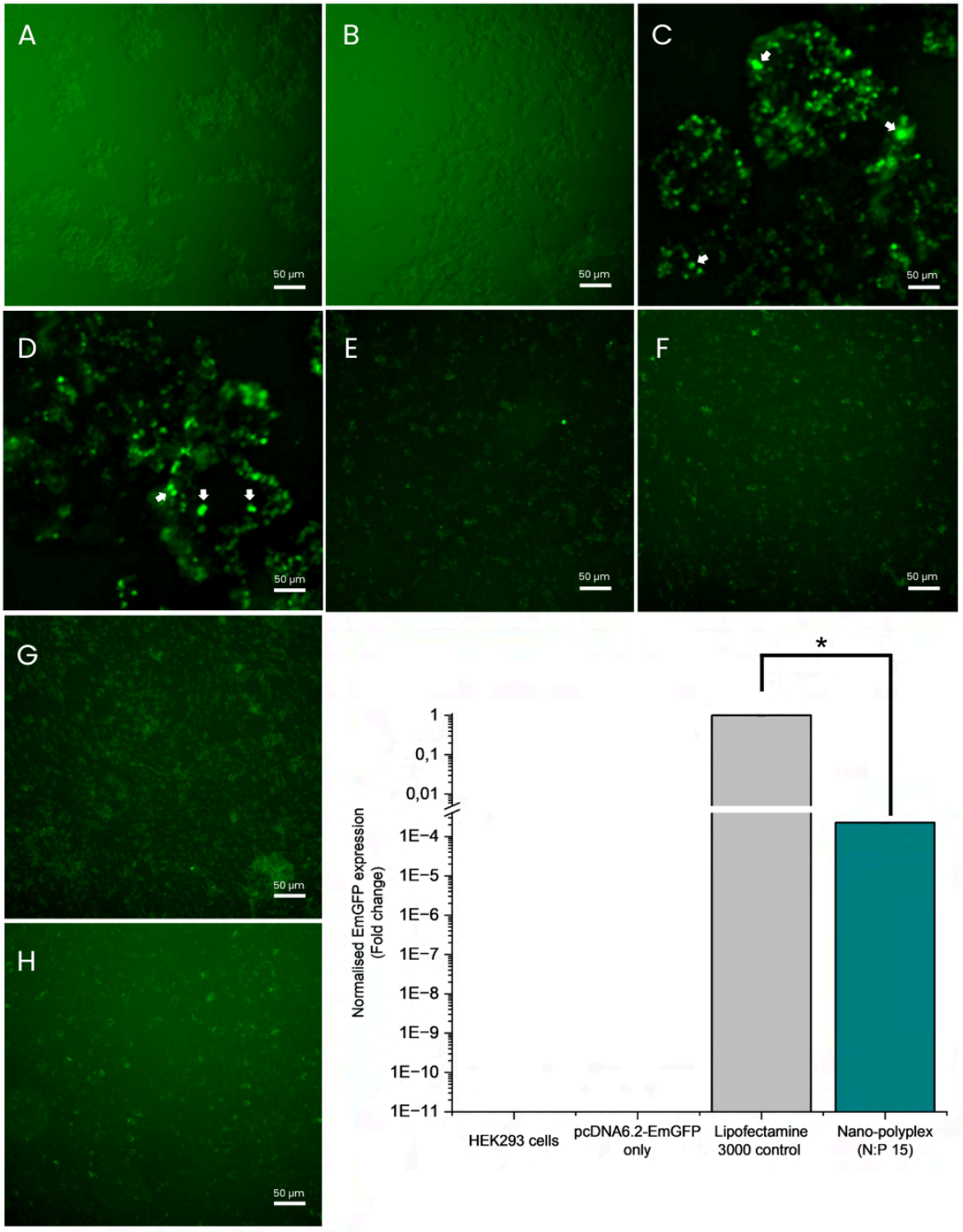

Figure 3.9: Assessment of the transfection efficiency of the nano-polyplex system in HEK293 and hRPE cells. Fluorescence microscopy images were captured 72 hours post-transfection to assess EmGFP expression. **Panels A–D** show HEK293 cells under the following conditions: (A) untreated control, (B) transfected with free pcDNA6.2-EmGFP plasmid, (C) transfected with Lipofectamine 3000/pcDNA6.2-EmGFP complex, (D) transfected with the nano-polyplex/pcDNA6.2-EmGFP complex. **Panels E–H** show hRPE cells under the same respective conditions: (E) untreated control, (F)

free plasmid, (G) Lipofectamine 3000 complex, (H) nano-polyplex complex. (I) Relative EmGFP mRNA expression quantified by qPCR. Results represent mean ± SD (n = 3). *p < 0.05 indicates statistical significance compared to the untreated control. **Scale bar = 50 µm.** Arrow indicates GFP expression/flouresence.

3.2.11.2. hRPE cells fail to express GFP following transfection

Regrettably, transfection of hRPE cells by lipofectamine 3000/pcDNA6.2-EmGFP and the nano-polyplex systems did not result in visible GFP expression (Figure 3.10). This was evidenced by lack of GFP signal in fluorescence microscopy and qPCR analysis. However, autofluorescence was detected in fluorescence micrographs, which can be attributed to the production of lipofuscin granules by hRPE cells *in vitro*, these granules are highly fluorescent when excited with blue light (470 nm) (Yung et al., 2016). Failure to detect GFP expression and thus achieve transfection using both lipofectamine 3000 and the nano-polyplex may be ascribed to the cells used in this study. During culturing, hRPE cells were noted to have potentially reached cellular senescence, inadvertently, transcription and translation processes may be limited to essential genes such as those involved in metabolic processes (Kumari and Jat, 2021). Notably, senescent cells inherently have low proliferative capacity, as such, the absence of nuclear membrane break down as a result of no replication, leads to low to no plasmid nuclear translocation and thus limited nuclear delivery and gene expression of genetic cargo (Pérez-Martínez et al., 2011). Additionally, cell senescence may limit the activity of machinery involved in endosomal processing and escape. Therefore, further optimisation of the nano-polyplex system and transfection process is required. This involves possible activation of the quiescent cells to stimulate the cell cycle via use of growth factors or signals, selection of a stronger constitutive promoter capable of achieving expression even in quiescent cells or further optimisation of the nano-polyplex system and lipofectamine 3000 alike.

3.3. Concluding remarks

The work presented in this chapter focused on the fabrication of a novel amphiphilic - cationic gene delivery vector (nano-polyplex system), its physicochemical characterisation and *in vitro* safety profile. The aim of this study was to establish the use of the nano-polyplex system as a viable candidate for gene delivery and subsequently gene expression. Accordingly, the nano-polyplex system was synthesised using biocompatible polymers; HA, 2-AB and the lipid, oleylamine to encapsulate and deliver the pcDNA6.2-EmGFP construct. A charge-dependent response in the nano-polyplex system's hydrodynamic size (73 nm to 3.5 µm), entrapment efficiency (19.5% to 99.7%) and release (<30% release across N:P ratios) was observed. Notably, the presence of a quaternary ion on the nano-polyplex system had a

significant effect on pcDNA6.2-EmGFP protection from degradation by endonucleases and formation of a stable nano-complex (28 days at 4°C).

Significantly, the nano-polyplex system proved feasible as a non-viral gene delivery vehicle in HEK293 cells. Using lipofectamine 3000 as a market comparator for the pcDNA6.2-EmGFP construct delivery demonstrated that the nano-polyplex system showed significant promise for sustained expression of exogenous genes (emGFP) in HEK 293 cells with no cytotoxic effects. Conversely, hRPE cells treated with lipofectamine 3000 and the nano-polyplex system achieved no visible GFP expression/signal and thus no transfection. Importantly, gene transfection and expression is affected by a number of factors: existing cellular barriers, the presence of nucleases, immunogenic behaviour of foreign genetic material which leads to its clearance by macrophages and the reticuloendothelial system, and the role of endosomes which have multiple nucleases resulting in an average endosomal escape of 4% (Wang et al., 2023). Additionally, an essential barrier to DNA delivery is the need for nuclear translocation, the size of the nuclear pore and its selectivity to macromolecules remain a key barrier as exogenous DNA relies on the rupture of the nuclear membrane during mitosis in order to enter the nucleus and allow for transcription. Therefore, the development and use of an efficient gene delivery vector is essential in overcoming these intra and extracellular barriers and remains the most promising approach for achieving efficient gene delivery. Despite the shortcomings of the nano-polyplex system to efficiently transfect hRPE cells, the findings from HEK 293 cells illustrate that the nano-polyplex system is a promising candidate for non-viral vector based gene delivery with prolonged gene release characteristics which are beneficial in the reduction of injections that may be required to achieve sustained therapeutic effect. Additionally, this approach renders it ideal for application in general delivery of nucleic acids such as mRNAs, siRNAs, oligonucleotides and particularly large gene cassettes which shows an upper hand compared to viral vectors as they have limited genetic cargo capacity (Lundstrom, 2023). Furthermore, modifications on the nano-polyplex system have to be undertaken to ensure versatility and efficiency in the transfection of quiescent or difficult to transfect cells particularly where gene delivery is required for the activation of dedifferentiation pathways necessary for achieving cell or tissue renewal.

Importantly, the nanopolyplex system developed, characterized, and validated for gene delivery and expression in HEK293 cells in this chapter will serve as the foundational vector for subsequent investigations. In Chapter 4, this system is incorporated into a hydrogel scaffold not only to enable sustained gene release but also to facilitate cell encapsulation for delivery. The chapter focuses on evaluating the structural integrity and behavior of the hydrogel, which is critical for understanding the release dynamics of the embedded nanopolyplex and optimising its performance for ocular applications. This platform is designed to overcome the need for repeated intraocular administration commonly associated

with therapies for retinal degenerative diseases. Building on these findings, Chapter 5 will assess the *in vivo* performance of the nanopolyplex-loaded hydrogel, with particular attention to safety and the ability to mediate efficient gene expression over time.

3.4. References

Adijanto, J., Naash, M.I., 2015. Nanoparticle-based Technologies for Retinal Gene Therapy. Eur. J. Pharm. Biopharm. Off. J. Arbeitsgemeinschaft Pharm. Verfahrenstechnik EV 95, 353–367. https://doi.org/10.1016/j.ejpb.2014.12.028

Alfei, S., 2023. Cationic Materials for Gene Therapy: A Look Back to the Birth and Development of 2,2-Bis-(hydroxymethyl)Propanoic Acid-Based Dendrimer Scaffolds. Int. J. Mol. Sci. 24, 16006. https://doi.org/10.3390/ijms242116006

Almalik, A., Karimi, S., Ouasti, S., Donno, R., Wandrey, C., Day, P.J., Tirelli, N., 2013. Hyaluronic acid (HA) presentation as a tool to modulate and control the receptor-mediated uptake of HA-coated nanoparticles. Biomaterials 34, 5369–5380. https://doi.org/10.1016/j.biomaterials.2013.03.065

Bishop, C.J., Kozielski, K.L., Green, J.J., 2015. Exploring the role of polymer structure on intracellular nucleic acid delivery via polymeric nanoparticles. J. Control. Release Off. J. Control. Release Soc. 219, 488–499. https://doi.org/10.1016/j.jconrel.2015.09.046

Brgles, M., Jurašin, D., Sikirić, M.D., Frkanec, R., Tomašić, J., 2008. Entrapment of Ovalbumin into Liposomes—Factors Affecting Entrapment Efficiency, Liposome Size, and Zeta Potential. J. Liposome Res. 18, 235–248. https://doi.org/10.1080/08982100802312762

Bulcha, J.T., Wang, Y., Ma, H., Tai, P.W.L., Gao, G., 2021. Viral vector platforms within the gene therapy landscape. Signal Transduct. Target. Ther. 6, 1–24. https://doi.org/10.1038/s41392-021-00487-6

Casper, J., Schenk, S.H., Parhizkar, E., Detampel, P., Dehshahri, A., Huwyler, J., 2023. Polyethylenimine (PEI) in gene therapy: Current status and clinical applications. J. Controlled Release 362, 667–691. https://doi.org/10.1016/j.jconrel.2023.09.001

Chandola, C., Casteleijn, M.G., Chandola, U.M., Gopalan, L.N., Urtti, A., Neerathilingam, M., 2019. CD44 aptamer mediated cargo delivery to lysosomes of retinal pigment epithelial cells to prevent age-related macular degeneration. Biochem. Biophys. Rep. 18, 100642. https://doi.org/10.1016/j.bbrep.2019.100642

Chiou, H.C., Tangco, M.V., Kormis, K., Levine, S.M., Robertson, D., Kormis, K., Wu, C.H., Wu, G.Y., 1994. Enhanced resistance to nuclease degradation of nucleic acids complexed to asialoglycoprotein-polylysine carriers. Nucleic Acids Res. 22, 5439–5446. https://doi.org/10.1093/nar/22.24.5439

Fan, H., Johnson, C., 2011. Insertional Oncogenesis by Non-Acute Retroviruses: Implications for Gene Therapy. Viruses 3, 398–422. https://doi.org/10.3390/v3040398

Federica Ponti, Matilde Campolungo, , Clara Melchiori, , Nina Bono, ,, Gabriele Candiani, 2021. Cationic lipids for gene delivery: many players, one goal. Chem. Phys. Lipids 235, 105032. https://doi.org/10.1016/j.chemphyslip.2020.105032

Fonseca, M., Jarak, I., Victor, F., Domingues, C., Veiga, F., Figueiras, A., 2024. Polymersomes as the Next Attractive Generation of Drug Delivery Systems: Definition, Synthesis and Applications. Materials 17, 319. https://doi.org/10.3390/ma17020319

Genetic Immunity, 2024. URL https://geneticimmunity.hu/ (accessed 10.14.24).

Goswami, R., Subramanian, G., Silayeva, L., Newkirk, I., Doctor, D., Chawla, K., Chattopadhyay, S., Chandra, D., Chilukuri, N., Betapudi, V., 2019. Gene Therapy Leaves a Vicious Cycle. Front. Oncol. 9, 297. https://doi.org/10.3389/fonc.2019.00297

Ha, T.T.N., Huy, N.T., Murao, L.A., Lan, N.T.P., Thuy, T.T., Tuan, H.M., Nga, C.T.P., Tuong, V.V., Dat, T.V., Kikuchi, M., Yasunami, M., Morita, K., Huong, V.T.Q., Hirayama, K., 2011. Elevated Levels of Cell-Free Circulating DNA in Patients with Acute Dengue Virus Infection. PLOS ONE 6, e25969. https://doi.org/10.1371/journal.pone.0025969

Han, L., Zhao, Y., Yin, L., Li, R., Liang, Y., Huang, H., Pan, S., Wu, C., Feng, M., 2012. Insulin-Loaded pH-Sensitive Hyaluronic Acid Nanoparticles Enhance Transcellular Delivery. AAPS PharmSciTech 13, 836–845. https://doi.org/10.1208/s12249-012-9807-2

Hill, A.B., Chen, M., Chen, C.-K., Pfeifer, B.A., Jones, C.H., 2016. Overcoming Gene-Delivery Hurdles: Physiological Considerations for Nonviral Vectors. Trends Biotechnol. 34, 91–105. https://doi.org/10.1016/j.tibtech.2015.11.004

Hillaireau, H., Couvreur, P., 2009. Nanocarriers' entry into the cell: relevance to drug delivery. Cell. Mol. Life Sci. 66, 2873–2896. https://doi.org/10.1007/s00018-009-0053-z

Honary, S., Zahir, F., 2013. Effect of Zeta Potential on the Properties of Nano-Drug Delivery Systems - A Review (Part 2). Trop. J. Pharm. Res. 12, 265–273. https://doi.org/10.4314/tjpr.v12i2.20

Hsiao, P. F., Peng, S., Tang, T. C., Lin, S. Y., & Tsai, H. C., 2016. Enhancing the in vivo transdermal delivery of gold nanoparticles using poly (ethylene glycol) and its oleylamine conjugate. International journal of nanomedicine, 1867-1878.

Hsu, M.-J., Chen, H.-K., Chen, C.-Y., Lien, J.-C., Gao, J.-Y., Huang, Y.-H., Hsu, J.B.-K., Lee, G.A., Huang, S.-W., 2022. Anti-Angiogenetic and Anti-Lymphangiogenic Effects of a Novel 2-Aminobenzimidazole Derivative, MFB. Front. Oncol. 12.

Javahershenas, R., Han, J., Kazemi, M. and Jervis, P.J., 2024. Recent Advances in the Application of 2‐Aminobenzothiazole to the Multicomponent Synthesis of Heterocycles. ChemistryOpen, 13(11), p.e202400185.

Jiang, B.-P., Zhang, L., Zhu, Y., Shen, X.-C., Ji, S.-C., Tan, X.-Y., Cheng, L., Liang, H., 2015. Water-soluble hyaluronic acid–hybridized polyaniline nanoparticles for effectively

targeted photothermal therapy. J. Mater. Chem. B 3, 3767–3776. https://doi.org/10.1039/C4TB01738B

Jun, Y.J., Park, M.K., Jadhav, V.B., Song, J.H., Chae, S.W., Lee, H.J., Park, K.S., Jeong, B., Choy, J.H., Sohn, Y.S., 2010. Tripodal amphiphiles tunable for self-assembly to polymersomes. J. Controlled Release 142, 132–137. https://doi.org/10.1016/j.jconrel.2009.10.004

Kita, K., Dittrich, C., 2011. Drug delivery vehicles with improved encapsulation efficiency: taking advantage of specific drug–carrier interactions. Expert Opin. Drug Deliv. 8, 329–342. https://doi.org/10.1517/17425247.2011.553216

Kumari, R., Jat, P., 2021. Mechanisms of Cellular Senescence: Cell Cycle Arrest and Senescence Associated Secretory Phenotype. Front. Cell Dev. Biol. 9. https://doi.org/10.3389/fcell.2021.645593

Li, S.-D., Huang, L., 2009. Nanoparticles Evading The Reticuloendothelial System: Role of The Supported Bilayer. Biochim. Biophys. Acta 1788, 2259–2266. https://doi.org/10.1016/j.bbamem.2009.06.022

Lisziewicz, J., Bakare, N., Calarota, S.A., Bánhegyi, D., Szlávik, J., Újhelyi, E., Tőke, E.R., Molnár, L., Lisziewicz, Z., Autran, B., Lori, F., 2012. Single DermaVir Immunization: Dose-Dependent Expansion of Precursor/Memory T Cells against All HIV Antigens in HIV-1 Infected Individuals. PLoS ONE 7, e35416. https://doi.org/10.1371/journal.pone.0035416

Lundstrom, K., 2023. Viral Vectors in Gene Therapy: Where Do We Stand in 2023? Viruses 15, 698. https://doi.org/10.3390/v15030698

Ma, K., Mi, C.-L., Cao, X.-X., Wang, T.-Y., 2021. Progress of cationic gene delivery reagents for non-viral vector. Appl. Microbiol. Biotechnol. 105, 525–538. https://doi.org/10.1007/s00253-020-11028-6

Massadeh, S., Al Aamery, M., 2016. Nano-materials for Gene Therapy: An Efficient Way in Overcoming Challenges of Gene Delivery. J. Biosens. Bioelectron. 07. https://doi.org/10.4172/2155-6210.1000195

Massahud, E., Ahmed, H., Babarao, R., Ehrnst, Y., Alijani, H., Darmanin, C., & Yeo, L. Y., 2023. Acoustomicrofluidic Defect Engineering and Ligand Exchange in ZIF‐8 Metal–Organic Frameworks. Small Methods, 7(6), 2201170.

Mehta, M.J., Kim, H.J., Lim, S.B., Naito, M. and Miyata, K., 2024. Recent progress in the endosomal escape mechanism and chemical structures of polycations for nucleic acid delivery. Macromolecular Bioscience, 24(4), p.2300366.

Mollé, L.M., Smyth, C.H., Yuen, D., Johnston, A.P.R., 2022. Nanoparticles for vaccine and gene therapy: Overcoming the barriers to nucleic acid delivery. WIREs Nanomedicine Nanobiotechnology 14, e1809. https://doi.org/10.1002/wnan.1809

Mourdikoudis, S., Menelaou, M., Fiuza-Maneiro, N., Zheng, G., Wei, S., Pérez-Juste, J.,

Polavarapu, L. and Sofer, Z., 2022. Oleic acid/oleylamine ligand pair: a versatile combination in the synthesis of colloidal nanoparticles. Nanoscale horizons, 7(9), pp.941-1015.

Mullen, P.M., Lollo, C.P., Phan, Q.-C., Amini, A., Banaszczyk, M.G., Fabrycki, J.M., Wu, D., Carlo, A.T., Pezzoli, P., Coffin, C.C., Carlo, D.J., 2000. Strength of conjugate binding to plasmid DNA affects degradation rate and expression level in vivo. Biochim. Biophys. Acta BBA - Gen. Subj. 1523, 103–110. https://doi.org/10.1016/S0304-4165(00)00104-5

Parveen, S., Gupta, P., Kumar, S., Banerjee, M., 2023. Lipid polymer hybrid nanoparticles as potent vehicles for drug delivery in cancer therapeutics. Med. Drug Discov. 20, 100165. https://doi.org/10.1016/j.medidd.2023.100165

Pérez-Martínez, F.C., Guerra, J., Posadas, I., Ceña, V., 2011. Barriers to Non-Viral Vector-Mediated Gene Delivery in the Nervous System. Pharm. Res. 28, 1843–1858. https://doi.org/10.1007/s11095-010-0364-7

Raana, S., Nouri, M., Agbolaghi, S., Roshangar, L., Sadrhaghighi, A., Seifalian, A.M., Keyhanvar, P., 2020. A summary on non-viral systems for gene delivery based on natural and synthetic polymers [WWW Document]. URL https://www.tandfonline.com/doi/epdf/10.1080/00914037.2020.1825081?needAccess=true (accessed 11.13.23).

Redrejo-Rodríguez, M., Muñoz-Espín, D., Holguera, I., Mencía, M., Salas, M., 2012. Functional eukaryotic nuclear localization signals are widespread in terminal proteins of bacteriophages. Proc. Natl. Acad. Sci. 109, 18482–18487. https://doi.org/10.1073/pnas.1216635109

Santa, P., Garreau, A., Serpas, L., Ferriere, A., Blanco, P., Soni, C., Sisirak, V., 2021. The Role of Nucleases and Nucleic Acid Editing Enzymes in the Regulation of Self-Nucleic Acid Sensing. Front. Immunol. 12.

Tan, E., Chin, C.S.H., Lim, Z.F.S., Ng, S.K., 2021. HEK293 Cell Line as a Platform to Produce Recombinant Proteins and Viral Vectors. Front. Bioeng. Biotechnol. 9, 796991. https://doi.org/10.3389/fbioe.2021.796991

Tomihata, K., Ikada, Y., 1997. Crosslinking of hyaluronic acid with water-soluble carbodiimide. J. Biomed. Mater. Res. 37, 243–251. https://doi.org/10.1002/(SICI)1097-4636(199711)37:2<243::AID-JBM14>3.0.CO;2-F

Vaughan, E.E., DeGiulio, J.V., Dean, D.A., 2006. Intracellular Trafficking of Plasmids for Gene Therapy: Mechanisms of Cytoplasmic Movement and Nuclear Import. Curr. Gene Ther. 6, 671–681.

Wang, C., Pan, C., Yong, H., Wang, F., Bo, T., Zhao, Y., Ma, B., He, W., Li, M., 2023. Emerging non-viral vectors for gene delivery. J. Nanobiotechnology 21, 272. https://doi.org/10.1186/s12951-023-02044-5

Wang, Y., Shahi, P.K., Wang, X., Xie, R., Zhao, Y., Wu, M., Roge, S., Pattnaik, B.R., Gong, S., 2021. In vivo targeted delivery of nucleic acids and CRISPR genome editors enabled by GSH-responsive silica nanoparticles. J. Controlled Release 336, 296–309. https://doi.org/10.1016/j.jconrel.2021.06.030

Wilson, B., Geetha, K.M., 2022. Lipid nanoparticles in the development of mRNA vaccines for COVID-19. J. Drug Deliv. Sci. Technol. 74, 103553. https://doi.org/10.1016/j.jddst.2022.103553

Xu, Y., Szoka, F.C., 1996. Mechanism of DNA Release from Cationic Liposome/DNA Complexes Used in Cell Transfection'. Biochemistry 35, 5616–5623. https://doi.org/10.1021/bi9602019

Xu, E., Saltzman, W.M. and Piotrowski-Daspit, A.S., 2021. Escaping the endosome: assessing cellular trafficking mechanisms of non-viral vehicles. Journal of Controlled Release, 335, pp.465-480.

Yaghobi, Z., Movassaghpour, A., Talebi, M., Abdoli Shadbad, M., Hajiasgharzadeh, K., Pourvahdani, S., Baradaran, B., 2021. The role of CD44 in cancer chemoresistance: A concise review. Eur. J. Pharmacol. 903, 174147. https://doi.org/10.1016/j.ejphar.2021.174147

Youm, I., Agrahari, V., Murowchick, J. B., & Youan, B. B. C., 2014. Uptake and cytotoxicity of docetaxel-loaded hyaluronic acid-grafted oily core nanocapsules in MDA-MB 231 cancer cells. Pharmaceutical research, 31, 2439-2452.

Yung, M., Klufas, M.A., Sarraf, D., 2016. Clinical applications of fundus autofluorescence in retinal disease. Int. J. Retina Vitr. 2, 12. https://doi.org/10.1186/s40942-016-0035-x

Zhao, Z., Anselmo, A.C., Mitragotri, S., 2021. Viral vector‐based gene therapies in the clinic. Bioeng. Transl. Med. 7, e10258. https://doi.org/10.1002/btm2.10258

CHAPTER FOUR

Preliminary Investigation of Smart Hydrogel System for cell encapsulation and delivery to promote ocular tissue regeneration

4. Introduction

Pairing regenerative medicine with gene therapy is fast gaining interest due to its promise in long term disease correction, targeting of disease etiology, cell restoration, possible reprogramming of healthy/degenerative cells and the multiple failures of conventional therapies. As a result of its uniqueness, this approach has garnered attention for the treatment of retinal degenerative diseases. Notably, the eye's inherent immune privilege, the opportunity for targeted administration, and the reduced variability associated with most clinical studies due to the need for a control group/cohort make the eye an ideal tissue for assessing the potential of this dual approach (Niederkorn, 2019; Park, 2021). The inherent association of retinal degenerative diseases with severe visual impairment and or blindness introduces complexities in the development of effective treatments. Due to the myriad of underlying causes, novel approaches to the treatment of retinal degeneration such as gene therapy, tissue engineering, stem cell therapy and optogenetics are necessary to bridge the gap. The synergistic approach of gene therapy and regenerative medicine for retinal degeneration can address shortfalls associated with conventional pharmacological therapies and the only FDA approved gene therapy, Luxturna® (Maguire et al., 2021; Byrne et al., 2025). Despite the advent of Luxturna®, which has significantly contributed to improved visual acuity in patients suffering from Leber congenital amaurosis 2, and the plethora of PSED pharmacological drugs; these therapies remain limited in their ability to halt the progressive degeneration of the retina and to regenerate, replace or restore lost retinal cells (photoreceptor cells and retinal pigment epithelial cells) which in the long run would improve patient outcomes (Chiu et al., 2021).

Therefore, the combination of gene therapy with tissue regeneration/engineering has the potential to address multiple challenges simultaneously as the inclusion of genetically engineered cells or stem cells, can tackle the regeneration question by conferring functional improvement to retinal cells and introducing beneficial properties normally associated with stem cell therapy (Huang et al., 2020). Genetically modified cells (particularly stem cells) have expanded functionality beyond self-renewal - differentiation - driving neuroprotection through neuronal cell apoptosis inhibitors (Watanabe et al., 2016), they have the potential to modify cell survival under degenerative conditions (oxidative stress, inflammatory, nutrient deficient and hypoxic amongst others), improve neuroplasticity, support cell integration and homing and treat underlying genetic disorders (Han et al., 2024; Salehi et al., 2022).

A combinatorial approach therefore offers a synergistic template for disease treatment as most degenerative diseases may require both cellular and molecular repair. An exciting avenue to achieve this approach is pairing gene delivery with cell delivery using a gene delivery nanosystem and cell scaffolds. This avenue of therapy can be referred to as genetically engineered cell therapy (Yong et al., 2018). Research has been conducted discussing the potential of merging these two forms of therapies, with the pertinent question arising - 'Why complicate the therapeutic process by combining these two approaches?' This approach offers the best of both worlds, enabling the modification of primary cells to achieve expression of tissue specific proteins capable of promoting cell de-differentiation and tissue renewal (Sheyn et al., 2010). An interesting example is the genetic modification of mesenchymal stem cells (MSCs) through the use of a lentivirus encoding the immunomodulatory cytokine, interleukin -13 (IL-13) to enhance their survival following subretinal transplantation (Huang et al., 2020). Normally, upon transplantation, MSCs are limited in their ability to repair injured tissue due to their susceptibility to oxidative stress, inflammation and nutrient starvation which restricts their viability in vivo (Herberg et al., 2013). Additionally, MSC subretinal transplantation promotes lesion formation and BRB destruction (Xian and Huang, 2015).

Therefore, genetic modification of MSCs with IL-13 was shown to alleviate BRB breakdown, adopt immuno-modulatory response mechanisms and thus enhance MSC survival following grafting (Huang et al., 2020). This strategy has also been used for promoting bone regeneration. Briefly, bone morphogenic protein (BMPs) was overexpressed in pluripotent mesenchymal cells for the induction of bone engraftment and regeneration as exogenous doses of BMPs (short half life) required to achieve osteogenic effect are toxic and often results in osteolysis and bone resorption at the site of the implant (Sheyn et al., 2010; Wang et al., 2003). Across the field of tissue regeneration, retinal degenerative diseases underscore the need for investigating genetically engineered cell therapy to tackle key limiting factors in their treatment. Interestingly, retinal pigment epithelial (RPE) cell suspensions transplanted into the subretinal space of patients have been shown to maintain vision, however the prevention or reversal of AMD is unknown (Gouras and Algvere, 1996). Importantly, transplanted cell suspensions and their resulting tissues are required to survive surgical delivery, engraft onto the Bruch's membrane, integrate with existing RPE cell layer and polarise without eliciting an immune response (MacLaren et al., 2016). Alternatively, the use of cell delivery scaffolds and more recently, cell sheets of RPE cells cultivated on artificial Bruch's membrane may eliminate existing challenges. A phase 1, safety and feasibility study for a designed patch carrying differentiated human embryonic stem cells derived RPE monolayer was conducted on patients with acute wet AMD (Da Cruz et al., 2018). According to Da Cruz et al (2018), the coated synthetic basement membrane patch - RPE system delivered in the subretinal space, resulted in improved visual acuity for 12 months.

Favourably, the patch enabled the group to bypass limitations commonly associated with the use of cell suspension in RPE replacement therapy.

Therefore, as part of this thesis, the adoption and preliminary investigation of the combinatorial approach, fabrication of a dual system that can act as a gene delivery system and cell scaffold was proposed. A composite system, henceforth referred to as the Gen-I system was designed for encapsulation and delivery of genetic material as well as serving as a "scaffold" for potential RPE cell regeneration. Construction of the Gen-I system was conducted by carefully selecting functional and biocompatible polymers to support gene delivery and cell viability, thus evading limitations such as cell loss as a result of reflux through retinotomy, cell damage due to shear stress and unlocalised delivery as commonly seen in the delivery of cell suspensions (Da Cruz et al., 2018). This investigation reports the capacity of the Gen-I system to act as an encapsulation network for genetic material and scaffold for cell growth by using a design of experiment approach to optimise an ideal injectable smart hydrogel system. Furthermore, the physicochemical (injectability, gelation time, viscosity & modulus and degradation) and cellular compatibility properties of the optimised system were investigated. The data collated in this study serves as a preliminary study for the use of smart hydrogels as cell scaffolds and nanoparticle delivery agents capable of providing structural support and nutrient rich environments for cell engraftment.

4.1. Materials and Methods

Pluronic ® F-127 (Poloxamer 407 - 12600 g/mol), chitosan oligosaccharide (Mn 5,000) were purchased from Sigma Aldrich (St Louis, MO, USA). Nanosystem was constructed by the WADDP group (reference), pcDNA was purchased from ThermoFischer (Waltham, MA USA). For cell culture, Dulbecco's modified Eagle's Medium (DMEM), foetal bovine serum (FBS), penicillin-streptomycin solution (10,000 U/mL), modified Eagle's Medium alpha (MEMalpha) and gentamicin purchased from Thermofischer (Waltham, MA USA). Phosphate-buffered saline (1×, pH 7.4) was purchased from Gibco. For microscopy, stains DAPI, CAPSIC, HOECHST ETC were obtained abcd. MTT (3-(4,5-Dimethylthiazol-2-yl)-2,5-diphenyltetrazolium bromide).

4.1.1. Construction and characterisation of the Gen-I system: Box-Behnken Design

To optimise the formulation of the Gen-I system, a Design of Experiment (DoE) approach was undertaken using the software Stat-Ease. A Box-Behnken Design was conducted, the experimental design considered two factors, namely; Pluronic ® F-127 and chitosan oligosaccharide, each evaluated at varying concentrations. Each factor was evaluated at three levels; low (-1), medium (0) and high (+1) (Table 4.1). The Box-Behnken Design matrix (BBD) provided 17 experimental runs with replicates at key factor levels included to estimate

experimental error and ensure reproducibility (Table 4.2). The Gen-I system formulations were prepared at the following concentrations - Pluronic® F-127 (17 - 22%), chitosan oligosaccharide lactate (0.1 - 1%) (w/v%) and nano-polyplex (1%) as per the experimental design. Briefly, the nano-polyplex system was prepared as outlined in Chapter 3, the respective amounts of chitosan oligosaccharide and Pluronic ® F-127 were dispersed in the nano-polyplex system and dissolved using the cold method by Schmolka (Schmolka, 1972) overnight prior to performing characterisation to ensure complete dissolution of Pluronic® F-127. Responses measured as part of this BBD approach included gelation time, gelation temperature and injectability (Table 4.1).

Table 4.1: Independent and dependent variables for factorial design.

Independent Variables Concentration	**Variable Levels**		
	Low (-1)	Medium (0)	High (+1)
X_1 = Pluronic F127	17	19.5	22
X_2 = Chitosan oligosaccharide	0.1	0.55	1
Dependent variables			
Y_1 = Gelation temperature	Maximum in °C		
Y_2 = Gelation time	Minimum in seconds		
Y_3 = Syringeability	Minimum in Newtons		

4.1.2. Gelation Characterisation and Injectability Assessment

To determine the critical gelation concentration and temperature, the inversion test tube method, which is considered an essential primary qualitative assessment for formulation gelation and viscosity, was conducted for all formulations. Previously prepared formulation solutions were equilibrated to room temperature (22 °C) prior conducting the test, 2 ml of each formulation was placed in a 5 ml glass vial and incubated in a 37 °C incubator. The critical gelation point (sol-gel transition) of each formulation was observed by absence of flow through the inversion of the vial and the time it takes the formulation to transition from sol to gel state otherwise known as gelation time was also recorded. The exact critical gelation temperature (Tgel) was determined using the ThermoHaake MARS Modular Advanced Rheometer (ThermoFischer Scientific, Karlsruhe, Germany) equipped with a temperature control chamber for thermal control. Briefly, formulated solutions were prepared and loaded

between the temperature controlled plates, a temperature ramp test was then performed with an angular frequency of 1 Hz at a heating rate of 1°C/min at a temperature range of 20 to 60°C. The storage modulus (G') and loss modulus (G'') was continuously monitored. Subsequently, injectability of the formulations was assessed across different needle sizes 21, 25 and 27 Gauges. Assessing ease of gel administration/injection is crucial to eliminate any potential variabilities in dosage or distribution that may arise due to poor injectability and loss of gel integrity. Injectability of the thermogels prepared in triplicate and pre-cooled to 8°C was assessed using the TA-XT2 Texture Analyser (Stable Micro Systems, Surrey, UK). Using a P/50R cylinder probe aligned to the plunger plate, pseudo manual injection of each formulation was conducted using Luer-lock syringes fitted with the appropriate needle. To expel the gel, the probe was also used for volume displacement by compression of the syringe plunger at compression speed of 1 mm/s and a distance of 20 mm and the maximum force was recorded (Naik et al., 2024). From these data, optimised formulation was provided by Stat-Ease and used for subsequent investigation,

4.1.3. Physicochemical and structural characterisation of hydrogels

The optimised Gen-I formulation computed by the Stat-Ease software (1% nano-polyplex, 0.22% oligosaccharide chitosan and 17.11% Pluronic® F-127) was used to composed final system, henceforth referred to as the Gen-I system. The physicochemical properties and stability of the Gen-I system was investigated and verified using Pluronic® only and Pluronic®_chitosan as the controls. Fourier transform infrared spectroscopy (PerkinElmer ATR, Spectrum 2000, Waltham, MA, USA) was used for investigating the chemical structure of the system and to detect chemical degradation or changes in response to stress and time over the wavelength range 4000 to 650 cm^{-1}. To understand the thermal behaviour of the systems, thermogravimetric analysis (PerkinElmer, TGA 4000, Llantrisant, Wales, UK) was utilised as it aids in understanding the effect of temperature on the thermal stability and degradation profile of the thermogel over a temperature range 30°C to 900°C at a heating rate of 10°C/min under inert N2 environment. Degradation thermograms were constructed as percentage weight loss over temperature. Morphological analyses were performed using scanning electron microscopy (Zeiss, Jena, Germany) to analyse the interior morphologies of lyophilized hydrogels following mounting on SEM aluminium stub and sputter coating with palladium-gold.

4.1.4. Rheological analysis of the Gen-I system

Rheological assessments (frequency sweep, thixotropy and yield stress) were performed using the ThermoHaake MARS Modular Advanced Rheometer (Thermo Fisher Scientific, Karlsruhe, Germany) affixed with a parallel plate having a gap measurement of 0.052 mm

and measuring geometry of C35/1° T1 and a solvent trap to minimise evaporation during testing. Prior to conducting each test, samples were applied on the Peltier temperature controlled stage and equilibrated to 37°C to ensure gelation. The viscoelastic behaviour/frequency sweep of the Gen-I system was analysed across a range of oscillatory shear frequencies, 0.01 Hz to 10 Hz at a constant strain. The viscosity (η), loss modulus (G'') and storage modulus (G') were noted as a function of frequency at 37°C. Shear thinning behaviour and thixotropic recovery of the Gen-I system's viscosity was evaluated by subjecting the system to varying shear rates and recording the viscosity at different shear rates. Lastly, to determine yield stress, parameters such shear stress (0.02 Pa to 2000 Pa vs rate over time was recorded.

4.1.5. Gen-I Degradation profile and stability

In a thermostatic bath, 800 µL of the Gen-I system was incubated in a 1.5 ml micro-tube until gelation. The microtubes were filled with simulated vitreous humour (Bonfiglio et al., 2015), incubated at 37 °C and the amount of weight loss after recovery of the samples was measured at different time intervals. The degradation profile was evaluated by measuring the weight loss (%) at each time point, where ***Wt*** is the weight of each respectively at specific time points and ***W0*** is the initial weight of each system.

$$\%\, Degradation \;=\; \frac{Wt-W0}{W0} \times 100 \qquad (4.1)$$

The stability of the Gen-I system was assessed using the following procedure: The Gen-I system and controls were prepared in sealable containers and stored at 4 °C for 1 month. At week four, the rheological properties (viscosity, gelation time and temperature) of the system along with the stability of nucleic acid was assessed.

4.1.6. Maintenance of Cell culture

Cells (MG63, HEK293, and hRPE) were cultured in Modified Eagle Medium alpha, Dulbecco's Modified Eagle Medium and Dulbecco's Modified Eagle's Medium/Nutrient Mixture F-12 Ham respectively. Media for each cell line was supplemented with 10% foetal bovine serum, 1% of 100 mg/mL streptomycin, 100 U/mL penicillin and 50 mg/mL gentamicin (only for MEM-alpha: MG63) (Thermofisher, South Africa). Cells were maintained in a humidified incubator at 37°C and 5% CO_2. Culture mediums were replaced every 2 days until cell confluence (80 - 90%) was reached.

4.1.7. Cell Viability and Proliferation assay

The equipment used for preparing the Gen-I system and controls was autoclaved, Pluronic f127, the nanosystem and chitosan were subsequently sterilised by UV irradiation before

formulation. The system was then prepared in cell culture medium and stored at 4°C overnight to achieve complete dissolution of the pluronic. The respective cell lines were cultured and seeded at a density of 5 × 10^4 cells/mL in 96-well plates and incubated at 37°C, 95% humidity, and 5% CO_2. Subsequently, cells were seeded in the Gen-I system (intervention) and treated with DMSO (negative control) for 48 and 72 hours, following which cell viability was assessed using MTT assay (Roche Cell Proliferation Kit) as per manufacturer's instructions. Briefly, 10 µL of MTT solution was added to each well, and the plates were incubated at 37°C under humidity and 5% CO_2 for 4 hours. Following incubation, 100 µL of MTT solubilizing agent was added to dissolve the formazan crystals, and the plates were left overnight. Cell viability was quantified by measuring absorbance at 570 nm (with reference at 620 nm) using a multimodal microplate reader (Victor X3, PerkinElmer, Waltham, MA, USA), with non-seeded cells used as a reference (positive control).

$$\%\, Cell\ viability = \frac{Absorbance\ of\ sample}{Absorbance\ of\ control} \times 100 \qquad (4.2)$$

To further support the data from the cell proliferation and viability assays, Casein AM staining was utilised to assess the biocompatibility of the Gen-I system for cell encapsulation and delivery. The Gen-I system was prepared as outlined in section 4.1.3 and cells cultured as previously described. After reaching 80 - 90% confluency, cells were trypsinized and the suspension was mixed with the hydrogels at a concentration of 0.5 x10^6 cells/ml. The gels were placed in 96 well plates containing appropriate complete cell media and incubated under cell culture conditions. Viability of the seeded cells was evaluated using live/dead cell staining with calcein acetoxymethyl ester (calcein AM) (Thermorfisher, South Africa). Prior staining, cells were washed in PBS and incubated in 1uM of calcein AM in serum free cell media under cell culture conditions for 60 minutes (Invitrogen, USA) in the dark for each timepoint. Following incubation, calcein AM was aspirated and excess stain was removed by washing cells with PBS**.** Cells were then stained with 30 nM DAPI for 30 minutes, washed twice with PBS and visualised using the Celina S (Logos Biosystems, South Korea) fluorescence microscope with brightfield, fluorescent and merged images taken 4x magnification and GFP- filter (Emission 475 nm and excitation 509 nm).

Excitation (Ex): 375 nm with a 28 nm bandwidth **Emission (Em):** 460 nm with a 50 nm bandwidth.

4.1.8. Statistical analysis

All data are expressed as the mean ± standard error, calculated from at least three independent replications. The statistical differences between the means were determined using one-way or two-way analysis of variance (ANOVA), followed by Tukey's multiple comparison test. $P < 0.05$ was considered statistically significant.

4.2. Results and Discussion

4.2.1. Design of Experiments - The Box-Behnken Design matrix

To investigate the use of the Gen-I system as a possible "depot"/ delivery system for genetic material and scaffold for cells, optimisation was conducted through a design of experiment approach, as it allows for the evaluation of the impact multiple factors have on specific responses. The aim of the experimental design was to investigate the impact of Pluronic® F127 and chitosan oligosaccharide on three important responses; gelation time, gelation temperature and injectability. Stat-Ease aided in the evaluation of possible interactions between the independent factors and resulting responses. The results were analysed to determine how varying concentrations of each polymer influenced the responses, based on the outcome further optimisation of the formulations was conducted to achieve desired downstream properties such as gene delivery (*in vivo*) cell viability, rate of degradation and cell encapsulation. The preparation of the composite thermogel (Gen-I) consisting of pluronic® F127, oligosaccharide chitosan and the nano-polyplex system (fabricated in Chapter 3) involved the use of the cold method with all components prepared in nuclease free water and autoclaved glassware. As per the DOE approach, 17 formulations (Table 4.2) were prepared and analysed pertinently for their gelation time, temperature and injectability using three different needle gauges (21, 25 and 27 Gauge). Mathematical models were generated which provided insight on factor-response interactions and the optimal conditions for the predicted responses.

Table 4.2: Summary of the Box-Behnken statistical design-generated formulations and responses obtained from i*n vitro* testing for the optimisation of the Gen-I system

Formulation	Pluronic F127 (%)	Nanosystem (%)	Chitosan (%)	Gelation Time (seconds)	Injectability (21 Gauge)	Injectability (25 Gauge)
F1	19.5	1	0.55	105	11.86	47.65
F2	17	1	0.55	156	10.71	42.19
F3	17	1	1	200	19.44	82.83
F4	17	1	0.1	105	8.25	35.49
F5	19.5	1	0.1	105	12.82	55.87
F6	19.5	1	0.1	105	12.61	57.56
F7	19.5	1	0.55	105	11.86	47.95

F8	19.5	1	0.55	105	12.21	46.58
F9	22	1	1	45	16.4	50.78
F10	19.5	1	0.55	105	11.32	47.14
F11	19.5	1	0.55	105	11.95	49.54
F12	22	1	0.55	45	14.62	59.14
F13	19.5	1	1	105	7.95	37.95
F14	19.5	1	1	105	7.91	36.85
F15	22	1	0.55	45	14.62	59.14
F16	17	1	0.55	155	9.95	41.45
F17	22	1	0.1	45	18.56	77.68

Gelation time is an important parameter to optimise as it influences drug loading, distribution and release. A wide distribution of gelation times is represented across formulations (Table 4.2). Formulations composed of higher X_1 concentrations showed faster gelation times (45 seconds) (Figure 4.1), which can be beneficial in ensuring precision in targeted cell or gene delivery, as this can minimise dispersion of therapeutics beyond the intended site of delivery (Bellotti et al., 2021). Additionally, faster gelation times can protect sensitive cells (stem and primary cells) from external environmental pressures (Hodjat et al., 2015), through the immediate formation of a three dimensional network/supportive cell matrix. Conversely, formulations composed of lower to moderate X_1 concentrations comparatively longer gelation times (Figure 4.1). Although this has its drawbacks particularly concerning possible immediate burst release of therapeutic, gradual gelation has some advantages. One factor to consider for cell and gene delivery is the need for homogeneity of encapsulated components. Gradual gelation enables uniform distribution of components within the *in-situ* forming matrix therefore potentially enhancing efficacy. Lastly, the potential introduction of chemical and mechanical stress to sensitive cells by faster gelation process can affect cell viability and integration into surrounding tissue.

Table 4.3: Regression analysis summary for responses Y_1, Y_2, Y_3 and Y_4

Model	R^2 Value	Adjusted R^2	Predicted R^2	F value	S.D.	CV%
Y_1	0.834	0.810	0.697	35.26	20.36	19.38
Y_2	0.977	0.967	0.905	96.16	$1.05e^{-06}$	11.06
Y_3	0.835	0.760	0.132	11.18	1.57	12.38
Y_4	0.789	0.741	0.642	16.27	2.71	14.42

Notably, a quadratic interactive model for gelation time was generated and represented in Equation (4.3). The model was significant ($p < 0.0001$), with X_1 reported as the significant factor in determining gelation time (Table 4.3).

$$Y_2 = 581\ 82549 - 52405000\ X_1 - 1416667\ X_2 \quad (4.3)$$

Importantly, shorter gelation times observed corresponded with higher viscosities and higher force requirements for injectability across the different needle gauges (Table 4.2). The confirmed models (quadratic - Equation 4.3 and 4.4) were significant ($p < 0.0001$) and the terms X_1, X_2, X_1X_2, X_1^2 and X_1^2 had a significant effect on response Y2 (Table 4.3). As shown in the contour plot (Figure 4.1), formulations with higher concentrations of X_1 and X_2 require more force for injectability as they do not pass easier through the needle. During *in vivo* intravitreal administration, this may clog the needle head resulting in increased intraocular pressure, patient discomfort and other complications. Conversely, lower X_1 and X_2 concentrations showed lower syringeability force (Figure 4.1) requirements which is beneficial for minimally invasive procedures such as intravitreal administration procedures which require precise delivery and for maintaining cell viability during administration or grafting.

$$Y_2 = -\ 8.14e^{-06} + 6.23e^{-06}\ X_1 - 0.000086\ X_2 + 3.35\ e^{-06}\ X_1\ X_2 - 2.47e^{-07}\ X_1^2 + 5.58e^{-06}\ X_2^2 \quad (4.4)$$

$$Y_3 = 130.35 - 13.5\ X_1 + 22.79\ X_2 - 0.73\ X_1 X_2 + 0.37\ X_1^2 - 0.75\ X_2^2 \quad (4.5)$$

As mentioned before, on visual inspection, formulations showed differing degrees of viscosity, therefore rheological analyses were conducted to elucidate the role of the different components in the composite on gelation temperature in particular which is one of the most significant responses to analysis.

Viscoelastic properties as a function of temperature under predetermined oscillatory conditions and a set linear viscoelastic region for each formulation were investigated. Using Stat-Ease software, the formulations were fitted to quadratic models for gelation temperature. The 3D surface response and contour plot showed that factor X_1 and X_2 had an inverse proportional relationship with gelation temperature (Y_1) as illustrated in Figure 4.1. Equation 4.6 demonstrates the quadratic model (p =0.0001) for Gen-I gelation temperature:

$$Y_4 = 17.20 - 5.60\ X_1 - 2.70\ X_2 + 3.41\ X_1^2 \quad (4.6)$$

Notably, factor X_1 and X_2 showed significant effect on the gelation temperature of the Gen-I system, with the model showing an F-value of 16.7 indicating there is only a 0.01% chance that an F-value this large could occur due to noise, further validating the significance of the model (Table 4.3). Specifically, according to rheological analysis, formulations constructed from high X_1 concentrations showed gelation below 20 °C (Figure S5) which is not ideal as the best temperature range for injectable hydrogels is 25–37 °C (Shaker et al., 2013). Lower X_1 formulations exhibited low loss moduli (G'') compared to storage modulus (G') (G"">G') in contrast to higher X_1 concentration with G'>G" at low temperatures (Figure S5). Moduli values G' and G" along with viscosity increased with temperature and at a critical temperature G' and G" crossover was observed which signifies the critical gelation temperature. Thus, the thermo responsiveness of the formulations is clearly conferred by X_1 concentration, however, X_2 clearly also has a role on the CGT, notably the presence of X_2 has been shown to interfere with gelation (Gratieri et al., 2010). Importantly, the gelation window was strongly dependent on the content of pluronic, with higher concentrations exhibiting quicker gelation below room temperature.

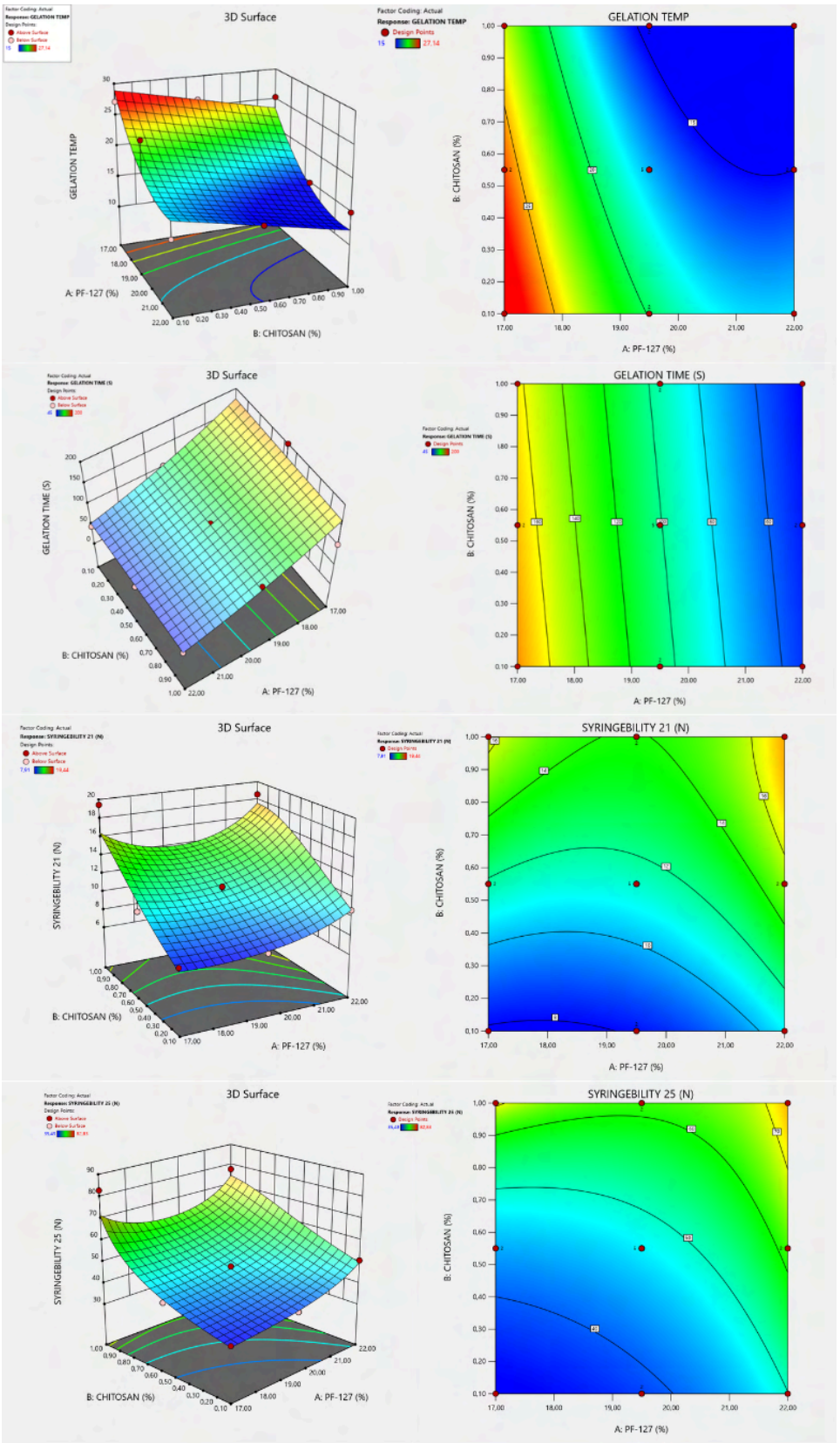

Figure 4.1: Three-dimensional (3D) and contour response surface plots depicting interactive effects of variables on (**A**) Gelation temperature, (**B**) Gelation temperature, (**C**) Injectability (21 Gauge needle), (**D**) Injectability (25 Gauge needle).

The ideal formulation comprising Pluronic®F127 (17.11%), CS (0.22%) and nano-polyplex (1%) was chosen for downstream experiments to yield the following responses a gelation temperature of 27.14 °C, gelation time 172.24 seconds and syringeability of 8.7 N and 36.8 N for 21 G, 25 G respectively. As per Stat-Ease analysis, the relationships between the independent parameters and responses showed that the models for each response were in reasonable agreement and were capable of making accurate predictions. The R^2 values of each model also showed that variability noted can be explained by the model itself and not external noise (Table 4.3).

4.2.2. Structural and Thermal Characterisation of the Gen-I system

4.2.2.1. Assessment of Gen-I chemical composition and molecular structure

Characterisation of the Gen-I system, chitosan and Pluronic®F127 was conducted to efficiently assess the composition of the individual polymers and the resulting composites, along with their thermal stability and microstructure. The FTIR spectra of Pluronic®F127, chitosan oligosaccharide, nano-polyplex and the Gen-I system, are shown in Figure 4.2. The spectrum of the final Gen-I system containing embedded nanoparticles demonstrated characteristic absorption peaks present in the chitosan and Pluronic®F127 polymers. Specifically, absorption bands corresponding to the functional group O-H bending (1341 cm^{-1}), C-O-C stretching vibrations (1093) of the ether bonds in the Pluronic®F127 backbone, C-H (2873) stretch vibrations of the $–CH_2$ and $–CH_3$ groups in present in Pluronic®F127 were detected in the composite. Additionally, C=O and N–H (± 1633 and 2876, respectively) stretching vibrations from chitosan or the nano-polyplex's carbonyl and amine groups, are present in the Gen-I system likely overlapping with any contributions from Pluronic®F127. Preservation of key structural features in the composite is indicative of the structural integrity within the hydrogel and possible interactions between the polymers. Distinct absorption peaks present in the embedded nano-polyplex are not as pronounced in the composite because Pluronic®F127 is abundant and the nano-polyplex is dispersed within the composite matrix (Gen-I) therefore showing successful integration of the nano-polyplex within the chitosan-Pluronic®F127 hydrogel. Further analysis was conducted to investigate the thermal stability and structural characteristics of the Gen-I system compared to the individual polymers.

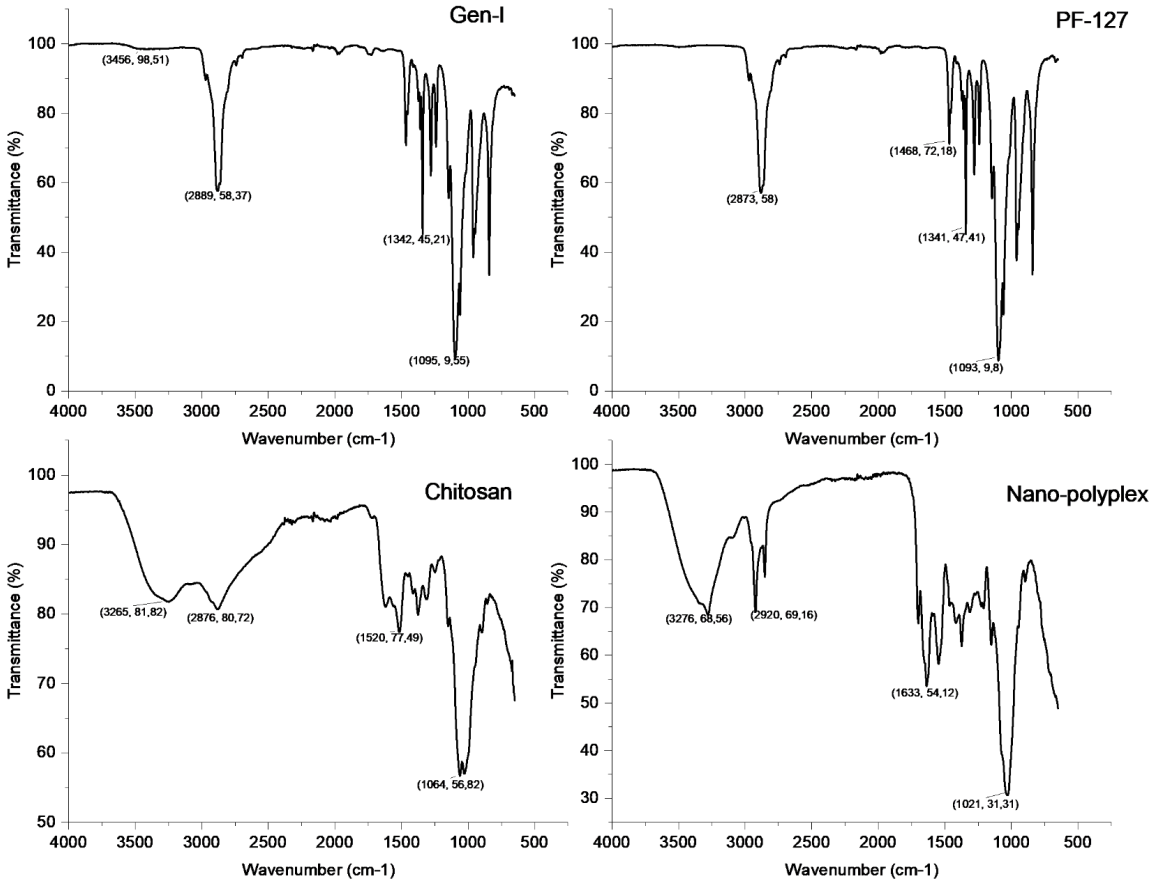

Figure 4.2: Structural analysis of theGen-I system, Pluronic®F127, Chitosan and the nano-poplex using FTIR.

4.2.2.2. Assessment of Gen-I system composition and thermal stability

The thermal profile of the Gen-I system resembles that of Pluronic®F127; the thermal properties of chitosan and the nano-polyplex system are overshadowed due to higher concentrations of the Pluronic®F127 (Figure 4.3). Residual mass of the Gen-I system is higher (4.55% weight) than that of Pluronic®F127 alone (1.70%) (Figure 4.3) indicating that the chitosan or the nano-polyplex maybe contributing to the more stable fraction of the composite despite the absence of distinct chitosan and nano-polyplex TGA signals. Furthermore, the absence of comparative degradation shifts in the Gen-I TGA spectra is indicative of the minimal interactions or bonding affinity between the polymers and the nano-polyplex, rightly indicating that the composite was formulated by mixing therefore resulting in the Gen-I system largely adopting the thermal behaviour of the Pluronic®F127 matrix. One approach to confer the results obtained from TGA and FTIR regarding the absence of key structural elements and essential decomposition patterns of the nanosystem masked by the hypothesised embedding of the nanosystem is to conduct structural analysis of the Gen-I system.

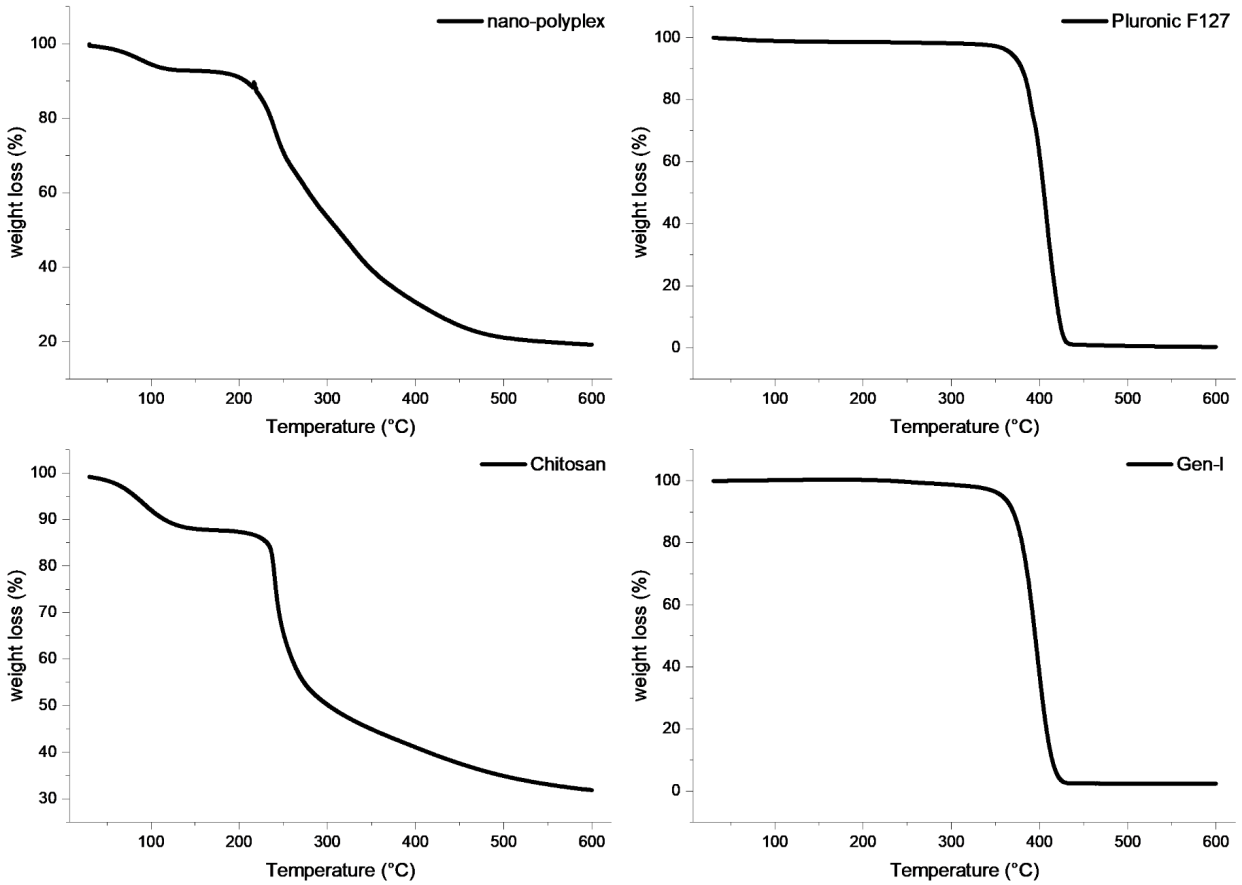

Figure 4.3: Thermograms of individual polymers and the composite Gen-I system as a function of temperature.

4.2.2.3. Electron microscopy for the evaluation of the surface topography and composition of the Gen-I system

Topographical and morphological features of the Gen-I system were investigated to understand the porosity of the composite, dispersion of the nano-polyplex system, and define the overall structure of the Gen-I system. The SEM micrographs (Figure 4.4) show the presence of embedded nano-polyplex and porous nanofibrous structures. Notably, nanofibrous scaffolds have been shown to possess ECM-like behaviour which is beneficial for maintaining cell viability (Dahlin et al., 2011), supporting cell infiltration, three dimensional cell growth through the ECM and lastly, promoting the development of healthy tissue (Onuwaje and Phillips, 2020). The fibrous microstructure of the Gen-I system is accompanied by relative porosity and high surface area which are attractive properties for use as tissue models. The relatively porous nature and high surface area to volume ratio of the Gen-I system renders it ideal for tissue regeneration as these properties allow for guided cell growth, migration, penetration and blood vessel infiltration (Annabi et al., 2010).

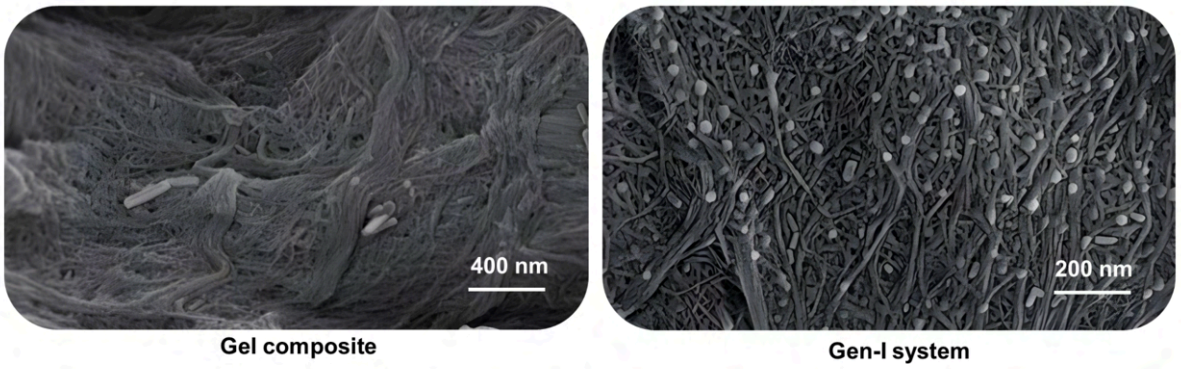

Figure 4.4: Scanning electron micrographs of the surface morphology of composite gel matrix (left) and Gen-I system (right).

4.2.3. Mechanical and rheological properties of the Gen-I system

Rheological analysis of materials, particularly biogels, aids in understanding how their properties can influence their application as cell delivery modalities, bio-inks for tissue printing and their role in promoting cell viability, growth, self-renewal and migration (Alam et al., 2020). Notably, rheological investigations also provide insights on how these properties influence biogel compatibility with target tissue, structure and behaviour following administration, and the degree of therapeutic release in localised tissue, in cases of drug delivery (Yan and Pochan, 2010). Therefore following physicochemical characterisation of the Gen-I system, rheological properties of the composite were investigated to elucidate its behaviour in comparison to the potential site of administration (vitreous humour). The thermogelling and viscoelastic behaviour of the Gen-I system was assessed and the storage modulus (G') and loss modulus (G'') as a function of temperature was recorded. The analysis was conducted around the temperature range 20°C to 60°C at a rate 1°C/min. The Gen-I system showed a crossover point (G'=G'') at 27.42°C, exhibiting solid-like behaviour (G'' < G') and formation of an elastic network characteristic of a gel state at temperature above 27.42°C (Figure 4.5 b). This crossover confirms the thermoresponsive nature of the Gen-I system, making it a promising candidate for applications requiring controlled gelation at physiological temperatures such as gene and cell delivery.

To evaluate/quantify shear thinning or thixotropy which is used to characterise structural changes due to deformation and the reversibility thereof, a flow ramp up and down test was conducted. Thixotropy analysis was performed at 37°C using a ThermoHaake MARS Modular Advanced Rheometer. The shear rate was ramped up from 0.001 to 100 s^{-1} in 140 seconds and then ramped back down. Figure 4.5 d demonstrated the shear thinning behaviour of the Gen-I system following application of shear stress (e.g. during injection) and its removal (in situ following injection) thus demonstrating the power lower behaviour $\tau \propto \dot{\gamma}^{-1}$.

As seen, viscosity decreases with increasing shear rate which is beneficial for easy administration. The recovery of the gel's viscoelastic properties with the removal of the shear results in structural recovery and stability which is an essential property for self-healing hydrogels which can be used as ink materials for 3D-bioprinting. Maintaining a consistency under physiological shear aids in avoiding premature erosion or migration to non target sites, therefore stability of the gel during shear states encountered under physiological conditions is essential as increases in shear rate changes microstructure of the hydrogels (Londhe et al., 2025).

To further understand the response of the Gen-I system to oscillating shear force at different frequencies and its viscoelastic properties, it was subjected to an oscillatory shear strain with a gradual frequency increase (0.01 to 10 Hz). This was performed at a constant strain within its linear viscoelastic region (LVR). Under normal physiological conditions, shear rate of vitreous humour is often less than $1s^{-1}$, however slight deviations from this as a result of eye movement occur, with huge variations being as a result of diseases such as age related macular degeneration (Parsons et al., 2003). Similar to studies conducted using vitreous humour from animal and human models, Gen-I has a higher storage modulus (G') than loss modulus (G"), additionally, as the frequency increased, G' increases whilst G'' and viscosity (n) decrease (Figure 4.5c), thus indicating that the Gen-I system behaves more like a solid under physiological conditions and its viscoelastic behaviour is comparable to that of the vitreous humour (Silva et al., 2017; Tram and Swindle-Reilly, 2018). As seen in Figure 4.5c, storage modulus is greater than loss modulus across different oscillatory stresses/forces (frequency range 0.01 - 10 Hz). Across different frequency ranges, the Gen-I system is stable and maintains its viscoelastic characteristics even under fast oscillations. The structure of the Gen-I system can withstand rapid stress and maintain its solid like properties within this range, which is typically considered the physiological frequency of the vitreous. The vitreous has been shown to dominantly show elastic behaviour over viscous nature in the frequency of shear movement ranging from 0.1 to 5 Hz, above this range the viscous behaviour is more dominant which is ideal during fast eye movement (As a result of high impact or collision) (Urbańska et al., 2024). At lower frequencies, the Gen-I systems showed loss modulus being greater than storage (G">G'), suggesting that the Gen-I system can flow under specific conditions which is useful for injectability or controlled release. Understanding the characteristic flow (yield stress) of biogels is essential in their application as injectable systems and importantly, as vectors for drug and cell encapsulation. Therefore, yield stress can provide insights into the internal structure and stability of the Gen-I system by highlighting key transition points (elastic to fluid state) and stability characteristics. Notably, the data follow Bingham liquid mode (equation 4.7) as at low shear rate relatively low

stresses are observed depicting a resistance to flow comparable with previous studies (Hvidt, 2013).

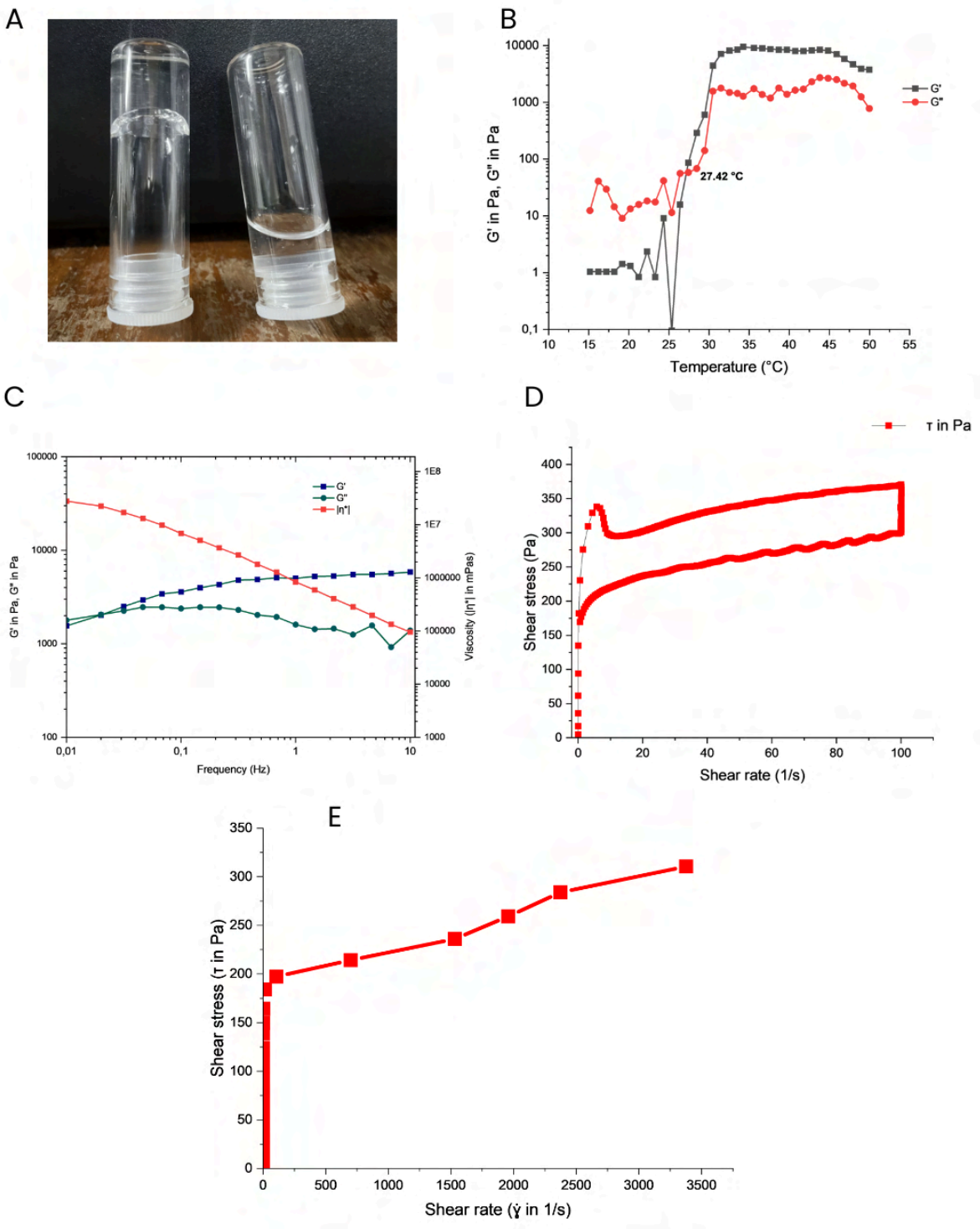

Figure 4.5: Rheological characterisation of the optimised Gen-I system. (a) Inversion test for the assessment of gelation behaviour. (b) Temperature ramp at constant shear rate. (c) Frequency sweep at 37 °C. (d) Shear thinning behaviour of the Gen-I system at 37 °C. (e) Steady shear stress ramps on the Gen-I system at 37 °C. Stress ramps from 0 to 350 Pa in 1000 s.

$\sigma = \sigma_y + \eta_b \gamma$ for $\sigma \geq \sigma_y$ (4.7)

A potential yield or transition point (197.31 Pa) of the Gen-I system is observed at 107 s^{-1} shear rate, depicting thixotropic behaviour. This is essential behaviour for a smart biogel as it indicates that the Gen-I system can remain stable under normal physiological low stress conditions, such as those observed in the vitreous humour (Shafaie et al., 2018), but can flow when required for injectability and controlled release requirements.

4.2.4. Gen- I system degradation rate

Investigating the degradation profile of the Gen-I system is essential to obtain insight into the rate of degradation of the system, which aids in the evaluation of its suitability as a cell and gene delivery carrier. In the case of tissue engineering, the rate of carrier/scaffold degradation affects the distribution of the extracellular matrix, migration of cell promoting proteins, and tissue deposition (Dhote et al., 2012). Therefore, the ability to predict the rate of degradation aids in the design of an optimised system. *In vitro* Gen-I system degradation was investigated by evaluating the weight loss of the Gen-I vs the Pluronic® F127 hydrogel across different time points at 37°C in simulated vitreous humour (pH 7.4). Pluronic® F127 hydrogel exhibited a significantly faster degradation profile than the Gen-I system between days 2 and 6 ($p < 0.05$), with almost complete degradation (97.25% ±1.85%) observed by day 21. In contrast, 36.07% ± 0.63% of the Gen-I system remained stable up to day 21 (Figure 4.6), consistent with findings from previous studies (Diniz et al., 2015). The Gen-I system had significantly improved stability and mechanical strength compared to the pluronic F127, this may have been attributed to the presence of chitosan at the ideal proportion supporting crosslinking of chitosan amines with free hydroxyls on the nanosystem, aiding in the preservation of the structural integrity of the Gen-I system particularly in aqueous environment (Berger et al., 2004). Notably, the degradation rate of the Gen-I system is well suited to support the different phases of tissue regeneration; immunomodulation (1 to 3 days), cell integration - survival (minutes to months), cell proliferation (3 to 10 days), extracellular matrix deposition and reorganisation (48 h to months) and tissue maintenance (extended period, weeks to months) (Jin et al., 2023; Kumar et al., 2015; Nauta et al., 2011). However, prolonged degradation study is required to monitor the long term degradation profile of the Gen-I system.

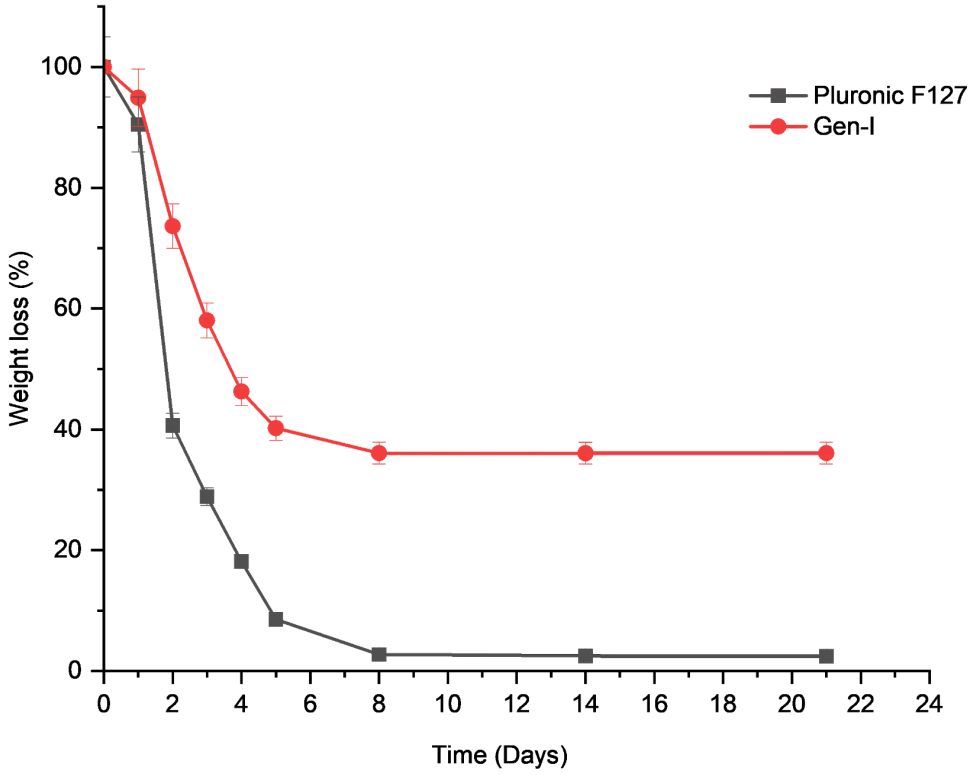

Figure 4.6: Degradation profiles of Gen-I system and Pluronic F127 in simulated vitreous humour (pH 7.4) at 37 °C (mean ± S.D., n = 3, $p < 0.05$).

4.2.5. Gen-I system safety profile and cell viability monitoring following cell seeding

Biocompatibility of any system is important to limit immune response or inflammation upon administration (Cao et al., 2021). To determine general safety of the Gen-I system for *in vivo* application, cell viability analysis was conducted using hRPE, MG63 and HEK 293 cell lines *in vitro*. Cells were seeded in 96 well plates in appropriate media, maintained in a humidified incubator at 37 °C and 5% CO_2 and cultured for 24 hours before treatment. Cell viability was conducted for 48 and 72 hours to determine possible toxicity of the Gen-I nanosystem. The control gel composed of pluronic and chitosan showed mild toxicity across different timepoints and cell lines (Figure 4.7 a,b). This can be attributed to the 3D nature of the matrix encapsulating the cells, possibly reducing oxygen and nutrient diffusion across the matrix thus affecting cell viability (Yap and Yang, 2020). Alternatively, the cationic nature of chitosan could possibly cause membrane disruption, although its presence is largely beneficial as it confers antimicrobial properties and stability of the gel. Surprisingly, cells treated with the Gen-I system displayed slightly similar levels of cell viability across different timepoints when compared to cells not treated with gels (2D-environment) which readily interact with their environment. Higher viability noted in Gen-I treated cells, particularly for HEK293 cells is

hypothesised to be due to the presence of hyaluronic acid within the Gen-I system that possibly crosslinks with chitosan and creates pores, allowing for the ease of nutrient and oxygen diffusion and thus promotion of cell growth (Pangjantuk et al., 2024).

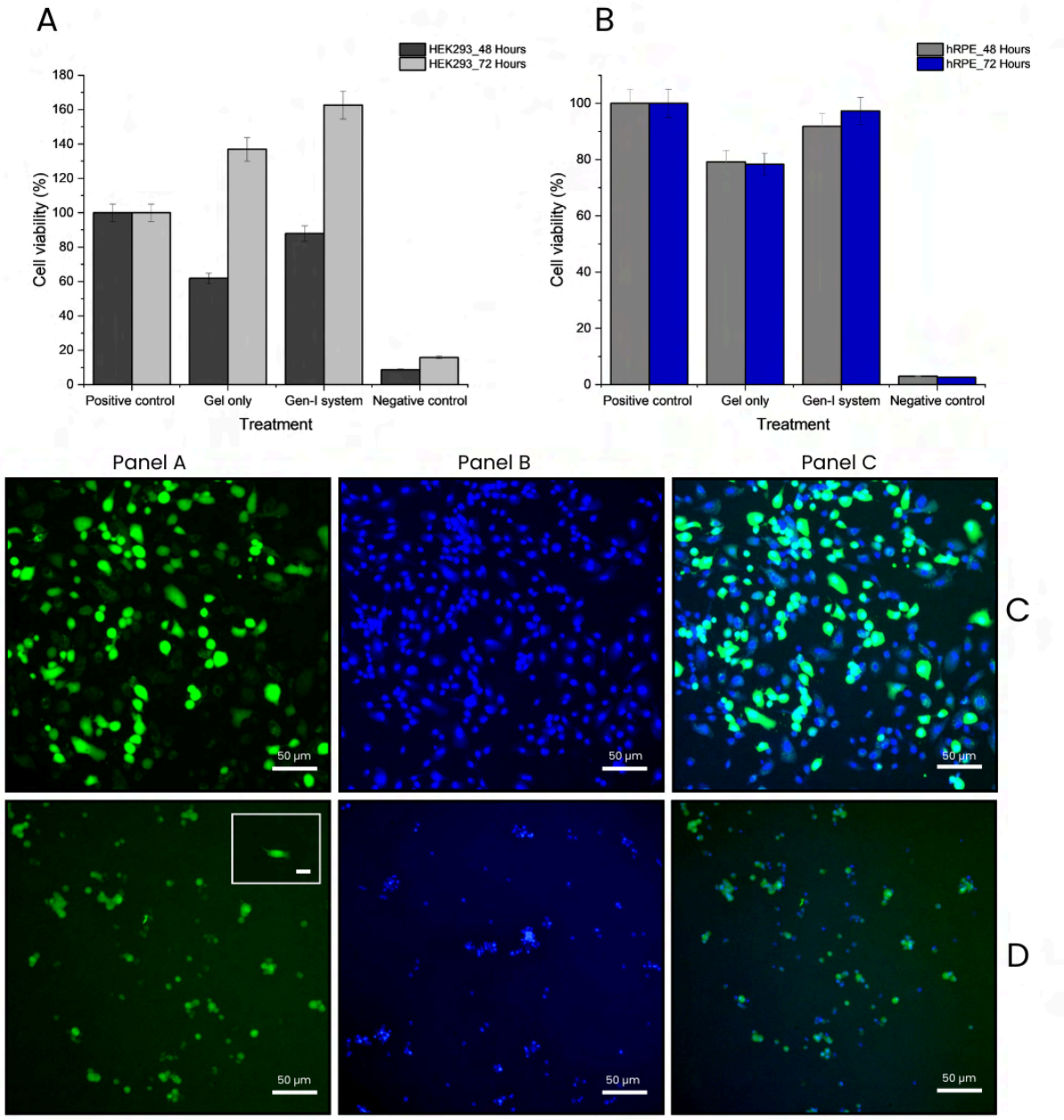

Figure 4.7: Cell viability assessment and live cell imaging of unencapsulated and Gen-I system encapsulated cells. A, B) Graphical representation of HEK293 and hRPE cells following encapsulation in Gen-I system using the MTT assay at 48h and 72 h. Fluorescence microscopy images showing viability and nuclear morphology of unencapsulated control hRPE cells (C) and Gen-I system encapsulated hRPE cells (D) stained with Calcein AM (green, live cells - panel A) and DAPI (blue, nuclei - panel B). Merged images (panel C) demonstrate cell viability and spatial organization within each condition. White square on

panel A shows attached/differentiated hRPE cells in the Gen-I system. Scale bar: 50 μm. (Data from experiments are presented as the mean ± SD, n = 3) ; *p < 0.05 indicates statistically significant differences.

In addition to creating a biocompatible, slow release gene delivery platform, the aim of this work was to develop an injectable cell scaffold to promote cell encapsulation, survival and eventually tissue regeneration. Viability of encapsulated hRPE cells was assessed for 72 hours. Calcein AM staining was conducted to evaluate the viability of seeded cells (Figure 4.7 c,d). Non-encapsulated cells adapted their normal flat, hexagonal shape which is synonymous to adhered cells, with some maintaining spherical morphology (dividing cells) (Figure 4.7 c). Significantly, cell adhesion is essential in processes such as wound healing, embryogenesis, immune response and metastasis (Hou et al., 2019; Koivisto et al., 2014). The cell morphology adapted following attachment is driven by adhesion cues such as cytoskeletal reorganisation (Hou et al., 2019). In contrast, encapsulated cells retained the spherical morphology synonymous with unattached cells (Figure 4.7d). The retention of the spherical-like morphology in cells encapsulated within the 3D hydrogel matrix has been reported in chondrocytes encapsulated in chitosan-pluronic hydrogels (Park et al., 2009), L929, rBMSCs, and HUVEC in silk acid derived hydrogel (Sun et al., 2024), osteosarcoma MG63 encapsulated in Pluronic F127, carboxymethyl hexanoyl chitosan (CA) and glyoxal (Gx) hydrogels (Yap and Yang, 2020) and retinal stem-progenitor cell encapsulated in hyaluronan and methylcellulose (Ballios et al., 2010); both showed retention of cell viability following injection using a needle (21 and 19 G × 1½ respectively).

A subset of the encapsulated cells exhibited a flattened, hexagonal morphology within the 3D Gen-I matrix similar to that observed in non-encapsulated attached cells (Figure 4.7d); however, their numbers were not statistically significant. The 3D matrix demonstrated a wide adaptability of cell morphologies, showing that the Gen-I system could potentially promote the delivery of cells in a suspension prior to engraftment, and subsequently cell attachment *in vivo* following targeted delivery. Conversely, despite minimal hRPE cell attachment to the Gen-I system, the presence of Gen-I adhered cells indicate the potential of the 3D matrix application in promoting *ex vivo* cell viability, cell-cell communication and possibly functional tissue integration and regeneration.

4.3. Concluding remarks

A Design of Experiments approach was adopted to ascertain the ideal formulation with favourable characteristics for protection and delivery of nucleic acid, along with maintaining the viability of cells within the Gen-I system for tissue regenerative purposes. The research detailed herein demonstrates the significant role of DOE via Box-Behnken design in formulation fabrication, understanding possible interaction/relationship between specific input

variables and responses and identifying optimal conditions in a statistically significant manner. The optimised Gen-I system prepared using the cold method showed favourable characteristics for cell encapsulation and compatibility with transplantation in soft tissue. Additionally, the hydrogel's capacity to offer tissue-like properties; tissue homeostasis through hyaluronic acid and cell proliferation supported by chitosan allows for versatility in application as explored in this study (Alkabli, 2024). In this work, the optimised Gen-I system demonstrated improvements in the thermogel's rheological properties and immunogenicity compared to a pluronic gel control. Importantly, beyond utilisation of the Gen-I system as a depot for sustained gene delivery, the system also demonstrated potential as a cell delivery scaffold, and could ultimately enable the co-delivery of genes and cells (stem cells). The ideal cell scaffold is capable of achieving multiple mechanisms essential for cell integration and tissue regeneration. These include providing mechanical support whilst promoting cell adhesion, migration, proliferation, differentiation and communication with local tissue to facilitate cell integration and tissue regeneration (Galocha-León et al., 2023). As demonstrated, the Gen-I system was capable of maintaining cell viability within the 3D matrix and supporting cellular processes. Further modifications to prolong scaffold degradation to at least 4 to 6 months in order to support optimal stem cell differentiation, ECM deposition, organisation and tissue maintenance (Gupta et al., 2023). Each of these mechanisms occur at different schedules, therefore prolonged maintenance of cell scaffold integrity would be required. For this reason, further optimisation of the Gen-I system is necessary to extend its degradation profile.

4.4. References

Alam, K., Iqbal, M., Hasan, A., Al-Maskari, N., 2020. Rheological Characterization of Biological Hydrogels in Aqueous State. J. Appl. Biotechnol. Rep. https://doi.org/10.30491/jabr.2020.109994

Alkabli, J., 2024. Recent advances in the development of chitosan/hyaluronic acid-based hybrid materials for skin protection, regeneration, and healing: A review. Int. J. Biol. Macromol. 279, 135357. https://doi.org/10.1016/j.ijbiomac.2024.135357

Annabi, N., Nichol, J.W., Zhong, X., Ji, C., Koshy, S., Khademhosseini, A., Dehghani, F., 2010. Controlling the Porosity and Microarchitecture of Hydrogels for Tissue Engineering. Tissue Eng. Part B Rev. 16, 371. https://doi.org/10.1089/ten.teb.2009.0639

Ballios, B.G., Cooke, M.J., Van Der Kooy, D., Shoichet, M.S., 2010. A hydrogel-based stem cell delivery system to treat retinal degenerative diseases. Biomaterials 31, 2555–2564. https://doi.org/10.1016/j.biomaterials.2009.12.004

Bellotti, E., Schilling, A.L., Little, S.R., Decuzzi, P., 2021. Injectable thermoresponsive hydrogels as drug delivery system for the treatment of central nervous system disorders: A review. J. Controlled Release 329, 16–35. https://doi.org/10.1016/j.jconrel.2020.11.049

Berger, J., Reist, M., Mayer, J.M., Felt, O., Peppas, N.A., Gurny, R., 2004. Structure and interactions in covalently and ionically crosslinked chitosan hydrogels for biomedical applications. Eur. J. Pharm. Biopharm. Off. J. Arbeitsgemeinschaft Pharm. Verfahrenstechnik EV 57, 19–34. https://doi.org/10.1016/s0939-6411(03)00161-9

Bonfiglio, A., Lagazzo, A., Repetto, R., Stocchino, A., 2015. An experimental model of vitreous motion induced by eye rotations. Eye Vis. 2, 10. https://doi.org/10.1186/s40662-015-0020-8

Cao, H., Duan, L., Zhang, Y., Cao, J., Zhang, K., 2021. Current hydrogel advances in physicochemical and biological response-driven biomedical application diversity. Signal Transduct. Target. Ther. 6, 1–31. https://doi.org/10.1038/s41392-021-00830-x

Chiu, W., Lin, T.-Y., Chang, Y.-C., Lai, H.I.-A.M., Lin, Shen-Che, Ma, C., Yarmishyn, A.A., Lin, Shiuan-Chen, Chang, K.-J., Chou, Y.-B., Hsu, C.-C., Lin, T.-C., Chen, S.-J., Chien, Y., Yang, Y.-P., Hwang, D.-K., 2021. An Update on Gene Therapy for Inherited Retinal Dystrophy: Experience in Leber Congenital Amaurosis Clinical Trials. Int. J. Mol. Sci. 22, 4534. https://doi.org/10.3390/ijms22094534

Da Cruz, L., Fynes, K., Georgiadis, O., Kerby, J., Luo, Y.H., Ahmado, A., Vernon, A., Daniels, J.T., Nommiste, B., Hasan, S.M., Gooljar, S.B., Carr, A.-J.F., Vugler, A., Ramsden, C.M., Bictash, M., Fenster, M., Steer, J., Harbinson, T., Wilbrey, A., Tufail, A., Feng, G., Whitlock, M., Robson, A.G., Holder, G.E., Sagoo, M.S., Loudon, P.T., Whiting, P., Coffey, P.J., 2018. Phase 1 clinical study of an embryonic stem cell–derived retinal

pigment epithelium patch in age-related macular degeneration. Nat. Biotechnol. 36, 328–337. https://doi.org/10.1038/nbt.4114

Dhote, V., Skaalure, S., Akalp, U., Roberts, J., Bryant, S.J., Vernerey, F.J., 2012. On the role of hydrogel structure and degradation in controlling the transport of cell-secreted matrix molecules for engineered cartilage. J. Mech. Behav. Biomed. Mater. 19, 61. https://doi.org/10.1016/j.jmbbm.2012.10.016

Diniz, I.M.A., Chen, C., Xu, X., Ansari, S., Zadeh, H.H., Marques, M.M., Shi, S., Moshaverinia, A., 2015. Pluronic F-127 hydrogel as a promising scaffold for encapsulation of dental-derived mesenchymal stem cells. J. Mater. Sci. Mater. Med. 26, 153. https://doi.org/10.1007/s10856-015-5493-4

Galocha-León, C., Antich, C., Voltes-Martínez, A., Marchal, J.A., Mallandrich, M., Halbaut, L., Rodríguez-Lagunas, M.J., Souto, E.B., Clares-Naveros, B., Gálvez-Martín, P., 2023. Development and characterization of a poloxamer hydrogel composed of human mesenchymal stromal cells (hMSCs) for reepithelization of skin injuries. Int. J. Pharm. 647, 123535. https://doi.org/10.1016/j.ijpharm.2023.123535

Gouras, P., Algvere, P., 1996. Retinal cell transplantation in the macula: New techniques. Vision Res. 36, 4121–4125. https://doi.org/10.1016/S0042-6989(96)00180-0

Gratieri, T., Gelfuso, G.M., Rocha, E.M., Sarmento, V.H., De Freitas, O., Lopez, R.F.V., 2010. A poloxamer/chitosan in situ forming gel with prolonged retention time for ocular delivery. Eur. J. Pharm. Biopharm. 75, 186–193. https://doi.org/10.1016/j.ejpb.2010.02.011

Gupta, S., Lytvynchuk, L., Ardan, T., Studenovska, H., Sharma, R., Faura, G., Eide, L., Shanker Verma, R., Znaor, L., Erceg, S., Stieger, K., Motlik, J., Petrovski, G., Bharti, K., 2023. Progress in Stem Cells-Based Replacement Therapy for Retinal Pigment Epithelium: In Vitro Differentiation to In Vivo Delivery. Stem Cells Transl. Med. 12, 536–552. https://doi.org/10.1093/stcltm/szad039

Han, H., Chen, B.-T., Liu, Y., Wang, Y., Xing, L., Wang, H., Zhou, T.-J., Jiang, H.-L., 2024. Engineered stem cell-based strategy: A new paradigm of next-generation stem cell product in regenerative medicine. J. Controlled Release 365, 981–1003. https://doi.org/10.1016/j.jconrel.2023.12.024

Herberg, S., Shi, X., Johnson, M.H., Hamrick, M.W., Isales, C.M., Hill, W.D., 2013. Stromal Cell-Derived Factor-1β Mediates Cell Survival through Enhancing Autophagy in Bone Marrow-Derived Mesenchymal Stem Cells. PLOS ONE 8, e58207. https://doi.org/10.1371/journal.pone.0058207

Hodjat, M., Rezvanfar, M.A., Abdollahi, M., 2015. A systematic review on the role of environmental toxicants in stem cells aging. Food Chem. Toxicol. 86, 298–308. https://doi.org/10.1016/j.fct.2015.11.002

Hou, H.-S., Lee, K.-L., Wang, C.-H., Hsieh, T.-H., Sun, J.-J., Wei, P.-K., Cheng, J.-Y., 2019.

Simultaneous assessment of cell morphology and adhesion using aluminum nanoslit-based plasmonic biosensing chips. Sci. Rep. 9, 7204. https://doi.org/10.1038/s41598-019-43442-w

Huang, L., You, J., Yao, Y., Xie, M., 2020. Interleukin-13 Gene Modification Enhances Grafted Mesenchymal Stem Cells Survival After Subretinal Transplantation. Cell. Mol. Neurobiol. 40, 725–735. https://doi.org/10.1007/s10571-019-00768-3

Hvidt, S., 2013. Yield Stress Value Determinations of a Physical Gel.

Jin, Y., Li, S., Yu, Q., Chen, T., Liu, D., 2023. Application of stem cells in regeneration medicine. MedComm 4, e291. https://doi.org/10.1002/mco2.291

Koivisto, L., Heino, J., Häkkinen, L., Larjava, H., 2014. Integrins in Wound Healing. Adv. Wound Care 3, 762–783. https://doi.org/10.1089/wound.2013.0436

Kumar, P., Satyam, A., Fan, X., Collin, E., Rochev, Y., Rodriguez, B.J., Gorelov, A., Dillon, S., Joshi, L., Raghunath, M., Pandit, A., Zeugolis, D.I., 2015. Macromolecularly crowded in vitro microenvironments accelerate the production of extracellular matrix-rich supramolecular assemblies. Sci. Rep. 5, 8729. https://doi.org/10.1038/srep08729

Londhe, P.V., Londhe, M.V., Salunkhe, A.B., Laha, S.S., Mefford, O.T., Thorat, N.D., Khot, V.M., 2025. Magnetic hydrogel (MagGel): An evolutionary pedestal for anticancer therapy. Coord. Chem. Rev. 522, 216228. https://doi.org/10.1016/j.ccr.2024.216228

MacLaren, R.E., Bennett, J., Schwartz, S.D., 2016. Gene Therapy and Stem Cell Transplantation in Retinal Disease: The New Frontier. Ophthalmology 123, S98–S106. https://doi.org/10.1016/j.ophtha.2016.06.041

Maguire, A.M., Bennett, J., Aleman, E.M., Leroy, B.P., Aleman, T.S., 2021. Clinical Perspective: Treating RPE65-Associated Retinal Dystrophy. Mol. Ther. 29, 442–463. https://doi.org/10.1016/j.ymthe.2020.11.029

Naik, K., du Toit, L.C., Ally, N., Choonara, Y.E., 2024. In vivo evaluation of a Nano-enabled therapeutic vitreous substitute for the precise delivery of triamcinolone to the posterior segment of the eye. Drug Deliv. Transl. Res. 14, 2668–2694. https://doi.org/10.1007/s13346-024-01566-1

Nauta, A., Gurtner, G., Longaker, M., 2011. Wound healing and regenerative strategies. Oral Dis. 17, 541–549. https://doi.org/10.1111/j.1601-0825.2011.01787.x

Niederkorn, J.Y., 2019. The Eye Sees Eye to Eye With the Immune System: The 2019 Proctor Lecture. Invest. Ophthalmol. Vis. Sci. 60, 4489–4495. https://doi.org/10.1167/iovs.19-28632

Pangjantuk, A., Kaokaen, P., Kunhorm, P., Chaicharoenaudomrung, N., Noisa, P., 2024. 3D culture of alginate-hyaluronic acid hydrogel supports the stemness of human mesenchymal stem cells. Sci. Rep. 14, 4436. https://doi.org/10.1038/s41598-024-54912-1

Park, K.M., Lee, S.Y., Joung, Y.K., Na, J.S., Lee, M.C., Park, K.D., 2009. Thermosensitive

chitosan–Pluronic hydrogel as an injectable cell delivery carrier for cartilage regeneration. Acta Biomater. 5, 1956–1965. https://doi.org/10.1016/j.actbio.2009.01.040

Park, S.S., 2021. Advantages of ocular regeneration research. Ann. Transl. Med. 9, 1269. https://doi.org/10.21037/atm-21-1793

Parsons, M.A., Start, R.D., Forrest, A.R.W., 2003. Concurrent vitreous disease may produce abnormal vitreous humour biochemistry and toxicology. J. Clin. Pathol. 56, 720.

Salehi, M.S., Safari, A., Pandamooz, S., Jurek, B., Hooshmandi, E., Owjfard, M., Bayat, M., Zafarmand, S.S., Miyan, J.A., Borhani-Haghighi, A., 2022. The Beneficial Potential of Genetically Modified Stem Cells in the Treatment of Stroke: a Review. Stem Cell Rev. Rep. 18, 412–440. https://doi.org/10.1007/s12015-021-10175-1

Schmolka, I.R., 1972. Artificial skin I. Preparation and properties of pluronic F-127 gels for treatment of burns. J. Biomed. Mater. Res. 6, 571–582. https://doi.org/10.1002/jbm.820060609

Shafaie, S., Hutter, V., Brown, M.B., Cook, M.T., Chau, D.Y.S., 2018. Diffusion through the ex vivo vitreal body – Bovine, porcine, and ovine models are poor surrogates for the human vitreous. Int. J. Pharm. 550, 207–215. https://doi.org/10.1016/j.ijpharm.2018.07.070

Shaker, D.S., Ghorab, M.K., Klingner, A., Teiama, M.S., 2013. IN-SITU INJECTABLE THERMOSENSITIVE GEL BASED ON POLOXAMER AS A NEW CARRIER FOR TAMOXIFEN CITRATE 5, 429–437.

Sheyn, D., Mizrahi, O., Benjamin, S., Gazit, Z., Pelled, G., Gazit, D., 2010. Genetically modified cells in regenerative medicine and tissue engineering☆. Adv. Drug Deliv. Rev. 62, 683–698. https://doi.org/10.1016/j.addr.2010.01.002

Silva, A.F., Alves, M.A., Oliveira, M.S.N., 2017. Rheological behaviour of vitreous humour. Rheol. Acta 56, 377–386. https://doi.org/10.1007/s00397-017-0997-0

Sun, Z., Liu, H., Dai, D., Lyu, H., Huang, R., Wang, W., Guo, C., 2024. Injectable cell-laden silk acid hydrogel. Chem. Commun. 60, 316–319. https://doi.org/10.1039/D3CC04280D

Youm, I., Agrahari, V., Murowchick, J. B., & Youan, B. B. C. 2014. Uptake and cytotoxicity of docetaxel-loaded hyaluronic acid-grafted oily core nanocapsules in MDA-MB 231 cancer cells. Pharmaceutical research, 31, 2439-2452.

Tram, N.K., Swindle-Reilly, K.E., 2018. Rheological Properties and Age-Related Changes of the Human Vitreous Humor. Front. Bioeng. Biotechnol. 6, 199. https://doi.org/10.3389/fbioe.2018.00199

Urbańska, M.A., Thakur, S.S., Kolenderska, S.M., 2024. OCT-based dynamic mechanical analysis of vitreous humour. Opt. Lasers Eng. 172, 107881. https://doi.org/10.1016/j.optlaseng.2023.107881

Wang, J.C., Kanim, L.E.A., Yoo, S., Campbell, P.A., Berk, A.J., Lieberman, J.R., 2003. Effect of Regional Gene Therapy with Bone Morphogenetic Protein-2-Producing Bone Marrow Cells on Spinal Fusion in Rats. JBJS 85, 905.

Watanabe, T., Nagai, A., Sheikh, A.Md., Mitaki, S., Wakabayashi, K., Kim, S.U., Kobayashi, S., Yamaguchi, S., 2016. A human neural stem cell line provides neuroprotection and improves neurological performance by early intervention of neuroinflammatory system. Brain Res. 1631, 194–203. https://doi.org/10.1016/j.brainres.2015.11.031

Xian, B., Huang, B., 2015. The immune response of stem cells in subretinal transplantation. Stem Cell Res. Ther. 6, 161. https://doi.org/10.1186/s13287-015-0167-1

Yan, C., Pochan, D.J., 2010. Rheological properties of peptide-based hydrogels for biomedical and other applications. Chem. Soc. Rev. 39, 3528. https://doi.org/10.1039/b919449p

Yap, L.-S., Yang, M.-C., 2020. Thermo-reversible injectable hydrogel composing of pluronic F127 and carboxymethyl hexanoyl chitosan for cell-encapsulation. Colloids Surf. B Biointerfaces 185, 110606. https://doi.org/10.1016/j.colsurfb.2019.110606

Yong, S.-B., Chung, J.Y., Song, Y., Kim, Y.-H., 2018. Recent challenges and advances in genetically-engineered cell therapy. J. Pharm. Investig. 48, 199–208. https://doi.org/10.1007/s40005-017-0381-1

CHAPTER FIVE

Pilot study: *In vivo* evaluation of Novel Gen-I system safety profile in New Zealand White Rabbit Eye Model

The in vivo study received approval from the Animal Research Ethics Committee (AREC) of the University of the Witwatersrand, clearance certificate number: AESC 21-04-016 (see Appendix A).

5. Introduction

The standard of care for posterior segment eye diseases such as age related macular degeneration (which affects over 8% of individuals over the age of 45 years) involves the intravitreal injection of anti-vascular endothelial growth factor (VEGF) agents, which require regular dosing (initial treatment requires monthly injections whilst maintenance phase requires 4 -8 week injections indefinitely) to ensure recovery of visual acuity (Iyer et al., 2019). Conversely, inherited retinal dystrophy (affecting 1 in 2000 individuals globally) treatments and management strategies are limited and largely dependent on genetic and prenatal counselling, low visual aids and retinal prosthesis (e.g. Argus II epiretinal prosthesis and Alpha IMS subretinal prostheses) for blind patients whose inner retinal structure and optic nerve remains intact (Murro et al., 2023; Talib and Boon, 2020). More recently, the RPE65 retinal dystrophy gene therapy, Luxturna, has shown immense promise in improving vision acuity. However, similar to existing therapies it has shown significant limitations: transient therapeutic effect and possible future immunogenicity challenges with more doses (Giannaccini et al., 2014). Notwithstanding these limitations, gene therapy remains a promising avenue for the treatment of ocular diseases, particularly those resulting from genetic mutations.

Blinding inherited ocular diseases often affect the retinal pigment epithelium (RPE), a layer of cells crucial for retinal health. Mutations in RPE-specific genes can lead to visual defects. Some of these genes are too large for viral vector (e.g. Adeno-associated viruses - AAV) packaging, a limitation overcome by polymer nanosystems which are capable of delivering large genetic cargo (Strauss et al., 2005). While AAV vectors have tissue tropism advantages, preexisting immunity can limit their therapeutic benefits (Strauss et al., 2005). Notably, nanoparticles (NPs) have a positive safety profile, as demonstrated in various studies (Ziady et al., 2003). Historically, challenges such as transient transgene expression and low transfection efficiency have hindered non-viral gene therapy. Recent advances in vector engineering and delivery technologies aim to address these issues by creating non-viral gene therapies, a promising approach for gene therapy delivery (Hoffman et al., 2005). Additionally, unlike viral gene delivery systems, most non-viral based vectors are capable of promoting prolonged and sustained gene delivery, without genome integration, to

avoid the need for multiple dosing activities which normally reduces patient compliance. Accordingly, the design and development of a polymer based sustained gene release system is a big leap in reducing the need for multiple injections events and achieving targeted delivery. To this end, a smart thermoresponsive biogel loaded with the nano-polyplex system (Gen-I system generated in Chapter four) was constructed for investigation *in vivo* using New Zealand White Rabbit as the animal model. While *in vitro* studies are essential for understanding basic cellular processes and safety, using animal models provides a more comprehensive and realistic environment that better simulates the complexities of living organisms and serves as a crucial intermediate step in gathering evidence for safety, efficacy, and mechanisms of action of the potential therapeutics (Peynshaert et al., 2018). Additionally, as demonstrated in Chapter 3, the hRPE cells used in the study had reached senescence, and no GFP was detected, thus employing animal models might serve as an improved model for its detection. Lastly, even though *in vitro* studies have demonstrated a satisfactory safety profile of the Gen-I system, *in vivo*, the immune response to the Gen-I system can vary significantly, as more responses such as intraocular pressure and local immune responses will enable us to gauge the tolerability of the delivered material. The aim of this pilot study was to determine the *in vivo* safety profile and tolerability of the Gen-I system, along with assessing its ability to provide prolonged stability and protection of genetic cargo from nuclease degradation while enabling sustained release. Additionally, this work evaluates the Gen-I system's potential to reduce the need for multiple dosing regimens, thereby improving patient compliance. The pilot extended our understanding of appropriate dosage volume as determined by intraocular pressure and immune response to the system, along with the potential duration of the study required to achieve significant levels of gene expression or detection.

5.1. Materials and Methods

This pilot study was undertaken in accordance with the recommendations of the Animal Research Ethics committee at the University of the Witwatersrand (AREC Number: AESC 21-04-016). Operational procedures were stringently conducted in accordance with the Laboratory Animal Requirements of Wits Research Animal Facility (WRAF). All New Zealand White (NZW) Rabbits were provided by Wits Research Animal Facility (WRAF) University of the Witwatersrand, Johannesburg, South Africa.

5.1.1. Materials

In vivo studies were conducted using New Zealand White (NZW) Rabbits (Oryctolagus cuniculus) weighing 2.5 to 4 kg. Interventions utilised for analysis in the study included Lipofectamine 3000 (Thermofischer), Gen-I system (designed in study) carrying

pcDNA6.2-EmGFP (Thermofischer). The following anaesthetics, analgesics and antibiotics were used during the study; Sodium pentobarbitone, Phenylephrine HCl drop, Chloramphenicol ointment 1% w/w (antibiotic), Xylazine HCl (sedation, anesthesia muscle relaxation, and analgesia), Ketamine HCl (dissociative anesthetic), Tropicamide, Tetracaine HCl (topical anaesthetic) 0.5% w/w Buprenorphine DNA/RNA Shield and formalin, were provided by WRAF.

5.1.2. Animal housing and welfare

Normal WRAF husbandry procedures were followed. Briefly, NZW rabbits (2.5 to 4 kg) were housed in stainless-steel cages, singly, under a 12-hour light/12-hour darkness photoperiod at a temperature of 20 ºC ± 2ºC and at 35% humidity. During acclimation/prior intervention (7 days), NZW rabbits were monitored daily, with comprehensive welfare markers (rabbit grimace scale, coat condition, hydration, food intake and defecation monitoring) noted daily.

5.1.3. Preparation of formulations and intravitreal administration of the intervention

For the pilot, the novel Gen-I system and lipofectamine 3000 loaded with pcDNA6.2-EmGFP plasmid DNA (used as the model genetic material) were prepared as described in Chapter 4. Prior to conducting surgery, all animals were monitored for overall health and weight assessments were conducted. The NZW rabbits were randomly assigned to different treatment groups, namely; Test (n = 2) and positive control (n = 2) (Figure 5.1). The sample size (n = 2) was adopted to adhere to ethical regulations considering this is a pilot. Following seven days post habituation, animals were randomly assigned to two treatment groups (Gen-I system and Lipofectamine 3000 both loaded with plasmid DNA - pcDNA6.2-EmGFP) and ophthalmological examinations were conducted, followed by general anaesthesia using an intramuscular injection of ketamine and xylazine (40 mg/kg and 10 mg/kg) (Figure 5.2).

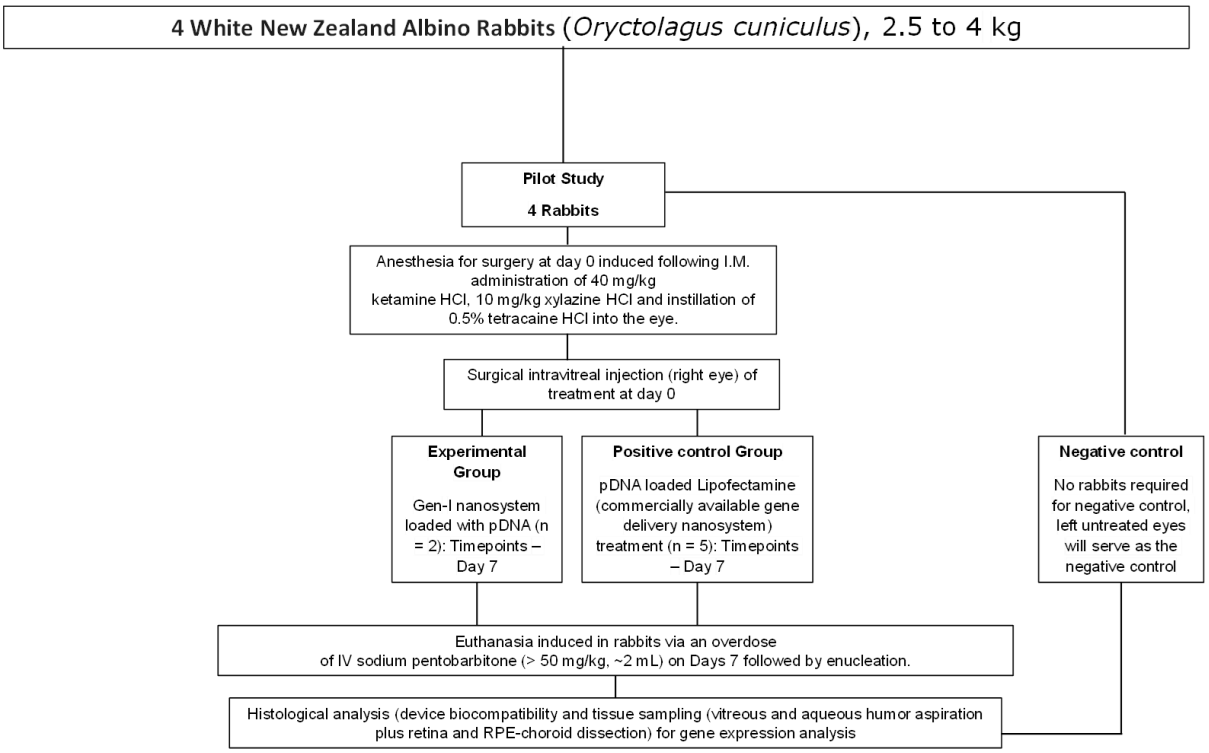

Figure 5.1: Pilot study design (allocation of animals to groups).

To keep the eye lid from closing, a wire speculum was inserted in the intervention eye followed by washing with several drops of 5% povidone/iodine and 0.2 mL lignocaine and local anaesthetic. Under optical ophthalmic microscope, 100 µL of the Gen-I system and lipofectamine 3000 system loaded with 1µg pcDNA6.2-EmGFP was intravitreally administered to the right eye of each animal using a 25 G syringes with the left eye considered as the negative control - receiving no intervention (Figure 5.2). Following surgery, Chloramphenicol ophthalmic ointment was administered to prevent postoperative infection (Figure 5.2). Subsequently, qualitative cage-side observations were conducted following the rabbit grimace scale (Keating et al., 2012) and their weights were measured weekly.

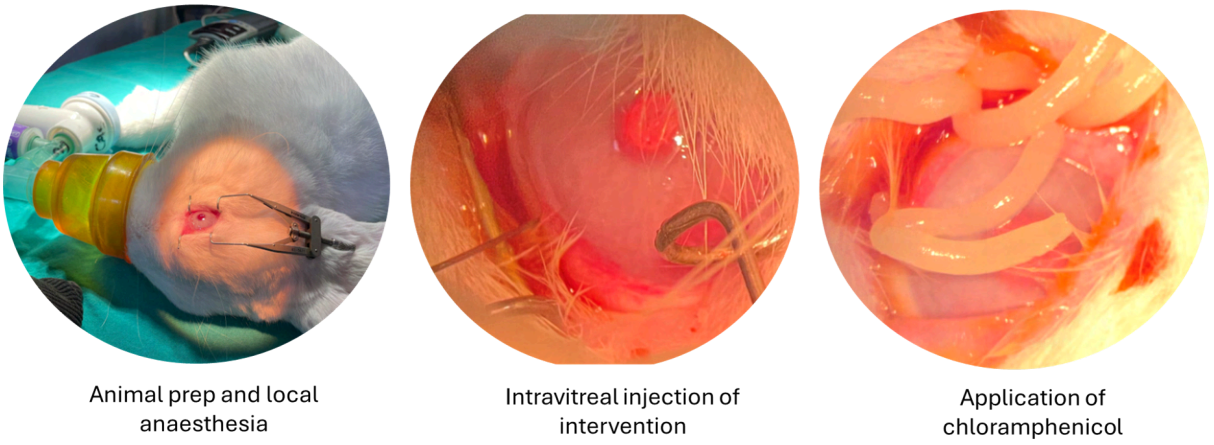

Figure 5.2: Depiction of surgical setup, intravitreal administration of intervention and postoperative application of chloramphenicol ointment.

5.1.4. Euthanisia, enucleation and sampling

NZW rabbits were euthanised 7 days after intervention. An overdose of IV sodium pentobarbital (> 50 mg/kg, 2 mL) was administered via the ear marginal vein for euthanisation followed by enucleation (removal of the eyeball) of the treated eye (right eye) and the negative control eye (left eye). Vitreous humour was aspirated from the ocular tissue, the remaining enucleated tissue was immersed either in 10% v/v buffered formalin for histomorphological or DNA/RNA Shield buffer for gene expression analysis.

5.1.5. Histomorphological and GFP expression analysis

Histomorphological analyses on the enucleated eyes were performed by IDEXX laboratories (Johannesburg South Africa), and green fluorescent protein (GFP) expression analysis using Quantitative PCR (qPCR) was performed by Inqaba Biotech (South Africa). For histomorphological analysis, eyes were prepared as per IDEXX SOP (IDEXXSA-AP-SOP-26) and processed using an automated tissue processor according to the histological tissue processing SOP (IDEXXSA-AP-SOP-27). Sections of the tissue were created (IDEXXSA-AP-SOP-30) and slides stained in an automated Haematoxylin and Eosin tissue stainer (IDEXXSA-AP-SOP-205) prior analysis. Histopathological grading was performed in accordance with IDEXX lab protocols to assess the level of inflammation in the tissue as follows; the infiltration of inflammatory cells into the vitreous cavity was visualized where Grade 0 = absent, Grade 1 = mild, Grade 2 = moderate, and Grade 3 = severe. Cellular infiltration (degree of infiltration by lymphocytes, plasma cells, and mononuclear and polymorphonuclear leukocytes) was graded from 0 to 3 +. For qPCR, upon reception of posterior ocular tissue, RNA extraction was performed to quantitatively determine the level of GFP expression in the posterior segment of the eye. The ocular tissue stored in DNA/RNA

Shield (Inqaba Biotech, South Africa) was homogenised to release RNA, the samples were processed as per Inqaba SOP. Reference gene β-ACTIN (Forward: 5'-CAGAAGGATTCCTATGTGGGC-3', Reverse: 5'-GAGGGCATACCCCTCGTAGAT-3') was quantified for normalising the expression levels of emGFP (Forward: 5'-GACGACGGCAACTACAAGAC -3', Reverse: 5 '- TGTCGGCGGTGATATAGACC- 3') in transfected cells.

5.1.6. pcDNA6.2-EmGFP *in vivo* Quantification

Following euthanasia, the aspirated vitreous humour was centrifuged (Eppendorf centrifuge 5804, Hamburg, Germany) at 10,000 x g for 10 min at 4°C to separate the cell fragments, proteins, and extracellular matrix components from the encapsulated genetic material. The supernatant was subsequently analysed using the Quant-iT PicoGreen assay (outlined in Section 3.1.7) at an excitation wavelength of 480 nm and emission of 520 nm. The absorbance readings were analysed via pcDNA6.2-EmGFP calibration curve to determine the stability of the encapsulated genetic cargo.

5.2. Results and Discussion

5.2.1. Animal postoperative assessment, recovery, and behaviour

Following surgery, postoperative monitoring was conducted paying close attention to the right eye for inflammation/irritation along with changes in body temperature, pulse, respiration and gastrointestinal function. Slight macroscopic changes such as discharge production and possible acute uveitis were observed in the treated eye (Gen-I and lipofectamine) compared to the untreated eye (negative control). This could be attributed to trauma resulting from the intravitreal injection and perhaps tissue sensitivity to the intervention (Palmieri et al., 2024). Rabbits were continually given appropriate doses of tramadol for pain management for three days post operation. Continuous monitoring showed an improvement in rabbit habitus, with observable inflammation visibly decreasing. Significantly, upon reception the rabbits weighed between 2.9 and 3.0 kg. Post-surgery, a weight loss ≤ 3% was observed for all rabbits. This weight reduction can be attributed to decreased food intake during the first three days following surgery, likely due to postoperative discomfort and stress (Jang et al., 2017). Gastrointestinal (GIT) function assessments revealed delayed recovery in these rabbits, with scores of ¾ post surgery, indicating partial impairment in digestive activity.

Important to note, continued monitoring of rabbit habitus demonstrated recovery in food intake, GIT function and overall alertness. Prior to termination, some of the rabbits had regained 0.1 kg, suggesting recovery in feeding behavior and GIT function. The remaining rabbits maintained their postoperative weight, which may indicate a prolonged impact on their metabolic recovery. Additionally, following intravitreal “therapy” injection in NZW rabbits, physiological parameters, including pulse rate and body temperature, were monitored over the first three days post-surgery to assess systemic responses to the treatment. Pulse rate varied amongst the animals, with the highest rate being 240 bpm, and the lowest being 142 bpm which is within the normal range (Cubík et al 2022). Slight fluctuations following the intervention may indicate post-surgical stress, inflammatory response, pain, or physiological compensation for transient hypotension (Bagley, 2007). Notably, the low pulse rates were observed among the positive control animals, fortunately, pulse rates stabilised by day 3 post treatment. This suggests adaptation and recovery from the initial stress response. Body temperature was monitored over three days post-injection. On Day 1, body temperatures were within the normal range (37.8–38.6°C). A drop in temperature was observed on Day 2 across all rabbits, reaching a minimum of 36.4°C, suggesting transient post-surgical hypothermia, altered autonomic regulation or reduced metabolic activity (Hart et al., 2011). By Day 3, both pulse rate and temperature trends suggest physiological stabilisation, indicating recovery from acute post-surgical stress. Further investigation into inflammatory markers and behavioral assessments provided additional insights into the systemic effects of the intervention. On the last day of the study (7 days post surgery) all rabbits were euthanised and enucleated.

5.2.2. Histological analysis of ocular tissue

To correlate these macroscopic observations with cellular-level changes, histomorphological investigations were subsequently conducted using Hematoxylin and Eosin (H&E) staining to assess the extent of inflammation microscopically (Figure 5.6). As expected, all ocular tissue layers from untreated eyes showed normal histological appearance. Both treatment groups (Gen-I system and Lipofectamine 3000), showed no morphological changes in the cornea, however enucleated eyes from the Gen-I system treatment group showed focal mild lymphoplasmacytic inflammation within the submucosa, at the limbus area of the Bulbar conjunctiva. Assessment of the anterior uvea of both treatment groups indicated mild edema, proliferating capillaries and lymphoplasmacytic infiltrate in the iris indicative of a mild and comparable inflammatory response in both groups.

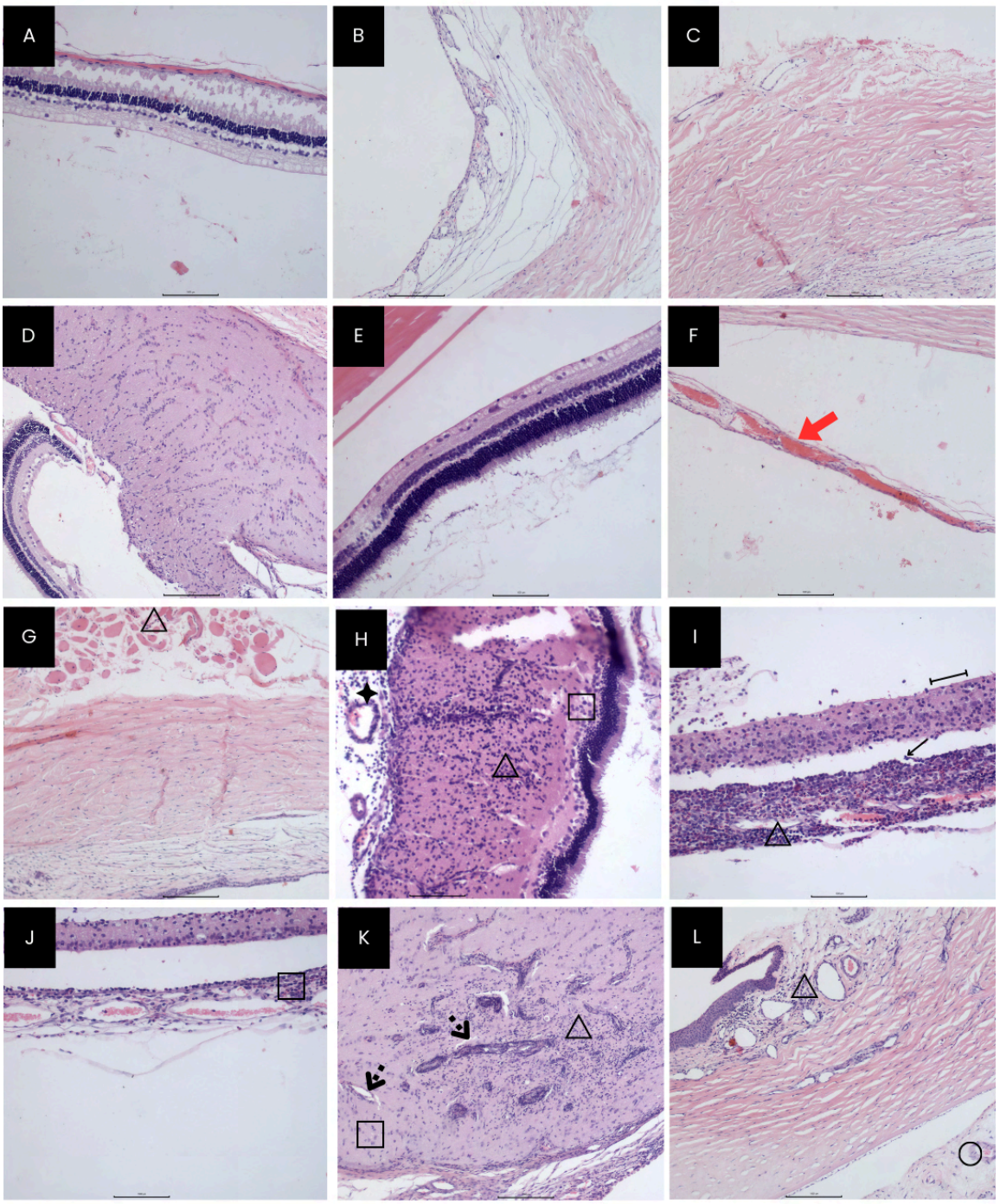

Figure 5.3: Histological slides of enucleated eyes at day 7. Tissue from negative control eyes showing (A) retina, (B) choroid, (C) sclera and (D) optic nerve at 10x and 20x magnification (Scale bar = 1000 µm) . (E - H) ocular tissue from Lipofectamine 3000_ pcDNA6.2-EmGFP (positive control) administered eyes (scale bar = 1000 µm). (I - L) histological images of ocular tissue from Gen-I system administered eyes (scale bar = 1000 µm). Symbols in the histopathological images indicate the following: circle = plasma cells; square =gliosis; triangle = lymphocytes; star = lymphocytic cuffing, dotted = vacuolization, black arrow = neutrophils, red arrow = congested vasculature.

Significantly, the sclera and retina of the lipofectamine treatment group showed normal histological appearance, however, some vascular congestion was observed in the choroid which is a sign of inflammation, increased/obstructed blood flow and irritation as a result of the surgical procedure (Figure 5.3 F). Moderate inflammation is noted by the infiltration of heterophils and single lymphocytes, macrophages and plasma cells in the choroid. Additionally a mild invasion of lymphocytes and plasma cells at the limbus of the sclera was observed along with moderate to large numbers of heterophils and few lymphocytes in the retina (Figure 5.3 E). In one of the test rabbits (Gen-I intervention), prominent hypertrophy/tombstoning (Figure 5.3 K,I) of the outer retinal epithelium compatible with retinal detachment was observed, which has been similarly reported in other studies following intravitreal injection (Ben Yahia et al., 2016; Thacker et al., 2021). This can be attributed to increased intraocular pressure as compared to lipofectamine 3000 only, the viscosity of the Gen-I system is higher and may have a greater impact on IOP. The inflammatory response observed seven days post operation is comparable to that observed in other studies and may resolve with longer timelines (Naik et al., 2024). Additionally, since the vitreous cavity has limited volume/capacity this highlights the need for vitreous volume compensation for gelling systems removing an equivalent amount of vitreous humor before administration. The elevated IOP can exert mechanical pressure on the retina, causing stress on the retinal layers, particularly the retinal pigment epithelium (RPE), leading to its detachment (Machiele et al., 2025). Additionally, traction from inflammatory changes may have contributed to the detachment of the retinal layers. Lastly, the optic nerve of both treatment groups showed moderate numbers of lymphocytes infiltrating the neuropil in association with gliosis and prominent cuffing of optic disc blood vessels (Figure 5.3 H,K). Furthermore, multifocal mild vacuolization within the neuropil indicating cellular damage and possibly some degree of tissue necrosis was observed in the Gen-I treated group. However, the deeper portions of the optic nerve displayed a normal histological appearance. Importantly, inflammation of ocular tissue is prominent following intravitreal surgery and was thus expected (Cox et al., 2021; Knickelbein et al., 2016).

5.2.3. Quantitative analysis of pcDNA6.2-EmGFP and GFP expression

The stability, clearance and expression kinetics of the nano-polyplex system were assessed using fluorometric and qualitative polymerase chain reaction (qPCR) analyses. Briefly, a calibration curve of pcDNA6.2-EmGFP was constructed as discussed in section 3.1.5 to determine the levels of pcDNA6.2-EmGFP in the aspirated vitreous humour of the rabbits following euthanasia. The pcDNA6.2-EmGFP levels detected in the vitreous humour reflect available pcDNA6.2-EmGFP from the nanosystems seven days post surgery. Notably, 6 ng/mL pcDNA6.2-EmGFP was detected in the vitreous humour of lipofectamine 3000 treated eyes (Figure 5.4). As lipid based systems are readily detected by the immune system and

thus rapidly cleared resulting in limited *in vivo* stability (Abbasi et al., 2023), low detection levels of pcDNA6.2-EmGFP can be attributed to these factors along with the immediate release of pcDNA6.2-EmGFP and clearance of the lipofectamine system by diffusion and or elimination via aqueous outflow or systemic circulation (del Amo et al., 2017). Additionally, the low levels of pcDNA6.2-EmGFP concentration and ultimately low dsDNA PicoGreen detection are a consequence of the rapid degradation of pcDNA6.2-EmGFP by vitreous endonucleases. Importantly, dsDNA PicoGreen is more sensitive to intact double stranded nucleic acids, therefore lower detection rates of PicoGreen are indicative of fragmented and thus degraded nucleic acids as reported in other studies (Sedlackova et al., 2013). Conversely, significantly higher pcDNA6.2-EmGFP (477.5 ng/mL; $p < 0.0001$) levels in the vitreous of Gen-I treated eyes was detected (Figure 5.4). This demonstrates that the Gen-I system is capable of protecting pcDNA6.2-EmGFP from nucleases, promoting nucleic acid stability and ensuring sustained nucleic acid entrapment and possibly release.

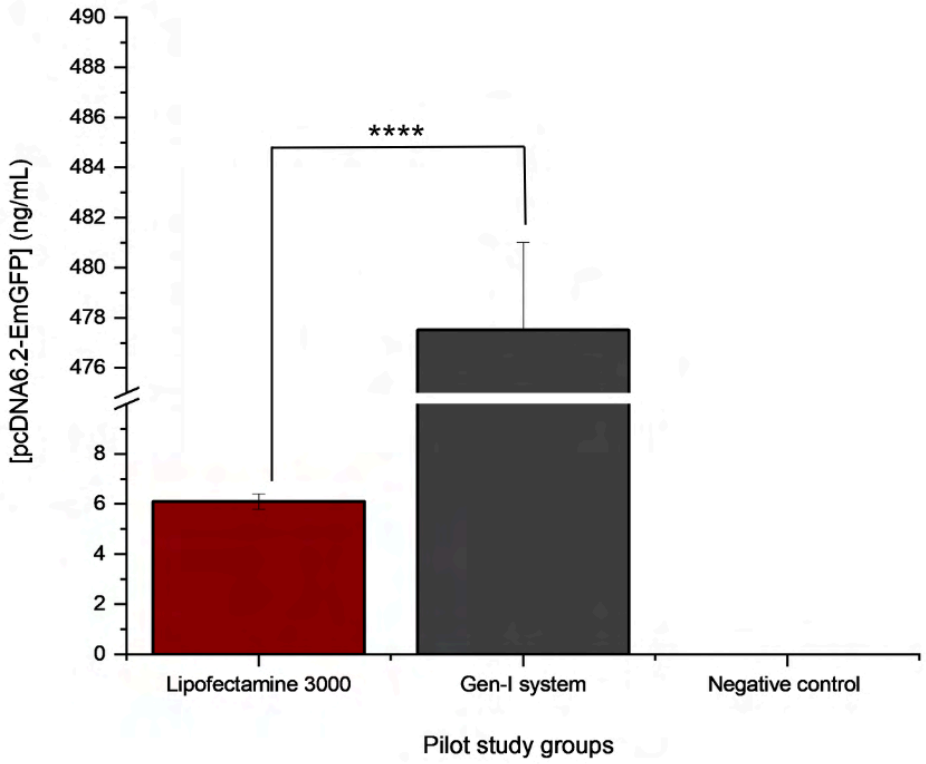

Figure 5.4: pcDNA6.2-EmGFP concentrations quantified in aspirated vitreous humour using the PicoGreen dsDNA assay. Data are presented as mean ± standard deviation (SD) from [n] biological replicates. Statistical significance was determined using ONE-WAY ANOVA, with $p < 0.0001$ (****) considered significant.

Additionally, qPCR was undertaken to determine GFP expression in NZW rabbits intravitreally injected with Lipofectamine 3000 and Gen-I system respectively loaded with 1ug pcDNA6.2-EmGFP. Lipofectamine was used as a market comparator as it has been utilised multiple times in *in vivo* gene delivery studies and its safety profile has been extensively

highlighted (Guo et al., 2024). Additionally, significant improvements on lipofectamine technology have broadened its transfection efficiency in a broad spectrum of cell lines and expanded its possible application in genome editing, stem cell manipulation, and immunotherapy (Andronikou et al., 2015). Following the enucleation of the NZW rabbits in the study, ocular tissue (posterior segment) from treated and untreated eyes was stored in RNA/DNA shield in preparation for RNA extraction and qPCR. Reverse transcription (RT-qPCR analysis showed expression of the housekeeping gene □ - actin which was used as the reference gene serving to normalise gene expression data to ensure observable variations result from biological factors rather than tissue quality and or quantity. Slight variations of □ - actin were observed between the controls and intervention samples (Table 5.1) which are normal and could be due to the quality of RNA extracted from the tissues. No GFP expression was detected in both treatment groups (lipofectamine and Gen-I) seven days post intravitreal administration under conditions used in this study (Table 5.1). The lack of GFP mRNA detection in the posterior tissue of treated eyes can be attributed to a myriad of factors, the probable ones with respect to the study are outlined as follows. Notably, although intravitreal gene delivery is a relatively safe and minimally invasive delivery method that effectively targets the upper layers of the retina (ganglion and muller ganglion cells), it achieves little success in delivering therapy to the outer cell layers of the retina (photoreceptor and RPE) due to barriers posed by the vitreous humor and the inner limiting membrane (Gupta and Huckfeldt, 2017), therefore resulting in insufficient gene delivery or bioavailability and overall no GFP expression. Briefly, the viscosity, biochemical components and negative charge of the vitreous humour along with the presence of inflammation significantly impact movement of nanoparticles therefore creating a significant barrier to nanoparticle translocation to retinal cells (Mains and Wilson, 2013). Delayed movement or nanoparticle retardation within the vitreous humor may indicate the need for an extended study duration to allow sufficient time for the system to traverse the vitreous and reach retinal cells for effective gene expression. Therefore, a study lasting longer than seven days may provide adequate time for meaningful results.

An alternative explanation, particularly for Gen-I treated eyes, was that notable inflammation was observed (Figure 5.3). The recruitment of immune cells could have increased the detection of the system and genetic material thus resulting in the degradation and elimination of the released plasmid DNA prior to the system transfecting RPE cells. Other possible causes for this include vector promoter issues, which have been shown to significantly impact target gene expression. Particularly, the CMV promoter casette in the pcDNA6.2-EmGFP plasmid responsible for facilitating GFP expression in cells, is susceptible to silencing *in vivo* resulting in transgene silencing (Calado et al., 2014; Radhakrishnan et al., 2008). The exact mechanism driving this is currently unknown, however, epigenetic

modifications (e.g., DNA methylation and histone modifications) have been shown to be involved in restricting CMV promoter activity, particularly in post-mitotic cells such as neuronal and RPE cells (Calado et al., 2014; Radhakrishnan et al., 2008).

Table 5.1: RT-PCR Cq Data

Gene	Sample	Cq
Em_GFP	Lipofectamine treated Eye - Positive Control	ND
Em_GFP	Lipofectamine treated Eye - Positive Control	ND
Em_GFP	Lipofectamine treated Eye - Positive Control	ND
Em_GFP	Gen-I system treated Eye	ND
Em_GFP	Gen-I system treated Eye	ND
Em_GFP	Gen-I system treated Eye	ND
Em_GFP	Negative Control Eye	ND
Em_GFP	Negative Control Eye	ND
Em_GFP	Negative Control Eye	ND
□-ACTIN	Lipofectamine treated Eye - Positive Control	25.26
□-ACTIN	Lipofectamine treated Eye - Positive Control	25.30
□-ACTIN	Lipofectamine treated Eye - Positive Control	25.34
□-ACTIN	Gen-I system treated Eye	28.15
□-ACTIN	Gen-I system treated Eye	28.22
□-ACTIN	Gen-I system treated Eye	28.34
□-ACTIN	Negative Control Eye	26.49
□-ACTIN	Negative Control Eye	26.55
□-ACTIN	Negative Control Eye	26.53

5.3. Concluding Remarks

The chronic nature of PSEDs requires multiple injections to achieve therapeutic efficacy as mentioned above. Therefore, the development of sustained drug release systems eliminates the need for frequent intraocular drug administration, therefore limiting possible risks associated with therapeutic delivery. Thus, the advent of strategies promoting controlled and prolonged drug delivery, such as the use of scaffolds, nanoparticles, and hydrogels serves as the basis for long term localised payload delivery. As highlighted above, this chapter reports a pilot study focused on assessing the efficacy of the designed hybrid gene delivery system, Gen-I, for achieving gene delivery, and for determining its safety profile. The intravitreal injection of the formulated smart hydrogel system led to a moderate immune response and first signs of retinal detachment which is common in intravitreal surgeries and may be due to

increased IOP as the Gen-I system was not compensated for prior administration. Notably, compared to the commercial gene delivery system, lipofectamine 3000, the Gen-I system achieves effective nucleic acid protection and stability *in vivo*, along with signs of prolonged nucleic acid release indicative of its potential application as a single dose - long term therapy delivery system. The absence of detectable GFP expression *in vivo*, despite promising *in vitro* results, underscores the significant challenges involved in translating gene delivery systems from controlled laboratory conditions to complex physiological environments. *In vitro* experiments often provide idealised conditions for cellular uptake, endosomal escape, and gene expression, including direct exposure of cells to the delivery system and optimal culture conditions. In contrast, *in vivo* applications introduce multiple physiological barriers such as tissue diffusion limits, enzymatic degradation, immune responses, and anatomical complexities, particularly within the ocular space. Additionally, the intravitreal route of administration may have limited the interaction between the nanopolyplex-loaded hydrogel and target retinal cells due to diffusion constraints across the vitreous and inner limiting membrane. These limitations illustrate the difficulty in predicting *in vivo* performance solely based on *in vitro* data and highlight the need for iterative optimisation of delivery routes, dosages, and release kinetics to bridge the gap between preclinical research and clinical application. Therefore, further *in vivo* studies (Phase I Clinical Trial) are required to ascertain the ideal characteristics (promoter selection, pDNA concentration and vitreous compensation before Gen-I injection) necessary for achieving nano-polyplex system transfection and nucleic acid translocation *in vivo*.

5.4. References

Abbasi, H., Kouchak, M., Mirveis, Z., Hajipour, F., Khodarahmi, M., Rahbar, N., Handali, S., 2023. What We Need to Know about Liposomes as Drug Nanocarriers: An Updated Review. Adv. Pharm. Bull. 13, 7–23. https://doi.org/10.34172/apb.2023.009

Andronikou, N., Yu, X., Wei, J., Sridharan, M., Quintanilla, R., Lakshmipathy, U., Welch, P., de, X., 2015. Lipofectamine 3000 reagent—efficient, reproducible transfection for biologically relevant cell models.

Bagley, R.S., 2007. World Small Animal Veterinary Association World Congress Proceedings, 2007. VIN.com.

Ben Yahia, S., Kahloun, R., Abroug, N., Kaibi, I., Laadhari, G., Jelliti, B., Khairallah, M., 2016. Comparative effect of topical diclofenac and topical dexamethasone on anterior chamber flare and postoperative pain following rhegmatogenous retinal detachment surgery. Int. Ophthalmol. 36, 623–628. https://doi.org/10.1007/s10792-015-0168-1

Calado, S.M., Oliveira, A.V., Machado, S., Haase, R., Silva, G.A., 2014. Sustained Gene Expression in the Retina by Improved Episomal Vectors. Tissue Eng. Part A 20, 2692–2698. https://doi.org/10.1089/ten.tea.2013.0672

Cox, J.T., Eliott, D., Sobrin, L., 2021. Inflammatory Complications of Intravitreal Anti-VEGF Injections. J. Clin. Med. 10, 981. https://doi.org/10.3390/jcm10050981

Cubík, J., Kepak, S., Wiedermannova, H., Vrtkova, A., Burckova, H., Zarubova, P., Fernandez, C., Pavlicek, J., Jargus, J. and Vasinek, V., 2022. Measuring respiratory and heart rate using a fiber optic interferometer: A pilot study in a neonate model. Frontiers in pediatrics, 10, p.957835.

del Amo, E.M., Rimpelä, A.-K., Heikkinen, E., Kari, O.K., Ramsay, E., Lajunen, T., Schmitt, M., Pelkonen, L., Bhattacharya, M., Richardson, D., Subrizi, A., Turunen, T., Reinisalo, M., Itkonen, J., Toropainen, E., Casteleijn, M., Kidron, H., Antopolsky, M., Vellonen, K.-S., Ruponen, M., Urtti, A., 2017. Pharmacokinetic aspects of retinal drug delivery. Prog. Retin. Eye Res. 57, 134–185. https://doi.org/10.1016/j.preteyeres.2016.12.001

Guo, S., Li, C., Wang, C., Cao, X., Liu, X., Liang, X.-J., Huang, Y., Weng, Y., 2024. pH-Responsive polymer boosts cytosolic siRNA release for retinal neovascularization therapy. Acta Pharm. Sin. B 14, 781–794. https://doi.org/10.1016/j.apsb.2023.09.001

Gupta, P.R., Huckfeldt, R.M., 2017. Gene therapy for inherited retinal degenerations: initial successes and future challenges. J. Neural Eng. 14, 051002. https://doi.org/10.1088/1741-2552/aa7a27

Hart, S.R., Bordes, B., Hart, J., Corsino, D., Harmon, D., 2011. Unintended Perioperative Hypothermia. Ochsner J. 11, 259–270.

Jang SJ, Kang SS, Son SJ, Lee JY, Kim G, Choi SH 2017. Cortisol levels and

gastrointestinal disorders after stressful surgery in rabbits. in vivo. 1;31(4):637-40.

Keating, S.C.J., Thomas, A.A., Flecknell, P.A., Leach, M.C., 2012. Evaluation of EMLA Cream for Preventing Pain during Tattooing of Rabbits: Changes in Physiological, Behavioural and Facial Expression Responses. PLOS ONE 7, e44437. https://doi.org/10.1371/journal.pone.0044437

Knickelbein, J.E., Chew, E.Y., Sen, H.N., 2016. Intraocular Inflammation Following Intravitreal Injection of Anti-VEGF Medications for Neovascular Age-Related Macular Degeneration. Ophthalmic Epidemiol. 23, 69–70. https://doi.org/10.3109/09286586.2015.1122067

Machiele, R., Motlagh, M., Zeppieri, M., Patel, B.C., 2025. Intraocular Pressure, in: StatPearls. StatPearls Publishing, Treasure Island (FL).

Mains, J. and Wilson, C.G., 2013. The vitreous humor as a barrier to nanoparticle distribution. Journal of ocular pharmacology and therapeutics, 29(2), pp.143-150.

Murro, V., Banfi, S., Testa, F., Iarossi, G., Falsini, B., Sodi, A., Signorini, S., Iolascon, A., Russo, R., Mucciolo, D.P., Caputo, R., Bacci, G.M., Bargiacchi, S., Turco, S., Fortini, S., Simonelli, F., 2023. A multidisciplinary approach to inherited retinal dystrophies from diagnosis to initial care: a narrative review with inputs from clinical practice. Orphanet J. Rare Dis. 18, 223. https://doi.org/10.1186/s13023-023-02798-z

Naik, K., du Toit, L.C., Ally, N., Choonara, Y.E., 2024. In vivo evaluation of a Nano-enabled therapeutic vitreous substitute for the precise delivery of triamcinolone to the posterior segment of the eye. Drug Deliv. Transl. Res. 14, 2668–2694. https://doi.org/10.1007/s13346-024-01566-1

Palmieri, F., Younis, S., Bedan Hamoud, A., Fabozzi, L., 2024. Uveitis Following Intravitreal Injections of Faricimab: A Case Report. Ocul. Immunol. Inflamm. 32, 1873–1877. https://doi.org/10.1080/09273948.2023.2293925

Peynshaert, K., Devoldere, J., De Smedt, S.C., Remaut, K., 2018. In vitro and ex vivo models to study drug delivery barriers in the posterior segment of the eye. Adv. Drug Deliv. Rev. 126, 44–57. https://doi.org/10.1016/j.addr.2017.09.007

Radhakrishnan, P., Basma, H., Klinkebiel, D., Christman, J., Cheng, P.-W., 2008. Cell type-specific activation of the cytomegalovirus promoter by dimethylsulfoxide and 5-Aza-2'-deoxycytidine. Int. J. Biochem. Cell Biol. 40, 1944–1955. https://doi.org/10.1016/j.biocel.2008.02.014

Sedlackova, T., Repiska, G., Celec, P., Szemes, T., Minarik, G., 2013. Fragmentation of DNA affects the accuracy of the DNA quantitation by the commonly used methods. Biol. Proced. Online 15, 5. https://doi.org/10.1186/1480-9222-15-5

Talib, M., Boon, C.J.F., 2020. Retinal Dystrophies and the Road to Treatment: Clinical Requirements and Considerations. Asia-Pac. J. Ophthalmol. 9, 159–179. https://doi.org/10.1097/APO.0000000000000290

Thacker, M., Tseng, C.-L., Lin, F.-H., 2021. Substitutes and Colloidal System for Vitreous Replacement and Drug Delivery: Recent Progress and Future Prospective. Polymers 13, 121. https://doi.org/10.3390/polym13010121

CHAPTER SIX
Conclusion and Recommendations

6. Conclusion

6.1. Concluding Insights

Gene therapy has the potential to offer longer-lasting transformational clinical benefits as it can circumvent limitations associated with conventional therapies by achieving sustained and controlled genetic modification of target tissues. Taking into consideration the lack of treatments for PSEDs, the emergence of the ocular gene therapy, Luxturna®, has revolutionised the treatment of *rpe65* mutation induced retinitis pigmentosa and improved patient quality of life. Continued research into PSED-targeted gene therapy has the unique ability to achieve durable and potentially curative clinical benefit through a single dose, enabling sustained production of therapeutic proteins endogenously and obviating the need for lifelong therapeutic administration. However, essential hurdles reported for Luxturna® such as its inability to address the continued degeneration of retinal cells and the activation of the innate and adaptive immune system by viral vectors and associated transgenes, continue to limit its effectiveness as the aforementioned factors have severe consequences commonly resulting irreversible damage to the retina and surrounding ocular tissue. An alternative encompasses the use of biocompatible non-viral vectors. Although potentially less immunogenic and capable of encapsulating larger genetic cargos compared to viral vectors, these require further modification to improve their cell/tissue specificity, promote endosomal escape and ensure nuclear translocation.

To this end, the present study explored targeted non-viral vector-based gene delivery as a viable alternative to viral vectors. Initially, an in-depth review highlighting current gene therapy advancements in the treatment of PSEDs, with a particular focus on the design and development of non-viral gene delivery systems was conducted. A novel CD44 targeting - cationic amphiphilic nanosystem (HA-2AB^{+}-OLA), composed of biodegradable and biocompatible polymers was developed and characterised employing various in-depth characterisation techniques. The formulated composite was used to encapsulate pcDNA6.2-EmGFP as the model genetic material for the study, forming a nano-polyplex exhibiting aqueous stability for 4 weeks at 4°C. The average size and zeta potential of the nano-polyplex ranged from 150 nm to 3.6 µm and 3.5 to 25 mV, respectively, with low to high encapsulation efficiencies (19.5 to 99.7%). The significant sustained release of pcDNA6.2-EmGFP was translated *in vitro*, showing slightly lower levels of GFP expression compared to lipofectamine 3000 following transfection of HEK293 cells due to slower but sustained release by the nano-polyplex as discussed in section 4. Sustained release is advantageous for achieving prolonged therapeutic effects, unlike Lipofectamine, which has a

rapid release profile and is therefore limited in applications requiring extended efficacy. Alternatively, no GFP expression was detected in hRPE cells following treatment with both nanosystems (positive control and nano-polyplex) which is maybe due to the senescence of hRPE cells *in vitro* as noted on their failure to propagate in culture.

Considering clinical trial studies conducted on Luxturna highlighted significant drawbacks of the therapy such as its failure to achieve sustained efficacy as photoreceptors steadily continue degenerating sometime after treatment matching those of untreated patients, the promotion of retinal cell regeneration combined with gene therapy is a potential key to achieving therapeutic efficacy for PSEDs (Fu et al., 2018; Wang et al., 2020). Furthermore, this study entailed the development of a hybrid system capable of serving as a vehicle for gene delivery, as well as for cellular support, highlighting its potential use for cell delivery, and aiding in the promotion of cell viability in the event of tissue regeneration. The cold method was used to formulate a smart hydrogel system based on Pluronic F127, chitosan and the nano-polyplex system. DOE strategy for formulation was utilised to determine the optimum formulation with desired characteristics. The rheological and physicochemical characterisation of the final formulation, the Gen-I system, was conducted using multiple techniques. The polymers selected for the formulation of the Gen-I system are known to have the propensity to mimic the extracellular matrix thus providing a 3D environment which provides structural support and promotes cell viability and proliferation. The rate of Gen-I degradation exceeded 21 days which is ideal for cell delivery, integration and ECM deposition. *In vitro* analyses highlighted that the Gen-I possessed an acceptable safety profile, with seeded cells maintaining viability and metabolic activity within the scaffold as depicted by live cell staining. Further studies focusing on regenerative processes, such as cell migration and cell differentiation will be necessary to establish the Gen-I system as a viable scaffold for tissue regeneration.

Furthermore, studies were conducted to assess the safety profile of the Gen-I system for gene delivery *in vivo* using New Zealand White (NZW) Rabbits. The *in vivo* pilot study was conducted to optimise the route of administration and assess the behaviour of the intravitreally injected Gen-I system as *in vitro* and *in vivo* conditions differ. As discussed in the previous chapter, intravitreal administration of Gen-I elicited a mild immune response potentially due to increased intraocular pressure caused by the smart hydrogel system and lack of vitreous volume compensation. Therefore, *in vivo* investigation of Gen-I aided in our understanding of the mechanism by which the system affects retinal structure and immunity. The data obtained showed that intravitreal delivery of Gen-I may require vitrectomy to account for the volume of the Gen-I smart hydrogel. Alternatively, a lower volume of the Gen-I system could be considered for delivery to avoid vitrectomy. Importantly, this pilot also

indicated the need for investigating alternative routes of administration such as subretinal and suprachoroidal injection, along with a prolonged study timeline.

While considerable challenges remain and further clinical investigations are required, advancements achieved in this study present a promising step toward safer, minimally invasive, and long-acting treatments for conditions such as age-related macular degeneration and inherited retinal dystrophies diseases for which durable therapeutic options remain limited. The above investigation contributes to the growing body of research focused on smart, biomaterial-based gene delivery platforms that enable precise spatial and temporal control of therapeutic release within sensitive tissues. Therefore, future Phase I clinical trials must carefully consider the translational and regulatory challenges associated with the development and application of gene therapy. Robust evidence of the safety, reproducibility, and long-term efficacy of the novel Gen-I system must be provided. Given the heightened concern over immunogenicity, off-target effects, and the risk of irreversible damage to delicate retinal structures, particular attention must be paid to dose selection to ensure both efficacy and safety. Additionally, scaling up the Gen-I system for use in a substantially larger animal group (72 New Zealand White rabbits) may introduce complexities such as maintaining batch consistency, sterility, and long-term stability. These considerations underscore the need to develop delivery platforms that are not only biologically effective but also scalable, safe, and compliant with regulatory standards for clinical application in treating retinal degenerative diseases.

6.2. Recommendations

The knowledge gained from this investigation could be used to design and construct gene therapy protocols that are safe, effective, and suitable for eventual use in human patients. This translational research has the potential to bring about novel therapeutic options for individuals suffering from retinal degenerative diseases. This study demonstrates the potential of a hybrid hydrogel/nanoparticle system for both sustained gene delivery and cell support applications. The nanoparticles ensured efficient genetic material encapsulation and controlled release, while incorporation into the hydrogel further sustained gene release. The smart hydrogel provided a supportive environment for cell survival and proliferation, maintaining high viability and metabolic activity. The combined system offers a multifunctional platform where gene-loaded nanoparticles can simultaneously deliver therapeutics and support cell-based treatments. Future work could optimise the system to balance gene release rates with cellular response for enhanced therapeutic efficacy. Furthermore, key priorities include improving the *in vivo* transfection efficiency and cell specificity of the nanopolyplex, ensuring long-term biocompatibility and biodegradation of the Gen-I system,

and establishing a robust safety profile. Additionally, *in vivo* studies using disease-relevant models will be critical for validating the therapeutic efficacy and functional recovery potential of the system.

Additionally, dvanced preclinical studies are recommended to optimise the route of administration particularly to ensure nano-polyplex translocation across the retina to achieve significant levels of gene expression. Additionally, studies beyond cell encapsulation, viability and survival are necessary to explore the role of the Gen-I system in promoting tissue regeneration, expanding on the results demonstrated in the preliminary study in chapter 4. To this end, future investigations on key tissue regeneration markers such as cell migration dynamics, cell proliferation markers, differentiation and inflammatory pathways amongst others in response to the Gen-I system will give some insights into the significance of the cell scaffold in tissue regeneration. Alternatively, a retinal degenerative zebrafish model can be used to study the delivery and impact of exogenous gene edited cells/stem cells employing the Gen-I system in driving retinal dedifferentiation and regeneration. This multi-component form of therapy has the potential to apply genes to drive tissue regeneration providing an opportunity to develop ‘one-time treatment options’.

6.3. References

Fu, X., Huu, V.A.N., Duan, Y., Kermany, D.S., Valentim, C.C., Zhang, R., Zhu, J., Zhang, C.L., Sun, X. and Zhang, K., 2018. Clinical applications of retinal gene therapies. Precision Clinical Medicine, 1(1), pp.5-20. https://doi.org/10.1093/pcmedi/pby004

Wang, X., Yu, C., Tzekov, R.T., Zhu, Y. and Li, W., 2020. The effect of human gene therapy for RPE65-associated Leber’s congenital amaurosis on visual function: a systematic review and meta-analysis. Orphanet Journal of Rare Diseases, 15, pp.1-9. https://doi.org/10.1186/s13023-020-1304-1.

Appendix A: Supplementary Material

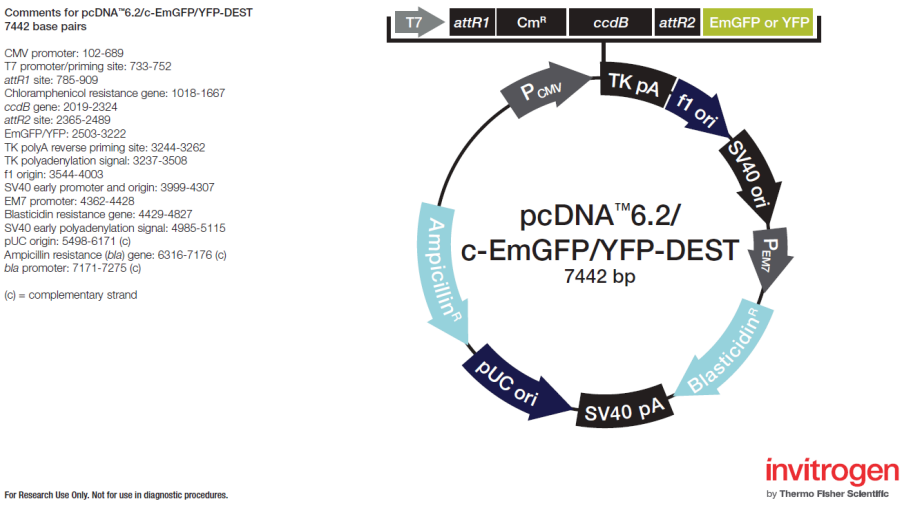

Figure S1: pcDNA6.2-EmGFP construct

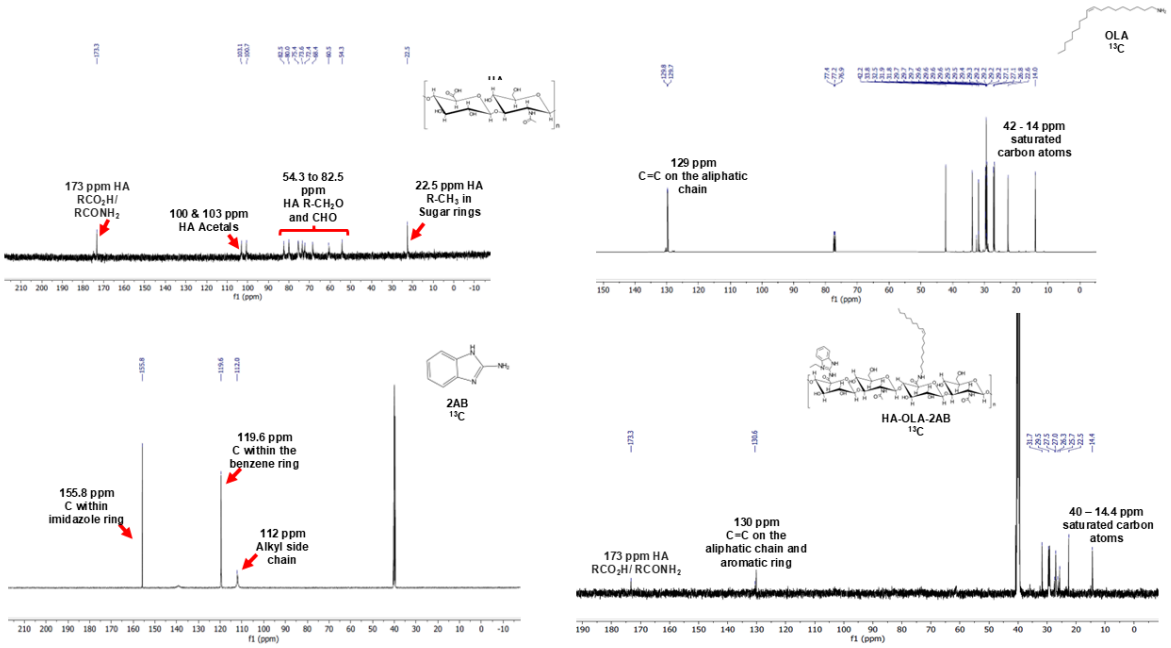

Figure S2: ^{13}C nuclear magnetic resonance (NMR) spectra of native polymers and the synthesised conjugate.

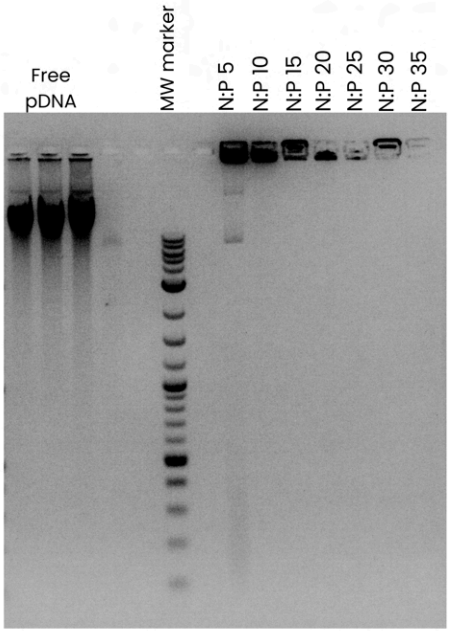

Figure S3: pcDNA6.2-EmGFP entrapment within the nanosystem depicted qualitatively using gel electrophoresis (Highlighting N:P 5).

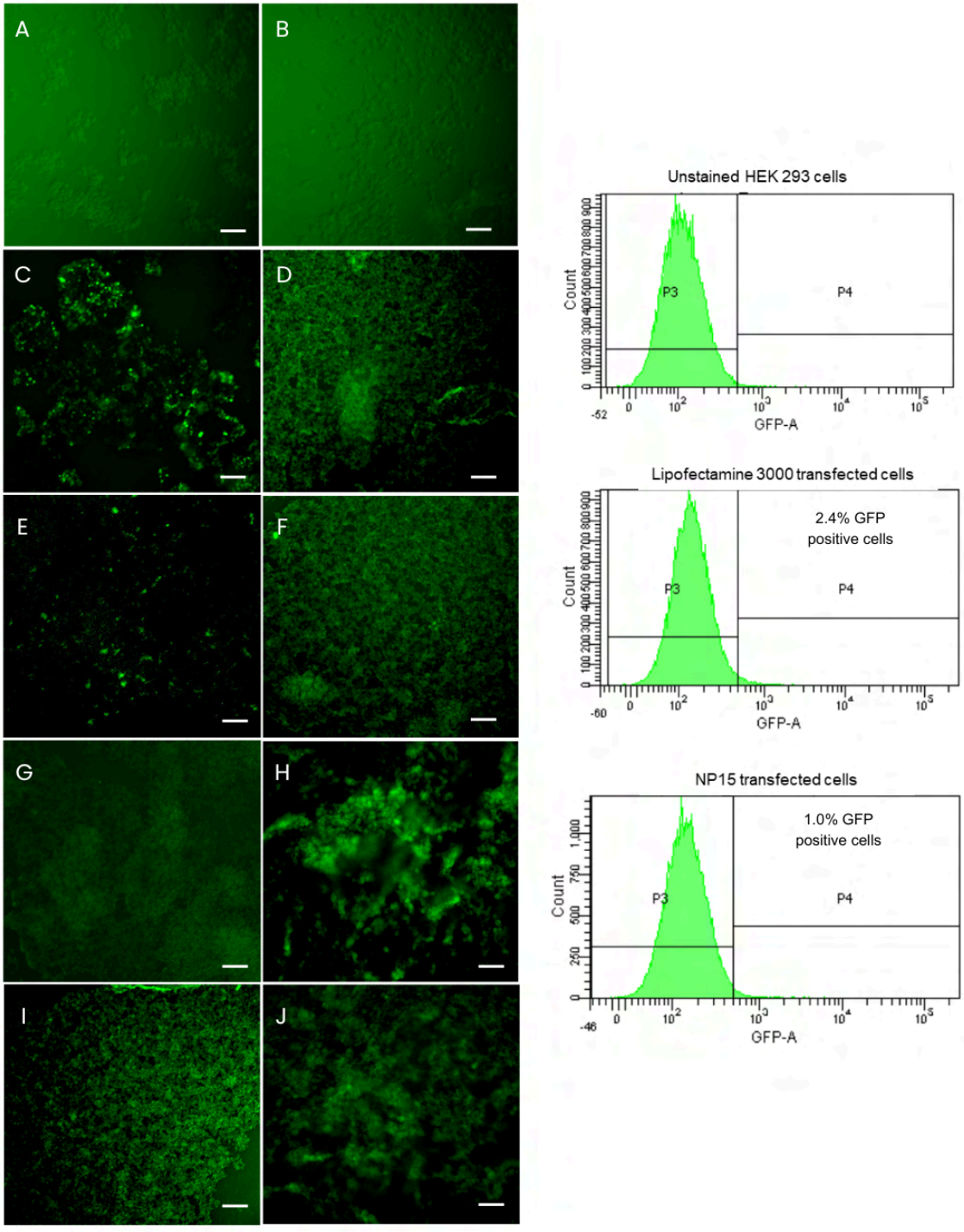

Figure S4: Transfection efficiency of HEK 293 cells by nano-polyplex system after 72 h. HEK 293 cells (A), free pcDNA6.2-EmGFP (B), Lipofectamine 3000/pcDNA6.2-EmGFP (C), N:P 10 (D), N:P 15 (E), N:P 20 (F), N:P 25 (G), N:P 30 (H), N:P 35 (I), N:P 40 (J) and Flow cytometry for emGFP detection (K).

Supplementary Table 1: RNA quality following extraction in HEK293 cells for qPCR

Sample	Concentration	A260/A280	A260/A230
Lipofectamine transfected cells RNA	97.9	1.85	2.18
Cells only RNA	191.6	2.12	2.18
Nano-polyplex transfected cells RNA	73.4	2.12	2.07

Supplementary Table 2:

Formulation	Pluronic F127 (%)	Nanosystem (%)	Chitosan (%)	Cross-over - Gelation temperature (°C)
F1	19.5	1	0.55	15
F2	17	1	0.55	26.18
F3	17	1	1	25.33
F4	17	1	0.1	27.14
F5	19.5	1	0.1	24.89
F6	19.5	1	0.1	24.89
F7	19.5	1	0.55	15
F8	19.5	1	0.55	15
F9	22	1	1	No crossover
F10	19.5	1	0.55	15
F11	19.5	1	0.55	No crossover
F12	22	1	0.55	No crossover
F13	19.5	1	1	15
F14	19.5	1	1	15
F15	22	1	0.55	No crossover

F16	17	1	0.55	26.18
F17	22	1	0.1	No crossover

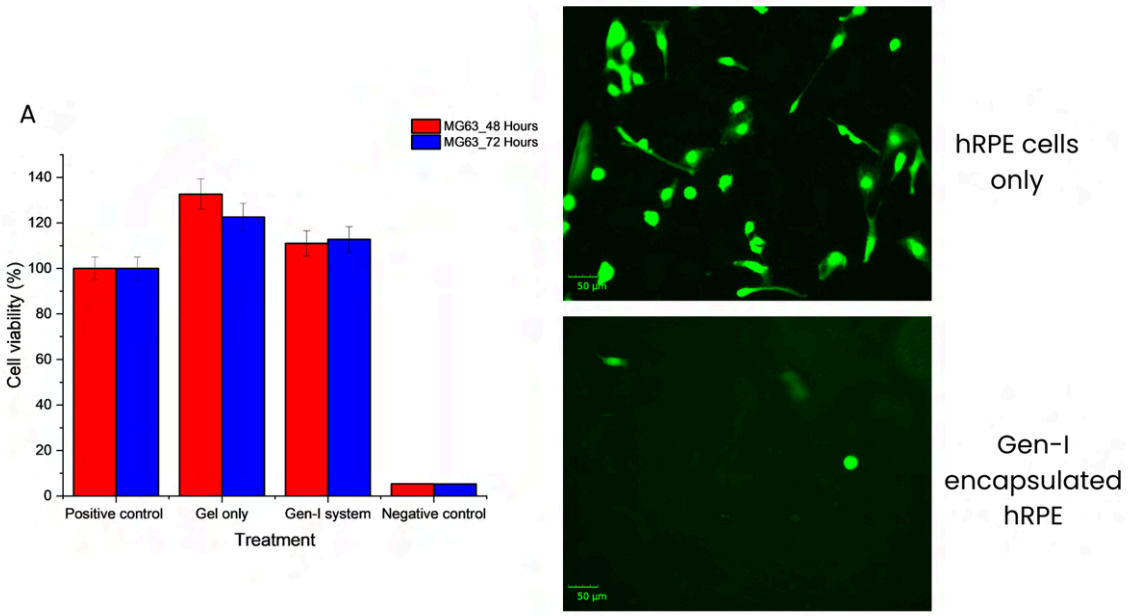

Figure S6: a) Safety profile of the Gen-I system on MG63 cells and hRPE cells. a) Cell viability of MG63 cells at 48h and 72 h. b) Live cell staining (Calcein AM) of non-encapsulated hRPE cells and Gen-I encapsulated hRPE cells at timepoint - 24 h.

Appendix B: Animal Ethics Clearance Certificate

ANIMALS RESEARCH ETHICS COMMITTEE (AREC)

UNIVERSITY OF THE WITWATERSRAND JOHANNESBURG

STRICTLY CONFIDENTIAL

CLEARANCE CERTIFICATE NUMBER: AESC21-04-016C

APPLICANT: Ms N Sikhosana
School: Therapeutic sciences; Department: Pharmacy and Pharmacology; Location: WRAF

PROJECT TITLE: In vivo analysis of the biocompatibility, gene release and expression following intraocular injection of a thermoresponsive gel nanosystem (Gen-I) in New Zealand white rabbits
Category: C; Species and Numbers involved: 73X, Either sex, 2.5 kg - 4 kg, New Zealand white rabbits, Rabbits

Approval is hereby given for the use of animals for the research project named above and described in the application reviewed by a quorate meeting of the AREC held on 25 September 2024. This approval remains valid until 6 October 2026 and is conditional to the following (if blank there are no special conditions):

Condition 1	Condition 2	Condition 3	Condition 4
Dr Naseer Ally (Ophthalmologist) to get authorisation from SAVC before any veterinary procedures			

All material changes to the approved research must be reported to the AREC before they are implemented. Failure to do so will invalidate this clearance certificate.

An annual progress report must be provided to the AREC.

The use of these animals is subject to AREC guidelines on the use and care of laboratory animals, is limited to the procedures described in the application and is subject to additional conditions listed below:

I, the Chair of the AREC (or my designated representative) am satisfied that the proposed research is ethical as judged by local law, international standards and University policy.

Signed: _____ _____ Date: _____09/10/2024___
(Chairperson of the AREC)

CC: Student supervisor: Prof Y Choonara
Acting Director Wits Research Animal Facility (WRAF): Sr A Rammekwa

Appendix C: Research Outputs

C1: 16th Early Career Scientist Convention, SAMRC, Cape Town Headquarters (Online), 25 - 26 October 2022.

SOUTH AFRICAN MEDICAL RESEARCH COUNCIL

30. Nano-embedded 3D-bioplatforms for Ocular Tissue Regeneration

N. Sikhosana[1], L. du Toit[1], N. Ally[2], Y.Choonara[1]

[1]Wits Advanced Drug Delivery Platform Research Unit, Department of Pharmacy and Pharmacology, School of Therapeutic Sciences, Faculty of Health Sciences, University of the Witwatersrand, Johannesburg, 7 York Road, Parktown, 2193, South Africa; [2] Division of Ophthalmology, Department of Neurosciences, School of Clinical Medicine, Faculty of Health Sciences, University of the Witwatersrand, Johannesburg, 7 York Road, Parktown 2193, South Africa

BACKGROUND

Posterior Segment Eye Diseases (PSEDs) such as age-related macular degeneration, retinitis pigmentosa, and diabetic retinopathy, affect tissues of the eye; vitreous humor, retina, optic nerve, and choroid, resulting in visual impairment and blindness. The complex anatomy and physiology of the eye poses significant barriers in efficient therapeutic delivery, necessitating intravitreal administration. However, current intravitreally delivered therapies have major drawbacks and low patient compliance. Efficient treatment of PSEDs remains a challenge and requires the development of more effective therapeutics capable of eliminating the need for repeat intraocular injections, achieving sustained and controlled therapeutic release, and promoting tissue regeneration via the body's healing mechanisms.

METHODS

Gene delivery nanocarriers targeting cluster of differentiation 44 (CD44) in retinal pigment epithelium cells (RPE) have been constructed for the treatment of retinal diseases. Nanocarriers based on hyaluronic acid (HA)-2 aminothiazole (HA_2AT) and HA- 2-aminobenzimidazole (HA_2AB) copolymers were developed. The copolymers were quaternized using iodoethane to enable the entrapment of genetic material. For preliminary studies, miR-128 was encapsulated into the nanoparticles. The copolymers and nanosystems were characterised using DLS, FTIR, NMR and SEM.

RESULTS

Following synthesis, nanoparticles were formulated, the charge, size and morphology of the nanosystems carrying miR-128 was determined. HA was used as a control and showed a charge of -12, HA_2AT_miR-128 charge was 5.54 and size was ~89 nm whilst HA_2Benzo_miR-128 NP charge was 6.27 and size was ~78 nm. SEM micrographs depicted all nanoparticles to be spherical.

CONCLUSION

Current therapies for retinal diseases cannot achieve sustained and targeted therapeutic delivery. The designed nanosystem uses HA to target the retina via CD44 receptors and utilises the positive charge on the nanosystem to promote gene encapsulation. The slightly positive charge, size and properties of the nanosystem are hypothesized to promote targeted and sustained gene delivery and expression, which are currently under investigation.

C2: Annual Young Scientists Conference 2023 (Oral Presentation). University of Venda, Thohoyandou, South Africa, June 12 -13, 2023

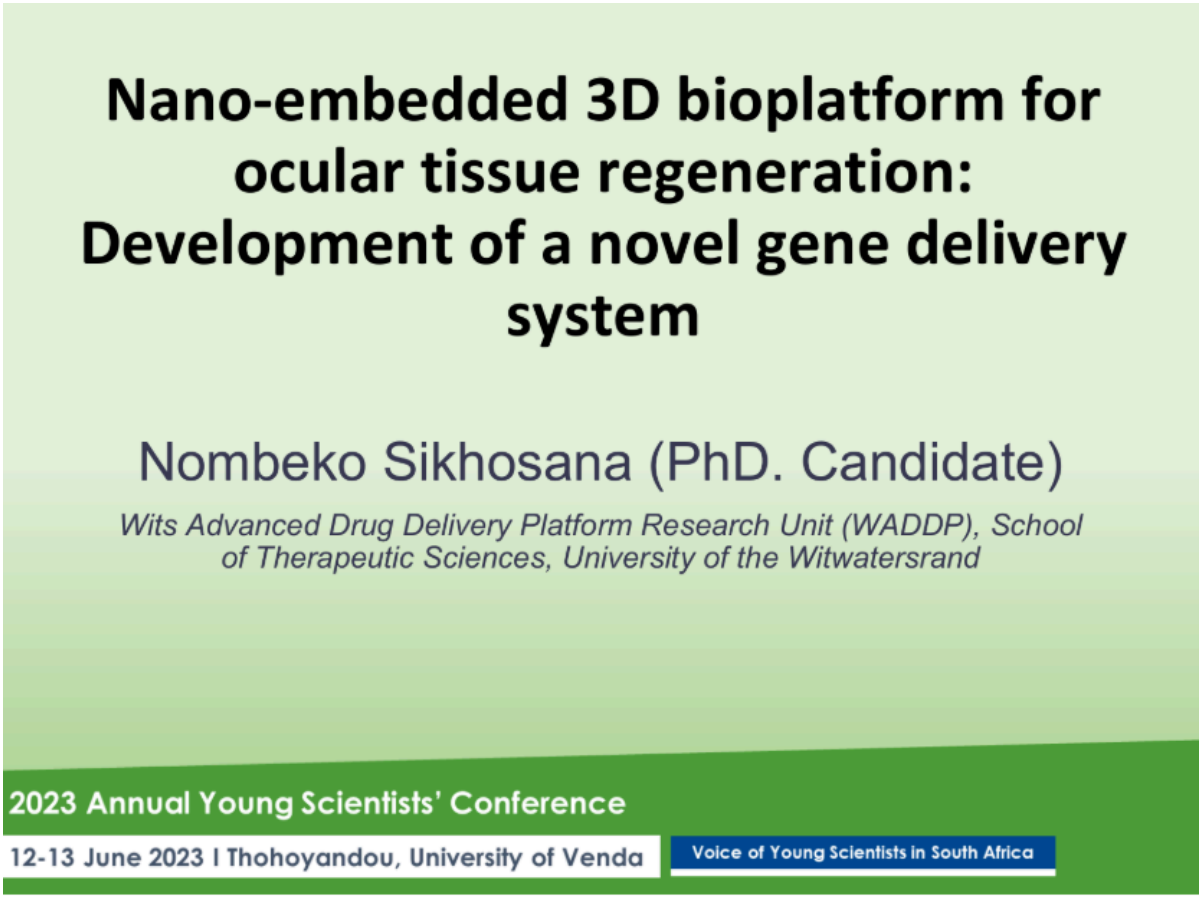

C3: APSSA 2023 Conference, University of KwaZulu Natal, The Capital Resort, Zimbali, 31 Aug - 02 September 2023.

The Academy of Pharmaceutical Sciences
of the Pharmaceutical Society of South Africa

PO Box 75769, Lynnwood Ridge, 0040 ♦ Tel: (012) 470 9562 ♦ Fax 0866 159 835
♦ email: info@pssa.org.za

27 July 2023

Dear Ms Sikhosana

It is a pleasure to inform you that the Academy Exco has accepted your abstract, to be presented at the APSSA conference which is being held at Zimbali Lodge, KwaZulu-Natal, from 31 August to 3 September 2023.

Details regarding the date, time and length of your presentation to follow.

Yours sincerely

aManolis

Nitsa Manolis
Email: nitsa@pssa.org.za

Appendix D: Originality report

PhD Thesis 2025-1.docx

ORIGINALITY REPORT

12%	7%	12%	1%
SIMILARITY INDEX	INTERNET SOURCES	PUBLICATIONS	STUDENT PAPERS

PRIMARY SOURCES

1	www.ncbi.nlm.nih.gov Internet Source	1%
2	www.mdpi.com Internet Source	<1%
3	Latavia Singh, Yahya E. Choonara, Lisa C. du Toit, Pradeep Kumar, Avirup Chakraborty, Viness Pillay. "Design, characterization and optimization of lamivudine-loaded amphiphilic HA- g -ECL nanoparticles", Journal of Drug Delivery Science and Technology, 2017 Publication	<1%
4	Li, Zhongyu. "Development of Non-Viral Nano-Carriers for Gene Delivery and COVID-19 Vaccines", New Jersey Institute of Technology, 2024 Publication	<1%
5	link.springer.com Internet Source	<1%